

TALLINN UNIVERSITY OF TECHNOLOGY
DOCTORAL THESIS
8/2019

**The Roles of Class XI Myosins in
Arabidopsis Development**

EVE-LY OJANGU



TALLINN UNIVERSITY OF TECHNOLOGY

School of Science

Department of Chemistry and Biotechnology, Division of Gene Technology

Dissertation was accepted for the defense: December 14, 2018

Supervisor:

Prof. Erkki Truve
Department of Chemistry and Biotechnology
Tallinn University of Technology
Tallinn, Estonia

Co-supervisor:

Dr. Heiti Paves
Optika & Diagnostika OÜ
Tallinn, Estonia

Opponents:

Prof. Luis Vidali
Biology and Biotechnology Department
Worcester Polytechnic Institute
Worcester, MA, U.S.A.

Prof. Hannes Kollist
Institute of Technology
University of Tartu
Tartu, Estonia

Time of defense: February 19, 2019, Tallinn

Declaration:

Hereby I declare that this doctoral thesis, my original investigation and achievement, submitted for the doctoral degree at Tallinn University of Technology has not been submitted for any degree or examination elsewhere.

Eve-Ly Ojangu

allkiri



Copyright: Eve-Ly Ojangu, 2019

ISSN 2585-6898 (publication)

ISBN 978-9949-83-392-4 (publication)

ISSN 2585-6901 (PDF)

ISBN 978-9949-83-393-1 (PDF)

TALLINNA TEHNIKAÜLIKOOL
DOKTORITÖÖ
8/2019

Klass XI müosiinide roll mürlooga arengus

EVE-LY OJANGU

*I dedicate this piece of work to my little scientist Paul-Erik – stay curious,
keep your head cool and heart warm, ♥.*

CONTENTS

LIST OF PUBLICATIONS	9
AUTHOR'S CONTRIBUTION TO THE PUBLICATIONS	10
INTRODUCTION	11
ABBREVIATIONS	13
TERMS	15
1 REVIEW OF THE LITERATURE.....	16
1.1 Actin cytoskeleton in <i>Arabidopsis</i>	16
1.1.1 Cytoskeleton-dependent morphogenesis of plant epidermal cells	16
1.1.2 Actin cytoskeleton-mediated signaling of gene expression.....	21
2 Myosin motors in plants	22
2.1 Roles of class XI myosins in <i>Arabidopsis</i>	26
3 Crosstalk between actomyosin cytoskeleton and auxin	33
3.1 Role of auxin in regulating flower development in <i>Arabidopsis</i>	35
4 Leaf senescence	38
4.1 Actin filament role in mediating cell death.....	40
4.2 Leaf senescence and auxin.....	40
4.2.1 Anthocyanins, auxin signaling, stress-response and senescence	41
5 AIMS OF THE STUDY.....	42
6 MATERIALS AND METHODS	43
7 RESULTS AND DISCUSSION.....	44
7.1 Downregulation of myosin XI-K affects epidermal cell growth in <i>Arabidopsis</i> (publication I).....	44
7.1.1 Myosin XI-K contributes to tip growth of root hairs (publication I).....	44
7.1.2 Myosin XI-K contributes to diffuse growth of trichomes (publication I).....	45
7.2 Simultaneous elimination of myosins XI-1, XI-2, and XI-K affects both cell size and organ growth in <i>Arabidopsis</i> (publication II).....	46
7.2.1 Simultaneous elimination of myosins XI-1, XI-2, and XI-K affects the growth of leaf epidermal cells to various extents (publication II)	47
7.2.2 Simultaneous elimination of myosins XI-1, XI-2, and XI-K affects the reproduction of myosin 3KO plants (publication II).....	49
7.3 Myosins XI-K, XI-2 and XI-1 contribute to auxin responses in <i>Arabidopsis</i> (publication III).....	50
7.4 Myosins XI-K, XI-2 and XI-1 contribute to leaf senescence in <i>Arabidopsis</i> (publication III).....	53
7.5 Modelling actomyosin cytoskeleton dependent processes in PAT and PCD signaling (publication III).....	55
CONCLUSIONS.....	58
REFERENCES	59
ACKNOWLEDGMENTS	77
ABSTRACT.....	78

KOKKUVÕTE	79
APPENDIX.....	81
Publication I	81
Publication II	93
Publication III.....	127
<i>CURRICULUM VITAE</i>	157
ELULOOKIRJELDUS	160

LIST OF PUBLICATIONS

The present dissertation is based on the following publications, which will be referred to in the text by their Roman numerals:

- I **Ojangu, E.-L., Järve, K., Paves, H. and Truve, E.** (2007). *Arabidopsis thaliana* myosin XIK is involved in root hair as well as trichome morphogenesis on stems and leaves. *Protoplasma* **230**:193–202. doi: 10.1007/s00709-006-0233-8.
- II **Ojangu, E.-L., Tanner, K., Pata, P., Järve, K., Holweg, C.L., Truve, E. and Paves, H.** (2012). Myosins XI-K, XI-1, and XI-2 are required for development of pavement cells, trichomes, and stigmatic papillae in *Arabidopsis*. *BMC Plant Biol.* **12**:81. doi: 10.1186/1471-2229-12-81.
- III **Ojangu, E.-L., Ilau, B., Tanner, K., Talts, K., Ihoma, E., Dolja, V.V., Paves, H., Truve, E.** (2018). Class XI myosins contribute to auxin response and senescence-induced cell death in *Arabidopsis*. *Front. Plant Sci.* **9**:1570. doi: 10.3389/fpls.2018.01570.

AUTHOR'S CONTRIBUTION TO THE PUBLICATIONS

- I The author performed the Northern blot analysis of *XI-K* transcripts, carried out trichome imaging and measurements, interpreted the results and participated in writing the manuscript.
- II The author created and characterized the double (*xi-2/xi-k*) and triple mutant line (*xi-1/xi-2/xi-k*; 3KO), measured the sizes of plant organs and circularity of pavement cells, extracted and measured trichomes, examined flower architecture with scanning electron microscope (SEM), performed Alexander's staining of anthers, aniline blue staining of pollen tubes, and reciprocal crossings, participated in statistical analysis, interpreted the results and wrote the manuscript.
- III The author characterized the stable expression of DR5::GUS, IAA2::GUS, PIN1::PIN1-GFP, and 35S::GFP-FABD2-GFP in 3KO mutant background: performed quantitative GUS-assays of plant extracts, examined flower architecture with SEM and green fluorescent protein (GFP) patterning with confocal laser scanning microscope (LSM), conducted preliminary measurements for anthocyanin accumulation, participated in RT-qPCR analysis (primer design, RNA extraction, and first strand synthesis), interpreted the results and wrote the manuscript.

INTRODUCTION

The dynamic actin filament (AF) system carries out multiple tasks during plant development such as transport of vesicles and organelles, and determination of cell growth and morphogenesis. A delicate balance has to be maintained between continuous rearrangement of AFs and membrane trafficking for providing instant cellular responses to developmental, physiological and environmental stimuli in plant cells. The organization, dynamics, and maintenance of actin arrays is determined by actin-binding proteins (ABPs) that exist in hundreds of different varieties. Myosins constitute a large superfamily of molecular motors, which move along actin tracks in an ATP-dependent manner and are key determinants in generating and maintaining membrane trafficking and cytoplasmic streaming in plant cells.

Originally, the goal of this study was to determine the roles of myosins in *Arabidopsis thaliana* (thale cress) by characterizing respective T-DNA insertional mutants. All mutants carrying a T-DNA insertion in a single myosin gene were found to have normal phenotypes under optimal growth conditions. However, a closer analysis revealed impaired growth of root hairs and trichomes in T-DNA insertional lines where myosin XI-K had been downregulated.

The absence of noticeable phenotypes in single mutants of the remaining myosin genes in *Arabidopsis* indicated strong functional redundancy among class XI myosins. Next, in order to study redundant roles of the class XI myosins, we established and characterize double and triple knock-out lines. For this, single mutant lines of three highly expressed class XI myosin genes, *XI-K*, *XI-1*, and *XI-2*, were used. Subsequent characterization of these mutant lines showed that the growth of myosin XI single, double, and triple knock-out plants decreased proportionally along with the reduction in cell size. This indicated that myosins XI-1, XI-2, and XI-K share overlapping roles in cell growth, and thus in whole plant development. Since simultaneous inactivation of three class XI myosins in a triple myosin knock-out mutant *xi1 xi2 xik* (3KO) caused severe deviations in inflorescence shoot architecture and leaf longevity, we hypothesized that myosin motors, similarly to their actin tracks, could be involved in mediating cellular signals in auxin- and senescence-related processes. Using flower and leaf development of 3KO plants as model systems, we revealed that the auxin- and senescence-related processes were indeed affected in tissues of the myosin 3KO plants.

Our findings demonstrated that myosins XI-1, XI-2, and XI-K in cooperation with actin regulate very versatile but still interrelated processes such as: cell growth, tissue morphogenesis, fertility, polar auxin transport (PAT), senescence-induced cell death, secondary metabolism, and expression of selected genes related to latter processes. Comparison of single, double and triple mutants showed that the elimination of myosin XI-K affected the growth of mutant plants to a greater extent than removal of XI-1 or XI-2. Moreover, stable expression of *XI-K* genomic sequence fused with yellow fluorescent protein (XI-K:YFP) in 3KO plants (3KOR) rescued almost all phenotypic defects described above.

In the next chapters, I will give an overview of how the knowledge about the roles of myosin in plants, specifically in *Arabidopsis*, have evolved during the last decade. In addition, I will cover the main developmental processes that are regulated by the actomyosin cytoskeleton in plants. The development of epidermal cells and signaling of auxin and senescence will be described in more detail. In light of current knowledge,

I will sum up how the functionality of plant organism is ensured by interactions among its independent organs, and how specific physiological processes described in this work are interconnected.

ABBREVIATIONS

ABA	abscisic acid
ABP	actin binding protein
ADF	actin depolymerizing factor
AF	actin filament
ARF	auxin response factor
Arp	actin-related protein
At	<i>Arabidopsis thaliana</i>
ATP	adenosine triphosphate
Ca ²⁺	calcium ion
Col	Columbia; ecotype of <i>Arabidopsis thaliana</i>
DNA	deoxyribonucleic acid
FABD2	fimbrin actin binding domain 2
F-actin	filamentous actin
FM	flower meristem
G-actin	globular actin
GFP	green fluorescent protein
GTPase	guanosine triphosphate hydrolase
GUS	β-glucuronidase
IAA	indole-3-acetic acid
IAA2	indole-3-acetic acid inducible 2
IM	inflorescence meristem
JA	jasmonic acid
LSM	laser scanning microscope
MT	microtubule
NPA	<i>N</i> -1-naphthylphthalamic acid
PAT	polar auxin transport
PCD	programmed cell death
PM	plasma membrane
PCR	polymerase chain reaction
qPCR	quantitative polymerase chain reaction
RNA	ribonucleic acid
ROP	Rho of plants; plant Rho-like small GTPase
ROS	reactive oxygen species
RT	reverse transcription
SAG	senescence-associated gene
SAM	shoot apical meristem
SAUR	small auxin up-regulated RNA gene
SCAR/WAVE	suppressor of cAMP receptor / WASP family verprolin-homologue

SEM	scanning electron microscopy
SI	self-incompatibility
T-DNA	transferred DNA
TF	transcription factor
UV-B	ultraviolet B
WT	wild type

TERMS

3KO	Triple knock-out mutant <i>xi-1/xi-2/xi-k</i> .
3KOR	Rescued 3KO line: genomic sequence of <i>XI-K</i> fused with YFP (<i>XI-K::YFP</i>) is stably expressed in 3KO plants.
DR5::GUS	Auxin-responsive reporter system: synthetic auxin-responsive DR5 promoter drives β -glucuronidase gene.
IQ motif	Calmodulin-binding motif is an amino acid sequence motif containing the following sequence: [FILV]Qxxx[RK]Gxxx[RK]xx[FILVWY]. IQ refers to the first amino acids of the motif, isoleucine and glutamine.
IAA2::GUS	Auxin-responsive reporter system: auxin-responsive IAA2 promoter drives β -glucuronidase gene. Indole-3-acetic acid inducible 2 is a short-lived transcriptional repressor of early auxin response genes.
PIN1::PIN1-GFP	Auxin efflux carrier PIN1 imaging construct: GFP is fused to N-termini of PIN1 under the control of the native PIN1 promoter.
35S::GFP-FABD2-GFP	F-actin imaging construct: GFP is fused both to N- and C-termini of fimbrin ABD2 under the control of the CaMV 35S promoter.
<i>distorted (dis)</i> mutants	A class of eight genes, called <i>DISTORTED (DIS)</i> , which are required for proper expansion of leaf trichomes in <i>Arabidopsis</i> .
Arp2/3 complex	Seven subunit protein complex that plays a major role in the nucleation of the actin cytoskeleton. ARP2 and ARP3 together serve as nucleation sites for new AFs. This complex is a major initiator of actin polymerization that promotes the formation of branched AF networks.
SCAR/WAVE complex	Major regulator of the Arp2/3 complex: these proteins activate the Arp2/3 complex to nucleate new AFs.
T-DNA	The transferable DNA segment (T-DNA) of the tumor-inducing (Ti) plasmid of pathogenic <i>Agrobacterium</i> species.
T-DNA insertional mutant	The T-DNA is transferred from <i>Agrobacterium</i> into the plant's nuclear DNA genome.
YUCCA genes	Encode flavin monooxygenase-like enzymes, which catalyze auxin biosynthesis <i>via</i> the tryptophan-dependent pathway.

1 REVIEW OF THE LITERATURE

A large number of cellular processes in plants are controlled by cytoskeleton. One of such processes is the trafficking of vesicles and organelles that is orchestrated mainly by actin cytoskeleton in plants. The balance between the dynamics of actin cytoskeleton and membrane trafficking is necessary for cell growth and thus for proper plant development. Constant remodeling of actin cytoskeleton, ensured by hundreds of actin binding proteins (ABPs), enables cellular responses to developmental and environmental signals. In the review of literature, I will first introduce fundamental aspects of actin-dependent processes in plants. As the emphasis of this thesis is on the myosin-dependent development of epidermal cells. Therefore, I will describe actin cytoskeleton-dependent growth of different epidermal cell types in *Arabidopsis*. Since actin and myosin motors work in close proximity at the cellular level, the possible functions of myosins in plant cells are closely linked to the functions of actin. Thus, I will also describe how major cellular processes, such as cell growth, morphogenesis, polar auxin transport, senescence-associated changes, cell death and regulation of gene expression are orchestrated by actin cytoskeleton, and how myosins contribute to these processes.

1.1 Actin cytoskeleton in *Arabidopsis*

In eukaryotic cells, intracellular transport, signaling, cell division and cell shape are coordinated by the cytoskeleton. In higher plants, the cytoskeleton is made up of two types of filaments: actin filaments (AFs), and microtubules (MTs) (reviewed in Reddy and Day, 2001). The actin cytoskeleton exists in two forms within eukaryotic cells: a globular monomer (G-actin) or as linear filamentous polymer (F-actin or AF), whereas both are essential for cellular functions. The AFs are highly dynamic structures present in all eukaryotic cells (Thomas *et al.*, 2009). The arrangement and dynamics of AFs, including single filament assembly and disassembly, formation of arrays, meshwork or bundles, and quick reorganization of these structures is established by a myriad of ABPs. The plant actin cytoskeleton is involved in processes such as cellular transportation, signaling, cell division, cytoplasmic streaming and morphogenesis. The huge variety of ABPs enables rapid and finely tuned changes in AF organization in response to developmental and environmental stimuli. A number of studies have shown that the levels of AF organization can be modified by changing expressions of different ABPs in plant cells (Higaki *et al.*, 2010; Thomas *et al.*, 2009).

1.1.1 Cytoskeleton-dependent morphogenesis of plant epidermal cells

The plant epidermal cell layer is a multifunctional tissue that keeps inner cells in place, decreases water loss, maintains an internal temperature and gas exchange, and resists the intrusion by external materials (Qian *et al.*, 2009). These different functions are ensured by a number of different epidermal cell types with distinct morphological specializations, such as pavement cells, stomatal guard cells, trichomes, root hairs, and stigmatic papillae. Mounting evidences suggest that even the less specialized cell types

of epidermis require certain signals to ensure their correct differentiation and patterning (reviewed in Hong *et al.*, 2018).

Plant cells use two growth strategies – polar (or tip) growth and diffuse expansion. While the tip growth is limited to the very apex of the cell, and diffuse growth occurs over a wide area of the cell. Morphologically, tip growing cells are filamentous or tubular (e.g. pollen tubes, root hairs and stigmatic papillae) and therefore the new cell wall material is delivered exclusively in the apex enriched with vesicles and cytoplasm (Franklin-Tong, 1999; Rounds and Bezanilla, 2013; Mendrinna and Persson, 2015). Diffuse growth is typical for cells such as pavement cells and guard cells that grow within boundaries of the surrounding tissue, where all cells are connected to their neighbors (reviewed in Szymanski and Staiger, 2018; Hong *et al.*, 2018).

Cytoskeleton plays an important role in plant cell morphogenesis. It is well documented that manipulations of cytoskeleton influence both the polar growth as well as the diffuse expansion of epidermal cells: MTs are necessary for establishing and maintaining growth polarity/directionality, whereas AFs are required for cell expansion/elongation (**Figure 1**) (Fowler and Quatrano, 1997; Kost *et al.*, 2002; Mathur and Hülskamp, 2002).

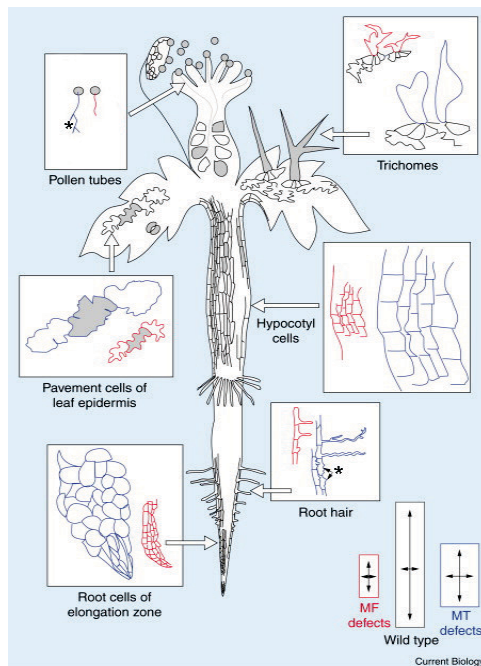


Figure 1. Schematic representation of common phenotypes of model cell types resulting from defects in actin (red) and microtubule (blue) cytoskeleton. The scheme at the bottom right of the figure compares cytoskeleton-related changes on cell growth with the wild type cell: actin cytoskeleton defects affect cell elongation/expansion (red), and MT defects affect growth focus, increase expansion and general rounding of the cell shape (blue). During root hair (RH) and pollen tube morphogenesis, specifically, both the selection of a site for tip growth (*) as well as the maintenance of tip growth are influenced by the MT cytoskeleton (Mathur and Hülskamp, 2002; used with permission).

Actin-dependent plant cell morphogenesis is a complex process. In growing cells, the organization of AF arrays, vesicle trafficking, and cell wall assembly are mutually interconnected and feedback each other in a temporal and spatial manner. The dynamics of the actin cytoskeleton and thus the cell growth is influenced mainly by ABPs and AF nucleating proteins (Szymanski and Staiger, 2018). In the cytoplasm of actively growing cells, short-lived fine AFs coexist side by side with long-lived stable AF bundles. The relationship between the extent of AF bundling and cell growth is well documented – it has been shown that the unbundled fine AF meshwork is a prerequisite for efficient elongation or expansion of the growing cell (**Figure 2**) (Mathur and Hülskamp, 2002; Nick *et al.*, 2009).

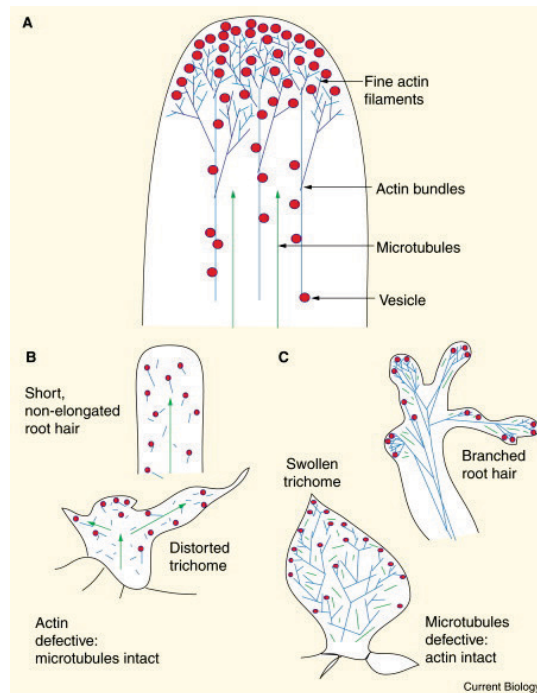


Figure 2. Hypothetical role of MTs and AFs in growing root hairs and trichomes. (A) In tip-growing root hair, fine AF (blue) are concentrated near the apex being branched out from thicker AF bundles. Fine AFs are most probably the final tracks for vesicles (carrying cell wall materials; red) that are released into vesicle incorporation zone. MTs (green) do not prevail in the zone occupied by fine AFs. In diffusely growing cells, the vesicle incorporation zone is much wider compared to tip-growing cells. **(B)** Defects in the actin cytoskeleton result in random movement of vesicles and aberrant deposition of cell-building material both in tip-growing (root hair, upper part) and diffusely growing cells (trichome, lower part), and leads to reduced cell size and distorted cell shape. **(C)** Defects in the MT cytoskeleton result in a loss of growth polarity. In the absence of a clear growth focus vesicles are released at numerous aberrant positions causing the formation of multiple growth apices in tip-growing cells (root hair, upper part), and loss of growth focus (up-swelling) of diffusely growing cells (trichomes, lower part) (Mathur and Hülskamp, 2002; used with permission).

Several studies have demonstrated that increased AF bundling affects the cell growth in a cell type-dependent manner differently (Fu *et al.*, 2002; Henty *et al.*, 2011; Nick *et al.*, 2009). For instance, *adf4* (*actin depolymerizing factor 4*) mutant plants have longer hypocotyls than wild type (WT) plants, because mutant cells exhibit enhanced AF bundling (Henty *et al.*, 2011).

1.1.1.1 Actin filament-dependent morphogenesis of *Arabidopsis* pavement cells

The most frequently occurring cells in the epidermal layer in plants are pavement cells which protect the inner tissues and ensure that more specialized epidermal cells are located correctly. In dicots, leaf pavement cells exhibit irregular shapes and resemble puzzle pieces interlocked between each other. The puzzle-like shape of leaf pavement cells gives the leaf its mechanical strength, and is reflected in the growth of a leaf blade that requires cell expansion in all directions. Pavement cells of stems and other elongated organs (petioles, pistils, petals etc.) are often more rectangular (or even elongated) in shape with their long axis being parallel to the direction of organ expansion (Glover, 2000; Zhang *et al.*, 2011a).

The mutations in genes regulating pavement cell morphogenesis lead to cell shape defects, such as the reduced lobe formation and gaps between lobe and neck regions. Various cellular processes, such as cytoskeletal dynamics, small GTPase signaling, endoreduplication, vesicle transport, and sugar metabolism are critical in the establishment of epidermal cell shape (Fu *et al.* 2005; Chary *et al.* 2008; Qian *et al.*, 2009). Several studies have shown that the plant cytoskeleton plays an important role in formation of the pavement cell shape (**Figure 1**) (Mathur and Hülskamp, 2002; Deeks and Hussey, 2003; Li *et al.*, 2003; Guimil and Dunand, 2007). In pavement cells, the lobe formation depends on AF patches, and the neck region formation relies on MT bands. Extensive mutant analysis has shown that actin nucleating complex ARP2/3 (actin-related protein 2/3) together with its regulator complex SCAR/WAVE (suppressor of cAMP receptor/WASP family verprolin-homologue) participates in the lobe formation of pavement cells *via* Rho of plant (ROP) GTPase signaling cascades (Qian *et al.*, 2009). However, in diffusely growing cells, tubulin and actin cytoskeletons cooperate to maintain mechanical properties of the cell wall and spatial architecture that supports cell expansion (Smith and Oppenheimer, 2005; Yanagisawa *et al.*, 2015).

1.1.1.2 Actin filament-dependent morphogenesis of *Arabidopsis* trichomes

Trichomes are large unicellular epidermal outgrowths with a characteristic three-dimensional architecture, covering the surface of *Arabidopsis* leaves and stems. It is thought that *Arabidopsis* trichomes form both a passive barrier against photo-damage and overheating as well as a mechano-sensing barrier which triggers plant responses after external stimulation (Zhou *et al.*, 2017). In the developing leaf primordia, trichomes are the first epidermal cells that begin to differentiate (Hülskamp *et al.*, 1994; Larkin *et al.*, 1996, 2003). After cell fate determination, the trichome precursor (protodermal cell) stops the mitotic cycle and switches to endoreduplication followed by branch initiation. After completion of the branch initiation, a rapid expansion of the branches begins (Schwab *et al.*, 2000). Trichome development can be divided into six stages. Stage 1 trichomes are defined as radially expanded cells within the epidermis. During stage 2, the transition to polar expansion (perpendicular to the plane of the leaf)

occurs. During stage 3 of trichome development, branch initiation occurs. Stage 4 trichomes are defined as cells that have expanded branches with a blunt tip. Stage 5 trichomes are defined as cells that contain branches with fine tips, and branch and stalk expansion during this stage yields the vast majority of the volume of the cell. At stage 6, trichome expansion is completed, and the cell wall acquires a papillate surface (Szymanski *et al.*, 1999). Mature leaf trichomes of WT plants are approximately 200-400 μm tall, and the average DNA content (after four endoreduplication cycles) is about 32C (Hülkamp *et al.*, 1994).

Trichomes are widely used to study how the cytoskeleton influences plant cell morphogenesis. It is well known that MT organization regulates the number of branches (Oppenheimer *et al.*, 1997; Folkers *et al.*, 2002), and AFs control the length and growth direction of the branches (**Figure 2**) (Mathur *et al.*, 1999; Szymanski *et al.*, 1999; Guimil and Dunand, 2007). It is proposed that the interaction of MTs and the AFs in trichome cell shape determination is orchestrated by a plant-unique kinesin (Tian *et al.*, 2015).

1.1.1.3 Actin filament-dependent morphogenesis of *Arabidopsis* root hairs

Root hairs are tubular extensions of root epidermal cells that are important for nutrient acquisition, plant anchorage, and microbe interactions (Grierson *et al.*, 2014). The development of root hairs begins with the bulge formation at the basal end of a trichoblast. Polarized (tip) growth from the bulge can be divided into two growth phases. The first growth phase is slow, but when the root hair has reached approximately 20-40 μm length, the rapid growth phase begins. During tip growth, secretory vesicles carrying cell wall components accumulate at the very tip, below which an organelle-enriched zone is located (**Figure 2**) (Mathur and Hülkamp, 2002). Defects in MT cytoskeleton affect root hair formation, and defects in actin cytoskeleton affect root hair expansion rate and growth directionality (Yanagisawa *et al.*, 2015).

In root hairs and pollen tubes, the well-documented mechanism of cytoplasmic streaming, named as “reverse fountain”, provides an actin cytoskeleton-dependent driving force for positioning and recycling of the cell wall materials (de Win *et al.*, 1999; Zhang *et al.*, 2011b). AFs form long-lived cortical cables that run from the base of the root hair cell to the tip, and short-lived fine AFs near the cell apex (**Figure 2**). The concentrated G-actin reservoir in the apex is necessary for formation of fine short-lived AFs (Mathur and Hülkamp, 2002). It is thought, that the actin polymerization exclusively near the cell apex promotes the reversion of the cytoplasmic streaming: the forward direction occurs at the cell’s edges, and the backward direction in the cell’s interior. The tip-focused formation of fine AFs supports transport and positioning of Golgi-derived vesicles carrying precursors for cell wall synthesis, indicating that precisely regulated dynamics of actin cytoskeleton contributes to cellular processes, such as endocytosis and exocytosis in growing root hair cells (de Win *et al.*, 1999; Zhang *et al.*, 2011b).

1.1.1.4 Actin filament-dependent morphogenesis of *Arabidopsis* stigmatic papillae

During pistil maturation, epidermal cells of the stigma, named papillae, extend to form elongated cells that are required for pollen grain attachment and germination (Edlund *et al.*, 2004). During pollination, factors essential for pollen germination (water, calcium, and boron) are actively transported from stigmatic papilla into a pollen grain.

In *Arabidopsis*, immature stigmas are able to promote pollen tube growth to some extent, although the immature pistil is then unable to support pollen tube navigation to the ovules (Nasrallah *et al.*, 1994).

Arabidopsis gynoecium development has been investigated extensively (Sessions, 1997; Bowman *et al.*, 1999; Sundberg and Ferrandíz, 2009), but the role of cytoskeleton in gynoecium patterning in general and in stigma development in particular still remains almost unstudied. The role of actomyosin cytoskeleton in the growth of stigmatic papillae has been demonstrated only by our group – we showed that in *Arabidopsis* myosin XI triple mutant plants the pre-anthesis elongation of stigmatic papilla, and the subsequent attachment of pollen are affected (publication II).

Only one study has shed light on the role of AFs in stigmatic papillae, although it was related to cross- and self-pollination events in *Brassica rapa*, a distant relative of *Arabidopsis*, and not to cell elongation directly (Iwano *et al.*, 2007). Namely, this work demonstrated the role of AFs of stigmatic papillae in mediating pollen hydration and germination. Briefly, cross-pollination increased AF bundle formation, whereas self-pollination induced AF reorganization and depolymerization, thus preventing pollen germination. In addition, during cross-pollination concomitant conformational change of the vacuolar network was detected. Therefore, a causal relationship between these processes was found, suggesting that AF reorganization regulates the structure and positioning of vacuoles in papillae during and after cross- or self-pollination in *Brassica rapa*. Hence, the actin cytoskeleton may indirectly regulate transport of ions and water to germinating pollen (Iwano *et al.*, 2007).

1.1.2 Actin cytoskeleton-mediated signaling of gene expression

The main function of actin cytoskeleton is associated with membrane trafficking, but several lines of evidence have emphasized the importance of actin also in gene expression (Burgos-Rivera *et al.*, 2008). Actin is an essential component of the cell nucleus (Bettinger *et al.* 2004; Meagher *et al.*, 2010), and some ABPs, such as actin depolymerizing factors (ADFs), are also located in the nucleus (Ruzicka *et al.* 2007). Therefore, it has been proposed that nuclear actin together with ADFs may participate in the control of gene expression at the level of transcription as well as of chromatin remodeling (Bettinger *et al.* 2004; Miralles and Visa 2006; Visa 2005).

Cytoplasmic actin together with ABPs provide a key target for many signaling events, and can also act as a signal transducer. It is well known that ABPs mediate extracellular signals *via* rearrangements of the cytoplasmic actin arrays (Staiger, 2000; Wasteneys and Galway, 2003; Porter and Day, 2015). Limited data indicate that there exists a crosstalk between the nuclear and cytoplasmic compartments of actin and ADFs, suggesting that some ADFs may function as couriers, mediating the status of cytoplasmic actin rearrangements to the nucleus. This crosstalk may provide dynamic guidance for both cytoplasmic as well as nuclear compartments of actin cytoskeleton throughout cell division, expansion, and organ development (Minakhina *et al.* 2005; Burgos-Rivera *et al.*, 2008; Kanellos *et al.*, 2015).

2 Myosin motors in plants

Myosins constitute a superfamily of ABPs called molecular motors that move along AF tracks in an adenosine triphosphate (ATP) dependent manner. Myosin motors are evolutionary conserved in eukaryotes mediating translocation of endomembranes and other macromolecular cargoes along the AFs in different cell types (Reddy and Day, 2001; Citovsky and Liu, 2017; Duan and Tominaga 2018). Myosin proteins have four domains in common: conserved N-terminal motor domain with ATPase and actin-binding activities, a neck domain (composed of IQ motifs) that binds calmodulin, a coiled-coiled domain for dimerization, and a variable C-terminal cargo-binding tail domain (**Figure 3**) (Reddy and Day, 2001). Phylogenetic analysis using sequences of conserved motor domains of 2.269 myosins from 328 organisms has revealed 35 myosin classes in eukaryotes of which plant myosins fall into two classes only, VIII and XI (Odrionitz and Kollmar, 2007).

More than a decade ago, myosins were well characterized in non-plant systems but the information about the presence and roles of these motors in plant cells just started to become available. As myosins utilize AFs for motility, it was proposed that the possible functions of myosins in plants might be closely linked to the functions of actin. Myosin-dependent processes in plant cells remained poorly understood, partly because pharmacological or immunological approaches had been mainly used. However, findings from these initial experiments suggested that myosins in plants could be involved in cellular processes such as cell division (Reichelt *et al.*, 1999), the movement of mitochondria (Van Gestel *et al.*, 2002) and chloroplasts (Liebe and Menzel, 1995), cytoplasmic streaming (Shimmen and Yokota, 1994), the rearrangement of transvacuolar strands (Hoffmann and Nebenführ, 2004), and statolith positioning (Braun *et al.*, 2002). First partial or full-length myosin sequences were identified from *Zea mays*, *Helianthus annuus*, algae *Chara corallina* and *Chlamydomonas reinhardtii* (reviewed in Reddy and Day, 2001), and *Arabidopsis* (Knight and Kendrick-Jones, 1993; Kinkema *et al.*, 1994; Kinkema and Schiefelbein, 1994; Reichelt *et al.*, 1999). However, the questions about the number of myosins, types and roles in plants remained unanswered until the completion of the sequencing of the *Arabidopsis* genome (Arabidopsis Genome Initiative, 2000). In 2001, Reddy and Day demonstrated that there are 17 highly conserved myosin-coding genes in *Arabidopsis* genome: 13 isoforms in class XI and 4 isoforms in class VIII (**Figure 3**). Class XI is similar to mammalian class V sharing similar domain structures and functions in organelle movement (Reddy and Day, 2001; Sparkes, 2011).



Figure 3. Schematic diagram of domain structures of *Arabidopsis myosins*. The motor domain, IQ domains, and coiled-coil domains are as indicated in the key. The bar represents 100 amino acids (Reddy and Day, 2001; used with permission).

Domain structure analysis of these two myosin classes revealed that in general the class XI myosins are much longer than the class VIII myosins: the neck region contains five or six IQ motifs (except for XI-K), and the length of the carboxy-terminal region following coiled-coil domain is much longer. Class VIII myosins contain three or four IQ motifs in the neck region, and a slightly longer amino-terminal region before the motor domain compared to class XI motors. The coiled-coil domains of all myosins vary considerably in length and number (Reddy and Day, 2001).

The division of high number of *Arabidopsis* myosin genes into just two classes was surprising since majority of non-plant organisms possess more than two myosin classes with only few members per each class. For example, the myosin genes of *Saccharomyces cerevisiae* are divided into three classes, and the ones of *Caenorhabditis elegans* and *Drosophila melanogaster* into seven and nine myosin classes, respectively. In the light of this knowledge, a number of questions about the roles of myosins in plants were raised. Why do higher plants have only two myosin classes? What is the biological need for the exceptionally high number of myosin genes in class XI? The phylogenetic analysis of full-length sequences of plant myosins revealed a clear dichotomy among *Arabidopsis* myosins. Class VIII myosins formed one subgroup with two pairs: ATM/VIIIA and VIIIB/ATM2. Class XI myosins formed two subgroups with three outliers: first subgroup

containing one myosin pair XIC/XIE and two unpaired myosins, XIK and MYA1; the second subgroup containing three myosin pairs – XI-B/MYA-2, XI-G/XI-H, and XI-D/XI-A. The rest of class XI myosins, XI-J, XI-F and XI-I, were positioned on separate branches. The similarity of myosin full length sequences within the class XI ranged from 40 to 85%, and the one for the class VIII myosins from 50 to 83%. Subsequent analysis of exon-intron composition revealed that the large number of myosin genes in class XI is the result of gene duplication events. Therefore, it was proposed that both the dichotomy as well as the high number of class XI myosins in *Arabidopsis* may reflect both functional redundancy as well as functional diversity (Reddy and Day, 2001).

In later years, genome sequencing of different plant group species such as green algae, mosses, monocots, and dicots has enabled to classify plant myosins in a more proper way. It was revealed that several higher plant species also possess increased number of class XI myosin isoforms. For example, while moss *Physcomitrella patens* has just two myosin XI genes, *Arabidopsis thaliana*, *Oryza sativa*, and *Brachypodium distachyon* have 13, 12, and 9 genes, respectively (Jiang and Ramachandran, 2004; Peremyslov *et al.*, 2011; Vidali *et al.*, 2010). The classification of plant myosins was further validated by Peremyslov and colleagues by using phylogenetic analysis of myosin motor domains (2011) (**Figure 4**). According to this, class VIII myosins were divided into two distinct lineages, VIII(A) and VIII(B), and class XI myosins into five lineages – XI(I), XI(G), XI(F), XI(K), and XI(J). The phylogenetic tree showed that green algae, the ancestors of land plants, possess also just two myosin classes (VIII and XI) (beige boxes in **Figure 4**). Previously, two algal myosins from *Acetabularia peniculus* were classified as belonging to a separate class XIII (Foth *et al.*, 2006), but later analysis showed their clear affiliation with class XI (Peremyslov *et al.*, 2011; **Figure 4**). Moss (*P. patens*) and lycopsid (*S. moellendorffii*) possessed also the same two classes of myosins (brown boxes in **Figure 4**), whereas moss class XI myosins clustered with flowering plant myosins. Authors concluded that the origin of the flowering plants was associated with several duplication events in class XI and a single duplication event in class VIII, suggesting a diversity of functions for the paralogous myosins. Only the group XI (F) myosins were not duplicated in any of the plant lineages analyzed. Moreover, authors showed that plant myosin genes exhibit an alternative splicing of their corresponding transcripts which may also increase myosin variants with distinct functions (Peremyslov *et al.*, 2011).

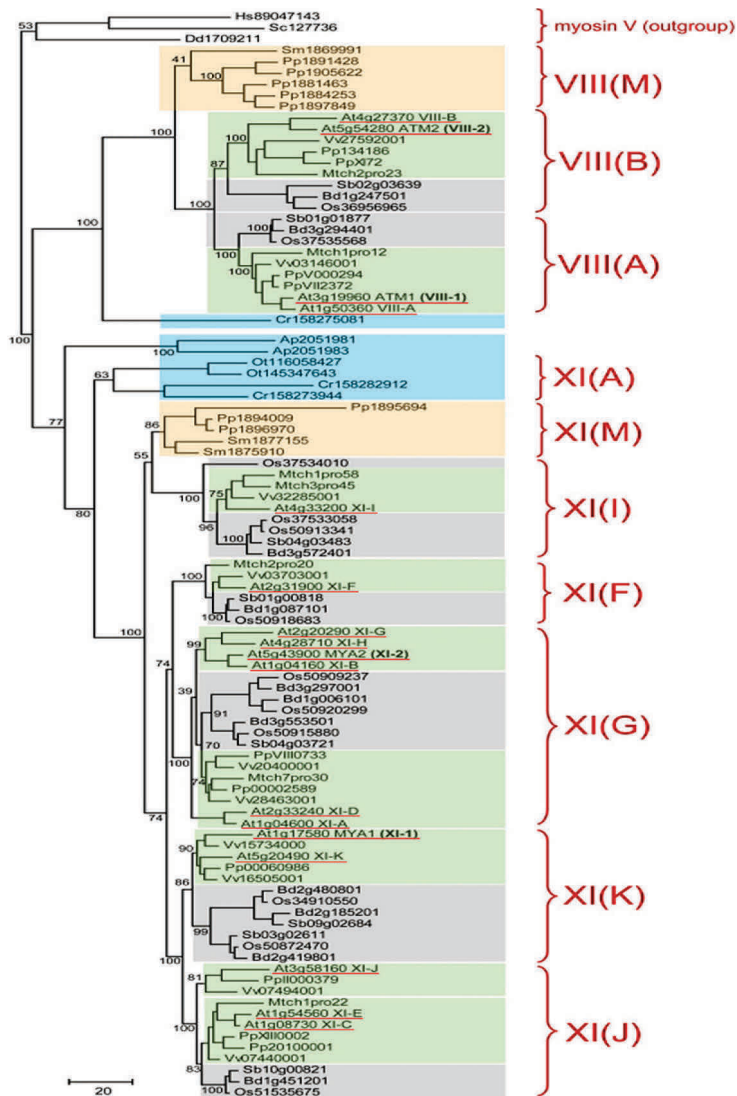


Figure 4. Phylogenetic tree of the motor domains of plant myosins. Each terminal node of the tree is labeled by the two-letter abbreviation of the corresponding species name and the unique myosin gene code. The myosin clusters are highlighted according to corresponding plant taxa as follows: algae in blue, mosses in beige, dicots in green, and monocots in gray. Abbreviations indicate: Hs, *Homo sapiens*; Sc, *Saccharomyces cerevisiae*; Dd, *Dictyostelium discoideum*; Ap, *Acetabularia peniculus*; Cr, *Chlamydomonas reinhardtii*; Ot, *Ostreococcus tauri*; Pp, *Physcomitrella patens*; Sm, *Selaginella moellendorffii*; At, *Arabidopsis thaliana*; Mt, *Medicago truncatula*; Pt, *Populus trichocarpa*; Vv, *Vitis vinifera*; Sb, *Sorghum bicolor*; Bd, *Brachypodium distachyon*; Os, *Oryza sativa*. For selected major branches, bootstrap support values (percentage) are shown. Braces at the right designate corresponding subfamilies of the class VIII and XI myosins. Red vertical lines indicate *Arabidopsis* myosins (Peremyslov et al., 2011; used with permission).

Authors complemented also the nomenclature of plant myosins proposed by Reddy and Day (2001) with some modifications as shown in **Table 1** (Peremyslov *et al.*, 2011). In the following text, I have used the myosin nomenclature as listed in **Table 1**.

Table 1. Nomenclature of the Arabidopsis class XI and class VIII myosins (Peremyslov *et al.*, 2011; used with permission).

Evolutionary Group	Gene Identifier	Proposed Name	Other Name
XI(F)	AT2G31900	XI-F	XIF
XI(G)	AT5G43900	XI-2	MYA2
	AT1G04160	XI-B	XIB
	AT2G20290	XI-G	XIG
	AT4G28710	XI-H	XIH
	AT1G04600	XI-A	XIA
	AT2G33240	XI-D	XID
XI(I)	AT4G33200	XI-I	XII
XI(J)	AT1G08730	XI-C	XIC
	AT1G54560	XI-E	XIE
	AT3G58160	XI-J	XIJ
XI(K)	AT5G20490	XI-K	XIK
	AT1G17580	XI-1	MYA1
VIII(A)	AT3G19960	VIII-1	ATM1
	AT1G50360	VIII-A	VIIIA
VIII(B)	AT5G54280	VIII-2	ATM2
	AT4G27370	VIII-B	VIIIB

2.1 Roles of class XI myosins in *Arabidopsis*

Progress in plant myosin research during last decade has been advanced due to emergence of novel approaches such as gene knock-out technologies, dominant negative inhibition, and RNA interference (publication I; Avisar *et al.*, 2008a, 2008b; Peremyslov *et al.*, 2008, 2010; Prokhnevsky *et al.*, 2008; Sparkes *et al.*, 2008; Natesan *et al.*, 2009; Sattarzadeh *et al.*, 2009; Ueda *et al.*, 2010; publication II). Initial characterization of class XI myosins revealed that in single mutant lines where myosins XI-K and XI-2 were inactivated the growth of root hairs was reduced (publication I; Peremyslov *et al.*, 2008). Additionally, *xi-k* mutants exhibited also mildly distorted trichomes (I). It was shown that at the cellular level these two myosins contribute to the transport of peroxisomes, Golgi stacks, mitochondria, and processing bodies (P-bodies) (Peremyslov *et al.*, 2008; Steffens *et al.*, 2014). Another single mutant, *xi-i*, showed defective nuclear shape and movement, though no visible defects were apparent at the whole plant level (Tamura *et al.*, 2013).

The absence of significant phenotypes among the single mutants of the rest of isoforms indicated a strong functional redundancy among class XI myosins in *Arabidopsis*, and several research groups started to create and describe various multiple knock-outs. Subsequent characterization of double knock-out mutants revealed that myosin XI-B is also involved in the root hair growth (Prokhnovsky *et al.*, 2008). Moreover, myosin XI-1 was shown to contribute to organ size development and organelle transport, but only when myosin XI-K had been simultaneously inactivated (Prokhnovsky *et al.*, 2008). Phenotypic analysis of double mutant *xi-1/xi-k* and *xi-2/xi-k* plants revealed that myosin XI-1, XI-2 together with XI-K significantly contribute to the development of aerial organs such as rosette leaves, and inflorescence shoots (Prokhnovsky *et al.*, 2008; publication II). Latter works also showed that another double mutant, *xi-f/xi-k*, displays stem hypergravitropism in response to light and gravity (Okamoto *et al.*, 2015), and *xi-c/xi-e* mutant exhibits defects in pollen tube growth (Madison *et al.*, 2015).

Studies using dominant negative inhibitions were consistent with knock-out mutant analysis. These results showed that the transient expression of myosin XI-1, XI-2, XI-C, XI-E, XI-I, and XI-K tail fragments inhibits Golgi stack movement in *Arabidopsis* plants (Sparkes *et al.*, 2008; Avisar *et al.*, 2008a, 2012). In addition, the expression of the XI-K tail fragment also inhibited the movement of the pre-vacuolar compartment and endosomes as well as cytoplasmic streaming, suggesting that myosin XI-K could be a major regulator of cytoplasmic dynamics (Avisar *et al.*, 2012). Similarly, using both RNA interference and dominant negative inhibition, it was shown that class XI myosins regulate the dynamics of chloroplast stromules (Natesan *et al.*, 2009; Sattarzadeh *et al.*, 2009).

Subsequently, studies using triple (3KO), quadruple (4KO) and quintuple (5KO) mutants emphasized that five myosins - XI-1, XI-2, XI-B, XI-I, and XI-K, critically contribute to both polarized and diffuse cell expansion, and thus to organ growth and whole plant development (Prokhnovsky *et al.*, 2008; Peremyslov *et al.*, 2010; publication II). Simultaneous myosin inactivation in 3KO, 4KO or 5KO background resulted in reduced cell size, stunted growth, delayed bolting, and reduced fertility (Peremyslov *et al.*, 2010, publication II). At the cellular level, 3KO, 4KO or 5KO plants exhibited cell-type specific changes in organization of AF bundles as well as in mobility of organelles, Golgi bodies, peroxisomes, and mitochondria (Peremyslov *et al.*, 2008; 2010; Prokhnovsky 2008; Ueda *et al.*, 2010). Ueda and colleagues showed that myosins XI-K, XI-1, and XI-2 are also responsible for the ER flow along AF bundles (2010).

Still, the exact mechanism by which myosins support plant cell growth remains unclear, i.e. whether large organelles or small vesicles constitute the main myosin cargoes. Analysis of subcellular localization of myosin XI-K:YFP revealed its association with vesicle-like compartments rather than with large organelles (Peremyslov *et al.*, 2012). Thus, a paradox was found here. Although total endomembrane trafficking (motility of organelles, vesicles, the trans-Golgi network, endosomes, and the entire cytoplasmic streaming) depended on class XI myosins (Peremyslov *et al.*, 2010; Avisar *et al.*, 2012), the major player, myosin XI-K, did not co-localize with these organelles or vesicles (Peremyslov *et al.*, 2012). Further studies were performed to identify possible cellular receptors for class XI myosins. It was found that myosin XI-K is indeed attached to membrane anchored myosin binding proteins (MyoBs) that decorate vesicles moving in a continuous and rapid manner distinct from the slower movement of organelles and major carrier vesicles. It was proposed that the vesicles decorated by MyoB and myosin XI form a specialized transport system, whereas organelles and carrier

vesicles are passively dragged along with it (Peremyslov *et al.*, 2013). Additionally, a few years later the same group identified also putative myosin adaptors (MadA and MadB), implying that the myosin XI interactor network is more complex than previously suspected (Kurth *et al.*, 2017). As myosin XI-dependent MyoB-decorated vesicles moved along AF bundles at the velocity of cytoplasmic streaming, the authors hypothesized that class XI myosins could play a major role in generating a motive force for cytoplasmic streaming (Peremyslov *et al.*, 2015). The detailed analysis of AF dynamics in 3KO cells revealed that three *Arabidopsis* class XI myosins contribute to actin remodeling by stimulating AF turnover and generating the force for AF shape change (Cai *et al.* 2014). This explained, why in cells of myosin multiple mutants the cytoplasmic streaming was slowed down, the elongation of epidermal cells was reduced, and plant size and fertility were affected (Tominaga *et al.*, 2013; Peremyslov *et al.*, 2015). Therefore, it was proposed that cytoplasmic streaming, generated by organelle-associated class XI myosins moving along AF bundles, is very likely a key determinant of plant size. This assumption was proven elegantly by using stable expression of high- and low speed myosin XI-2 chimeras in *Arabidopsis*. This experiment showed that size change of these transgenic plant lines correlated with acceleration and deceleration, respectively, of cytoplasmic streaming (Tominaga *et al.*, 2015).

Most recent studies, using myosin triple mutant 3KO plants as a model system, have revealed that class XI myosins mediate fundamental cellular responses such as gravitropism, auxin responses, and cell division (Scheuring *et al.*, 2016; Talts *et al.*, 2016; Abu-Abied *et al.*, 2018). In the first paper we showed that 3KO inflorescence stems exhibit impaired stem gravitropism, which was related to physical features, actin cytoskeleton, and amyloplast sedimentation (Talts *et al.*, 2016). A publication by another group reported that myosin 3KO root cells show moderate unresponsiveness to exogenous auxin treatment, exhibiting partially auxin-insensitive vacuoles (Scheuring *et al.*, 2016). Using root development as a model, the authors of a third study revealed that class XI myosin together with actin contribute to polar auxin transport (PAT) and cell division (Abu-Abied *et al.*, 2018). The most recent study showed the role of myosin XI in exocytosis of cellulose synthase complexes (Zhang *et al.*, 2018).

All developmental defects related to class XI myosins in *Arabidopsis* described above, are listed in **Table 2**, and expression patterns are summarized in **Figure 5** (reviewed by Duan and Tominaga, 2017).

Table 2. Developmental defects related to class XI myosins (modified from Duan and Tominaga, 2017; used with permission).

Root		
Root elongation and branching	XI-1, XI-2, XI-K	Root elongation of 3KO seedlings is decreased, and root branching is increased (inducible by dark treatment).
Root hair elongation	XI-1, XI-2, XI-K, XI-B	Root hair elongation is inhibited in single mutant <i>xi-k</i> (I) and <i>xi-2</i> , and the phenotype is amplified in respective double (II), triple (II) and quadruple mutants.
AF organization and dynamics	XI-1, XI-2, XI-K, XI-I	AF dynamics is moderately decreased in <i>xi-k</i> root hairs, and significantly affected in 3KO and 4KO mutants since they exhibit less dense and more bundled AFs in the epidermal cells.
Nuclear shape and dynamics	XI-I	In root hairs of <i>xi-i</i> mutant nuclear shape and movement are affected.
Organelle motility	XI-2, XI-K	XI-2 and XI-K play major roles in organelle trafficking in root hairs.
Auxin transport	XI-1 XI-2 XI-K	In 3KO mutant seedlings, the activity of auxin responsive DR5 promoter is decreased, and root cells exhibit partial loss of PIN1 polarization.
Leaf		
Cell expansion/leaf growth	XI-1, XI-2, XI-K, XI-B, XI-I	The diffuse growth of epidermal cells is inhibited in double, triple (II), and quadruple mutants.
Trichome development	XI-1, XI-2, XI-K, XI-I	Single mutant <i>xi-k</i> , double mutant <i>xi-k/xi-2</i> , and triple mutant exhibit distorted trichome phenotype (I, II).
AF organization	XI-1, XI-2, XI-K, XI-I	AF organization is affected in leaf midvein epidermal cells of <i>xi-k/xi-2</i> , 3KO, and 4KO mutants.
Nuclear shape	XI-2, XI-K, XI-I	Trichome nuclei of <i>xi-1</i> , <i>xi-2</i> , <i>xi-k</i> , <i>xi-1/xi-2</i> and <i>xi-1/xi-k</i> and 3KO plants exhibit abnormally elongated nuclei (II). <i>xi-i</i> single mutant has more spherical nuclei.
Organelle motility	XI-1, XI-2, XI-K, XI-B, XI-I	XI-2 and XI-K play major roles in organelle trafficking in leaf epidermal cells.
Cell death	XI-1, XI-2, XI-K	3KO mutant plants exhibit premature leaf senescence accompanied by the loss of chlorophyll, and up-regulation of the stress-inducible early senescence associated <i>SAG13</i> gene (III).
Inflorescence stem		
Bolting	XI-1, XI-2, XI-K, XI-B, XI-I	Late bolting phenotype in 3KO (II) and 4KO mutants.
Bolt height	XI-1, XI-2, XI-K, XI-B, XI-I	Inhibited bolt height in double (II), 3KO (II), and 4KO mutants.
Shoot branching	XI-1, XI-2, XI-K	Increased formation of secondary and tertiary branches on primary inflorescence stem of 3KO mutant plants (III).

Straightening	XI-1, XI-2, XI-K, XI-F	Delayed sedimentation of amyloplasts in 3KO mutant stem. XI-F exhibits specific expression in the fiber cells of stem.
Flower /Reproduction		
Stigma development	XI-1, XI-2, XI-K	Delayed elongation of stigmatic papillae of 3KO mutant pistils (II).
Pollen tube growth	XI-A, XI-D, XI-C, XI-E	Double mutants <i>xi-a xi-d</i> and <i>xi-c xi-e</i> have slower pollen tube growth rates <i>in vivo</i> .
Seed set	XI-1, XI-2, XI-K XI-A, XI-D, XI-C, XI-E	Reduced seed-set phenotype in 3KO mutant (II) and in double mutants <i>xi-a/xi-d</i> and <i>xi-c/xi-e</i> .
Auxin transport	XI-1, XI-2, XI-K	Decreased activity of DR5 promoter in 3KO mutant bolts is accompanied with partial loss of PIN1-GFP polarization in triple mutant pistils (III).

Taken together, studies of class XI myosin have shown that these molecular motors drive the motility of different vesicles and organelles (Avisar *et al.*, 2008, 2009; Peremyslov *et al.*, 2008, 2010, 2013; Prokhnevsky *et al.*, 2008; Sparkes *et al.*, 2008; Ueda *et al.*, 2010; Tamura *et al.*, 2013), influence cytoplasmic streaming (Shimmen and Yokota, 2004; Avisar *et al.*, 2012; Tominaga *et al.*, 2013; Peremyslov *et al.*, 2015), modulate AF organization, and thereby affect cell expansion, plant morphology (publication I, II; Peremyslov *et al.*, 2008, 2010; Prokhnevsky *et al.*, 2008; Park and Nebenführ, 2013; Madison *et al.*, 2015; Okamoto *et al.*, 2015), and responses to external/environmental stimuli (Scheuring *et al.*, 2016; Talts *et al.*, 2016; Abu-Abied *et al.*, 2018).

Expression analysis of *Arabidopsis* myosins (using public Affymetrix DNA microarray data and Genevestigator tools) revealed that myosin XI genes can be roughly divided into three groups (Peremyslov *et al.*, 2011). The first one includes five highly expressed genes (*XI-K*, *XI-1*, *XI-2*, *XI-H*, and *XI-I*), suggestive of having important roles in plant development. Indeed, data available for these myosin functions confirms that they have major, albeit redundant, roles in intracellular dynamics, cell expansion, and organ growth (as discussed above). The genes (*XI-B*, *XI-F*, *XI-G*, and *XI-J*) in the second group are transcribed at intermediate levels, indicating that they might be less relevant for plant development or alternatively have more specialized roles (Peremyslov *et al.*, 2011). Accordingly, the specific function of the *XI-F* is related to plant stem responses to gravity and light (Okamoto *et al.*, 2015), whereas *XI-B* contributes to root hair growth (Prokhnevsky *et al.*, 2008; Peremyslov *et al.*, 2010). On the other hand, the *XI-B* and *XI-J* genes are preferentially expressed in pollen, implying a specific role in pollen tube growth. The third group of myosins (*XI-A*, *XI-C*, *XI-D*, and *XI-E*), seem to have very specialized roles, since they are all expressed exclusively in stamen and pollen (Peremyslov *et al.*, 2011). Indeed, experiments with double mutant *xi-c/xi-e* confirmed that myosins *XI-C* and *XI-E* are required for efficient pollen tube growth (Madison *et al.*, 2015).

Nonetheless, the functions of class XI myosins are not yet fully understood. Very recent research elegantly shows that specific roles of class XI myosins in plants could be also related to their distinct motile and enzymatic activities (Haraguchi *et al.*, 2018). Based on *in vitro* motility assays of recombinant myosins, 13 class XI myosins were broadly classified into three groups, where a rough correlation between tissue-specific expression and velocity groups was found. Briefly, high-velocity group contained mainly pollen-specific myosins (*XI-A*, *XI-C*, *XI-D*, *XI-E*, *XI-F*, *XI-G*), medium-velocity group

contained mainly widely expressed myosins (XI-1, XI-2, XI-B, XI-H, XI-J, XI-K), and the low-velocity group contained only one myosin, XI-I. The authors concluded that they did not find a correlation between the myosin grouping generated using velocity analysis and the one generated using phylogenetic analysis (Haraguchi *et al.*, 2018).

3 Crosstalk between actomyosin cytoskeleton and auxin

Majority of plant growth processes rely on controlled levels of, and responses to, phytohormone auxin. Indole-3-acetic acid (IAA) is the principal naturally occurring auxin which plays critical regulatory roles in plant development since it regulates both expansion and polarity of individual cells, as well as initiation and patterning of organs. Auxin is believed to be active in the form of free acid synthesized from the precursor tryptophan, though endogenous levels of the hormone are controlled also by processes such as oxidation and conjugation. IAA-conjugates (IAA-amino acids, IAA-sugar, and IAA-methyl ester) are believed to be involved in IAA transport and storage, and for controlling of the pool of the free IAA (Östin *et al.*, 1998).

Since auxin action depends on its differential distribution in plant tissues, it has to be transported from the sites of synthesis (shoot and root meristem, organ primordia) to the sites of action – primarily downward from shoots and upward from roots. Long-distance auxin transport occurs passively, *via* phloem, and short-distance transport occurs from cell to cell. Depending on the protonation state, auxin can diffuse either passively (IAAH) from cell to cell or require active (IAA⁻) transporters located at the plasma membrane. The major determinant of auxin actions is differential auxin distribution (local auxin maxima or gradients between cells) which is created by directional cell to cell transport mechanism known as polar auxin transport (PAT) (Petrášek and Friml, 2009). These transient auxin concentration gradients underlie developmental processes such as meristem initiation, organ primordia formation, embryo morphogenesis, lateral root formation, as well as regulation of phyllotaxy and vascular tissue differentiation, photo- and gravitropic responses (Berleth and Sachs, 2001; Vanneste and Friml, 2009; Cardarelli and Cecchetti, 2014; Adamowski and Friml, 2015). PAT is mediated by auxin uptake permeases and efflux carrier proteins that localize to PM in an asymmetric manner. PIN-FORMED (PIN) and ATP-binding cassette transporters/P-glycoprotein (ABCB/PGP) families are principal auxin efflux carriers whereas members of Auxin-Resistant 1/LIKE-AUX1 (AUX1/LAX) family are major auxin uptake carriers (Okada *et al.*, 1991; Bennett *et al.*, 1996; Gälweiler *et al.*, 1998; Luschnig *et al.*, 1998; Marchant *et al.*, 1999; Swarup *et al.*, 2001; Geisler and Murphy, 2006; Krecek *et al.*, 2009; Zažímalová *et al.*, 2010; Swarup and Péret, 2012; Adamowski and Friml, 2015). The regulation of PAT mainly depends on the action of auxin efflux carriers of the PIN and ABCB/PGP families (Geisler and Murphy, 2006; Vanneste and Friml, 2009; Adamowski and Friml, 2015). Both auxin influx permease AUX1, as well as efflux carriers (PINs and ABCBs) cycle between the plasma membrane and endosomal compartments (Geldner *et al.*, 2001; Kleine-Vehn *et al.*, 2006; Cho *et al.*, 2007; Kleine-Vehn and Friml, 2008; Titapiwatanakun *et al.*, 2009; Kleine-Vehn *et al.*, 2011; Swarup and Péret, 2012; Cho and Cho, 2013; Wang *et al.*, 2013).

In addition to being essential for cell integrity, actin cytoskeleton contributes to PAT. Various genetic and pharmacological studies have revealed a tight interplay between auxin signaling and actin cytoskeleton. On the one hand, the patterning of AF arrays is modulated by auxin (**Figure 6**); on the other hand, auxin transport depends on the organization and dynamics of AFs (Nick *et al.*, 2009; Zhu and Geisler, 2015; Wu *et al.*, 2015; Zhu *et al.*, 2016; Eggenberger *et al.*, 2017; Huang *et al.*, 2017).

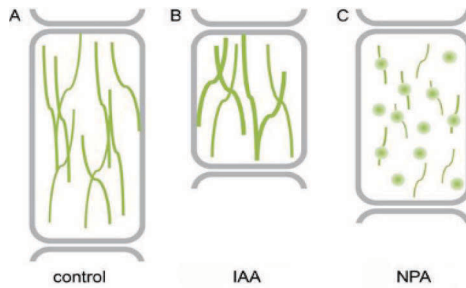


Figure 6. Effect of auxin and auxin transport inhibitor on AF stability and cell growth in the root elongation zone. In comparison to the control **(A)** (thick green lines), exogenous IAA application significantly reduces cell length, which is accompanied by AF bundling **(B)** (thick green lines). In contrast, auxin export inhibitor, 1-N-Naphthylphthalamic acid (NPA) decreases cell elongation moderately which is accompanied by partial depolymerization of AFs **(C)** (fragmented green lines and punctuated structures) (modified from Zhu and Geisler, 2015; used with permission).

The existence of a crosstalk between auxin and actin is also supported by findings that both localization and recycling of auxin importers and exporters depends partially on AFs (Geldner *et al.*, 2001; Kleine-Vehn *et al.*, 2006; Dhonukshe *et al.*, 2008; Wu *et al.*, 2015; Zhu and Geisler, 2015). Therefore, it has been proposed that AFs both determine the localization of auxin efflux carrier complexes at membranes and mediate vesicle delivery between the plasma membrane and internal cellular compartments (**Figure 7**) (Muday and DeLong, 2001).

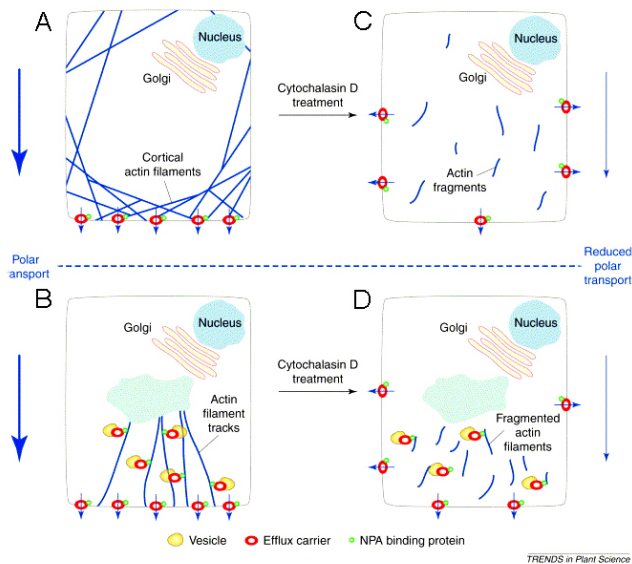


Figure 7. The effect of cytochalasin D on PAT. In control cells, cortical AFs localize the auxin efflux carrier complexes at membranes **(A)** and/or AFs serve tracks for vesicle delivery between the plasma membrane and internal cellular compartments **(B)**. The PAT is reduced in cells treated with actin polymerization inhibitor (cytochalasin D), **(C, D)** since the loss of AFs affects the correct localization of the efflux carrier complexes at membranes **(C)** and/or prevents AF-mediated vesicle cycling **(D)** (modified from Muday and DeLong, 2001; used with permission).

However, the exact role of the actin cytoskeleton in PAT is still unresolved. It has been suggested that interactions between auxin and actin are not only dose- and time-dependent, but also species- and organ-dependent (Zhu and Geisler, 2015).

In roots, the main function of auxin is to inhibit cell elongation while in shoots it stimulates cell elongation. The importance of AF bundling in auxin-controlled cell growth has been demonstrated also. Therefore, the auxin-actin interaction in these different organs (shoot versus root) can be summarized as follows: auxin-induced cell elongation is accompanied by debundling of AFs in the shoot, while auxin-inhibited cell elongation in root cells is associated with enhanced AF bundling (Holweg et al., 2004; Nick, 2010; Rahman et al., 2007; Li et al., 2014). Although auxin transport has been well characterized in both roots and shoots, the information about auxin transport and its role in elongation is limited. In particular, it is not clear whether the proteins mediating PAT are separate from the protein mediating auxin action on cell elongation or whether these two processes might be mediated by the same receptor. It has been proposed that this root-shoot puzzle could be explained by the action of hypothetical auxin-actin integrators which may have opposite effects on AF stability and dynamics in a tissue-specific manner (reviewed in Zhu and Geisler, 2015).

Even though myosin and AFs act in concert, the potential role of myosins in auxin responses has begun to be revealed recently. First, one of the studies reported that myosin 3KO roots show moderate unresponsiveness to exogenous auxin treatment, exhibiting partially insensitive vacuoles (Scheuring *et al.*, 2016). Because both the AF architecture and dynamics are altered in myosin 3KO cells (Ueda *et al.*, 2010; Peremyslov *et al.*, 2010; Cai *et al.*, 2014; Scheuring *et al.*, 2016), it is likely that the mutant cells are less responsive to stimuli such as auxin signaling. Second, very recent findings (Abu-Abied *et al.*, 2018) have shown that there is a correlation between altered architecture of 3KO roots, reduced auxin gradient, and partial loss of PIN1 polarization in stele cells. These results provide the first line of evidence that PAT could be, at least partly, myosin-mediated process in *Arabidopsis*.

3.1 Role of auxin in regulating flower development in *Arabidopsis*

During the transition from vegetative phase to flowering, the shoot apical meristem (SAM) becomes the inflorescence meristem (IM) (Hempel and Feldman, 1995). The IM generates the floral meristems (FM) on its flanks, and FMs produce floral primordia (Alvarez-Buylla *et al.*, 2010). Floral organs are initiated sequentially by the FM which produces four whorls: the outermost whorl of sepals, second whorl of petals, a third whorl of stamens and innermost whorl of carpels. *Arabidopsis* flower development before fertilization is summarized in **Figure 8** (Larsson *et al.*, 2014). During first two stages, FM and primordium are formed. First floral organs to arise from FM are sepals. Next, the petal and stamen primordia are formed, and the last organ to bulge out from FM is gynoecium. During late growth stages, organ growth continues and the last tissue which develops on the top of the gynoecium is stigma. By stages 10-11, pistil growth is completed. At the stage 12 petals are equal in length to stamens, and the onset of flower bud opening (anthesis) begins at stage 13, followed by self-fertilization at stage 14. For self-fertilization to occur, anthers must reach the stigma for proper pollination (Aloni *et al.*, 2006; Larsson *et al.*, 2014).

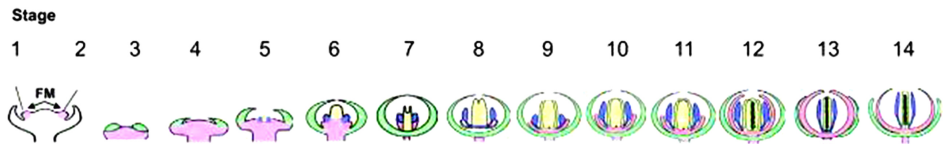


Figure 8. Schematic diagram showing 14 stages of *Arabidopsis* flower development. At stages 1 and 2, the floral meristem and primordium are formed. At stage 3, sepal primordia become visible and continue growing until enclosing the flower meristem (until to stage 6). At stage 5, petal and stamen primordia start to form. At stage 6, gynoecium primordium becomes visible. At stages 7 and 8, the growth of floral organs continues and by stage 9, stigmatic papillae appear at the top of the gynoecium. At stage 12, petals are similar in length to stamens. Anthesis occurs at stage 13, fertilization occurs at stage 14. Floral meristems (FM), pink; sepals, green; petals, bright pink; stamens, blue; gynoecia, yellow; ovules, dark green (adapted from Alvarez-Buylla *et al.*, 2010; used with permission).

The emergence and morphogenesis of the gynoecia and stamens, the most modified floral organs, requires elevated auxin production (Okada *et al.*, 1991; Sessions *et al.*, 1997; Nemhauser *et al.*, 2000; Aloni *et al.*, 2006; Cheng *et al.*, 2006; Cecchetti *et al.*, 2008; Sundberg and Ferrandíz, 2009; Hawkins and Liu, 2014). During floral organ development, auxin gradients are formed by local auxin biosynthesis and PAT, which leads to organ outgrowth and tissue differentiation. **Figure 9** illustrates gradual changes in sites of free IAA production (detected by DR5::GUS expression) during *Arabidopsis* flower development (Aloni *et al.*, 2006).

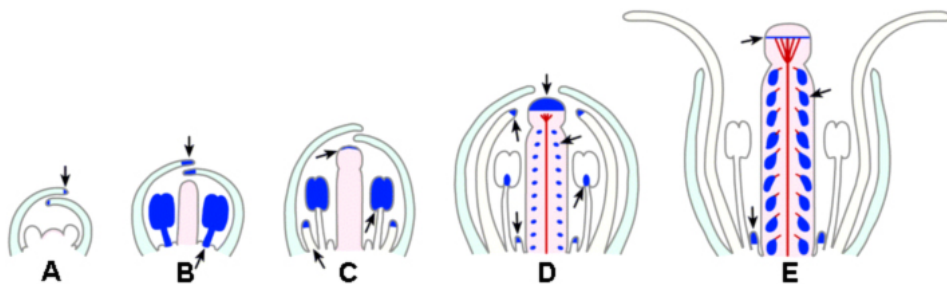


Figure 9. Schematic diagram illustrates gradual changes in the sites of free-IAA production. Free-IAA production was detected with auxin-responsive promoter-reporter system DR5::GUS (blue color). **(A-E)** Flower organ development in *Arabidopsis*. **(A)** In young floral bud, free-IAA accumulates at the tip of the developing sepals (the bud is loaded with conjugated auxin). **(B)** Free-IAA production at the sepal tips and massive auxin production in the stamens demonstrates stamen dominance and petal suppression. **(C)** Decreased free-IAA production in the stamens (DR5::GUS activity limited to the anthers) is followed by emergence of free-IAA auxin production in the growing stigma and petals. **(D)** Elevated free-IAA production in the stigma; low auxin production in ovules, nectaries, petal tips and stamen-filament tips. **(E)** Residual free-IAA production beneath the stigma, elevated auxin production in developing seeds, and continuous production in nectaries. Arrows mark sites of auxin production. Red lines indicate short xylem veinlets induced by developing seeds (adapted from Aloni *et al.*, 2006; used with permission).

Briefly, dynamic auxin distribution within the periphery of the IM specifies the site of FM initiation, while auxin maxima present at the tips of developing floral organ primordia mediate organ growth and patterning. For example, the elevated auxin accumulation in growing stamens becomes limited when the petal growth is initiated.

According to Nemhauser's model, the auxin gradient spreads along the apical-basal axis of the emerging gynoecium drives pistil development, which means that apically synthesized auxin is transported downward (Nemhauser *et al.*, 2000). Thereat, high auxin levels specify stigma and style identity, intermediate auxin levels specify ovary identity, and lower auxin levels specify gynophore identity. More than a decade later both by Hawkins and Liu as well as Larsson and colleagues have proposed an alternate model for auxin-dependent patterning of gynoecium (2014) (**Figure 10**). This model suggests that auxin-mediated adaxial-abaxial polarity of the gynoecial primordium drives pistil development. According to this model, auxin is synthesized at the basal end of the primordium and delivered to apices *via* basipetal transport. Thereat, two oppositely-oriented auxin flows in epidermis determine a change of auxin transport direction toward the interior of the primordium. Since PAT now takes place in two laterally localized foci, adaxial-abaxial symmetry of the developing gynoecia is generated (Hawkins and Liu, 2014; Larsson *et al.*, 2014). This theory is supported by studies showing that the auxin efflux carrier PIN1 accumulates apically in epidermal cells of developing gynoecia, indicating upward auxin transport (Sorefan *et al.*, 2009; Grieneisen *et al.*, 2013; Larsson *et al.*, 2014).

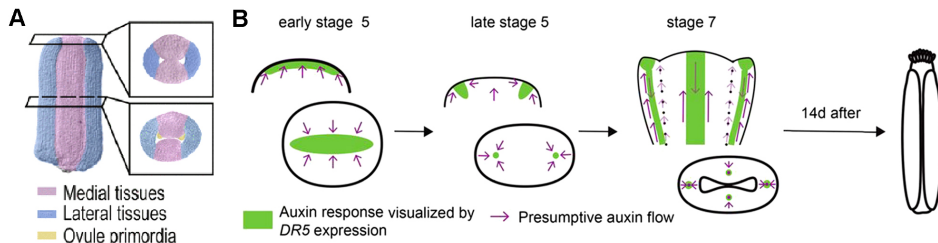


Figure 10. Model of the auxin-dependent patterning during early gynoecium development. (A) Gynoecium at floral stage 8. False colors indicate lateral (abaxial) and medial (adaxial) tissues (domains), and ovule primordia. (B) The outgrowth of two carpel primordia from floral meristem depends on PIN1-mediated lateral auxin maxima as well as subsequent internal auxin drainage. At early floral stage 5, auxin transport occurs toward emerging carpel primordium, and the auxin maximum is generated along the lateral plane of the primordium. At late floral stage 5 (just before the gynoecium bulges out) PAT is organized into two laterally localized foci: opposing auxin flows converge on the epidermal centers of each carpel primordium and create auxin response maxima. These convergence sites mark boundaries between the adaxial and abaxial tissues. At floral stage 7, both medial and lateral domains are provided with auxin from the base. Later the cylindrical tube of gynoecium differentiates into stigma/style at the apex and gynophore at the base (Modified from Larsson *et al.*, 2014; used with permission).

4 Leaf senescence

Senescence in plants is a highly regulated degeneration of cells, tissues, organs or the whole organisms that occurs as a part of development or can be induced prematurely by stress (Buchanan-Wollaston *et al.*, 2003; Kim *et al.*, 2016). Senescence in plants is most distinctive at the organ (leaf) or organismal (whole plant) level (Kim *et al.*, 2016). The emergence and growth of new leaves requires nutrients from the rest of the plant. The mature leaf is the primary source of nutrients for plant development. When the leaf is no longer contributing to the growth of the whole plant, the senescence process is induced. Senescence, the terminal phase in leaf development, is programmed degradation of cellular components that results in programmed cell death (PCD) (Buchanan-Wollaston *et al.*, 2003; Lim *et al.*, 2003). The degradation products of senescing tissues are recycled to support the growth of newly forming organs such as leaves, roots, tubers, shoots, flowers, fruits, and seeds (Himelblau and Amasino, 2001; Maillard *et al.*, 2015). In *Arabidopsis*, the initiation of leaf senescence usually coincides with the switching to flowering that is accompanied by termination of vegetative meristem activity. Senescence progresses until fruit development and maturation are complete, and ends with the death of leaf tissues. Without external stress, leaf longevity depends on two parameters: leaf age, and age of the whole plant (Zentgraf *et al.*, 2004; reviewed in Bresson *et al.*, 2018).

Leaf senescence is characterized by loss of chlorophyll, degradation of organelles, autolysis of the tonoplast and subsequent removal of the cytoplasm (Weaver *et al.*, 1998; Lin and Wu, 2004; Zentgraf *et al.*, 2004; Hou *et al.*, 2013; Watanabe *et al.*, 2013; Woo *et al.*, 2013; Kim *et al.*, 2016). Leaf senescence can be divided into three stages: initiation, reorganization, and termination. The initiation of senescence is driven by multiple simultaneously coordinated signals mediated by hormones, sugars, reactive oxygen species (ROS), and calcium, which will activate a regulatory transcriptional network (Lim *et al.*, 2007). During the reorganization phase, the cells are intensively restructured, macromolecules are degraded, and nutrients are recycled. These processes involve many proteases and their regulators, and transportation of degradation products. Chloroplasts are the first organelles that are affected by the degradation process, and the breakdown of chlorophyll is one of the main visible symptoms for leaf senescence giving the leaf a characteristic yellowish color. It has been suggested also that chloroplasts might regulate the senescence in leaves by generating ROS, which damage cell structures and functions (Zapata *et al.*, 2005; Zimmermann and Zentgraf, 2005). ROS-signaling has been shown to promote senescence and age-induced PCD *via* induction of senescence associated genes (SAGs) (Rogers 2013; reviewed in van Hautegeem *et al.*, 2014). Anti-oxidative enzymes, such as catalases and peroxidases, have a key role in detoxifying ROS generated during cellular component breakdown (Buchanan-Wollaston *et al.*, 2003). Similarly, increased accumulation of anthocyanins during senescence has also been reported to protect against ROS-induced stress. The detoxification is important for maintaining the functionality of nuclei and mitochondria and for preserving transcriptional control and energy supply throughout the process (reviewed in Bresson *et al.*, 2018). During the termination phase, cell death is initiated – vacuoles are disrupted, and subsequent release of nucleases and proteases initiates the acidification of cytoplasm, which leads to the gradual degradation of the cytoplasm, fragmentation of nuclear DNA and

organelles, and weakening of the membranes (Zimmermann and Zentgraf, 2005; reviewed in Bresson *et al.*, 2018).

As mentioned above, senescence can be either a developmentally controlled process or be induced prematurely by a number of different environmental stresses such as pathogen infection, nutrient deficiency, drought, darkness, detachment, ozone or UV-B. During stress-induced senescence certain parts of the plant are sacrificed to ensure the survival of the rest of the plant. For example, pathogen infection of a single leaf will induce the senescence in that particular leaf (Beers and McDowell, 2001; Bresson *et al.*, 2018).

A major question in leaf senescence concerns the nature of the mechanisms initiating this process. In the light of current advances, it is known that radical cellular changes are transformed to cellular responses *via* changes in transcription. At the gene expression level, many transcription factors, chromatin-modifying factors, post-translational regulators, receptors, signaling components for hormones and stress responses, and metabolism regulators are differentially expressed over the time course of leaf senescence (reviewed in Bresson *et al.*, 2018; Kim *et al.*, 2016). For example, several transcriptomic, metabolomics or reverse genetic approaches have revealed that almost 6400 genes are differentially regulated throughout the leaf senescence in *Arabidopsis*. Based on their differential expression patterns, these genes were grouped into 48 clusters indicating the complexity of the regulatory networks, and providing a global view how distinct pathways become active at different time points of senescence (Breeze *et al.*, 2011; Bresson *et al.*, 2018). Large number of genes encoding proteins that drive breakdown of cellular components, including short-chain alcohol dehydrogenase SAG13, and cysteine protease SAG12, are up-regulated during leaf senescence (Weaver *et al.*, 1997; Buchanan-Wollaston *et al.*, 2003; Lin and Wu, 2004; Zentgraf *et al.*, 2004; Watanabe *et al.*, 2013; Woo *et al.*, 2013; Kim *et al.*, 2016). It is well established that SAG12 gene is up-regulated only late in senescence, in yellowing tissues (Swartzberg *et al.*, 2006), and that it is one of the few genes from the group which is specifically induced by developmental senescence. The expression of SAG13 is triggered early in senescence, prior to the onset of visible aging symptoms and its levels then increase with the progression of senescence. Its expression is enhanced by various senescence-inducing stress-treatments, such as detachment, hormonal treatment, darkness, drought, wounding, and pathogen attack. In contrast, SAG12 only rarely responds to these treatments. Therefore, it is proposed that SAG12 could be the best marker for age-related developmental-senescence and SAG13 for stress-induced senescence or general cell-death (Schippers *et al.*, 2007).

In *Arabidopsis*, the rate of senescence in different rosette leaves and in different cells within the same leaf is not synchronous. Therefore, the dark-treatment method has been widely used for inducing and synchronizing the senescence processes in leaves. Weaver and colleagues (1998) showed already two decades ago that several SAGs were differentially expressed after stress treatments, including darkness.

4.1 Actin filament role in mediating cell death

The actin cytoskeleton is a major target and effector of signaling cascades in both animal and plant cells. Several findings have shown that alterations in the cytoskeleton polymerization status are critical for triggering PCD in plants (Smertenko *et al.*, 2003; Thomas *et al.*, 2006; Breeze *et al.*, 2011; Keech, 2011; Smertenko and Franklin-Tong, 2011; Chang *et al.*, 2015). First evidences that actin dynamics is regulating PCD were obtained by investigating self-incompatible (SI) *Papaver rhoeas* pollens. In incompatible field poppy pollen, SI triggers a calcium-signaling cascade which leads to growth inhibition, AF depolymerization, and PCD. Using actin-stabilizing and depolymerizing drugs (jasplakinolide and latrunculin B, respectively), it was shown that changes in AF dynamics are sufficient to induce PCD in SI pollen evidenced by the activation of a caspase-like enzyme upstream of DNA fragmentation (Thomas *et al.*, 2006).

The integrity of AFs and the cytosolic Ca²⁺ reservoir play important roles also in stress-induced PCD signaling in plants. It has been shown that the actin related protein 2 (Arp2) acts as a regulator of cytosolic Ca²⁺ in response to salt stress in *Arabidopsis*. Plants lacking Arp2 or other proteins of the conserved ARP2/3 complex have disordered organization of AF bundles, exhibit salt-induced increases in cytosolic Ca²⁺ level, decreased movement of mitochondria, and hypersensitivity to salt. Mitochondria-related changes in *arp2* mutant are associated with salt-induced cell death. The results indicate that the AF organization regulates mitochondria-dependent Ca²⁺ signaling in response to salt stress. Because mitochondria move along AFs and function as Ca²⁺ stores in plant cells, any stress changing these events can induce mitochondria-mediated PCD processes in plant cells (Zhao *et al.*, 2013).

The contribution of actin cytoskeleton to senescence was shown indirectly by analyzing transcriptomic profiles of *Arabidopsis* leaves undergoing developmental senescence. It was found that the AFs, their myosin motors and the villin/profilin ABPs appeared to be more stable (upregulated) than the components of the tubulin cytoskeleton in senescing leaves. Therefore, the author proposed that the functions of actin cytoskeleton could be more important than those of MT cytoskeleton during leaf senescence (Keech, 2011).

4.2 Leaf senescence and auxin

Phytohormones play key roles in senescence processes. Senescence is accelerated by the hormones ethylene, abscisic acid (ABA), and jasmonic acid (JA) that mediate plant responses to biotic and abiotic stresses (Kim *et al.*, 2011). Auxin's involvement in senescence has been observed over two decades (Noodén and Noodén, 1985; Lim *et al.*, 2010; Kim *et al.*, 2011; Ren and Gray, 2015; Cha *et al.*, 2016), but its role in leaf senescence has remained unclear due to controversial results reporting either negative or positive effect of auxin (Lim *et al.*, 2010; Kim *et al.*, 2011; Hou *et al.*, 2013; Ren and Gray, 2015; Cha *et al.*, 2016). From one hand, exogenous application of auxin, mutations in auxin response factor genes (*ARF1* and *ARF2*) (Lim *et al.*, 2010), and over-expression of flavin monooxygenase coding *YUCCA6* gene (Kim *et al.*, 2011) delay chlorophyll loss and down-regulate or retard the expression of *SAG12* gene. These findings suggest that auxin could be a negative regulator of leaf senescence. On the other hand, it has been

shown that in senescing leaves of *Arabidopsis*, the concentration of free IAA is twice as high as in non-senescing leaves (Quirino *et al.*, 1999) and transcription of many genes involved in auxin biosynthesis (tryptophane synthase *TSA1* and nitrilases (*NIT1–NIT4*)) are up-regulated (Quirino *et al.*, 1999; van der Graaff *et al.*, 2006). These results suggest that auxin has a senescence-promoting effect. Recent advances in this field show that overexpression of small auxin up RNA gene *SAUR36* promotes leaf senescence in *Arabidopsis*, indicating that auxin acts indeed as positive regulator of leaf senescence (Hou *et al.*, 2013).

4.2.1 Anthocyanins, auxin signaling, stress-response and senescence

Anthocyanins, a group of pink, red, purple or blue pigments, are naturally occurring secondary metabolites in plants that belong to flavonoids. Anthocyanins are present in many tissues such as leaves, stems, roots, tubers, fruits, and seeds (Williams and Grayer, 2004). Accumulation of anthocyanins in tissues has been related to auxin signaling, stress responses (Solfanelli *et al.*, 2006) and senescence processes (Brown *et al.*, 2001; Feild *et al.*, 2001; Buer and Muday, 2004; Besseau *et al.*, 2007; Schippers *et al.*, 2007; Falcone Ferreyra *et al.*, 2012). In *Arabidopsis*, anthocyanins accumulate in variable amounts in leaves and stems in light and nutrition-dependent manner (Holton and Cornish, 1995; Gou *et al.*, 2011), and have been shown to be potentially protective agents against photo-oxidative damage (Havaux and Kloppstech, 2001).

Numerous investigations point to the auxin's role in modulating flavonoid biosynthesis, whereas flavonoids, in turn, are considered to be endogenous regulators of auxin efflux carriers, suggesting a mutual crosstalk between these processes (Murphy *et al.*, 2000; Brown *et al.*, 2001; Buer and Muday, 2004; Peer *et al.*, 2004; Besseau *et al.*, 2007; Peer and Murphy, 2007; Santelia *et al.*, 2008; Zažímalová *et al.*, 2010; Lewis *et al.*, 2011; Kuhn *et al.*, 2016). In particular, auxin transport is elevated in inflorescences, hypocotyls, and roots of plants of the flavonoids-deficient mutants (Murphy *et al.*, 2000; Brown *et al.*, 2001; Lewis *et al.*, 2011).

Anthocyanin accumulation in *Arabidopsis* is also an easily visible marker of plant response to stress conditions. Environmental stresses such as nutrient (nitrogen and/or phosphorus) deficiency, wounding, pathogen attack, JA treatment, drought, and various light conditions (UV, visible, and far-red radiation) have all been associated with anthocyanin accumulation in various tissues (Diaz *et al.*, 2006; Misiyura *et al.*, 2013). Accumulation of anthocyanins and acceleration of senescence are also well documented under certain stress conditions including reduced nitrogen levels and high light intensity. During senescence, anthocyanins reduce the risk of photo-oxidative damage in leaf cells and thereby may help to retrieve nutrients from senescing tissues (Feild *et al.*, 2001; Peng *et al.*, 2008; Misyura *et al.*, 2013).

5 AIMS OF THE STUDY

Over the previous decades several kinds of evidence suggested that myosins are present in plant cells. The sequencing of the first plant genome, *Arabidopsis*, revealed a number of myosin genes. However, a systematic analysis of myosin functions in plants was missing. Thus, the aims of the current study were:

- to reveal the roles of individual *Arabidopsis* myosins in plant development by characterizing the phenotypes of T-DNA insertional mutants;
- to study the highly redundant roles of class XI myosins by establishing double and triple mutant lines, and to characterize major developmental disorders of these mutant lines;
- to determine whether important developmental processes such as auxin- and senescence-associated responses are mediated by actomyosin cytoskeleton in plant cells by using the development of inflorescences and leaves of myosin XI triple mutant plants as the model systems.

6 MATERIALS AND METHODS

The following experimental methods described in the indicated publications were used during this study:

- Northern blot analysis of *XI-K* transcripts (publication I)
- Trichome isolation, imaging and measurements (publications I, II)
- Double and triple mutant generation (crossings); DR5::GUS, IAA2::GUS and PIN1::PIN1-GFP crossing into *xi-1/xi-2/xi-k* background; homozygous plant selection (publications II, III)
- Phenotyping: measuring sizes of plant organs and circularity of pavement cells (publication II)
- SEM imaging of floral organs (publications II, III)
- Alexander's staining of anthers (publication II)
- Aniline blue staining of pollen tubes *in vivo* (publication II)
- Quantitative GUS assays of plant extracts and histochemical GUS assay of intact plant tissues (publication III)
- Confocal imaging of fluorescent proteins in plant tissues (publications II, III)
- Measurement of anthocyanin accumulation (publication III)
- RNA isolation and reverse transcription polymerase chain reaction (RT-PCR) analysis (publications II, III)
- Polymerase chain reaction (PCR) (publications I, II, III)

7 RESULTS AND DISCUSSION

7.1 Downregulation of myosin XI-K affects epidermal cell growth in *Arabidopsis* (publication I)

The existence of multiple myosin genes in fully sequenced *Arabidopsis* genome was originally confirmed by phylogenetic analysis performed by Reddy and Day in 2001, but the systematic analysis of mutants was not available at that time. Thus, our first aim was to systematically characterize the possible phenotypes of T-DNA insertional mutants of all 17 *Arabidopsis* myosins. According to our results, only the mutant lines where T-DNA was inserted into myosin *XI-K* gene showed different phenotypic features in comparison with WT Columbia plants (publication I). To genetically characterize the functions of *XI-K*, we used three different mutant lines that carried homozygous T-DNA insertions in the first intron, the fifth exon and the 29th exon of the *XI-K* gene. Mutant lines were named *xik-1*, *xik-2*, and *xik-3*, respectively (Figure 11; publication I).



Figure 11. Schematic diagram of *Arabidopsis* myosin *XI-K* gene with the positions of the T-DNA insertions. Black boxes indicate the exons and black lines introns. Positions of T-DNA insertions in mutant lines *Xik-1*, *Xik-2*, and *Xik-3* are indicated. LB, left border; RB, right border of T-DNA (publication I).

RT-PCR based analysis showed that *XI-K* is expressed throughout the development of *Arabidopsis* plants – in seedlings, roots, leaves, stems, flowers, and siliques. The presence of *XI-K* transcripts in mutant lines was analyzed by both RT-PCR and Northern blotting. With RT-PCR, using amplification of regions upstream and downstream of T-DNA insertion sites, we were able to detect the *XI-K* transcripts in mutant seedlings (data not shown). However, the Northern blot analysis revealed the *XI-K* transcripts in WT plants only, but not in any of *xik* mutant lines (publication I). Thus, we concluded that the phenotypic changes of *xik* mutant lines (described below) were due to insufficient amount of functional *XI-K* gene product. Several years later, using more accurate RT-qPCR method, the significantly decreased expression levels of *XI-K* gene in single mutants, *xik-1* and *xik-2*, were confirmed by our group (Talts *et al.*, 2016).

7.1.1 Myosin XI-K contributes to tip growth of root hairs (publication I)

Phenotypic analysis of *xik* mutant lines revealed that downregulation of *XI-K* in all three mutant lines affected the growth of specialized epidermal cells – root hairs and trichomes. Elongation of the root hairs of seedlings grown on sugar-free medium was reduced up to 50% in *xik-1* and *xik-2* lines, and up to 23% in *xik-3* line, when compared

to WT plants. This indicated that mutations located in the beginning of the gene sequence influence the phenotype, more than those at end of the gene. The average growth rate of root hairs, measured in *xik-2* line, was approximately 30% slower in comparison with WT cells. Our results, both the decreased length and the slower growth rate of mutant root hairs, supported the notion that myosin XI-K contributes to the root hair development *via* tip growth (publication I). This was later confirmed by the observation that full length and functional XI-K fused to YFP (XI-K:YFP) exhibits enriched localization in the tip area of root hairs where it associates with vesicles moving along the longitudinal AF bundles (Peremyslov *et al.*, 2012).

Interestingly, when grown in the medium supplemented with 1% of sucrose or glucose, the root hairs of all three mutant lines remained shorter than those of WT, and also exhibited a significantly curled phenotype (publication I). In contrast, root hairs of *xik* mutant seedlings grown in sucrose-free medium were straight. Since sugars, at low concentrations, act as growth promoters, the curled phenotype of *xik* mutant root hairs could be caused by unbalanced transport of plasma membrane and/or cell wall components. The misdistribution of plasma membrane or cell wall components in actively growing mutant cells may indeed affect growth direction (publication I). This hypothesis was supported by the recent work of Zhang and colleagues who showed that class XI myosins are involved in exocytosis of cellulose synthase complexes in etiolated hypocotyl epidermal cells of *Arabidopsis* seedlings (2018).

7.1.2 Myosin XI-K contributes to diffuse growth of trichomes (publication I)

Since the root hairs represent only one type of plant hairs, the hairs of aerial organs, trichomes on stems and leaves, were also examined in *xik* mutant plants. The difference between WT and *xik* mutant trichomes was evident in shape and size. Most striking was the changed shape of mutant trichomes, whereas the number of trichomes per leaf did not differ from that of the WT (publication I). In WT, leaf trichomes normally consist of three to four branches of equal length symmetrically arranged on the top of the stalk. In *xik* mutants, the equal length and symmetrical arrangement of trichomes branches was affected: up to 60% of mutant leaf trichomes exhibited bent shape, abnormally decreased branch length, and/or expanded interbranch zone. The proportion of trichomes with abnormally shorter branches was doubled in mutant lines (publication I).

It is well known that actin cytoskeleton is essential for normal trichome morphogenesis. Interestingly, the phenotype of *xik* trichomes was somewhat similar to the trichomes described in *distorted* mutants, albeit the phenotype of *xik* trichomes was much weaker. Despite the weak phenotypic correlation between *distorted* and *xik* mutants, it was tempting to speculate that myosin XI-K may contribute to AF regulation (publication I). This assumption turned out to be correct as it was confirmed first by Ueda and colleagues (2010) three years later, who showed that inactivation of XI-K affected the ER movement, formation of thick ER strands, and formation of AF bundle-dependent transvacuolar cytoplasmic strands.

During early trichome development (stages 1 and 2), actin is organized into short and fine filaments that form thicker bundles as the trichome matures (at stage 3). After completion of the branch initiation a rapid expansion of the branches begins (stages 4 and 5), and AFs form thick bundles parallel to the long axis of elongating branches. Near the branch tip, fine, transversely aligned AFs are present (Mathur *et al.*, 1999; Tian *et al.*, 2015), suggesting similar situation as in tip growing cells. The trichome phenotype

of *xik* mutants indicated that myosin XI-K is particularly important for the normal elongation of trichome branches (publication I).

7.2 Simultaneous elimination of myosins XI-1, XI-2, and XI-K affects both cell size and organ growth in *Arabidopsis* (publication II)

At this stage, the data about the functionality of individual myosins was still limited, since only three publications had demonstrated the role of single class XI myosins in plants: XI-K and XI-2 in the growth of *Arabidopsis* root hairs and trichomes (I publication; Peremyslov *et al.*, 2008), and XI-B in the development of rice pollen (Jiang *et al.*, 2007).

According to phylogenetic analysis, *Arabidopsis* myosins XI-K and XI-2 belong to two paralogous groups, XI-1/XI-K and XI-2/XI-B, suggesting that their functions might be overlapping or redundant (Reddy and Day, 2001). To reveal the redundant roles of paralogous myosins XI-K and XI-1 and non-paralogous myosin XI-2, we generated and characterized double and triple mutant lines *xi-1/xi-2*, *xi-1/xi-k*, *xi-2/xi-k*, and *xi-1/xi-2/xi-k* (3KO) (publication II). T-DNA insertion sites for single mutant lines which were used for obtaining double and triple mutant lines are shown in **Figure 12** (publication II).

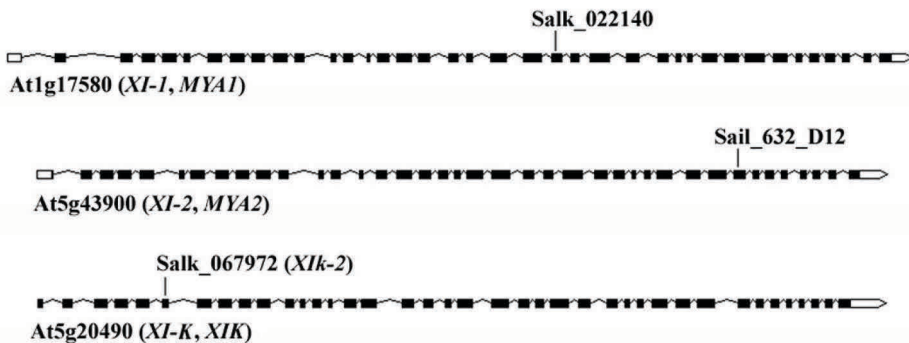


Figure 12. A schematic diagram of *Arabidopsis* myosin XI-1, XI-2, and XI-K genes with the positions of the T-DNA insertions. Black boxes represent exons, black lines introns, and empty boxes represent 5' and 3' untranslated regions, respectively (publication II).

To confirm that the T-DNA was indeed inserted solely into single myosin loci, the homozygous single mutant lines used for this work were checked using adapter ligation-mediated PCR method (O'Malley *et al.*, 2007) (K. Talts and K. Tanner, unpublished data).

Phenotypic characterization of these mutant lines showed that the growth and architecture of myosin XI single, double, triple knock-out plants was decreased progressively along with the reduction in cell size (publications I and II):

- *xi-1* - no phenotype
- *xi-2* - short root hairs
- *xi-k* - short root hairs, mildly distorted trichomes with shorter branches
- *xi-1/xi-2* - comparable to *xi-2* (short root hairs)
- *xi-1/xi-k* - comparable to *xi-k* (short root hairs, mildly distorted trichomes)

- *xi-2/xi-k* - root hair and trichome phenotype of single mutants was augmented; size of rosette leaves and flowers, as well as height of inflorescence shoots was affected

- *xi-1/xi-2/xi-k* (3KO) - root hair, trichome, and rosette leaf phenotype of *xi-2/xi-k* line was augmented; bolting time, flower development, and fertility (silique size) were affected.

Prior to our study, double mutant analysis of paralogous myosins XI-K/XI-1 and XI-2/XI-B was performed by Prokhnevsky and colleagues (2008). Their results indicated that the myosins XI-K, XI-2, and XI-B, but not XI-1, exhibited overlapping and additive roles in the root hair elongation. Moreover, using triple and quadruple mutants, they demonstrated redundant roles of myosins XI-1, XI-2, XI-K, XI-B, and XI-I in determining the rosette size, shoot height and fertility (Peremyslov *et al.*, 2010). Our results were consistent with these data since similar developmental defects were observed in the double mutant and 3KO plants (publication II). Moreover, we showed that myosin XI-K together with XI-2 and XI-1 significantly contributes to the growth of trichome branches and lobe formation of pavement cells (publication II). We also found that decreased elongation of stigmatic papillae was partially responsible for the reproduction defects in 3KO plants (publication II).

7.2.1 Simultaneous elimination of myosins XI-1, XI-2, and XI-K affects the growth of leaf epidermal cells to various extents (publication II)

Since the growth of *xi-2/xi-k* and 3KO rosettes was decreased in comparison with WT plants, it was investigated further. First, our measurements showed that the petiole elongation of *xi-2/xi-k* (76% of WT) and 3KO (60% of WT) plants was affected more than the elongation of leaf blades (79% of WT for 3KO). Epidermal cell size measurement revealed that both *xi-2/xi-k* and 3KO leaves had smaller (17% and 35%, respectively) pavement cells than WT. At the same time, pavement cells of 3KO leaves were significantly less lobed (i. e. more round) (publication II). According to phenotype analysis, it seemed that the growth of elongated (or tubular-shaped) cells was more affected than the growth of other cell types in 3KO background. Therefore, 3KO rosettes looked very small. Most probably, this was due to cell shape differences between these two tissues – tube shaped cells of the petiole versus pavement cells of the leaf blade. This suggests that at a certain developmental stage, the growth spurt of tubular-shaped cells is fast and intense, and demanding more cellular resources, such as myosin XI mediated vesicular transport. Consistent with this, the largest effect on AF organization and vesicle distribution was observed in leaf midvein epidermal cells (also tubular-shaped cells) of 3KO plants (Premyslov *et al.*, 2010; publication III).

In addition, the trichome phenotype of the *xik* single mutant was significantly enhanced both in *xi-2/xi-k* and in 3KO background – the length and growth direction of trichome branches was markedly affected, whereas the branch number was not altered (publication II). The average branch length of *xi-2/xi-k* and 3KO plants was 70% and 40% of WT, respectively. Also, trichomes of *xi-1/xi-k*, *xi-2/xi-k* and 3KO plants exhibited abnormally elongated stalks. In WT, the stalk height constitutes approximately half of the branch length, whereas in *xi-2/xi-k* and 3KO the height of trichome stalk constitutes 70% and 90% of the branch length, respectively. In the case of 3KO, the length of trichome stalks was equal (or slightly longer) to the branch length. SEM analysis revealed that in *xi-2/xi-k* and 3KO mutants, the irregular trichome phenotype became apparent by late

stage 5 of trichome development, indicating that class XI myosins are required for the rapid elongation of trichome branches (publication II).

The comparison of *xi-2/xi-k* and 3KO plants with those of *distorted* group mutants revealed an apparent similarity in the trichome phenotype of the 3KO with *pirogi* and *xi-2/xi-k* with *spirrig* plants. Nevertheless, the overall phenotype severity of *xi-2/xi-k* and 3KO plants was weaker than that of *distorted* mutants. For example, gaps between adjacent cells in cotyledons and hypocotyls, typical for *distorted* mutants, were not apparent in myosin mutants. On the other hand, the abnormal elongation of trichome stalks (typical for *xi-2/xi-k* and 3KO trichomes) has not been reported for *distorted* mutants. The lobe formation of pavement cells and branch elongation of trichomes are known to depend on the AF organization and dynamics. The phenotypic similarity between myosin mutants and *distorted* mutants suggests AF defects in these mutants. Indeed, AF defects in myosin mutants has been proven to be true by several authors (Peremyslov *et al.*, 2010; Uead *et al.*, 2010; Cai *et al.*, 2014; publication III; E.-L. Ojangu, unpublished data, **Figure 13**).

Hülkamp and colleagues found that mutants with smaller trichomes may contain less DNA, whereas mutants with increased cell size were found to have higher DNA content (1999). We therefore tested whether the decreased size of trichomes in myosin mutants might be related to the reduced ploidy level. Although we did not detect differences in ploidy level, the trichome nuclei had a markedly elongated shape in *xi-2/xi-k* and 3KO mutants. Trichomes of all single mutants and double mutants *xi-1/xi-2* and *xi-1/xi-k* had spherically shaped nuclei, similar to WT. Quantification of sphericity revealed that nuclei of WT trichomes had the most circular shape while *xi-2/xi-k* and 3KO trichome nuclei had significantly elongated shape (publication II).

The role of AFs in movement of nuclei has been investigated (Ketelaar *et al.*, 2002; Higa *et al.*, 2014), but not their role in determining shape of nuclei. In fully developed epidermal cells, nuclei are associated with (or pulled by) longitudinal AF bundles running throughout the cell (Higa *et al.*, 2014). Since AF organization in epidermal cells of both *xi-2/xi-k* and 3KO plants is significantly affected, a clear correlation between nuclear shape and AF orientation can be drawn. **Figure 13** illustrates AF organization in WT Columbia (Col) and 3KO trichomes (E.-L. Ojangu, unpublished data).

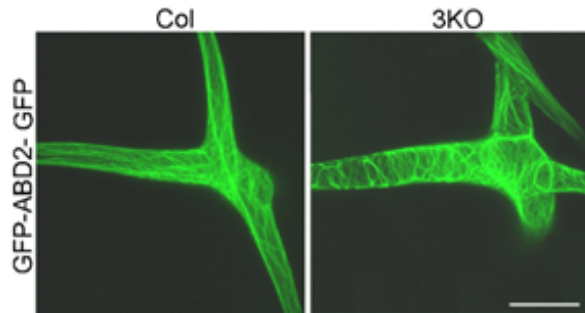


Figure 13. AF organization in trichomes of WT Columbia (Col) and 3KO plants. AFs are visualized with actin tracer GFP-ABD2-GFP. In Col, AF bundles are oriented in parallel to the long axis of the branches. The 3KO trichome displays perpendicular orientation of AF bundles. Scale bar is 50 μ m. (E.-L. Ojangu, unpublished data).

It is possible that misoriented AFs in *xi-2/xi-k* and 3KO trichomes physically stretch the nucleus thereby decreasing its sphericity. Interestingly, the roles of AFs and myosin XI-I in shaping the nucleus and mediating its relocation (through binding nuclear envelope protein WIT2) have been described (Tamura *et al.*, 2013; Zhou *et al.*, 2015). Moreover, the most recent data show that mCherry-tagged myosin XI-K (XI-K:mCherry) in *Arabidopsis* localizes both along thick cortical arrays (corresponding to AF bundles) and in thinner arrays surrounding the nucleus, as well as inside the nucleus (Kurth *et al.*, 2017).

Taken together, the phenotypic comparison of single, double and 3KO mutant plants indicates that myosins XI-1, XI-2 and XI-K have redundant functions in the polarized and diffuse growth of epidermal cells in *Arabidopsis*. Myosin XI-K has a leading role and XI-1 and XI-2 have minor roles in growth of plant cells, and myosin XI-2 contributes to the cell elongation more than XI-1 (publication II). Therefore, we conclude that among class XI myosins, XI-K is a key player regulating cell growth and plant development in *Arabidopsis*.

7.2.2 Simultaneous elimination of myosins XI-1, XI-2, and XI-K affects the reproduction of myosin 3KO plants (publication II)

To assess the fertility of mutant lines, the number and length of the siliques per plant were measured and the number of seeds per silique was counted. Fertility of single and double mutant lines was comparable to WT and was therefore not further investigated. In 3KO plants, we found that after onset of flowering, up to 60% of siliques emerging on the primary shoot remained mostly seedless. SEM analysis revealed that these 3KO siliques contained mostly unfertilized ovules. About three weeks after bolting, there was a “switch” and plants started to produce siliques only slightly underdeveloped or normal in size. Such siliques comprised up to 28% of unfertilized ovules. Interestingly, the variations in silique size were readily apparent on primary shoots and less obvious on axillary shoots of 3KO plants (publication II).

Since the reproduction defect in 3KO was manifested as unfertilized ovules, and not embryo abortion, we decided to evaluate the fertilization process in this mutant. For self-fertilization to occur, anthers should reach to the stigma for proper pollination, meaning that successful reproduction in *Arabidopsis* depends on interactions between

pollen grains and stigmatic papillae (Edlund *et al.*, 2004). First, anthers were examined to identify whether the decreased fertility of triple mutant was caused by defects in male reproductive organs. Surprisingly, neither pollen viability nor the pollen tube growth were affected in 3KO plants (publication II). Next, reciprocal crosses were performed to further test the role of male (anthers, pollens) and female (pistil) organs in fertilization in 3KO plants. Aniline blue staining of pollen tubes in cross-pollinated pistils confirmed that 3KO pollens were able to attach to WT stigmas and thus form pollen tubes *in vivo*. In contrast, 3KO pistils being pollinated with WT pollen developed very heterogeneously. We observed that the WT pollen attachment to the surface of 3KO pistils was frequently disturbed since only few pollen tubes were initiated. A similar phenotype was observable both in 3KO pistils cross-pollinated with WT as well as in self-pollinated 3KO pistils. Thus, reciprocal crosses revealed that the reduced fertility of 3KO mutant is female reproductive tract specific, implying defective stigma development (publication II).

The stigma is an epidermal structure composed of tubular-shaped elongated cells, papillae. In mature pistils, stigmatic papillae are properly extended being receptive to the recognition, attachment and germination of pollen grains (Alvarez-Buyilla *et al.*, 2010). For SEM analysis of stigmas, pistils were dissected from floral buds just before opening (stage 12) and from freshly opened flowers (stage 13 or 14) because WT pistils at these developmental stages are mature and receptive to pollination. Comparison of 3KO and WT stigmas revealed that the elongation of papillae of 3KO pistils at developmental stage 12 was often reduced, being comparable with WT stigmas at developmental stage 10 or 11. At stage 13 and 14 of flower development, the growth of 3KO stigmas varied from normal to stunted. We noticed that in some cases the development of entire gynoecia remained perturbed until late stages of 3KO flower development (publication II).

It has been shown that immature stigmas are less receptive to pollen grains in *Arabidopsis* (Kandadsamy *et al.*, 1994). Our results also indicated that insufficient development/maturation of stigmatic papillae prevents successful pollination and is therefore the main reason for the reduced fertility of 3KO plants (publication II). We suggest that the class XI myosins in the stigmatic papillae may fulfill a similar role as in other tubular-shaped tip-growing cells. Few years later, we showed that the pre-anthesis elongation of anther filaments of 3KO plants is also delayed. This means that during anthesis, the 3KO anthers do not reach to the stigma in time, and thus pollens are poorly delivered from the anthers to the stigma (publication III). We conclude that myosins XI-1, XI-2 and XI-K together are needed for normal development of floral organs.

7.3 Myosins XI-K, XI-2 and XI-1 contribute to auxin responses in *Arabidopsis* (publication III)

Flower development of 3KO plants was used as a model system for examining myosin-dependent auxin-responsive processes in *Arabidopsis*. When investigating the overall morphology of 3KO plants, we observed that the inflorescence shoots frequently displayed partially reduced apical dominance and increased formation of axillary branches. Inflorescence development can be evaluated by four traits: bolting time, length of the reproductive phase, number of rosette leaves at bolting, number of axillary branches and fruits (Ungerer *et al.*, 2002; Pouteau and Albertini, 2009). In myosin 3KO

plants, all these traits are affected: bolting time is delayed, reproductive phase is expanded, more rosette leaves are formed, the shoot branching architecture is changed, and silique size is decreased. The initiation and outgrowth of axillary meristem during inflorescence shoot development is mainly regulated by phytohormones auxin, cytokinin, and strigolactone (Domagalska and Leyser, 2011). In WT *Arabidopsis* plants, the auxin flow from shoot apex toward the base suppresses axillary meristem outgrowth, and leads to apical dominance, thus controlling the axillary branch formation (Davies *et al.*, 1966; Wang *et al.*, 2014). Well-regulated local auxin gradients in axillary shoot meristems are created by auxin importers together with PIN1 exporter (Bainbridge *et al.*, 2008).

To determine if the developmental defects of 3KO plants are auxin-dependent, we used the auxin-responsive promoter-reporters DR5::GUS and IAA2::GUS, widely used markers for studying endogenous auxin responses (Ulmasov *et al.*, 1997; Shibasaki *et al.*, 2009; Rusak *et al.*, 2010). We found that the auxin responsiveness was significantly reduced in seedlings and inflorescence stems of 3KO plants stably expressing DR5::GUS. Histochemical analysis of IAA2::GUS in flowers revealed reduced GUS staining in 3KO gynoecia – in stigma, style and the transmitting tract. We also analyzed the effect of a PAT inhibitor, NPA, on IAA2::GUS expression and found that 3KO pistils exhibited partial insensitivity to NPA. NPA treatment is also known to affect the organization of AFs and extent of actin bundling (Zhu *et al.*, 2016). We therefore propose that the partial NPA-resistance of 3KO pistils can be caused by AF defects which occur in 3KO cells already prior to NPA treatment. Thus, our results show that simultaneous inactivation of three highly expressed class XI myosins indeed reduces the auxin responses of different *Arabidopsis* tissues (publication III).

As the aberrant shoot development in 3KO plants correlated with the reduced auxin responses, we investigated if this was due to misdistribution of auxin efflux carrier PIN1, since it plays an essential role in flower and inflorescence formation (Okada *et al.*, 1991; Gälweiler *et al.*, 1998; Benková *et al.*, 2003; Adamowski and Friml, 2015). Towards this end, the effect of stable expression of PIN1::PIN1-GFP in 3KO and Columbia plants was examined. Surprisingly, we found that the previously described semi-sterile phenotype of 3KO plants (publication II) was exacerbated in the 3KO PIN1-GFP line (publication III). The development of flowers as well as architecture of inflorescences was significantly affected in 3KO PIN1-GFP line – some flowers showed completely arrested development and others exhibited a range of morphologies, from nearly normal to severely deformed. Undeveloped flowers did not contain inner whorl organs (pistils, petals or anthers), and consisted often of one to three sepals only. However, the most prevalent flower deformation in 3KO PIN1-GFP background was related to gynoecium development: significantly bent shape, delayed apical closure (stigma development) and abnormal valve and style growth. Similar gynoecium phenotypes have been described upon genetic or pharmacological disruption of auxin signaling (Sessions *et al.*, 1997; Nemhauser *et al.*, 2000; Cheng *et al.*, 2006; Zúñiga-Mayo *et al.*, 2014). It is well established that the finely tuned auxin gradient is necessary for gynoecium patterning in general and style and stigma development in particular (Nemhauser *et al.*, 2000). Thus, flower development defects of 3KO PIN1-GFP plants provide genetic evidence that even modest overexpression of PIN1 under native promoter may perturb auxin responses, and thus affect developmental decisions, when the actomyosin cytoskeleton is simultaneously affected. To further validate this notion, the PIN1-GFP expression was examined throughout flower development. The PIN1-GFP distribution in flower tissues of Columbia

plants was visible in septum or valve margins of pistils, as well as in floral primordia. The overall pattern of the PIN1-GFP expression during late stages (9-13) of flower development in 3KO plants was broadly the same with some exceptions – in heavily deformed pistils (valveless gynoecia with enlarged style), the PIN1-GFP signal was spread all over the gynoecium. Next, we examined PIN1-GFP polarization in epidermal cells of developing gynoecia since significant deformation of gynoecium was the most prominent phenotype of the 3KO PIN1::PIN1-GFP line. In epidermal cells of WT Columbia gynoecia (at stage 8), the PIN1-GFP exhibited prominently polar localization at apical membranes, whereas epidermal cells of 3KO gynoecia had a nonpolar distribution of PIN1-GFP both in apical and lateral membranes. Quantitative analysis showed that only 14% of 3KO cells exhibit highly polarized PIN1 distribution, whilst the frequency of polarized localization in Columbia was 39%. The gynoecium is the last organ to initiate from the floral meristem, and style and stigma are the last structures to emerge during gynoecium development (Larsson *et al.*, 2014). The partial loss of PIN1 polarization in epidermal cells of 3KO PIN1-GFP developing gynoecia indicates that the apical domains of the mutant gynoecia may not be sufficiently supplied with auxin and therefore the normal development of valves, style and stigma is affected. However, the PIN1 polarization defects are most probably present already at very early stages of floral primordium development as indicated by vast (and more severe) defects in flowers and inflorescences of 3KO PIN1-GFP plants. Collectively, these results imply that class XI myosins contribute to the localization of PIN1 during floral development at least partially.

One of the mechanisms by which auxin alters cellular responses is transcriptional regulation (Paponov *et al.*, 2008). To ascertain whether elimination of multiple class XI myosins or stable expression of PIN1::PIN1-GFP affect the regulation of the auxin-responsive genes, we measured the relative expression levels of the selected mRNAs in different tissues of WT Columbia, 3KO, 3KO PIN1-GFP, and Col PIN1-GFP plants. We found that auxin-responsive genes *AUX1*, *PIN1*, *PIN7*, *IAA2* were downregulated approximately twofold in 3KO parental line, in comparison with WT.

Since the PIN1 is the principal member of the PIN-family, even modest overexpression of PIN1 under native promoter may affect developmental processes (D. van Damme, personal communication). The RT-qPCR analysis showed that both in Col PIN1-GFP and 3KO PIN1-GFP plants, the *PIN1* expression was increased by 1.5- to 2-fold, in comparison with WT. As expected, the stable expression of PIN1::PIN1-GFP affected also the expression of the auxin-responsive genes both in 3KO and Columbia background, in comparison with parental lines. However, the down-regulation of two auxin-responsive genes, *IAA2* and *PIN7*, in 3KO PIN1-GFP was significantly higher than in Col PIN1-GFP plants. Our results indicate that both the down-regulation (in 3KO) as well as up-regulation (in 3KO PIN1-GFP) of *PIN1* affects auxin responses, and thus plant development, in a negative manner. At the same time, the up-regulation of *PIN1* in 3KO PIN1-GFP line is even more critical (in comparison to parental 3KO line), since the disrupted actomyosin cytoskeleton is unable to properly allocate an excess of PIN1, and increases developmental disorders during floral development (publication III).

Despite of class XI myosins sharing functional redundancy, it is known that myosin XI-K plays a major role in membrane trafficking, cell expansion and division, plant growth, and fertility (I, II; Peremyslov *et al.*, 2008, 2010, 2012; Avisar *et al.*, 2012; Park and Nebenführ, 2013; Abu-Abied *et al.*, 2018). To confirm the role of XI-K in flower development, we analyzed line stably expressing myosin XI-K:YFP in 3KO background (3KOR), and found that normal flower development, including the elongation of stigmas

and anther filaments, was restored. In addition, we demonstrated for the first time that the YFP-tagged myosin XI-K (XI-K:YFP) is highly expressed in floral primordia as well as in developing and mature flowers, indicating its role in floral development. Unlike PIN-GFP, the XI-K:YFP was expressed in stigmas and anther filaments at significant levels. The partial overlap in the expression patterns of XI-K:YFP and PIN1-GFP in flower primordia and pistils is consistent with their possible cooperation during flower development. Our results confirmed that myosin XI-K:YFP is functional and in addition to its roles in vegetative plant growth (Peremyslov *et al.*, 2012) and gravitropic response (Talts *et al.*, 2016), also contributes to floral development.

Our results complement recently published data demonstrating that the abnormal production of lateral and adventitious roots in 3KO plants was accompanied by changes in auxin gradient due to partial loss of PIN1 polarization in stele cells (Abu-Abied *et al.*, 2018). These authors also revealed the myosin XI-K role in cell division in both the root and shoot meristem (Abu-Abied *et al.*, 2018). Bearing that in mind, the loss of proper auxin distribution and myosin XI-K function in meristem could explain the enhanced branching of mutant roots and shoots in parental 3KO line. Although these two studies (publication III and Abu-Abied *et al.*, 2018) used different models (flowers and leaves versus roots) and different experimental approaches, both highlight the functional connection between myosin and auxin.

7.4 Myosins XI-K, XI-2 and XI-1 contribute to leaf senescence in *Arabidopsis* (publication III)

Leaf development of 3KO plants was used as a model system for examining myosin-dependent senescence-associated processes in *Arabidopsis*. Despite the delayed bolt formation and extended lifespan, described earlier (Peremyslov *et al.*, 2010; publication II), we found that the 3KO plants display premature leaf senescence. Significant yellowing of cotyledons was particularly striking in 12-day-old 3KO seedlings. Furthermore, 23-day-old rosettes of the 3KO plants produced 27% more leaves than those of Columbia (publication III). The correlation between leaf number and bolting time is well documented since late flowering plants have usually more rosette leaves (Pouteau and Albertini, 2009; Schmalenbach *et al.*, 2014). Conversely, there is a little data on the role of actin cytoskeleton in senescence and cell death of plant cells (Smertenko *et al.*, 2003; Keech *et al.*, 2010; Keech, 2011; Smertenko and Franklin-Tong, 2011).

These observations prompted us to further explore myosin's role in senescence-related processes. First, we used dark induced senescence assay of detached leaves to compare total chlorophyll content of rosette leaves (5th and 6th) of Columbia control and 3KO plants. Surprisingly, 3KO leaves exhibited significant loss of chlorophyll already before dark treatment. Second, using trypan blue staining, we found that dying cells prevailed in 3KO dark-treated leaves compared to WT Columbia leaves. Third, to monitor the cell integrity and architecture of actin arrays in abaxial epidermal cells of the fifth rosette leaf, we used stable expression of an AF tracer, GFP-ABD2- GFP. Since the cell growth and AF defects of 3KO plants are most pronounced in longest cells, such as root hairs and petiole cells (Peremyslov *et al.*, 2010), epidermal cells of leaf petioles were selected for examination. Cell integrity and organization of the AFs was examined in leaves of 21- and 28-day-old rosettes. GFP-ABD2-GFP decorated thick longitudinal cables in

epidermal cells of Columbia leaf petioles, whilst thin and prominently transverse filaments were visible in 3KO cells. Moreover, at 28 day of growth, all 3KO leaves examined, showed massive plasmolysis of petiole epidermal cells. Cell deformation defects were less pronounced in Columbia, since only 66% of petioles showed partial plasmolysis, and only 25% of petioles showed massive plasmolysis. This indicated that in 3KO plants, the cell death of older leaves was significantly progressed in comparison to WT. Taken together, observation of decreased chlorophyll content, increased trypan blue staining, and premature plasmolysis in 3KO mutant indicate that the loss of integrity of actomyosin cytoskeleton induces premature senescence and thus cell death in *Arabidopsis* leaves.

All these radical cellular changes occurring during senescence processes are mediated by changes in gene expression. A large number of genes encoding proteins that mediate degradation of cellular components are up-regulated during leaf senescence (Weaver *et al.*, 1997; Buchanan-Wollaston *et al.*, 2003; Lin and Wu, 2004; Zentgraf *et al.*, 2004b; Watanabe *et al.*, 2013; Woo *et al.*, 2013; Kim *et al.*, 2016). Among these, expression of the *SAG12* gene is specifically induced by developmental senescence, whereas expression of *SAG13* is enhanced by various senescence-inducing stresses, such as detachment, hormonal treatment, darkness, drought, wounding and pathogen attack. Therefore, it is considered that *SAG12* could be the best marker for age-related developmental senescence and *SAG13* for stress-induced senescence or general cell-death marker (Schippers *et al.*, 2007). We used RT-qPCR to analyze transcriptional activity of SAGs and found that *SAG13*, but not *SAG12*, was considerably up-regulated both in 7-day-old seedlings as well as in rosette leaves of 3KO plants when compared to WT.

We showed that the abnormal accumulation of anthocyanins in 3KO plants is in accordance with the fact that increased flavonoid production (e.g., anthocyanins) is associated with stress and senescence responses (Solfanelli *et al.*, 2006). Moreover, as the anthocyanin accumulation and *SAG13* up-regulation were detectable already in very young 3KO seedlings, we assumed that the premature leaf senescence of 3KO mutants is not typical developmental senescence but can be caused by some cellular stress such as altered membrane trafficking, AF rearrangement, or misregulation of auxin responses. We tested this possible causal link between AF defects and stress-responses (*SAG13* up-regulation), and showed that the expression level of *SAG13* in latrunculin B-treated WT seedlings increased almost twofold in comparison with untreated control. Thus, it is tempting to speculate that in 3KO cells, the loss of integrity of actomyosin cytoskeleton activates the stress-signaling pathway, and as a consequence of this premature senescence and cell death of rosette leaves is initiated. Moreover, the accumulation of anthocyanins and up-regulation of senescence-related auxin-regulated *SAUR36* gene in 3KO plants indicates a dialogue between auxin- and senescence-dependent processes.

It has been proposed that leaf senescence could be one of the major factors that mediates the compromise between photosynthetic and reproductive activity in plants. A study using inbred *Arabidopsis* lines of two different ecotypes, Cape Verde and Landsberg *erecta*, showed that leaf senescence and post-bolting longevity are under strong genetic control, and are inversely related with flowering time - earlier-flowering lines exhibited longer post-bolting duration of the rosette, compared with later-flowering ecotypes. It has been suggested that there are two different energy production strategies for the reproduction in *Arabidopsis*: early-flowering populations/ecotypes utilize photosynthates, whereas late-flowering ones recycle nutrients from old rosette

leaves (Luquez *et al.*, 2006). Studies using recombinant inbred lines revealed also that early- and later-emerging leaves of the single rosette may have different biological roles. For example, senescence of first six leaves contributes to the growth of newly emerging leaves rather than reproduction (Diaz *et al.*, 2008). These examples, described above, shed light upon the contradictory phenotype of 3KO plants exhibiting delayed bolting and expanded longevity at the whole organism level, and increased leaf number and premature foliar senescence at the organ/tissue level.

7.5 Modelling actomyosin cytoskeleton dependent processes in PAT and PCD signaling (publication III)

Our results provide genetic evidence that the integrity of actomyosin cytoskeleton contributes to the signaling of auxin- and senescence-responses, as well as secondary metabolism and gene expression related with these processes. All these processes are mutually connected as illustrated in a tentative model (Figure 14, publication III).

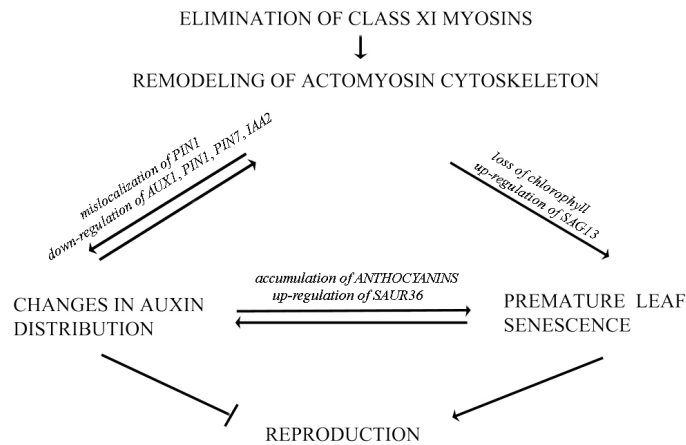


Figure 14. Hypothetical model illustrating mutual connections between actomyosin cytoskeleton, auxin transport and leaf senescence in 3KO plants. The actomyosin cytoskeleton mediated signaling of PAT involves both the distribution of auxin transporter PIN1 and regulation of the expression of auxin-responsive genes. The actomyosin cytoskeleton mediated signaling of leaf senescence involves the control of expression of early senescence-associated gene SAG13. Senescence and auxin signaling are mutually influenced by secondary metabolism and by expression of auxin-responsive SAUR36 gene. The auxin distribution and leaf senescence could affect inflorescence biomass production in opposite directions. The bidirectional arrows imply mutual influences between these processes, indicating that if one is unbalanced then the others will be affected to various degrees (modified from publication III; used with permission).

According to this, remodeling of actomyosin cytoskeleton affects not only the distribution of auxin transporters, but also the expression of auxin-responsive and senescence-associated genes. We propose that the levels of auxin-responsive genes (e.g., *AUX1*, *IAA2*, *PIN1*, *PIN7*) are influenced indirectly, through feedback signaling mechanisms, mediated by changes in auxin distribution and level. The actomyosin-mediated signaling in

leaf senescence involves the control of expression of early senescence-associated gene *SAG13*. Senescence and auxin signaling could be mutually regulated by secondary metabolites (e.g., anthocyanins) and by expression of auxin-responsive *SAUR* genes (e.g., *SAUR36*). All these processes are mutually interconnected, and if one process is unbalanced then the others are also affected. It is tempting to speculate that changes in auxin and senescence signaling influence reproduction of 3KO plants in opposite directions (**Figure 14**, publication III). On the one hand, the decreased auxin responses impair flower development; on the other hand, the premature leaf senescence could constitute a rescue mechanism for supporting the production of inflorescence biomass in conditions where flower development has been compromised.

All different phenotypes of 3KO plants described so far are assembled into a summarizing scheme (**Figure 15**).

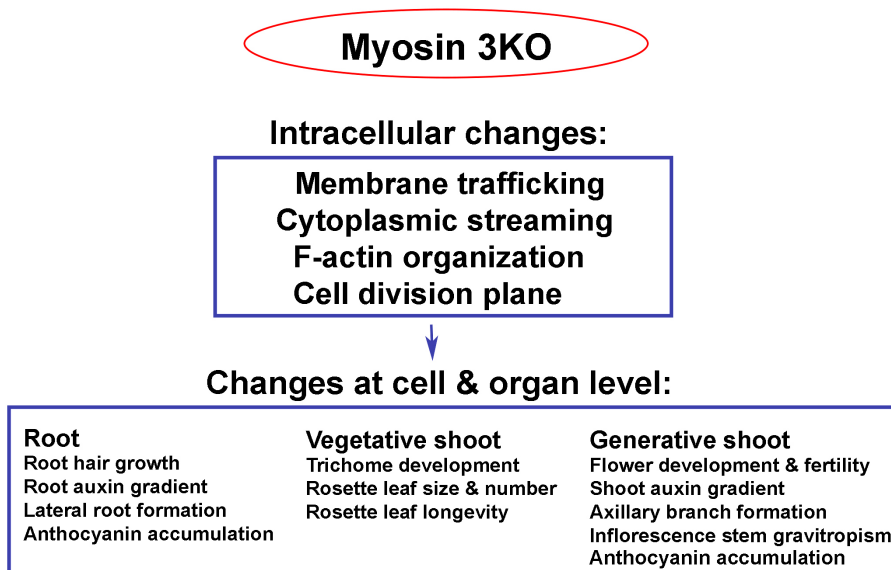


Figure 15. Phenotypic scheme for the *Arabidopsis myosin 3KO* mutant. The myosin 3KO mutant has many phenotypes as indicated with blue boxes. We propose that four main intracellular phenotypes are responsible for the downstream changes at the cellular and tissue level. Causal relationships between these phenotypes can be found, though the high variety of phenotypes emphasizes that we should view the different phenotypes as being at least partially independent.

Though all these different phenotypes of 3KO plants seem to be interrelated, it still remains elusive to know what is the cause and what is the effect in myosin 3KO plants, and the establishment of further causal relationships needs additional research. There are several questions that remain unanswered. Could it be that the changes in PAT are the basis for the secondary metabolism and/or cell death defects? Are the changes in the gene expression caused by AF defects or by auxin response defects or by something else? How is the reorganization of metabolism achieved in cells with drastically affected actomyosin cytoskeleton? What are the mechanisms by which the three class XI myosins, XI-K, XI-2, and XI-1 contribute to auxin, stress or senescence responses – through AF shaping, ER reorganization or *via* mitochondria-mediated Ca²⁺-signaling processes?

It has been interpreted that auxin transport and cell division may serve independent functions of class XI myosins. The auxin related defects seen in 3KO plants may result from reduced cytoplasmic streaming and its effect on PIN1 distribution. The cell division plane related phenotype of 3KO plants may point toward role of class XI myosins in AF guidance (Abu-Abied *et al.*, 2018). We propose that auxin transport, senescence-related processes, secondary metabolism, and signaling of the gene expression are mutually connected processes suggesting the existence of the myosin XI-dependent guidance of AFs (publication III). It is possible, that changes in actomyosin cytoskeleton of 3KO plants are converted into cellular responses *via* changes in gene expression, as indicated by conspicuously high up-regulation of stress-inducible marker gene *SAG13*.

This thesis highlights the importance of actomyosin cytoskeleton in auxin-, stress- and senescence-responses. Important aspect of future studies include the identification of myosin cargoes that affect auxin signaling and senescence. These cargoes could be formed by MyoB myosin receptors that appear to drive cytoplasmic streaming (Peremyslov *et al.*, 2013, 2015) or newly identified myosin adaptors of MadA and MadB families (Kurth *et al.*, 2017) that presumably mediate more specialized myosin-dependent processes.

CONCLUSIONS

This work, dedicated to the plant myosin family, does not reveal the exact roles of every single myosin in *Arabidopsis*, but rather offers pieces of information that should lead to understanding of the bigger picture of myosin functions in plants.

The principal findings of the present work are:

- *Arabidopsis* class XI myosin XI-K is required for normal elongation of specialized epidermal cells – root hairs and trichomes.
- Three class XI myosins, XI-1, XI-2 and XI-K, contribute together to the growth of different types of epidermal cells of vegetative (root hairs, trichomes, pavement cells) and generative (stigmatic papillae, anther filaments) tissues and organs, and thereby regulate organ size and reproduction of *Arabidopsis* plants.
- Contribution of XI-1, XI-2 and XI-K to the tissue growth is proportional to the cell size and shape – larger cells with more elongated shapes (root hairs, trichomes, petiole cells, anther filament cells, stigmatic papillae) are affected the most by the simultaneous loss of these three myosins.
- Significant expression of the XI-K:YFP in stigmatic papillae and anther filaments of developing flowers reveals an important role for XI-K in flower development.
- Myosins XI-1, XI-2 and XI-K together with actin contribute to the auxin-dependent developmental processes in *Arabidopsis* by mediating the activity of auxin-dependent promoters, polarization of major auxin efflux carrier PIN1, expression of some auxin-responsive genes, and accumulation of anthocyanins.
- Similar expression patterns of myosin XI-K:YFP and auxin efflux carrier PIN1:PIN1-GFP in *Arabidopsis* flowers suggests a functional connection between actomyosin cytoskeleton and auxin transport during floral development.
- Myosins XI-1, XI-2 and XI-K together with actin contribute to the stress-induced senescence and cell death processes in *Arabidopsis* leaves by mediating the up-regulation of stress-inducible *SAG13* expression, massive loss of chlorophyll, accumulation of anthocyanins, and increased cell death.
- Actomyosin cytoskeleton, auxin distribution and leaf senescence are mutually interconnected as suggested by elevated levels of anthocyanins and auxin-dependent senescence-associated *SAUR36* gene expression in 3KO plants.
- Since expression of *XI-K* in triple mutant plants rescues almost all phenotypic defects, the myosin XI-K is the key player in the processes described above, although myosins XI-2 and XI-1 also contribute significantly to the development of *Arabidopsis*.

REFERENCES

- Abu-Abied, M., Belausov, E., Hagay, S., Peremyslov, V., Dolja, V., Sadot, E. (2018). Myosin XI-K is involved in root organogenesis, polar auxin transport and cell division. *J. Exp. Bot.* 69, 2869–2881.
- Adamowski, M. and Friml, J. (2015). PIN-dependent auxin transport: action, regulation, and evolution. *Plant Cell* 27, 20–32.
- Aloni, R., Aloni, E., Langhans, M., Ullrich, C.I. (2006). Role of auxin in regulating *Arabidopsis* flower development. *Planta* 223, 315–328.
- Alvarez-Buylla, E.R., Benítez, M., Corvera-Poiré, A., Chaos Cador, A., de Folter, S., Gamboa de Buen, A., Garay-Arroyo, A., García-Ponce, B., Jaimes-Miranda, F., Pérez-Ruiz, R.V., Piñeyro-Nelson, A., Sánchez-Corrales, Y.E. (2010). Flower development. In: *Arabidopsis Book* 8, e0127.
- Arabidopsis Genome Initiative. (2000). Analysis of the genome sequence of the flowering plant *Arabidopsis thaliana*. *Nature* 408, 796–815.
- Avisar, D., Prokhnevsky, A.I., Makarova, K.S., Koonin, E.V., Dolja, V.V. (2008a). Myosin XI-K is required for rapid trafficking of Golgi stacks, peroxisomes, and mitochondria in leaf cells of *Nicotiana benthamiana*. *Plant Physiol.* 146, 1098–1108.
- Avisar, D., Prokhnevsky, A.I., Dolja, V.V. (2008b). Class VIII myosins are required for plasmodesmatal localization of a closterovirus Hsp70 homolog. *J. Virol.* 82, 2836–2843.
- Avisar, D., Abu-Abied, M., Belausov E., Sadot, E., Hawes, C., Sparkes, I.A. (2009). A comparative study of the involvement of 17 *Arabidopsis* myosin family members on the motility of Golgi and other organelles. *Plant Physiol.* 150, 700–709.
- Avisar, D., Abu-Abied, M., Belausov, E., Sadot, E. (2012). Myosin XIX is a major player in cytoplasm dynamics and is regulated by two amino acids in its tail. *J. Exp. Bot.* 63, 241–249.
- Bainbridge, K., Guyomarc'h, S., Bayer, E., Swarup, R., Bennett, M., Mandel, T., Kuhlemeier, C. (2008). Auxin influx carriers stabilize phyllotactic patterning. *Genes Dev.* 22, 810–823.
- Beers, E.P. and McDowell, J.M. (2001). Regulation and execution of programmed cell death in response to pathogens, stress and developmental cues. *Curr. Opin. Plant Biol.* 4, 561–567.
- Benková, E., Michniewicz, M., Sauer, M., Teichmann, T., Seifertová, D., Jürgens, G., Friml, J. (2003). Local, efflux-dependent auxin gradients as a common module for plant organ formation. *Cell* 115, 591–602.

- Bennett, M.J., Marchant, A., Green, H.G., May, S.T., Ward, S.P., Millner, P.A., Walker, A.R., Schulz, B., Feldmann, K.A. (1996). *Arabidopsis* AUX1 gene: a permease-like regulator of root gravitropism. *Science* 273, 948–950.
- Berleth, T., and Sachs, T. (2001). Plant morphogenesis: long-distance coordination and local patterning. *Curr. Opin. Plant Biol.* 4, 57–62.
- Besseau, S., Hoffmann, L., Geoffroy, P., Lapierre, C., Pollet, B., Legrand, M. (2007). Flavonoid accumulation in *Arabidopsis* repressed in lignin synthesis affects auxin transport and plant growth. *Plant Cell* 19, 148–162.
- Bettinger, B.T., Gilbert, D.M., Amberg, D.C. (2004). Actin up in the nucleus. *Nat. Rev. Mol. Cell Biol.* 5, 410–415.
- Bowman, J.L., Baum, S.F., Eshed, Y., Putterill, J., Alvarez, J. (1999). Molecular genetics of gynoecium development in *Arabidopsis*. *Curr. Top. Dev. Biol.* 45, 155–205.
- Braun, M., Buchen, B., Sievers, A. (2002). Actomyosin-mediated statolith positioning in gravisensing plant cells studied in microgravity. *J. Plant Growth Regul.* 21, 137–145.
- Breeze, E., Harrison, E., McHattie, S., Hughes, L., Hickman, R., Hill, C., Kiddle, S., Kim, Y.S., Penfold, C.A., Jenkins, D., Zhang, C., Morris, K., Jenner, C., Jackson, S., Thomas, B., Tabrett, A., Legaie, R., Moore, J.D., Wild, D.L., Ott, S., Rand, D., Beynon, J., Denby, K., Mead, A., Buchanan-Wollaston, V. (2011). High-resolution temporal profiling of transcripts during *Arabidopsis* leaf senescence reveals a distinct chronology of processes and regulation. *Plant Cell* 23, 873–894.
- Bresson, J., Bieker, S., Riestler, L., Doll, J., Zentgraf, U. (2018). A guideline for leaf senescence analyses: from quantification to physiological and molecular investigations. *J. Exp. Bot.* 69, 769–786.
- Brown, D.E., Rashotte, A.M., Murphy, A.S., Normanly, J., Tague, B.W., Peer, W.A., Taiz, L., Muday, G.K. (2001). Flavonoids act as negative regulators of auxin transport in vivo in *Arabidopsis*. *Plant Physiol.* 126, 524–535.
- Buchanan-Wollaston, V., Earl, S., Harrison, E., Mathas, E., Navabpour, S., Page, T., Pink, D. (2003). The molecular analysis of leaf senescence – a genomics approach. *Plant Biotechnol. J.* 1, 3–22.
- Buer, C.S. and Muday, G.K. (2004). The transparent testa4 mutation prevents flavonoid synthesis and alters auxin transport and the response of *Arabidopsis* roots to gravity and light. *Plant Cell* 16, 1191–1205.
- Burgos-Rivera, B., Ruzicka, D.R., Deal, R.B., McKinney, E.C., King-Reid, L., Meagher, R.B. (2008). *ACTIN DEPOLYMERIZING FACTOR9* controls development and gene expression in *Arabidopsis*. *Plant Mol. Biol.* 68, 619–632.

- Cai, C., Henty-Ridilla, J.L., Szymanski, D.B., Staiger, C.J. (2014). *Arabidopsis* myosin XI: a motor rules the tracks. *Plant Physiol.* 166, 1359–1370.
- Cardarelli, M. and Cecchetti, V. (2014). Auxin polar transport in stamen formation and development: how many actors? *Front. Plant Sci.* 5, 333.
- Cecchetti, V., Altamura, M.M., Falasca, G., Costantino, P., Cardarelli, M. (2008). Auxin regulates *Arabidopsis* anther dehiscence, pollen maturation, and filament elongation. *Plant Cell* 20, 1760–1774.
- Cha, J.-Y., Kim, M.R., Jung, I.J., Kang, S.B., Park, H.J., Kim, M.G., Yun, D.J., Kim, W.Y. (2016). The thiol reductase activity of YUCCA6 mediates delayed leaf senescence by regulating genes involved in auxin redistribution. *Front. Plant Sci.* 7, 626.
- Chang, X., Riemann, M., Liu, Q., Nick, P. (2015). Actin as deathly switch? How auxin can suppress cell-death related defence. *PLoS One* 10, e0125498.
- Chary, S.N., Hicks, G.R., Choi, Y.G., Carter, D., Raikhel, N.V. (2008). Trehalose-6-phosphate synthase/phosphatase regulates cell shape and plant architecture in *Arabidopsis*. *Plant Physiol.* 146, 97–107.
- Cheng, Y., Dai, X., Zhao, Y. (2006). Auxin biosynthesis by the YUCCA flavin monooxygenases controls the formation of floral organs and vascular tissues in *Arabidopsis*. *Genes Dev.* 20, 1790–1799.
- Cho, M., Lee, S.H., Cho, H.-T. (2007). P-glycoprotein4 displays auxin efflux transporter-like action in *Arabidopsis* root hair cells and tobacco cells. *Plant Cell* 19, 3930–3943.
- Cho, M. and Cho, H.-T. (2013). The function of ABCB transporters in auxin transport. *Plant Signal Behav.* 8, e22990.
- Citovsky, V., and Liu, B. (2017). Myosin-driven transport network in plants is functionally robust and distinctive. *Proc. Natl. Acad. Sci. U.S.A.* 114, 1756–1758.
- Davies, C.R., Seth, A.K., Wareing, P.F. (1966). Auxin and kinetin interaction in apical dominance. *Science* 151, 468–469.
- de Win, A.H., Pierson, E.S., Derksen, J. (1999). Rational analyses of organelle trajectories in tobacco pollen tubes reveal characteristics of the actomyosin cytoskeleton. *Biophys. J.* 76, 1648–1658.
- Deeks, M.J., and Hussey, P.J. (2003). Arp2/3 and “the shape of things to come.” *Curr. Opin. Plant Biol.* 6, 561–567.

- Dhonukshe, P., Grigoriev, I., Fischer, R., Tominaga, M., Robinson, D.G., Hasek, J., Paciorek, T., Petrásek, J., Seifertová, D., Tejos, R., Meisel, L.A., Zazimalová, E., Gadella, T.W. Jr., Stierhof, Y.D., Ueda, T., Oiwa, K., Akhmanova, A., Brock, R., Spang, A., Friml, J. (2008). Auxin transport inhibitors impair vesicle motility and actin cytoskeleton dynamics in diverse eukaryotes. *Proc. Natl. Acad. Sci. U.S.A.* 105, 4489–4494.
- Diaz, C., Saliba-Colombani, V., Loudet, O., Belluomo, P., Moreau, L., Daniel-Vedele, F., Morot-Gaudry, J.F., Masclaux-Daubresse, C. (2006). Leaf yellowing and anthocyanin accumulation are two genetically independent strategies in response to nitrogen limitation in *Arabidopsis thaliana*. *Plant Cell Physiol.* 47, 74–83.
- Diaz, C., Lemaître, T., Christ, A., Azzopardi, M., Kato, Y., Sato, F., Morot-Gaudry, J.F., Le Dily, F., Masclaux-Daubresse, C. (2008). Nitrogen recycling and remobilization are differentially controlled by leaf senescence and development stage in *Arabidopsis* under low nitrogen nutrition. *Plant Physiol.* 147, 1437–1449.
- Domagalska, M.A. and Leyser, O. (2011). Signal integration in the control of shoot branching. *Nat. Rev. Mol. Cell. Biol.* 12, 211–221.
- Duan, Z. and Tominaga, M. (2018). Actin-myosin XI: an intracellular control network in plants. *Biochem. Biophys. Res. Comm.* 506, 403–408.
- Edlund, A.F., Swanson, R., Preuss, D. (2004). Pollen and stigma structure and function: the role of diversity in pollination. *Plant Cell* 16, S84–S97.
- Eggenberger, K., Sanyal, P., Hundt, S., Wadhvani, P., Ulrich, A.S., Nick, P. (2017). Challenge integrity: the cell-penetrating peptide BP100 interferes with the auxin-actin oscillator. *Plant Cell Physiol.* 58, 71–85.
- Field, T.S., Lee, D.W., Holbrook, N.M. (2001). Why leaves turn red in autumn. The role of anthocyanins in senescing leaves of red-osier dogwood. *Plant Physiol.* 127, 566–574.
- Folkers, U., Kirik, V., Schöbinger, U., Falk, S., Krishnakumar, S., Pollock, M.A., Oppenheimer, D.G., Day, I., Reddy, A.S., Jürgens, G., Hülskamp, M. The cell morphogenesis gene *ANGUSTIFOLIA* encodes a CtBP/BARS-like protein and is involved in the control of the microtubule cytoskeleton. *EMBO J.* 21, 1280–1288.
- Foth, B.J., Goedecke, M.C., Soldati, D. (2006.) New insights into myosin evolution and classification. *Proc. Natl. Acad. Sci. U.S.A.* 103, 3681–3686.
- Fowler, J.E., and Quatrano, R.S. (1997). Plant cell morphogenesis: plasma membrane interactions with the cytoskeleton and cell wall. *Annu. Rev. Cell Dev. Biol.* 13, 697–743.

- Franklin-Tong, V.E. (1999). Signaling and the modulation of pollen tube growth. *Plant Cell* 11, 727–738.
- Fu, Y., Li, H., Yang, Z. (2002). The ROP2 GTPase controls the formation of cortical fine F-actin and the early phase of directional cell expansion during *Arabidopsis* organogenesis. *Plant Cell* 14, 777–794.
- Fu, Y., Gu, Y., Zheng, Z., Nicks, G., Yang, Z. (2005). *Arabidopsis* interdigitating cell growth requires two antagonistic pathways with opposing action on cell morphogenesis. *Cell* 120, 687–700.
- Haraguchi, T., Ito, K., Duan, Z., Rula, S., Takahashi, K., Shibuya, Y., Hagino, N., Miyatake, Y., Nakano, A., Tominaga, M. (2018). Functional diversity of class XI myosins in *Arabidopsis thaliana*. *Plant Cell Physiol.* 59, 2268–2277.
- Harvaux, M. and Kloppstech, K. (2001). The protective functions of carotenoid and flavonoid pigments against excess visible radiation at chilling temperature investigated in *Arabidopsis* npq and tt mutants. *Planta* 213, 953–966.
- Hempel, F.D., and Feldman, L.J. (1995). Specification of chimeric flowering shoots in wild-type *Arabidopsis*. *Plant J.* 8, 725–731.
- Henty, J.L., Bledsoe, S.W., Khurana, P., Meagher, R.B., Day, B., Blanchoin, L., Staiger, C.J. (2011). *Arabidopsis* actin depolymerizing factor4 modulates the stochastic dynamic behavior of actin filaments in the cortical array of epidermal cells. *Plant Cell* 23, 3711–3726.
- Holton, T. and Cornish, E. (1995). Genetics and biochemistry of anthocyanin biosynthesis. *Plant Cell* 7, 1071–1083.
- Hou, K., Wu, W., Gan, S.-S. (2013). SAUR36, a small auxin up RNA gene, is involved in the promotion of leaf senescence in *Arabidopsis*. *Plant Physiol.* 161, 1002–1009.
- Hülkamp, M., Misra, S., Jürgens, G. (1994). Genetic dissection of trichome cell development in *Arabidopsis*. *Cell* 76, 555–566.
- Gälweiler, L., Guan, C., Müller, A., Wisman, E., Mendgen, K., Yephremov, A., Palme, K. (1998). Regulation of polar auxin transport by AtPIN1 in *Arabidopsis* vascular tissue. *Science* 282, 2226–2230.
- Geisler, M. and Murphy, A.S. (2006). The ABC of auxin transport: the role of p-glycoproteins in plant development. *FEBS Lett.* 580, 1094–1102.
- Geldner, N., Friml, J., Stierhof, Y.-D., Jürgens, G., Palme, K. (2001). Auxin transport inhibitors block PIN1 cycling and vesicle trafficking. *Nature* 413, 425–428.
- Glover, B. J. (2000). Differentiation in plant epidermal cells. *J Ex.p Bot.* 51, 497–505.

- Gou, J.-Y., Felippes, F.F., Liu, C.-J., Weigel, D., Wang, J.-W. (2011). Negative regulation of anthocyanin biosynthesis in *Arabidopsis* by a miR156-targeted SPL transcription factor. *Plant Cell* 23, 1512–1522.
- Grieneisen, V.A., Maré, A.F.M., Østergaard, L. (2013). Juicy stories on female reproductive tissue development: coordinating the hormone flows. *J. Integr. Plant Biol.* 55, 847–863.
- Grierson, C., Nielsen, E., Ketelaar, T., Schiefelbein, J. (2014). Root hairs. In: *Arabidopsis Book*. 12, e0172.
- Guimil, S., and Dunand, C. (2007). Cell growth and differentiation in *Arabidopsis* epidermal cells. *J. Exp. Bot* 58, 3829–3840.
- Hawkins, C. and Liu, Z. (2014). A model for an early role of auxin in *Arabidopsis* gynoecium morphogenesis. *Front. Plant Sci.* 5, 327.
- Henty, J.L., Bledsoe, S.W., Khurana, P., Meagher, R.B., Day, B., Blanchoin, L., Staiger, C.J. (2011). *Arabidopsis* actin depolymerizing factor4 modulates the stochastic dynamic behavior of actin filaments in the cortical array of epidermal cells. *Plant Cell* 23, 3711–3726.
- Higa, T., Suetsugu, N., Kong, S.G., Wada, M. (2014). Actin-dependent plastid movement is required for motive force generation in directional nuclear movement in plants. *Proc. Natl. Acad. Sci. U.S.A.* 111, 4327–4331.
- Higaki, T., Kojo, K.H., Hasezawa, S. (2010). Critical role of actin bundling in plant cell morphogenesis. *Plant Signal Behav* 5, 484–488.
- Himmelblau, E. and Amasino, R.M. (2001) Nutrients mobilized from leaves of *Arabidopsis thaliana* during leaf senescence. *J. Plant. Physiol.* 158, 1317–1323.
- Hoffmann, A., and Nebenführ, A. (2004). Dynamic rearrangements of transvacuolar strands in BY-2 cells imply a role of myosin in remodeling the plant actin cytoskeleton. *Protoplasma* 224, 201–210.
- Holweg, C., Süßlin, C., Nick, P. (2004). Capturing in vivo dynamics of the actin cytoskeleton stimulated by auxin or light. *Plant Cell Physiol.* 45, 855–863.
- Hong, L., Dumond, M., Zhu, M., Tsugawa, S., Li, C.-B., Boudaoud, A., Hamant, O., Roeder, A.H.K. (2018). Heterogeneity and robustness in plant morphogenesis: from cells to organs. *Annu. Rev. Plant Biol.* 69, 469–495.
- Hoffmann, A. and Nebenführ, A. (2004). Dynamic rearrangements of transvacuolar strands in BY-2 cells imply a role of myosin in remodeling the plant actin cytoskeleton. *Protoplasma.* 224, 201–210.

- Huang, X., Maisch, J., Nick, P. (2017). Sensory role of actin in auxin-dependent responses of tobacco BY-2. *J. Plant Physiol.* 218, 6–15.
- Hülkamp, M., Misra, S., Jürgens, G. (1994). Genetic dissection of trichome cell development in *Arabidopsis*. *Cell* 76, 555–566.
- Hülkamp, M., Schnittger, A., Folkers, U. (1999). Pattern formation and cell differentiation: trichomes in *Arabidopsis* as a genetic model system. *Int. Rev. Cytol.* 186, 147–178.
- Iwano, M., Shiba, H., Matoba, K., Miwa, T., Funato, M., Entani, T., Nakayama, P., Shimosato, H., Takaoka, A., Isogai, A., Takayama, S. (2007). Actin dynamics in papilla cells of *Brassica rapa* during self- and cross-pollination. *Plant Physiol.* 144, 72–81.
- Jiang, S., and Ramachandran, S. (2004). Identification and molecular characterization of myosin gene family in *Oryza sativa* genome. *Plant Cell Physiol.* 45, 590–599.
- Jiang, S.Y., Cai, M., Ramachandran, S. (2007). *Oryza sativa* myosin XI B controls pollen development by photoperiod-sensitive protein localizations. *Dev. Biol.* 304, 579–592.
- Kandasamy, M.K., Nasrallah, J.B., Nasrallah, M.E. (1994). Pollen-pistil interactions and developmental regulation of pollen tube growth in *Arabidopsis*. *Development* 120, 3405–3418.
- Kanellos, G., Zhou, J., Patel, H., Ridgway, R.A., Huels, D., Gurniak, C.B., Sandilands, E., Carragher, N.O., Sansom, O.J., Witke, W., Brunton, V.G., Frame, M.C. (2015). ADF and Cofilin1 control actin stress fibers, nuclear integrity, and cell survival. *Cell Rep.* 13, 1949–1964.
- Keech, O., Pesquet, E., Gutierrez, L., Ahad, A., Bellini, C., Smith, S.M., Gardeström, P. (2010). Leaf senescence is accompanied by an early disruption of the microtubule network in *Arabidopsis*. *Plant Physiol.* 154, 1710–1720.
- Keech, O. (2011). The conserved mobility of mitochondria during leaf senescence reflects differential regulation of the cytoskeletal components in *Arabidopsis thaliana*. *Plant Signal. Behav.* 6, 147–150.
- Ketelaar, T., Faivre-Moskalenko, C., Esseling, J.J., de Ruijter, N.C.A., Grierson, C.S., Dogterom, M., Emons, A.M.C. (2002). Positioning of nuclei in *Arabidopsis* root hairs: an actin-regulated process of tip growth. *Plant Cell* 14, 2941–2955.
- Kim, J.I., Murphy, A.S., Baek, D., Lee, S.W., Yun, D.J., Bressan, R.A., Narasimhan, M.L. (2011). YUCCA6 over-expression demonstrates auxin function in delaying leaf senescence in *Arabidopsis thaliana*. *J. Exp. Bot.* 62, 3981–3992.

- Kim, J., Woo, H.R., and Nam, H.G. (2016). Toward systems understanding of leaf senescence: an integrated multi-omics perspective on leaf senescence research. *Mol. Plant* 9, 813–825.
- Kinkema, M. and Schiefelbein, J. (1994). A myosin from a higher plant has structural similarities to class V myosins. *J. Mol. Biol.* 239, 591–597.
- Kinkema, M., Wang, H., Schiefelbein, J. (1994). Molecular analysis of the myosin gene family in *Arabidopsis thaliana*. *Plant Mol. Biol* 26, 1139–1153.
- Kleine-Vehn, J., Dhonukshe, P., Swarup, R., Bennett, M., Friml, J. (2006). Subcellular trafficking of the *Arabidopsis* auxin influx carrier AUX1 uses a novel pathway distinct from PIN1. *Plant Cell* 18, 3171–3181.
- Kleine-Vehn, J., and Friml, J. (2008). Polar targeting and endocytic recycling in auxin-dependent plant development. *Annu. Rev. Cell Dev. Biol.* 24, 447–473.
- Kleine-Vehn, J., Wabnik, K., Martinière, A., Łangowski, Ł., Willig, K., Naramoto, S., Leitner, J., Tanaka, H., Jakobs, S., Robert, S., Luschnig, C., Govaerts, W., Hell, S.W., Runions, J., Friml, J. (2011). Recycling, clustering, and endocytosis jointly maintain PIN auxin carrier polarity at the plasma membrane. *Mol. Syst. Biol.* 7, 540.
- Knight, A.E. and Kendrick-Jones, J. (1993). A myosin-like protein from a higher plant. *J. Mol. Biol.* 231, 148–154.
- Kost, B., Bao, Y.-Q., Chua, N.-H. (2002). Cytoskeleton and plant organogenesis. *Philos. Trans. R. Soc. Lond. B. Biol. Sci.* 357, 777–789.
- Krecek, P., Skupa, P., Libus, J., Naramoto, S., Tejos, R., Friml, J., Zazimalová, E. (2009). The PIN-FORMED (PIN) protein family of auxin transporters. *Genome Biol.* 10, 249.
- Kuhn, B.M., Errafi, S., Bucher, R., Dobrev, P., Geisler, M., Bigler, L., Zažímalová, E., Ringli, C. (2016). 7-rhamnosylated flavonols modulate homeostasis of the plant hormone auxin and affect plant development. *J. Biol. Chem.* 291, 5385–5395.
- Kurth, E.G., Peremyslov, V.V., Turner, H.L., Makarova, K.S., Iranzo, J., Mekhedov, S.L., Koonin, E.V., Dolja, V.V. (2017). Myosin-driven transport network in plants. *Proc. Natl. Acad. Sci. U.S.A.* 114, E1385–E1394.
- Larkin, J. C., Brown, M. L., Schiefelbein, J. (2003). How do cells know what they want to be when they grow up? Lessons from epidermal patterning in *Arabidopsis*. *Annu. Rev. Plant. Biol.* 54, 403–430.
- Larkin, J.C., Young, N., Prigge, M., Marks, M.D. (1996). The control of trichome spacing and number in *Arabidopsis*. *Development* 122, 997–1005.

- Larsson, E., Roberts, C.J., Claes, A.R., Franks, R.G., Sundberg, E. (2014). Polar auxin transport is essential for medial versus lateral tissue specification and vascular-mediated valve outgrowth in *Arabidopsis gynoecia*. *Plant Physiol.* 166, 1998–2012.
- Lewis, D.R., Ramirez, M.V., Miller, N.D., Vallabhaneni, P., Ray, W.K., Helm, R.F., Winkel, B.S., Muday, G.K. (2011). Auxin and ethylene induce flavonol accumulation through distinct transcriptional networks. *Plant Physiol.* 156, 144–164.
- Li, S., Blanchoin, L., Yang, Z., Lord, E.M. (2003). The putative *Arabidopsis* arp2/3 complex controls leaf cell morphogenesis. *Plant Physiol.* 132, 2034–2044.
- Li, G., Liang, W., Zhang, X., Ren, H., Hu, J., Bennett, M.J., Zhang, D. (2014). Rice actin-binding protein RMD is a key link in the auxin–actin regulatory loop that controls cell growth. *Proc. Natl. Acad. Sci. U.S.A.* 111, 10377–10382.
- Liebe, S. and Menzel, D. (1995). Actomyosin-based motility of endoplasmic reticulum and chloroplasts in *Vallisneria* mesophyll cells. *Biol. Cell* 85, 207–222.
- Lim, P., Woo, H.R., Nam, H.G. (2003). Molecular genetics of leaf senescence in *Arabidopsis*. *Trends Plant Sci.* 8, 272–278.
- Lim, P.O., Kim, H.J., Nam, H.G. (2007). Leaf senescence. *Annu. Rev. Plant Biol.* 58, 115–136.
- Lim, P.O., Lee, I.C., Kim, J., Kim, H.J., Ryu, J.S., Woo, H.R., Nam, H.G. (2010). Auxin response factor 2 (ARF2) plays a major role in regulating auxin-mediated leaf longevity. *J. Exp. Bot.* 61, 1419–1430.
- Lin, J.-F. and Wu, S.-H. (2004). Molecular events in senescing *Arabidopsis* leaves. *Plant J.* 39, 612–628.
- Luquez, V.M., Sasal, Y., Medrano, M., Martín, M.I., Mujica, M., Guamét, J.J. (2006). Quantitative trait loci analysis of leaf and plant longevity in *Arabidopsis thaliana*. *J. Exp. Bot.* 57, 1363–1372.
- Luschnig, C., Gaxiola, R.A., Grisafi, P., Fink, G.R. (1998). EIR1, a root-specific protein involved in auxin transport, is required for gravitropism in *Arabidopsis thaliana*. *Genes Dev.* 12, 2175–2187.
- Madison, S.L., Buchanan, M.L., Glass, J.D., McClain, T.F., Park, E., Nebenführ, A. (2015). Class XI myosins move specific organelles in pollen tubes and are required for normal fertility and pollen tube growth in *Arabidopsis*. *Plant Physiol.* 169, 1946–1960.

- Maillard, A., Diquelou, S., Billard, V., Laine, P., Garnica, M., Prudent, M., Garcia-Mina, J.M., Yvin, J.C., Ourry, A. (2015). Leaf mineral nutrient remobilization during leaf senescence and modulation by nutrient deficiency. *Front. Plant Sci.*, 6:317.
- Marchant, A., Kargul, J., May, S.T., Muller, P., Delbarre, A., Perrot-Rechenmann, C., Bennett, M.J. (1999). AUX1 regulates root gravitropism in *Arabidopsis* by facilitating auxin uptake within root apical tissues. *EMBO J.* 18, 2066–2073.
- Mathur, J., Spielhofer, P., Kost, B., Chua, N. (1999). The actin cytoskeleton is required to elaborate and maintain spatial patterning during trichome cell morphogenesis in *Arabidopsis thaliana*. *Development* 126, 5559–5568.
- Mathur, J. and Hülskamp, M. (2002). Microtubules and microfilaments in cell morphogenesis in higher plants. *Curr. Biol.* 12, R669–676.
- Meagher, R.B., Kandasamy, M.K., Smith, A.P., McKinney, E.C. (2010). Nuclear actin-related proteins at the core of epigenetic control. *Plant Signal Behav.* 5, 518–522.
- Mendrinna, A. and Persson, S. (2015). Root hair growth: it's a one way street. *F1000Prime Rep* 7, 23.
- Minakhina, S., Myers, R., Druzhinina, M., and Steward, R. (2005). Crosstalk between the actin cytoskeleton and Ran-mediated nuclear transport. *BMC Cell Biol.* 6, 32.
- Miralles, F. and Visa, N. (2006). Actin in transcription and transcription regulation. *Curr. Opin. Cell Biol.* 18, 261–266.gene
- Misyura, M., Colasanti, J., Rothstein, S.J. (2013). Physiological and genetic analysis of *Arabidopsis thaliana* anthocyanin biosynthesis mutants under chronic adverse environmental conditions. *J. Exp. Bot.* 64, 229–240.
- Muday, G.K. and DeLong, A. (2001). Polar auxin transport: controlling where and how much. *Trends Plant Sci.* 6, 535–542.
- Natesan, S.K., Sullivan, J.A., Gray, J.C. (2009). Myosin XI is required for actin-associated movement of plastid stromules. *Mol. Plant.* 2, 1262–1272.
- Nasrallah, J.B., Stein, J.C., Kandasamy, M.K., and Nasrallah, M.E. (1994). Signaling the arrest of pollen tube development in self-incompatible plants. *Science* 266, 1505–1508.
- Nemhauser, J.L., Feldman, L.J., Zambryski, P.C. (2000). Auxin and ETTIN in *Arabidopsis* gynoecium morphogenesis. *Development* 127, 3877–3888.
- Nick, P., Han, M.-J., An, G. (2009). Auxin stimulates its own transport by shaping actin filaments. *Plant Physiol.* 151, 155–167.

- Noodén, L.D. and Noodén, S.M. (1985). Effects of morphactin and other auxin transport inhibitors on soybean senescence and pod development. *Plant Physiol.* 78, 263–266.
- Odronitz, F. and Kollmar, M. (2007). Drawing the tree of eukaryotic life based on the analysis of 2,269 manually annotated myosins from 328 species. *Genome Biol.* 8, R196.
- Okada, K., Ueda, J., Komaki, M., Bell, C., Shimura, Y. (1991). Requirement of the auxin polar transport system in early stages of *Arabidopsis* floral bud formation. *Plant Cell* 3, 677–684.
- Okamoto, K., Ueda, H., Shimada, T., Tamura, K., Kato, T., Tasaka, M., Morita, M.T., Hara-Nishimura, I. (2015). Regulation of organ straightening and plant posture by an actin-myosin XI cytoskeleton. *Nat. Plants* 1, 15031.
- O'Malley, R.C., Alonso, J.M., Kim, C.J., Leisse, T.J., Ecker, J.R. (2007). An adapter ligation-mediated PCR method for high-throughput mapping of T-DNA inserts in the *Arabidopsis* genome. *Nat. Protoc.* 2, 2910–2917.
- Oppenheimer, D.G., Pollock, M.A., Vacik, J., Szymanski, D.B., Ericson, B., Feldmann, K., Marks, M.D. (1997). Essential role of a kinesin-like protein in *Arabidopsis* trichome morphogenesis. *Proc. Natl. Acad. Sci. U. S. A.* 94, 6261–6266.
- Östin, A., Kowalyczk, M., Bhalerao, R.P., Sandberg, G. (1998). Metabolism of indole-3-acetic acid in *Arabidopsis*. *Plant Physiol.* 118, 285–296.
- Paponov, I.A., Paponov, M., Teale, W., Menges, M., Chakrabortee, S., Murray, J.A.H., Palme, K. (2008). Comprehensive transcriptome analysis of auxin responses in *Arabidopsis*. *Mol. Plant* 1, 321–337.
- Park, E. and Nebenführ, A. (2013). Myosin XIX of *Arabidopsis thaliana* accumulates at the root hair tip and is required for fast root hair growth. *PLoS One* 8:e76745.
- Peer, W.A. and Murphy, A.S. (2007). Flavonoids and auxin transport: modulators or regulators? *Trends Plant Sci.* 12, 556–563.
- Peng, M., Hudson, D., Schofield, A., Tsao, R., Yang, R., Gu, H., Bi, Y.M., Rothstein, S.J. (2008). Adaptation of *Arabidopsis* to nitrogen limitation involves induction of anthocyanin synthesis which is controlled by the NLA gene. *J. Exp. Bot.* 59, 2933–2944.
- Peremyslov, V.V., Prokhnevsky, A.I., Avisar, D., Dolja, V.V. (2008). Two class XI myosins function in organelle trafficking and root hair development in *Arabidopsis*. *Plant Physiol.* 146, 1109–1116.

- Peremyslov, V.V., Prokhnevsky, A.I., Dolja, V.V. (2010). Class XI myosins are required for development, cell expansion, and F-actin organization in *Arabidopsis*. *Plant Cell* 22, 1883–1897.
- Peremyslov, V.V., Mockler, T.C., Filichkin, S.A., Fox, S.E., Jaiswal, P., Makarova, K.S., Koonin, E.V., Dolja, V.V. (2011). Expression, splicing, and evolution of the myosin gene family in plants. *Plant Physiol.* 155, 1191–1204.
- Peremyslov, V.V., Klocko, A.L., Fowler, J.E., Dolja, V.V. (2012). *Arabidopsis* myosin XI-K localizes to the motile endomembrane vesicles associated with F-actin. *Front. Plant Sci.* 3, 184.
- Peremyslov, V.V., Morgun, E.A., Kurth, E.G., Makarova, K.S., Koonin, E.V., Dolja, V.V. (2013). Identification of myosin XI receptors in *Arabidopsis* defines a distinct class of transport vesicles. *Plant Cell* 25, 3022–3038.
- Peremyslov, V.V., Cole, R.A., Fowler, J.E., Dolja, V.V. (2015). Myosin-powered membrane compartment drives cytoplasmic streaming, cell expansion and plant development. *PLoS ONE* 10, e0139331.
- Petrášek, J. and Friml, J. (2009). Auxin transport routes in plant development. *Development* 136, 2675–2688.
- Pouteau, S., and Albertini, C. (2009). The significance of bolting and floral transitions as indicators of reproductive phase change in *Arabidopsis*. *J. Exp. Bot.* 60, 3367–3377.
- Prokhnevsky, A.I., Peremyslov, V.V., Dolja, V.V. (2008). Overlapping functions of the four class XI myosins in *Arabidopsis* growth, root hair elongation, and organelle motility. *Proc. Natl. Acad. Sci. U.S.A.* 105, 19744–19749.
- Qian, P., Hou, S., Guo, G. (2009). Molecular mechanisms controlling pavement cell shape in *Arabidopsis* leaves. *Plant Cell Rep.* 28, 1147–1157.
- Quirino, B.F., Normanly, J., Amasino, R.M. (1999). Diverse range of gene activity during *Arabidopsis thaliana* leaf senescence includes pathogen-independent induction of defense-related genes. *Plant Mol. Biol.* 40, 267–278.
- Rahman, A., Bannigan, A., Sulaman, W., Pechter, P., Blancaflor, E.B., Baskin, T.I. (2007). Auxin, actin and growth of the *Arabidopsis thaliana* primary root. *Plant J.* 50, 514–528.
- Reddy, A.S., and Day, I.S. (2001). Analysis of the myosins encoded in the recently completed *Arabidopsis thaliana* genome sequence. *Genome Biol.* 2, RESEARCH0024.1-RESEARCH0024.17.

- Reichelt, S., Knight, A.E., Hodge, T.P., Baluska, F., Samaj, J., Volkmann, D., Kendrick-Jones, J. (1999). Characterization of the unconventional myosin VIII in plant cells and its localization at the post-cytokinetic cell wall. *Plant J.* 19, 555–567.
- Ren, H., Gray, W.M. (2015). SAUR proteins as effectors of hormonal and environmental signals in plant growth. *Mol. Plant* 8, 1153–1164.
- Rogers, H.J. (2013). From models to ornamentals: how is flower senescence regulated? *Plant Mol. Biol.* 82, 563–574.
- Rounds, C.M. and Bezanilla, M. (2013). Growth mechanisms in tip-growing plant cells. *Annu. Rev. Plant Biol.* 64, 243–265.
- Rusak, G., Cerni, S., Stupin Polancec, D., Ludwig-Müller, J. (2010). The responsiveness of the IAA2 promoter to IAA and IBA is differentially affected in *Arabidopsis* roots and shoots by flavonoids. *Biol. Plantar.* 54, 403–414.
- Ruzicka, D.R., Kandasamy, M.K., McKinney, E.C., Burgos-Rivera, B., Meagher, R.B. (2007). The ancient subclasses of *Arabidopsis* actin depolymerizing factor genes exhibit novel and differential expression. *Plant J.* 52, 460–472.
- Santelia, D., Henrichs, S., Vincenzetti, V., Sauer, M., Bigler, L., Klein, M., Bailly, A., Lee, Y., Friml, J., Geisler, M., Martinoia, E. (2008). Flavonoids redirect PIN-mediated polar auxin fluxes during root gravitropic responses. *J. Biol. Chem.* 283, 31218–31226.
- Sattarzadeh, A., Krahmer, J., Germain, A.D., Hanson, M.R. (2009). A myosin XI tail domain homologous to the yeast myosin vacuole-binding domain interacts with plastids and stromules in *Nicotiana benthamiana*. *Mol. Plant* 2, 1351–1358.
- Scheuring, D., Löffke, C., Krüger, F., Kittelmann, M., Eisa, A., Hughes, L., Smith, R.S., Hawes, C., Schumacher, K., Kleine-Vehn, J. (2016). Actin-dependent vacuolar occupancy of the cell determines auxin-induced growth repression. *Proc. Natl. Acad. Sci. U.S.A.* 113, 452–457.
- Schippers, J., Jing, H.-C., Hille, J., Dijkwel, P. (2007). Developmental and hormonal control of leaf senescence. *Annu. Plant Rev.* 26, 145–170.
- Schmalenbach, I., Zhang, L., Reymond, M., Jiménez-Gómez, J.M. (2014). The relationship between flowering time and growth responses to drought in the *Arabidopsis* Landsberg *erecta* x Antwerp-1 population. *Front. Plant Sci.* 5, 609.
- Schwab, B., Folkers, U., Ilgenfritz, H., Hülskamp, M. (2000). Trichome morphogenesis in *Arabidopsis*. *Philos. Trans. R. Soc. Lond. B. Biol. Sci.* 355, 879–883.
- Sessions, A., Nemhauser, J.L., McColl, A., Roe, J.L., Feldmann, K.A., Zambryski, P.C. (1997). ETTIN patterns the *Arabidopsis* floral meristem and reproductive organs. *Development* 124, 4481–4491.

- Shibasaki, K., Uemura, M., Tsurumi, S., Rahman, A. (2009). Auxin response in *Arabidopsis* under cold stress: underlying molecular mechanisms. *Plant Cell* 21, 3823–3838.
- Shimmen, T., and Yokota, E. (1994). Physiological and biochemical aspects of cytoplasmic streaming. In: *International Review of Cytology*, eds. K.W. Jeon and J. Jarvik (Academic Press), 97–139.
- Smertenko, A.P., Bozhkov, P.V., Filonova, L.H., von Arnold, S., Hussey, P.J. (2003). Re-organisation of the cytoskeleton during developmental programmed cell death in *Picea abies* embryos. *Plant J.* 33, 813–824.
- Smertenko, A. and Franklin-Tong, V.E. (2011). Organisation and regulation of the cytoskeleton in plant programmed cell death. *Cell Death Differ.* 18, 1263–1270.
- Smith, L.G., and Oppenheimer, D.G. (2005). Spatial control of cell expansion by the plant cytoskeleton. *Annu. Rev. Cell Dev. Biol.* 21, 271–295.
- Solfanelli, C., Poggi, A., Loreti, E., Alpi, A., Perata, P. (2006). Sucrose-specific induction of the anthocyanin biosynthetic pathway in *Arabidopsis*. *Plant Physiol.* 140, 637–646.
- Sorefan, K., Girin, T., Liljegren, S.J., Ljung, K., Robles, P., Galván-Ampudia, C.S., Offringa, R., Friml, J., Yanofsky, M.F., Østergaard, L. (2009). A regulated auxin minimum is required for seed dispersal in *Arabidopsis*. *Nature.* 459, 583-586.
- Sparkes, I.A., Teanby, N.A., Hawes, C. (2008). Truncated myosin XI tail fusions inhibit peroxisome, Golgi, and mitochondrial movement in tobacco leaf epidermal cells: a genetic tool for the next generation. *J. Exp. Bot.* 59, 2499–2512.
- Sparkes, I. (2011). Recent advances in understanding plant myosin function: life in the fast lane. *Mol. Plant.* 4:805–812.
- Staiger, C.J. (2000). Signaling to the actin cytoskeleton in plants. *Annu. Rev. Plant Physiol. Plant Mol. Biol.* 51, 257–288.
- Steffens, A., Jaegle, B., Tresch, A., Hülkamp, M., Jakoby, M. (2014). Processing-body movement in *Arabidopsis* depends on an interaction between myosins and DECAPPING PROTEIN1. *Plant Physiol.* 164, 1879–1892.
- Sundberg, E. and Ferrandíz, C. (2009). Gynoecium patterning in *Arabidopsis*: a basic plan behind a complex structure. In: *Fruit development and seed dispersal Annual Plant Reviews* 38, 35–69.
- Swartzberg, D., Dai, N., Gan, S., Amasino, R., Granot, D. (2006). Effects of cytokinin production under two SAG promoters on senescence and development of tomato plants. *Plant Biol.* 8, 579–586.

- Swarup, R., Friml, J., Marchant, A., Ljung, K., Sandberg, G., Palme, K., Bennett, M. (2001). Localization of the auxin permease AUX1 suggests two functionally distinct hormone transport pathways operate in the *Arabidopsis* root apex. *Genes Dev.* 15, 2648–2653.
- Swarup, R., and Péret, B. (2012). AUX/LAX family of auxin influx carriers – an overview. *Front. Plant Sci.* 3, 225.
- Szymanski, D.B., Jilk, R.A., Pollock, S.M., Marks, M.D. (1998). Control of GL2 expression in *Arabidopsis* leaves and trichomes. *Development* 125, 1161–1171.
- Szymanski, D.B., Marks, M.D., Wick, S.M. (1999). Organized F-actin is essential for normal trichome morphogenesis in *Arabidopsis*. *Plant Cell* 11, 2331–2347.
- Szymanski, D.B., and Staiger, C.J. (2018). The actin cytoskeleton: functional arrays for cytoplasmic organization and cell shape control. *Plant Physiol.* 176, 106–118.
- Talts, K., Ilau, B., Ojangu, E.-L., Tanner, K., Peremyslov, V.V., Dolja, V.V., Truve, E., Paves, H. (2016). *Arabidopsis* myosins XI1, XI2, and XIK are crucial for gravity-induced bending of inflorescence stems. *Front. Plant Sci.* 7, 1932.
- Tamura, K., Iwabuchi, K., Fukao, Y., Kondo, M., Okamoto, K., Ueda, H., Nishimura, M., Hara-Nishimura, I. (2013). Myosin XI-i links the nuclear membrane to the cytoskeleton to control nuclear movement and shape in *Arabidopsis*. *Curr. Biol.* 23, 1776–1781.
- Thomas, S.G., Huang, S., Li, S., Staiger, C.J., Franklin-Tong, V.E. (2006). Actin depolymerization is sufficient to induce programmed cell death in self-incompatible pollen. *J. Cell Biol.* 174, 221–229.
- Thomas, C., Tholl, S., Moes, D., Dieterle, M., Papuga, J., Moreau, F., Steinmetz, A. (2009). Actin bundling in plants. *Cell Motility* 66, 940–957.
- Tian, J., Han, L., Feng, Z., Wang, G., Liu, W., Ma, Y., Yu, Y., Kong, Z. (2015). Orchestration of microtubules and the actin cytoskeleton in trichome cell shape determination by a plant-unique kinesin. *eLife* 4, e09351.
- Titapiwatanakun, B., Blakeslee, J.J., Bandyopadhyay, A., Yang, H., Mravec, J., Sauer, M., Cheng, Y., Adamec, J., Nagashima, A., Geisler, M., Sakai, T., Friml, J., Peer, W.A., Murphy, A.S. (2009). ABCB19/PGP19 stabilises PIN1 in membrane microdomains in *Arabidopsis*. *Plant J.* 57, 27–44.
- Tominaga, M., Kimura, A., Yokota, E., Haraguchi, T., Shimmen, T., Yamamoto, K., Nakano, A., Ito, K. (2013). Cytoplasmic streaming velocity as a plant size determinant. *Dev. Cell* 27, 345–352.
- Tominaga, M. and Ito, K. (2015). The molecular mechanism and physiological role of cytoplasmic streaming. *Curr. Opin. Plant Biol.* 27, 104–110.

- Ueda, H., Yokota, E., Kutsuna, N., Shimada, T., Tamura, K., Shimmen, T., Hasezawa, S., Dolja, V.V., Hara-Nishimura, I. (2010). Myosin-dependent endoplasmic reticulum motility and F-actin organization in plant cells. *Proc. Natl. Acad. Sci. U.S.A.* 107, 6894–6899.
- Ulmasov, T., Murfett, J., Hagen, G., Guilfoyle, T.J. (1997). Aux/IAA proteins repress expression of reporter genes containing natural and highly active synthetic auxin response elements. *Plant Cell* 9, 1963–1971.
- Ungerer, M.C., Halldorsdottir, S.S., Modliszewski, J.L., Mackay, T.F.C., Purugganan, M.D. (2002). Quantitative trait loci for inflorescence development in *Arabidopsis thaliana*. *Genetics* 160, 1133–1151.
- van der Graaff, E., Schwacke, R., Schneider, A., Desimone, M., Flügge, U.I., Kunze, R. (2006). Transcription analysis of arabidopsis membrane transporters and hormone pathways during developmental and induced leaf senescence. *Plant Physiol.* 141, 776–792.
- Van Gestel, K., Köhler, R.H., Verbelen, J.-P. (2002). Plant mitochondria move on F-actin, but their positioning in the cortical cytoplasm depends on both F-actin and microtubules. *J. Exp. Bot.* 53, 659–667.
- Van Hautegeem, T., Waters, A.J., Goodrich, J., Nowack, M.K. (2015). Only in dying, life: programmed cell death during plant development. *Trends Plant Sci.* 20, 102–113.
- Vanneste, S. and Friml, J. (2009). Auxin: a trigger for change in plant development. *Cell* 136, 1005–1016.
- Vazquez, L.A.B., Sanchez, R., Hernandez-Barrera, A., Zepeda-Jazo, I., Sánchez, F., Quinto, C., Torres, L.C. (2014). Actin polymerization drives polar growth in *Arabidopsis* root hair cells. *Plant Signal Behav* 9, e29401.
- Vidali, L., Burkart, G.M., Augustine, R.C., Kerdavid, E., Tüzel, E., Bezanilla, M. (2010). Myosin XI is essential for tip growth in *Physcomitrella patens*. *Plant Cell* 22, 1868–1882.
- Wang, C., Yan, X., Chen, Q., Jiang, N., Fu, W., Ma, B., Liu, J., Li, C., Bednarek, S.Y., Pan, J. (2013). Clathrin light chains regulate clathrin-mediated trafficking, auxin signaling, and development in *Arabidopsis*. *Plant Cell* 25, 499–516.
- Wang, Q., Kohlen, W., Rossmann, S., Vernoux, T., Theres, K. (2014). Auxin depletion from the leaf axil conditions competence for axillary meristem formation in *Arabidopsis* and tomato. *Plant Cell* 26, 2068–2079.
- Wasteneys, G.O. and Galway, M.E. (2003). Remodeling the cytoskeleton for growth and form: an overview with some new views. *Annu. Rev. Plant Biol.* 54, 691–722.

- Watanabe, M., Balazadeh, S., Tohge, T., Erban, A., Giavalisco, P., Kopka, J., Mueller-Roeber, B., Fernie, A.R., Hoefgen, R. (2013). Comprehensive dissection of spatiotemporal metabolic shifts in primary, secondary, and lipid metabolism during developmental senescence in *Arabidopsis*. *Plant Physiol.* 162, 1290–1310.
- Weaver, L.M., Himelblau, E., Amasino, R.M. (1997). Leaf senescence: gene expression and regulation. *Genetic Eng.* 19, 215–234.
- Weaver, L.M., Gan, S.S., Quirino, B., Amasino, R.M. (1998). A comparison of the expression patterns of several senescence-associated genes in response to stress and hormone treatment. *Plant Mol. Biol.* 37, 455–469.
- Williams, C.A. and Grayer, R.J. (2004). Anthocyanins and other flavonoids. *Nat. Prod. Rep.* 21, 539–573.
- Woo, H.R., Kim, H.J., Nam, H.G., Lim, P.O. (2013). Plant leaf senescence and death – Regulation by multiple layers of control and implications for aging in general. *J. Cell Sci.* 126, 4823–4833.
- Wu, S., Xie, Y., Zhang, J., Ren, Y., Zhang, X., Wang, J., Guo, X., Wu, F., Sheng, P., Wang, J., Wu, C., Wang, H., Huang, S., Wan, J. (2015). VLN2 regulates plant architecture by affecting microfilament dynamics and polar auxin transport in rice. *Plant Cell* 27, 2829–2845.
- Yanagisawa, M., Desyatova, A.S., Belteton, S.A., Mallery, E.L., Turner, J.A., Szymanski, D.B. (2015). Patterning mechanisms of cytoskeletal and cell wall systems during leaf trichome morphogenesis. *Nature Plants* 1, 15014.
- Zapata, J.M., Guera, A., Esteban-Carrasco, A., Martin, M., Sabater, B. (2005). Chloroplasts regulate leaf senescence: delayed senescence in transgenic *ndhF*-defective tobacco. *Cell Death and Differentiation* 12, 1277–1284.
- Zažimalová, E., Murphy, A.S., Yang, H., Hoyerová, K., Hošek, P. (2010). Auxin transporters – why so many? *Cold Spring Harb. Perspect. Biol.* 2, a001552.
- Zentgraf, U., Jobst, J., Kolb, D., Rentsch, D. (2004). Senescence-related gene expression profiles of rosette leaves of *Arabidopsis thaliana*: leaf age versus plant age. *Plant Biol.* 6, 178–183.
- Zhang, C., Halsey, L.E., Szymanski, D.B. (2011a). The development and geometry of shape change in *Arabidopsis thaliana* cotyledon pavement cells. *BMC Plant Biol.* 11, 27.
- Zhang, Y., Xiao, Y., Du, F., Cao, L., Dong, H., Ren, H. (2011b). *Arabidopsis* VILLIN4 is involved in root hair growth through regulating actin organization in a Ca²⁺-dependent manner. *New Phytol.* 190, 667–682.

- Zhang, W., Cai, C., Staiger, C.J. (2018). *Arabidopsis* myosins XI are involved in exocytosis of cellulose synthase complexes. *Cold Spring Harb. The preprint server for biology* <https://doi.org/10.1101/492629>.
- Zhao, Y., Pan, Z., Zhang, Y., Qu, X., Zhang, Y., Yang, Y., Jiang, X., Huang, S., Yuan, M., Schumaker, K.S., Guo, Y. (2013). The actin-related protein2/3 complex regulates mitochondrial-associated calcium signaling during salt stress in *Arabidopsis*. *Plant Cell* 25, 4544–4559.
- Zhou, X., Groves, N.R., Meier, I. (2015). Plant nuclear shape is independently determined by the SUN-WIP-WIT2-myosin XI-i complex and CRWN1. *Nucleus* 6, 144–153.
- Zhou, L.H., Liu, S.B., Wang, P.F., Lu, T.J., Xu, F., Genin, G.M., Pickard, B.G. (2017). The *Arabidopsis* trichome is an active mechanosensory switch. *Plant Cell Environ.* 40, 611–621.
- Zhu, J., Bailly, A., Zwiewka, M., Sovero, V., Di Donato, M., Ge, P., Oehri, J., Aryal, B., Hao, P., Linnert, M., Burgardt, N.I., Lücke, C., Weiwad, M., Michel, M., Weiergräber, O.H., Pollmann, S., Azzarello, E., Mancuso, S., Ferro, N., Fukao, Y., Hoffmann, C., Wedlich-Söldner, R., Friml, J., Thomas, C., Geisler, M. (2016). TWISTED DWARF1 mediates the action of auxin transport inhibitors on actin cytoskeleton dynamics. *Plant Cell* 28, 930–948.
- Zhu, J. and Geisler, M. (2015). Keeping it all together: auxin-actin crosstalk in plant development. *J. Exp. Bot.* 66, 4983–4998.
- Zimmermann, P. and Zentgraf, U. (2005). The correlation between oxidative stress and leaf senescence during plant development. *Cell Mol. Biol. Lett.* 10, 515–534.
- Zúñiga-Mayo, V.M., Reyes-Olalde, J.I., Marsch-Martinez, N., de Folter, S. (2014). Cytokinin treatments affect the apical-basal patterning of the *Arabidopsis* gynoecium and resemble the effects of polar auxin transport inhibition. *Front. Plant Sci.* 5, 191.

ACKNOWLEDGMENTS

This work was carried out at the Laboratory of Molecular Genetics, National Institute of Chemical Physics and Biophysics, and at the Department of Gene Technology, Tallinn University of Technology.

First and foremost, I would like to thank my supervisors Erkki Truve and Heiti Paves for their guidance, enthusiasm, and patience during all these years. I also would like to take the opportunity to acknowledge all the people worked in Erkki's lab during these years for creating a friendly and relaxed atmosphere. Thank you so much – Lenne, Cecilia, Signe, Birger, Kristiina, Merike, Maarja, Eliis, Krista, Kristel, Marju, Allan, Liivi, Kairi, Jaanus, Mariliis, Silva, Tiina, Grete, Kristjan, and Gabriela! Special thanks will go to people who made up our “myosin team” – Birger, Kristel, Kristiina, Krista, Eliis, Ann-Katriin and of course, Heiti! With all my heart I thank you, Heiti, introducing me the wonderful world of microscopy! I thank Signe for gently taking care of my plants, and Allan being always so helpful by fixing my computer problems. I thank Merike for being my roommate and discussion partner during last year. I thank Richard, Cecilia, and Birger for thoroughly proofreading the manuscript. I thank you, my dear friends, for all your friendship! I thank all colleagues from the institute for the friendly atmosphere you created, for sharing knowledge, chemical supplies, encouragement, constructive criticism and good words: Merike Kelve, Anne Kuusksalu, Annika Lopp, Mart Speek, Andres Veske, Lilian Järvekülg, Piret Michelson, Robert Tsanev, Piret Tiigimägi, Tiina Kirsipuu, Anne Pink, Ljuda Timofejeva, Kadri Järve, Tiit Lukk, Epp Ints, Vello Tõugu and many others. And of course Ants, our multifunctional handyman, unique with his never ending enthusiasm. And last but not least, I thank our volleyball team “for all the volleyball we played” through these years - Kristel, Andres, Erkki, Piret, Allan, Anne, Torben, Robi, Tiina, Indrek, Richard and many others. It was such a great period.

I am also thankful for my first supervisor Maia Kivisaar and her group at the University of Tartu for leading my first steps to the world of molecular biology. I remind you warmly - Riho, Andres, Jana, Rita, Lagle, Viia, Eve, Lele, Heili and Robi – many of you became my closest friends, though we do meet maybe twice a year.

I am extremely thankful to my family – my dear Renee and Paul-Eerik, mom and dad, Hannes and Marian, Assu and Anneli – for their emotional support and love during my studies – you never understood what and why I am doing, but at that you never doubted in “it”. I love you all!

This work was supported by Estonian Research Council (Institutional Research Funding IUT19-3); Estonian Science Foundation (Research Grants ETF8604, ETF6559, ETF5939, G4298); Archimedes Foundation (Centre of Excellence in Environmental Adaptation ENVIRON); European Space Agency (Research Grant VA529); Ministry of Education and Research (Grants SF0222604s03 and T220A). This work has been partially supported by “TUT Institutional Development Program for 2016-2022” Graduate School in Biomedicine and Biotechnology receiving funding from the European Regional Development Fund under program ASTRA 2014-2020.4.01.16-0032 in Estonia.

ABSTRACT

The Roles of Class XI Myosins in *Arabidopsis* Development

Actin filaments, together with the myosin motors moving on them form an important part of the cell's skeleton. Myosins deliver vesicles, organelles, and other possible cargoes within the cell. Only two classes, VIII and XI, out of all 35 known eukaryotic myosin classes, represent higher plant myosins.

The purpose of the current work was to describe the possible roles of class XI myosins in model organism *Arabidopsis thaliana*. Initially, only the number of myosin genes in newly sequenced *Arabidopsis* genome was known, but not their functions. Therefore, the purpose of the work was: (I) to reveal the functions of individual *Arabidopsis* myosins by characterizing the phenotypes of T-DNA insertional mutants; (II) to study the redundant roles of class XI myosins by establishing double and triple mutant lines, and to characterize major developmental disorders of these mutant lines; (III) to use the flower and leaf development of triple mutant plants as model systems for determining whether main developmental processes such as polar auxin transport and leaf senescence are mediated by actomyosin cytoskeleton.

The results of the work show that myosin XI-K is key player regulating the size and shape of different epidermal cells, such as root hairs and trichomes (publication I). Moreover, simultaneous inactivation of three class XI myosins genes (*XI-1*, *XI-2*, *XI-K*) affects the size and shape of epidermal cells to such an extent that the growth of different organs as well as plant fertility are perturbed. Double mutant analysis revealed that while myosin XI-K plays a major role in these processes, myosin XI-2 has a smaller role, whereas the impact of myosin XI-1 is the smallest (publication II). At the cellular level, actin and myosins work interdependently, and this cooperation is illustrated by the fact that in myosin triple mutant cells, the actin filament organization is disturbed. Next, we studied whether actin-dependent processes, such as auxin transport and senescence, are affected in myosin triple mutant. Our results showed that the activity of auxin-dependent promoters, the expression of selected auxin-responsive genes, and the distribution of auxin efflux carrier PIN1 in developing gynoecium are indeed affected in triple mutant plants. In addition, the massive up-regulation of the stress-inducible senescence associated gene, *SAG13*, implies that premature senescence and cell death of rosette leaves in triple mutant plants is caused by defects in actomyosin cytoskeleton. Moreover, these two processes – auxin distribution and leaf senescence, are mutually interconnected, suggested by elevated levels of anthocyanins and auxin-dependent senescence-associated *SAUR36* gene expression. Interestingly, on the one hand, the overall lifespan of triple mutant plants is extended, since bolting is delayed, and generative growth period is longer. On the other hand, despite the extended overall lifespan, the rosette leaves of triple mutant plants exhibit premature senescence. This indicates that the whole organism lifespan versus organ lifespan are not proportionally related in plants (publication III).

In summary, this work shows that three class XI myosins, XI-1, XI-2 and XI-K, are necessary for the normal development and functioning of different tissues and organs in plants. In addition, we demonstrate that actomyosin cytoskeleton is necessary for mediating both the dialogue between different developmental processes (like senescence and reproduction) as well as between different tissues (vegetative and generative) in plants, and for ensuring the functional integrity of the whole organism.

KOKKUVÕTE

Klass XI müosiinide roll müürlooga arengus

Aktiinifilamendid koos müosiinidega moodustavad osa raku tsütoskeletist, mis on pidevas liikumises ja reaktsioonivalmiduses, võimaldades rakkudel kasvada ja kuju muuta. Müosiinid, aktiinifilamentidel liikuvad mootorvalgud, vastutavad vesiikulite ja organellide transpordi eest rakus ning seeläbi vahendavad ka arenguliste või väliskeskonnast tulevatele signaalide vastuseid. Eukarüootsetes organismides on praeguseks identifitseeritud 35 klassi müosiine, millest vaid kaks klassi, VIII ja XI, esindavad taimede müosiine.

Käesoleva töö eesmärgiks oli kirjeldada klass XI müosiinide funktsioone mudelorganismis harilik müürlook (*Arabidopsis thaliana*). Algselt oli teada vaid võimalik müosiinigeenide arv müürlooga 2000. aastal sekveneeritud genoomis, kuid midagi polnud teada nende funktsioonide kohta. Sellest tulenevalt olid käesoleva töö eesmärkideks: (I) kasutades T-DNA insertioonilisi mutante kirjeldada müürlooga üksikute müosiinide bioloogilisi funktsioone; (II) kasutades kaksik- ja kolmikmutantide analüüsi, iseloomustada klass XI müosiinide kattuvaid rolle taime arengus; (III) uurides klass XI müosiinide kolmikmutandi öie ja lehe arengut, teha kindlaks müosiinide võimalik roll fütohormooni auksiini polaarses transpordis ja lehe vananemises.

Töö tulemused näitavad, et müosiin XI-K on oluline teatud epidermiserakkude, nagu juurekarvad ja trihhoomid, suurust ja kuju mõjutav valk (artikkel I). Kolme klass XI müosiinigeeni (*XI-1*, *XI-2*, *XI-K*) samaaegne inaktiveerimine kolmikmutandis mõjutab epidermiserakkude suurust ja kujul sel määral, et on häiritud erinevate organite kasv ja suurus ning ka taime viljakus. Kuigi kolmikmutandi analüüs näitas, et kõik kolm müosiini omavad kattuvaid rolle müürloogas, siis kaksikmutantide analüüs täpsustas, et kõige rohkem mõjutab neid protsesse müosiin XI-K, seejärel XI-2 ning kõige vähemal määral müosiin XI-1 (artikkel II). Aktiinifilamentide ja müosiinide vastastikust sõltuvust ilmestab fakt, et müosiini kolmikmutandis on märkimisväärselt häiritud ka aktiinifilamentide paigutus ning dünaamika. Sellest lähtuvalt tõstatasime küsimuse – mil määral on müosiini kolmikmutandis häiritud sellised aktiinist sõltuvad protsessid nagu auksiini polaarne transport ja vananemine. Meie tulemused näitavad, et kolmikmutandis on häiritud nii auksiini-tundlike promootorite aktiivsus, teatud auksiin-sõltuvate geenide ekspressioonitase kui ka auksiini eksporterit, PIN1, polarisatsioon emaka epidermise rakkudes. Lisaks tundub rosetilehtede enneaegne vananemine ja suremine kolmikmutandis olevat tingitud aktiini-müosiini rakuskeleti defektide poolt põhjustatud rakustressist, millele viitab stressi poolt indutseeritava vananemise markergeeni, *SAG13*, väga kõrge ekspressioonitase mutantides. Enamgi veel, auksiini gradiendid ja lehe vananemine on kolmikmutandis omavahel seotud nagu näitavad muutused antotsüaniinide hulgas ning auksiin-sõltuva vananemise markergeeni, *SAUR36*, ekspressioonitasemes. Ühelt poolt on kolmikmutandi taimede üldine eluiga pikem kui metsiktüübil, sest õitsemine hilineb ja paljunemise faas on edasi lükatud. Teisalt, vaatamata üldisele eluea pikenedamisele, vananevad kolmikmutandi rosetilehed enneaegselt. See näitab, et taimede üldine eluiga ja üksiku organi eluiga ei ole võrdelises seoses (artikkel III).

Kokkuvõttes kirjeldavad antud töö tulemused seda, millistes arenguetappides ning organites ja kudedes on müosiinid XI-1, XI-1 ja XI-K müürloogas vajalikud. Lisaks näitab antud töö ka seda, et aktiini-müosiini rakuskelett vahendab dialoogi eri bioloogiliste

protsesside (nagu vananemine ja paljunemine) ning erinevate kudede ja organite (vegetatiivsete ja generatiivsete) vahel taimedes, mis on omakorda vajalik taime organismi funktsionaalse terviklikkuse tagamiseks.

APPENDIX

Publication I

Ojangu E.-L., Järve K., Paves H., Truve E. (2007). *Arabidopsis thaliana* myosin XIK is involved in root hair as well as trichome morphogenesis on stems and leaves. *Protoplasma* 230:193–202.

Arabidopsis thaliana myosin XIX is involved in root hair as well as trichome morphogenesis on stems and leaves

E.-L. Ojangu, K. Järve, H. Paves*, and E. Truve

Department of Gene Technology, Tallinn University of Technology, Tallinn

Received February 21, 2006; accepted April 12, 2006; published online April 24, 2007
© Springer-Verlag 2007

Summary. Myosins form a large superfamily of molecular motors that move along actin filaments. The functions of myosins in plant cells are thought to be related to various processes: cell division, movement of mitochondria and chloroplasts, cytoplasmic streaming, rearrangement of transvacuolar strands, and statolith positioning. Class VIII and XI myosins are represented in the *Arabidopsis thaliana* genome by 4 and 13 potential genes, respectively. The roles of individual class XI myosins and their cellular targets in *A. thaliana* are still unclear. In this work we implemented a reverse genetic approach to analyse the loss-of-function mutants of XIX, a representative of class XI myosins in *A. thaliana*. Three different T-DNA insertion mutants in the myosin XIX gene showed similar phenotypes: impaired growth of root hair cells, twisted shape of stem trichomes, and irregular size, branch positioning, and branch expansion of leaf trichomes. Morphometric analysis of mutant seedlings showed that the average length of root hairs was reduced up to 50% in comparison with wild-type root hairs, suggesting an involvement of the class XI myosin XIX in tip growth. On leaves, the proportion of trichomes with short branches was doubled in mutant plants, and the mutant trichomes possessed a mildly twisted shape. Therefore, we concluded that myosin XIX is involved also in the elongation of stalks and branches of trichomes.

Keywords: Myosin; *Arabidopsis thaliana*; Root hair; Tip growth; Trichome.

Abbreviations: EST expressed sequence tag; MS medium Murashige and Skoog medium; WT wild type.

Introduction

Myosins constitute a large superfamily of molecular motors able to slide along actin filaments by the force-generating hydrolysis of ATP. Myosin proteins have three major regions: an amino-terminal motor domain that interacts with actin filaments in an ATP-dependent manner, a calmod-

ulin or light-chain binding neck domain, and a variable carboxy-terminal tail domain. In the phylogenetic analysis of the conserved motor domain, myosins of various organisms are divided into at least 18 classes (Cope et al. 1996, Mermall et al. 1998, Yamashita et al. 2000). Classes VIII, XI, and XIII are specific to plants and algae. The higher-plant myosins identified so far fall into classes VIII and XI, whereas class XIII is represented only in green algae *Acetabularia cliftonii* (Hodge and Cope 2000, Reichelt and Kendrick-Jones 2000). Representatives of class VIII and class XI myosins have been detected in all the higher-plant species studied (reviewed in Jiang and Ramachandran 2004).

The main sources of information about the functions of plant myosins are immunolocalisation studies with antibodies against animal and plant myosins or the exploitation of inhibitors of myosins and microfilaments. Findings from these experiments suggest that myosins in higher plants are involved in a wide range of cellular processes like cell division (Liu et al. 2001, Reichelt et al. 1999), the movement of mitochondria (Van Gestel et al. 2002) and chloroplasts (Liebe and Menzel 1995), cytoplasmic streaming (Kamiya and Kuroda 1956, Shimmen and Yokota 1994, Liebe and Quader 1994), the rearrangement of transvacuolar strands (Hoffmann and Nebenführ 2004), and statolith positioning (Braun et al. 2002).

Computational analysis of the *A. thaliana* genome has identified 17 putative myosin-coding genes: 4 from class VIII and 13 from class XI (Reddy and Day 2001). Studies that used an antibody to an *A. thaliana* class VIII myosin, ATM1, localised this myosin to the plasmodesmata and to the newly formed cross walls in maize root cells. Therefore, it is assumed that class VIII myosins

* Correspondence and reprints: Department of Gene Technology, Tallinn University of Technology, Akadeemia tee 15, 19086 Tallinn, Estonia.
E-mail: heiti.paves@ttu.ee

could be involved in the maturation of the cell plate and they could have a structural role in regulating transport through the plasmodesmata (Reichert et al. 1999; Baluška et al. 2000, 2001). It is known that the efficiency and velocity of a myosin motor is proportional to the number of IQ (IQXXRGGXXR) motifs in the calmodulin binding domain (Uyeda et al. 1996, Sakamoto et al. 2003). Because there are 3 or 4 IQ motifs in class VIII and 5 or 6 in class XI *A. thaliana* myosins (Reddy and Day 2001), it has been suggested that class XI myosins might be involved in the transport of large vesicles because of the larger number of IQ motifs (Liu et al. 2001). Recently, it has been shown that a 175 kDa class XI myosin isolated from cultured tobacco cells exhibits the fastest known processive movement along actin filaments in vitro (Tominaga et al. 2003). Only one *A. thaliana* class XI myosin, MYA2, has been characterised by intracellular localisation. Immunolocalisation studies have shown that MYA2 colocalises predominantly with actin filaments and partially with peroxisomes in leaf epidermal cells, root hair cells, and suspension-cultured cells (Hashimoto et al. 2005). Myosin MYA2 is also the only member of *A. thaliana* class XI myosins that is characterised by loss-of-function mutations, although different mutant lines display controversial phenotypes. First, it has been demonstrated that *mya2-1* mutants have a very severe phenotype: flower sterility, dwarf growth, reduction of cell elongation, and cytoplasmic streaming (Holweg and Nick 2004). In contrast, it has also been reported that a different MYA2 knockout line lacks any visible disorders (Hashimoto et al. 2005). Hence, the functions of the class XI myosins in *A. thaliana* are still unclear.

Here we report the effects of loss-of-function mutations of *A. thaliana* class XI myosin XIK. The phenotype of XIK mutants is restricted only to epidermal cells – root hairs, stem trichomes, and leaf trichomes, showing impaired growth and irregular shape of root hair cells and trichomes. Our study suggests that *A. thaliana* class XI myosin XIK is involved in the tip growth of root hair cells and in the elongation of trichome stalk and branches.

Material and methods

Plant material and growth conditions

Three different *Arabidopsis thaliana* T-DNA insertional lines of XIK were used. Information about the T-DNA insertional lines of XIK (At5g20490) was obtained from the Salk Institute Genomic Analysis Laboratory (<http://signal.salk.edu>). Seeds of T-DNA insertional lines XIK-1 and XIK-2 (corresponding to SALK_136682 and SALK_067972) were provided by the Arabidopsis Biological Resource Center at Ohio State University and seeds of line XIK-3 (SALK_018764) by the Nottingham Arabidopsis Stock Centre at University of Nottingham

(Alonso et al. 2003). The *A. thaliana* ecotype of all knockout lines as well as wild-type (WT) plants was Columbia-0. Plants were grown at 23 to 24 °C under a photoperiod of 16 h light and 8 h dark. To observe the roots, seeds were sterilized with 10% sodium hypochlorite (Fluka, Buchs, Switzerland) for 10 min, with 70% ethanol for 1 min, and rinsed 4 times with water. Surface sterilized seeds were held in water at 4 °C for 2 to 4 days and germinated on 0.5× Murashige and Skoog (MS) basal salt mixture (Duchefa Biochemie, Haarlem, The Netherlands) containing 0.05% 2-(N-morpholino)ethanesulfonic acid (Duchefa Biochemie) and 1% sucrose at pH 5.7, unless noted otherwise.

Identification of the transgenes

PCR using T-DNA left-border-specific primer LBB1 (5'-GCGTGGACC GCTTGCTGCAACT-3') and two XIK-specific primers flanking the insertion was performed to confirm T-DNA insertions. Primers for the three T-DNA insertional lines were as follows: for XIK-1, 5'-TCTGCAA TGGCAAACACATGG-3' and 5'-TATTGTCTGGTTTTCGGGGA-3'; for XIK-2, 5'-TCATGTGATTACAGAACC-3' and 5'-TGGGGAAA GTGGTGCTGGTAA-3'; for XIK-3, 5'-TCCATATATCTTCGAGGA ATG-3' and 5'-CGGGAACAGAGTCTGAGGAGA-3'. The genomic DNA was isolated from 4- to 6-week-old leaves, as reported by Dellaporte et al. (1983). Lines with homozygotic T-DNA insertions were selected and used in further experiments.

cDNA construction and expression analysis

Expressed sequence tag (EST) clone AB01B09 (GenBank accession nr. BE038557), corresponding to the 3' region of XIK (from the 20th to the 38th exon) was obtained from Dr. H. J. Bohnert (University of Arizona). The 5' region of XIK cDNA was amplified with two pairs of primers: for a 1077 bp fragment (named cDNA5'-1) primers XIK-ATG-Fw (5'-ATG AAGGAAACTGAGGGAAATGCGC-3') and XIK-7EXON-Rev (5'-TAC TGCAGCTGGATAATAGTAGCAGCCTT-3'), and for a 2052 bp fragment (named cDNA5'-2) primers XIK-067972-Fw (5'-TCATGTGATTACA GAACGCC-3') and XIK-Pst-Rev (5'-TACTGCAGCTGGATAATAGTA GCAGCCTT-3') were used. Two overlapping cDNA fragments, cDNA5'-1 and cDNA5'-2, comprised sequences from exon 1 to 6 and from exon 5 to 20, respectively. For the first-strand synthesis, RevertAid H Minus M-MuLV Reverse Transcriptase (Fermentas, Vilnius, Lithuania) and for the PCR amplification, AmpliTaq Gold DNA Polymerase (Applied Biosystems, Foster City, Calif., U.S.A.) were used. Sequencing reactions were performed with the BigDye Terminator Cycle Sequencing Kit (Applied Biosystems).

The total RNA was isolated from roots, leaves, stems, flowers, and siliques of mature plants as well as from the 2-week-old seedlings, following the standard protocol (Logemann et al. 1987). Genomic DNA contamination was eliminated by DNase I (Ambion, Austin, Tex., U.S.A.) treatment.

For the reverse transcriptase (RT)-PCR reactions, the first strand of cDNA was synthesized by gene-specific reverse primers for XIK and for the constitutively expressed B subunit of chloroplast glyceraldehyde-3-phosphate dehydrogenase (*GAPB*, At1g42970). To examine the expression of XIK mRNA in WT plant organs, gene-specific primers XIK-1700-Fw (5'-AACCAAGCTATCTCGGACCAGC-3') and XIK-Pst-Rev (5'-TACTGCAGCTGGATAATAGTAGCAGCCTT-3') were used for the RT-PCR analysis. For the amplification of *GAPB* cDNA fragment (396 bp), primers 5'-CTTAACATATAGTTTTCATCAGAC-3' and 5'-CGCCCTCTGTCTC TGTTGAC-3' were used.

Approximately 20 µg of the total RNA was used for the RNA gel blot analysis. RNA was separated on agarose gel containing formaldehyde and blotted onto positively charged nylon membranes (Amersham Biosciences, Piscataway, N.J., U.S.A.) following the standard protocol (Sambrook and Russell 2001). The blot was hybridized with the ³²P-labelled PCR product of XIK cDNA. For the probe, a 410 bp fragment corresponding to the 3' untranslated region (UTR) of XIK was obtained

with primers XIK-4300-Fw (5'-GTGCTAAGTATACAACAGCTATACA GAAT-3') and XIK-cDNA-UTR-Rev (5'-AAAAATAAGATGTGCAACCTATATAAAT-3') and cutting the amplified fragment with *Eco47I* (Fermentas). A ³²P-labelled probe for *GAPB* (obtained by RT-PCR, as described above) was used to ensure an equal loading of RNA. Hybridization conditions were as follows: 50% (w/v) formamide, 5× Denhardt reagent, 0.5% (w/v) sodium dodecyl sulfate (SDS), 5× SSPE buffer (750 mM NaCl, 10 mM sodium phosphate, 1 mM EDTA, pH 7.4) and 100 µg of denatured salmon sperm DNA per ml at 42 °C overnight. The membrane was washed twice for 15 min in 2× SSC (1× SSC is 0.15 M NaCl plus 0.015 M sodium citrate) and 0.1% SDS at 42 °C.

Morphometry

To compare root hair cell sizes of WT and mutant plants, root images of 4-day-old seedlings were taken with a digital camera (Kappa, Gleichen, Federal Republic of Germany) installed on a light microscope (Olympus AHBT-513), with a 10× objective. 90 to 120 optical sections were obtained, deconvoluted with AutoDeblur Gold WF 9.3 (AutoQuant Imaging, Troy, N.Y., U.S.A.), and combined to the entire root images. The length of root hairs was measured by Image Tool 3.0 (University of Texas Health Science Center in San Antonio, U.S.A.). Statistical evaluation with Student's *t* test at the 95% significance level was made from 100 root hair cells measured in at least 12 different plants. For root hair tip growth measurements, seedlings were grown on inclined agar surfaces, and photographed at 10 min intervals.

For the trichome branch length measurement, images of young first leaf pairs and mature rosette leaves were captured with an Olympus SZ40 stereomicroscope and an Olympus Camedia C-5050 digital camera. Trichomes with visible branches approximately parallel to the image plane were selected. Trichome branches were measured by Image Tool 3.0. For single trichome images, leaf trichomes were dissected from 6-week-old leaves using a fine forceps, followed by immediate photography.

Scanning electron microscopy

Trichomes on the stems were observed in the region between the last vegetative leaf and the first cauline leaf. Freshly cut stems were imaged by scanning electron microscopy in a Philips XL-30 ESEM at 0.5–0.6 torr (ca. 0.07–0.08 Pa), 20 kV.

Results and discussion

XIK gene structure and expression

A possible structure of the myosin *XIK* gene was first proposed by Reddy and Day (2001), who used computer analysis and showed that *XIK* might consist of an open reading frame of 4638 base pairs containing 39 exons. *XIK* is regarded as being a 1521-amino-acid protein belonging to myosin class XI, composed of a short amino-terminal region, a conserved myosin motor domain, calmodulin binding IQ motifs followed by a coiled-coil domain, and a long carboxy-terminal tail region (Reddy and Day 2001).

To validate the predicted *XIK* gene structure (Reddy and Day 2001), two overlapping cDNA fragments (cDNA5'-1 and cDNA5'-2) corresponding to the 5' region of *XIK* were amplified, since the 3' region of *XIK* was covered by the EST clone AB01B09 (Fig. 1). Differences were observed between the predicted and isolated 5' regions of *XIK*

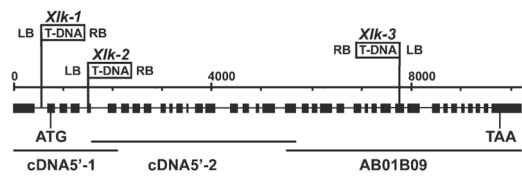


Fig. 1. Genomic structure of *XIK*. Black boxes indicate the localisation of exons. T-DNA insertions in mutant lines *Xik-1*, *Xik-2*, and *Xik-3* are marked in the first intron, 5th exon, and 29th exon, respectively. LB, left border; RB, right border of T-DNA. cDNA5'-1, cDNA5'-2, and AB01B09 designate two cDNA fragments and an EST clone, correspondingly

```
5' ATGAAGGAAACTGAGGAAATGCCAGTGTGTTGCTACTTTGTTGTGTTCTTA
Agtgagtggttctctctagattatagggcagtggttattgtcctggttttggcggaaatt
ttaaactctataaacattagttactcttogggttttaggttoggatgtctggtgccaatctatt
tcaactgcttgaactgatgataatttggattttgaagaggaacttatgtaaacagctt
gttgagggttattaaaactcttgtaccctcaoctcttcaaatatttgtatcttttggtag
gttggccocagTCAATATAAATAGTTGGTTCATGTTGGATTGAAGATCCTGGAGCG
GCATGGATTGATGGTGAAGTTGTCAAAATAATAGCCGAAGAGTTCATGCACATACC
ACAAATGGGAAGACCgtaagttgtctatcctcctcctccactgcttttgcagttaaattt
ccttttgagaataaattgtcaactggaatgaatagggtgtttctgcttaggtgtctgtt
ttaactttgaaacaaaatgtcaactagctctcctcctcctccactgcttttgcagttaaattt
taactcctcctcaacatgatgatttggcatgacatgacatccctatttcataattatata
tatacaatcattgaaccagattatgatacaatcaatcaaattaatttcaag
TTGTGGCAAATTCGCAACGTTATTCCAAAGGATACAGAGGCTCCCCTGGGGGTG
TTGATGACATGACAAAGCTCTCATATTTACATGAACCAGGCTTTTTGAAATAACTTGG
CCATGAGATATGAGTTGAACGAATTTAT... 3'
```

Fig. 2. Genomic structure of *XIK* 5' region. Sequences of exons and introns predicted by computational analysis are indicated with capital and lowercase letters, respectively. The sequence of the first experimentally proved exon is shadowed. Translation start site is boxed, in-frame stop codons are underlined

cDNA. Sequence analysis of the amplified cDNA fragments showed that the *XIK* gene was split by only 37 introns, while the first previously proposed intron proved to be part of the cDNA (Figs. 1 and 2). Thus, the first de facto exon of *XIK* included the first two exons and the first intron predicted computationally previously (Fig. 2). In addition, the new first exon contained 6 termination codons and therefore the putative translation start codon was shifted to the second de facto exon (Figs. 1 and 2). The calculated *XIK* resulted in a shorter protein, consisting of 1465 amino acid residues and retaining all the domains predicted previously, except the short amino-terminal region.

RT-PCR was performed to examine the expression pattern of *XIK* in WT plants. Our analysis revealed that *XIK* transcripts were present both in seedlings and in all the major organs of adult plants (roots, leaves, stems, flowers, and siliques) (Fig. 3). The ubiquitous expression pattern of *XIK* mRNA is supported by information from microarrays and EST databases (TAIR, www.arabidopsis.org).

Identification of *XIK* T-DNA insertional mutants

To describe genetically the functions of *XIK*, we characterised three different lines with a homozygous T-DNA in-

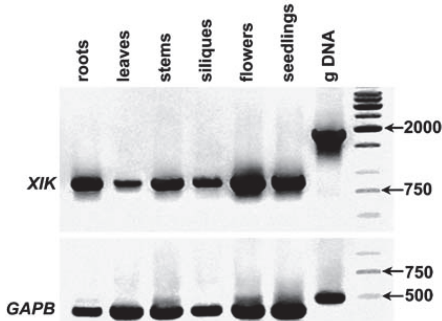


Fig. 3. RT-PCR analysis of *XIK* expression in different organs of adult plants and seedlings. Genomic DNA (*g DNA*) of WT *A. thaliana* and constitutively expressed B subunit of chloroplast glyceraldehyde-3-phosphate dehydrogenase (*GAPB*) were used as reaction controls

sertion in this gene: *Xik-1*, *Xik-2*, and *Xik-3* (Fig. 1). In the case of *Xik-1*, the T-DNA insertion resides in the first intron, while lines *Xik-2* and *Xik-3* carry the T-DNA insertions in the coding region (in the 5th and 29th exon, respectively) (Fig. 1). RT-PCR and Northern blot hybridization were performed to observe the effects of mutant background on the expression of *XIK* transcripts. Fragments of the *XIK*-specific transcript were detectable in both WT and mutant seedlings by RT-PCR analysis (data not shown). In contrast, Northern blot analysis showed the *XIK* transcript in WT plants only, but not in mutant lines (Fig. 4). The constitutively expressed *GAPB* of *A. thaliana* was used as loading control (Fig. 4). Results of the Northern blot analysis revealed only a weak signal for WT plants, suggesting that *XIK* is expressed at low levels, thus allowing the detection of truncated or defective transcripts by RT-PCR only. We concluded that although the RT-PCR analysis detected

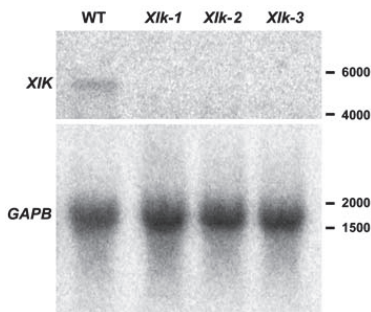


Fig. 4. Northern blot analysis of *XIK* transcripts in the total RNA isolated from WT and mutant plants. Constitutively expressed B subunit of chloroplast glyceraldehyde-3-phosphate dehydrogenase (*GAPB*) was used as a loading control

Xik transcripts in the T-DNA insertional lines, the phenotypic changes described below were most probably due to insufficient amounts of functional *XIK* gene products.

XIK involvement in tip growth of root hairs

The *Xik* mutant phenotype was first identified by screening the T-DNA-mutagenised seedlings for altered root growth phenotypes on inclined agar surfaces containing the culture medium with 1% sucrose. Three independent homozygous *Xik* mutant lines showed a normal root

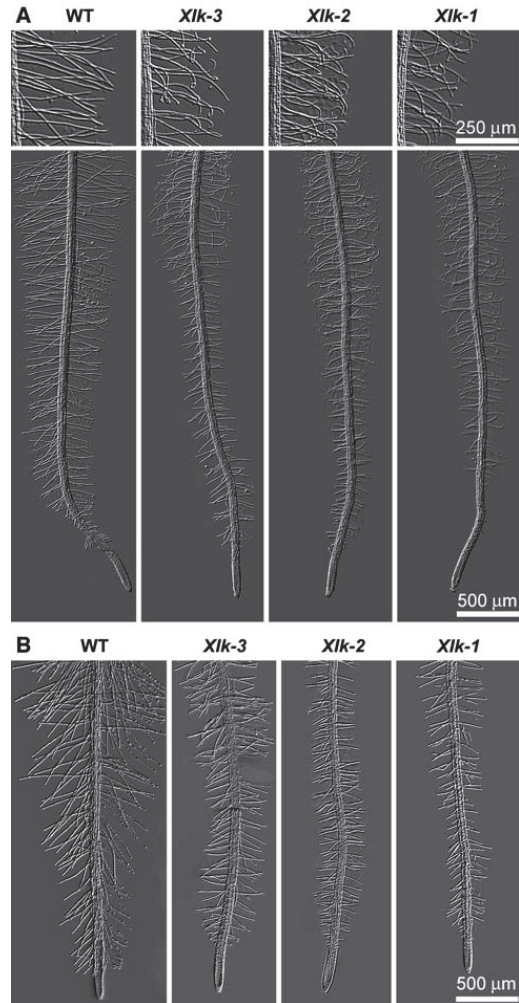


Fig. 5 A, B. Root hair morphology of WT and *Xik*⁻ plants. **A** Roots of 4-day-old seedlings grown in the MS medium with 1% sucrose. **B** Roots of 4-day-old seedlings grown in sucrose-free MS medium

growth rate when compared to WT plants. However, the morphology of root hair cells was different: the root hairs of all three T-DNA mutants were shorter than WT root hairs and had a hooked phenotype (Fig. 5A). A curled mutant root hair phenotype was apparent also when the culture medium contained 1% glucose (data not shown). Sugars are known as growth signalling factors and as carbon sources that promote germination and seedling development when added to the growth medium at low concentration (Leon and Sheen 2003). The hooked shape of XIK^- root hairs on the medium supplemented with sugar might be caused by inadequate transport of cell wall components in root hairs that are growing faster due to the presence of sugar.

Root hairs of seedlings of both WT and mutant plants grown in a sugar-free medium were straight (Fig. 5B). To gain quantitative information about the differences between WT and mutant root hairs, the length of all root hair cells of 4-day-old seedlings grown in a sugar-free medium was measured. Root hairs of all three *Xik* mutant lines were shorter than root hairs of WT plants in a sugar-free medium: the average root hair lengths of *Xik-3*, *Xik-2*, and *Xik-1* were 77, 50, and 49% of WT, respectively (Fig. 6A, B). Measurements of root hair growth rate showed that the difference between WT and mutants was caused by a slower tip growth of mutant root hairs from the very beginning of the cell's growth, after swelling formation. The growth rate of root hairs was approximately 30% decreased in mutant plants (Fig. 6C).

Root hairs as well as pollen tubes elongate by tip growth as new cell wall material is synthesised and precisely secreted to a single site on the cell surface – to the cell tip. The normal duration of tip growth, and hence, the normal length of root hairs requires a certain arrangement of microfilaments: longitudinally oriented actin cables along the length of the root hair, and a dense meshwork of fine actin filaments near the subapical region (Ketelaar et al. 2002, Miller et al. 1999). Indeed, loss-of-function and presumed partial-function mutations in the *A. thaliana* *ACTIN 2* (*ACT2*) gene (major actin of the vegetative tissue) produced defects in root hair growth. Different *ACT2* mutants, *act2-1* (Gilliland et al. 2002) and *deformed root hairs 1* (*der1*) (Ringli et al. 2002), have been reported to show a strong decrease in root hair length similar to that of the *Xik* mutant phenotype described in this paper. Additionally, *act2-1* and *der1* plants show enlarged basis and irregular diameter of root hairs (a phenotype not detected in *Xik* mutants). Therefore, it is proposed that *ACT2* is not only involved in the tip growth of root hairs but also required for the correct selection of the bulge site

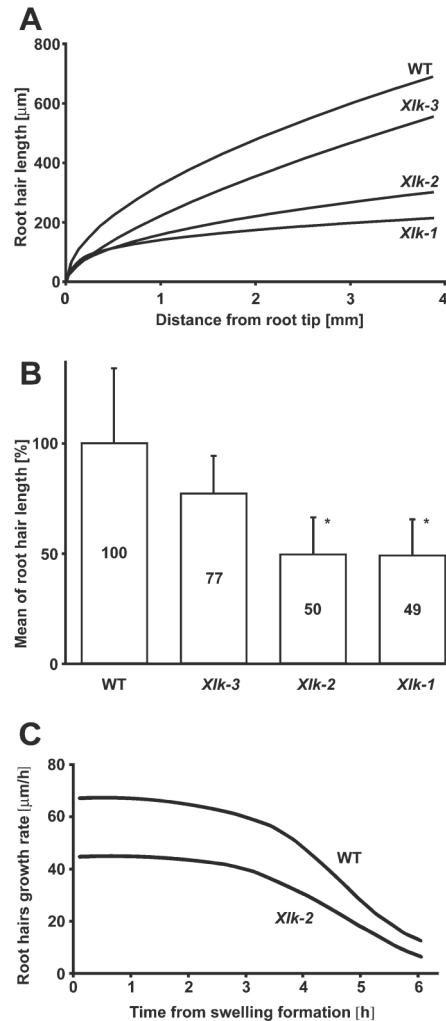


Fig. 6 A–C. Effects of *XIK* mutation on root hair length and rate of tip growth. **A** and **B** Root hair length of 4-day-old seedlings grown in the sucrose-free MS medium. Significant differences from WT ($P < 0.05$) are marked with asterisks. The number of individual root hairs measured is indicated in the bars. **C** Growth rates of WT and *Xik-2* root hair cells during fast tip growth

on the epidermal cell (Gilliland et al. 2002, Ringli et al. 2002). Our data indicate that myosin XIK is probably involved in the former but not in the latter process. Earlier studies have demonstrated that myosins most likely support tip growth by driving the movement of Golgi-derived vesicles along longitudinally oriented actin cables toward the tip and/or through the dense actin mesh from the sub-

apical region to the apex of the root hair (Boevink et al. 1998, Hepler et al. 2001). However, recent pharmacological experiments have shown that for early endosome motility, and thus for tip growth, actin polymerisation rather than direct myosin activity is needed (Voigt et al. 2005).

Our results, both the decreased length and the slower growth rate of XIK⁻ root hairs, support the idea that XIK is implicated in root hair development during tip growth. The possible role of myosin XIK in either long-range transport or in subapical transport of vesicles in root hair growth remains to be resolved.

Down-regulation or over-expression of several other actin-related proteins also affects root hair elongation. In

recent years, it has become evident that the actin-related protein2/3 complex (Arp2/3), needed for the nucleation of new actin filaments from the sides of existing actin filaments, is present in plants and has a role in plant epidermis morphogenesis (Mathur 2005). Among other disorders, mutation in the *DISTORTED1 (DIS1)* gene (coding *A. thaliana* ARP3 ortholog) causes mild differences in root hair phenotype, displaying relatively short, stubby root hairs with varying degrees of waviness (Mathur et al. 2003). Furthermore, Van Gestel et al. (2003) have shown that a putative plant Arp3 homolog immunolocalises to the tips of maize root hairs. Also, down-regulation of profilin (Ramachandran et al. 2000) and actin-interacting protein 1 (Ketelaar

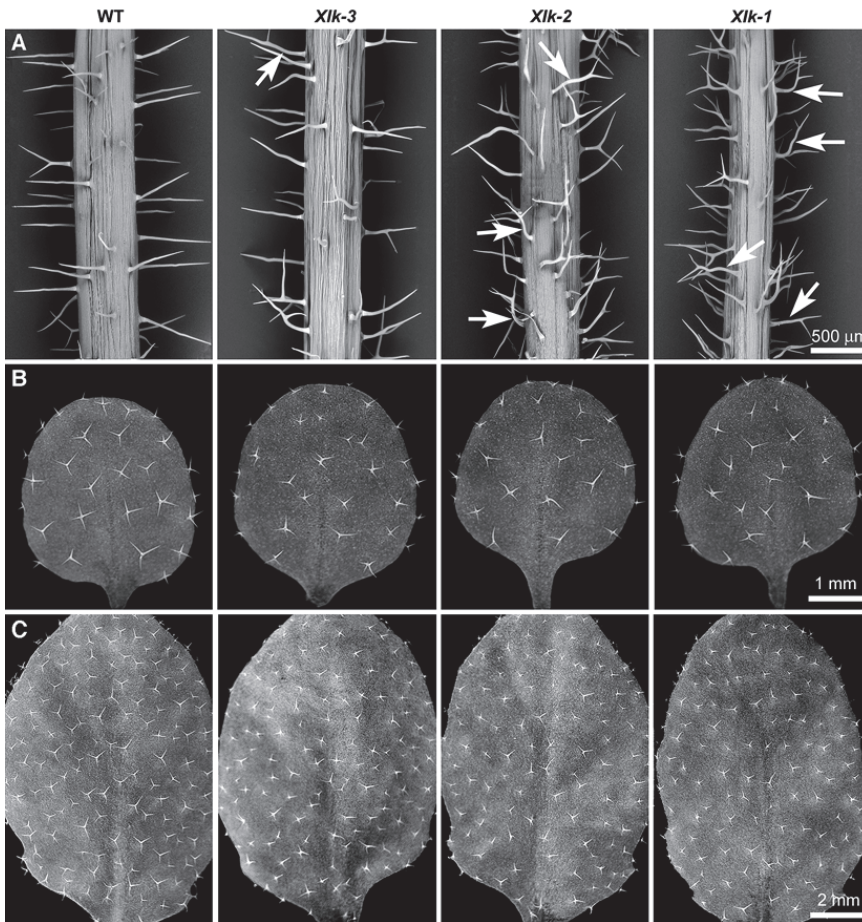


Fig. 7 A–C. Effects of *XIK* mutations on trichome morphology. **A** Scanning electron microscopy images of stem trichomes between the last vegetative leaf and the first cauline leaf from 8-week-old plants. Arrows indicate abnormally elongated trichome stalks. **B** First leaves from 2-week-old plants. **C** Rosette leaves from 6-week-old plants

et al. 2004) and over-expression of actin-depolymerising factor 1 (ADF1) (Dong et al. 2001) reduces the length of root hairs as well as the expansion of other cell types. Although these short root hair phenotypes are more or less similar to those in the *Xik* loss-of-function plants, the overall phenotype in these plants was different. Possible links between XIK, Arp2/3 complex, and ADF1 are further discussed below.

XIK involvement in development of stem and leaf trichomes

Root hairs represent only one of several epidermal cell fates; other cell types in the epidermis include unspecialised epidermal cells, stomatal guard cells, and trichomes. This fact served as motivation for a careful observation of epidermal cells of leaves and shoots of *Xik* loss-of-function plants.

The difference between WT and *Xik* mutant lines appeared in the morphology of trichomes both on stems and leaves. The changed phenotype was most obvious on the plant main stem and on mature rosette leaves. Branched and unbranched trichomes on the stems of all three *Xik* mutant lines were obviously crooked and wavy (Fig. 7A). In addition, stalks of branched stem trichomes were often abnormally elongated (2- to 3-fold) in T-DNA-mutagenised lines (Fig. 7A). The extent of the disturbed stem trichome phenotype was indistinguishable among the three different *Xik* mutant lines. The patterning and number of trichomes on the stems of WT and homozygous mutant plants was identical (data not shown).

Two types of abnormal phenotypes of leaf trichomes were detected in *Xik* mutants: irregular size and irregular shape. First, on the young and mature rosette leaves of *Xik* mutants, a larger proportion of small trichomes and a smaller proportion of large trichomes were observed (Fig. 7B, C). Mature rosette leaves with equal size and age were chosen to measure differences in branch lengths between the WT and mutant trichomes. All three *Xik* mutant lines had approximately two times more short (50–150 μm) trichome branches and two times less long (200–350 μm) trichome branches compared with the WT (Fig. 8). The proportion of short and long trichome branches on the young, 2-week-old leaves was similar (data not shown) to mature rosette leaves (Fig. 8). Again, the total number of trichomes did not differ from that of the WT (data not shown).

WT leaf trichomes normally consist of three or four branches of equal length symmetrically arranged on the top of the stalk. All three *Xik* lines had trichomes with a normal

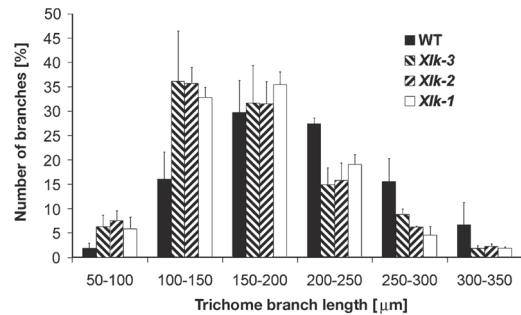


Fig. 8. Effects of *XIK* mutations on the distribution of leaf trichome branches with different lengths. Values are mean percentages (with standard deviation) of trichome branches in the indicated length categories. The numbers of individual branches measured for WT and *Xik*⁻ plants were the following: WT, 1240; *Xik3*, 554; *Xik2*, 609; *Xik1*, 1013

number of branches, but 30–60% of trichomes on leaves exhibited mild irregularities: twisted shape of branches (Fig. 9B–D), defects in branch length (Fig. 9B) and branch position (Fig. 9C) or presented all deviations together (Fig. 9D). A mildly twisted shape of branches was the most obvious defect of the *Xik* trichomes (Fig. 9B–D). *Xik* trichomes with an irregular branch length had typically one branch out of three or four branches clearly longer or shorter (Fig. 9B). The defects in the branching position of *Xik* trichomes were due to an abnormally elongated inter-branch zone (Fig. 9C) compared with the WT (Fig. 9A). In addition, mutant trichomes occasionally displayed mild swelling of stalk (Fig. 9B, C) or branches (data not shown). Compared with mutant plants, only 5–8% of trichomes on WT leaves showed twisted or irregular shape. As all the *Xik* lines represented the same phenotype, examples of trichome irregular shapes are given for *Xik-1* (Fig. 9).

Unlike root hairs, trichomes exhibit a coordinated diffuse expansion in which the incorporation of new cell wall material is broadly distributed across the cell surface. Both microtubules and microfilaments are important in trichome development: microtubules in trichome branching and microfilaments in the coordinated expansion of branches (Mathur et al. 1999, Szymanski et al. 1999, Szymanski 2000). The importance of the actin cytoskeleton in controlling the direction of trichome branch expansion has been shown by several genetic and pharmacological experiments. For example, the dominant negative mutant of ACT2, *act2-D*, exhibits trichome shape defects (wavy, irregularly elongated branches) among other dramatic disorders (Nishimura et al. 2003). Cytochalasin D, a filamentous-actin-disrupting drug, produces trichomes that phenocopy class *distorted* mutants, inhibiting coordinated

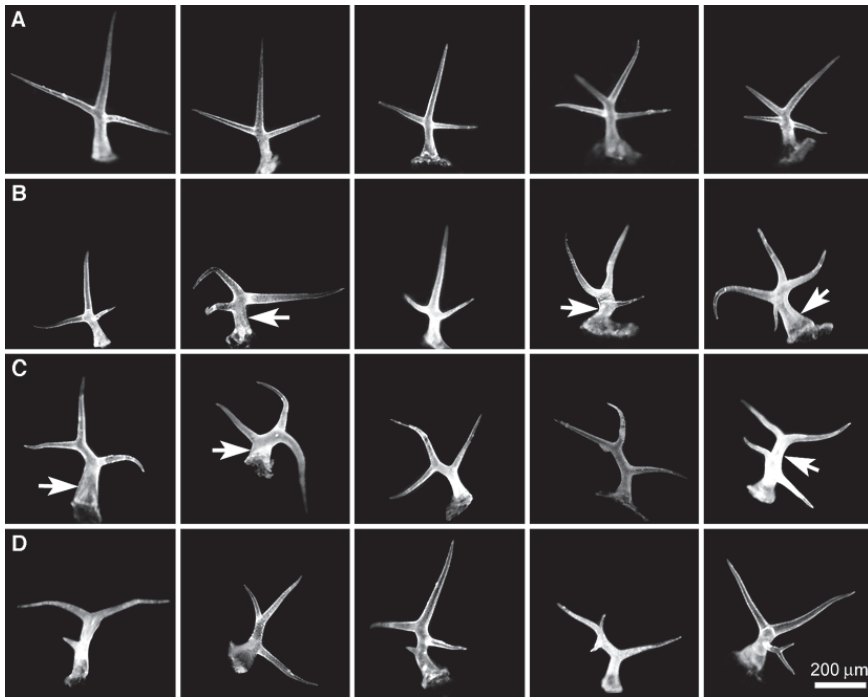


Fig. 9 A–D. Effects of *XIK* mutations on leaf trichome shape. **A** WT trichomes displaying symmetrical arrangement of branches. **B** *XIK-1* trichomes show irregular branch lengths. **C** *XIK-1* trichomes with abnormally elongated interbranch zone. **D** *XIK-1* trichomes showing irregular branch lengths and an elongated interbranch zone. Arrows indicate the mild swelling of the stalk

expansion of branches and stalks of trichomes (Mathur et al. 1999, Szymanski et al. 1999, Szymanski 2000). It is known that several *DISTORTED* genes encode proteins needed for proper actin filament organisation: subunits of Arp2/3 complex (Li et al. 2003, Mathur et al. 2003) and subunits of Arp2/3 activator complex Scar/WAVE (suppressor of cyclic AMP receptor/WASp family verpulin-homologs protein) (Basu et al. 2005, Zhang et al. 2005). Trichomes on the stems and leaves of homozygous T-DNA insertion mutants of some Arp2/3 complex subunits had a strongly stunted branch outgrowth and unrestricted stalk expansion (Li et al. 2003). Scar/WAVE subunit SCAR2 mutants *irregular trichome branch 1* (*itb1*) and *distorted3* (*dis3*) have trichome morphology defects, similar (although less severe) to those observed in the Arp2/3 complex subunit mutants (Basu et al. 2005, Zhang et al. 2005). The irregular phenotype of *Xik* leaf and stem trichomes is basically similar, being less serious compared with the Arp2/3 complex subunit mutants, but phenocopying clearly *dis3* mutant trichomes defined as “trichomes with mild phenotype” (Basu et al. 2005). Interestingly, *A.*

thaliana plants over-expressing ADF1 (Dong et al. 2001) share a similar phenotype. In addition to the reduced length of root hairs, these plants frequently have trichomes with curved and shortened branches (Dong et al. 2001). Our data show that class XI myosin, XIK, is required for proper expansion of trichome branches and stalks, maybe through interactions with actin nucleation and polymerisation machinery.

Phenotypic changes similar to those discussed above were observed in three independent mutant lines, meaning that the phenotypes result from the disruption of the *XIK* gene and not from the secondary effects of T-DNA insertion. Although *Xik* mutants displayed changes in the morphology of certain specialised epidermal cells (root hairs and trichomes), the overall plant architecture was normal in all of the three lines analysed.

Conclusions

We have elucidated the correct gene organisation for the *A. thaliana* myosin *XIK* gene and shown that this gene is

expressed ubiquitously, although at low levels. The phenotypic changes of *Xik* loss-of-function plants described in the present work indicate that *A. thaliana* myosin XIX is required both for the tip growth of root hairs and for the coordinated expansion of trichome branches and stalks.

The epidermis-related phenotype of *Xik* mutants is similar to the morphology found in different mutants where proper microfilament organisation and dynamics are disturbed. The *Xik*⁻ root hair phenotype was similar to the phenotypes found in *act2-1* (Gilliland et al. 2002) and *der1* mutants (Ringli et al. 2002) and in ADF1-over-expressing plants (Dong et al. 2001). Focusing on the trichome disorders, *Xik* mutants copy the mild phenotype of *dis3* trichomes (Basu et al. 2005) and ADF1-over-expressing plants (Dong et al. 2001). It is tempting to speculate that myosin XIX might be involved in the tip growth of root hairs as well as in the diffuse growth of trichomes through its direct or indirect interaction with the actin nucleating machinery. Indeed, it has been demonstrated that at least yeast myosin-1 has a role in actin assembly through interactions with the Arp2/3 complex (Evangelista et al. 2000, Lee et al. 2000, Sirotkin et al. 2005). At the same time, this does not rule out the possibility that XIX is also involved in the vesicular transport in these epidermal cells, a role proposed for myosins at least in the tip-growing cells (Hepler et al. 2001).

Acknowledgments

We thank M. Toomet (Estonian Forensic Service Centre) for help in SEM imaging; H. J. Bohnert for the EST clone; F. Baluška and D. Volkman for helpful discussions; the Salk Institute Genomic Analysis Laboratory for providing the sequence-indexed *A. thaliana* T-DNA insertion mutants; the ABRC/NASC Stock Centre for seeds; I. Altsaar, B. Ilau, C. Sarmiento, and M.-A. Laane for critical reading of the manuscript, and S. Nõu for excellent plant care. The work was supported by Estonian Science Foundation grants 5939 and 6559.

References

Alonso JM, Stepanova AN, Leisse TJ, Kim CJ, Chen H, Shinn P, Stevenson DK, Zimmerman J, Barajas P, Cheuk R, Gadrinab C, Heller C, Jeske A, Koesema E, Meyers CC, Parker H, Prednis L, Ansari Y, Choy N, Deen H, Geralt M, Hazari N, Hom E, Karnes M, Mulholland C, Ndubaku R, Schmidt I, Guzman P, Aguilar-Henonin L, Schmid M, Weigel D, Carter DE, Marchand T, Risseeuw E, Brogden D, Zeko A, Crosby WL, Berry CC, Ecker JR (2003) Genome-wide insertional mutagenesis of *Arabidopsis thaliana*. *Science* 301: 653–657

Baluška F, Barlow PW, Volkman D (2000) Actin and myosin VIII in developing root apex cells. In: Staiger CJ, Baluška F, Volkman D, Barlow PW (eds) Actin: a dynamic framework for multiple plant cell functions. Kluwer Academic, Dordrecht, pp 457–476

Baluška F, Cvrckova F, Kendrick-Jones J, Volkman D (2001) Sink plasmodesmata as gateways for phloem unloading. Myosin VIII and cal-

reticulum as molecular determinants of sink strength? *Plant Physiol* 126: 39–46

Basu D, Le J, El-Essal SEI-D, Huang S, Zhang C, Mallery EL, Koliantz G, Staiger CJ, Szymanski DB (2005) DISTORTED3/SCAR2 is a putative *Arabidopsis* WAVE complex subunit that activates the Arp2/3 complex and is required for epidermal morphogenesis. *Plant Cell* 17: 502–524

Boevink P, Oparka K, Santa Cruz S, Martin B, Betteridge A, Hawes C (1998) Stacks on tracks: the plant Golgi apparatus traffics on an actin/ER network. *Plant J* 15: 441–447

Braun M, Buchen B, Sievers A (2002) Actomyosin-mediated statolith positioning in gravisensing plant cells studied in microgravity. *J Plant Growth Regul* 21: 137–145

Cope MJ, Whisstock J, Rayment I, Kendrick-Jones J (1996) Conservation within the myosin motor domain: implications for structure and function. *Structure* 4: 969–987

Dellaporté SL, Wood J, Hicks JB (1983) A plant DNA miniprep, version II. *Plant Mol Biol Rep* 1: 19–21

Dong CH, Xia GX, Hong Y, Ramachandran S, Kost B, Chua NH (2001) ADF proteins are involved in the control of flowering and regulate F-actin organization, cell expansion, and organ growth in *Arabidopsis*. *Plant Cell* 13: 1333–1346

Evangelista M, Klebl BM, Tong AH, Webb BA, Leeuw T, Leberer E, Whiteway M, Thomas DY, Boone C (2000) A role for myosin-I in actin assembly through interactions with Vrp1p, Bee1p, and the Arp2/3 complex. *J Cell Biol* 148: 353–362

Gilliland LU, Kandasamy MK, Pawloski LC, Meagher RB (2002) Both vegetative and reproductive actin isoforms complement the stunted root hair phenotype of the *Arabidopsis act2-1* mutation. *Plant Physiol* 130: 2199–2209

Hashimoto K, Igarashi H, Mano S, Nishimura M, Shimmen T, Yokota E (2005) Peroxisomal localization of a myosin XI isoform in *Arabidopsis thaliana*. *Plant Cell Physiol* 46: 782–789

Hepler PK, Vidali L, Cheung AY (2001) Polarized cell growth in higher plants. *Annu Rev Cell Dev Biol* 17: 159–187

Hodge T, Cope MJ (2000) A myosin family tree. *J Cell Sci* 113: 3353–3354

Hoffmann A, Nebenführ A (2004) Dynamic rearrangements of transvacuolar strands in BY-2 cells imply a role of myosin in remodeling the plant actin cytoskeleton. *Protoplasma* 224: 201–210

Holweg C, Nick P (2004) *Arabidopsis* myosin XI mutant is defective in organelle movement and polar auxin transport. *Proc Natl Acad Sci USA* 101: 10488–10493

Jiang S, Ramachandran S (2004) Identification and molecular characterization of myosin gene family in *Oryza sativa* genome. *Plant Cell Physiol* 45: 590–599

Kamiya N, Kuroda K (1956) Velocity distribution of the protoplasmic streaming in *Nitella* cells. *Bot Mag Tokyo* 69: 544–554

Ketelaar T, Faivre-Moskalenko C, Esseling JJ, De Ruijter NC, Grierson CS, Dogterom M, Emons AM (2002) Positioning of nuclei in *Arabidopsis* root hairs: an actin-regulated process of tip growth. *Plant Cell* 14: 2941–2955

Ketelaar T, Allwood EG, Anthony R, Voigt B, Menzel D, Hussey PJ (2004) The actin-interacting protein AIP1 is essential for actin organization and plant development. *Curr Biol* 14: 145–149

Lee WL, Bezanilla M, Pollard TD (2000) Fission yeast myosin-I, Myo1p, stimulates actin assembly by Arp2/3 complex and shares functions with WASp. *J Cell Biol* 151: 789–800

Leon P, Sheen J (2003) Sugar and hormone connections. *Trends Plant Sci* 8: 110–116

Li S, Blanchoin L, Yang Z, Lord EM (2003) The putative *Arabidopsis* Arp2/3 complex controls leaf cell morphogenesis. *Plant Physiol* 132: 2034–2044

Liebe S, Menzel D (1995) Actomyosin-based motility of endoplasmic reticulum and chloroplasts in *Vallisneria* mesophyll cells. *Biol Cell* 85: 207–222

- Liebe S, Quader H (1994) Myosin in onion (*Allium cepa*) bulb scale epidermal cells: involvement in dynamics of organelles and endoplasmic reticulum. *Physiol Plant* 90: 114–124
- Liu L, Zhou J, Pesacreta TC (2001) Maize myosins: diversity, localization, and function. *Cell Motil Cytoskeleton* 48: 130–148
- Logemann J, Schell J, Willmitzer L (1987) Improved method for the isolation of RNA from plant tissues. *Anal Biochem* 163: 16–20
- Mathur J (2005) The ARP2/3 complex: giving plant cells a leading edge. *Bioessays* 27: 377–387
- Mathur J, Spielhofer P, Kost B, Chua N (1999) The actin cytoskeleton is required to elaborate and maintain spatial patterning during trichome cell morphogenesis in *Arabidopsis thaliana*. *Development* 126: 5559–5568
- Mathur J, Mathur N, Kernebeck B, Hülskamp M (2003) Mutations in actin-related proteins 2 and 3 affect cell shape development in *Arabidopsis*. *Plant Cell* 15: 1632–1645
- Mermall V, Post PL, Mooseker MS (1998) Unconventional myosins in cell movement, membrane traffic, and signal transduction. *Science* 279: 527–533
- Miller DD, De Ruijter NCA, Bisseling T, Emons AMC (1999) The role of actin in root hair morphogenesis: studies with lipochito-oligosaccharide as a growth stimulator and cytochalasin as an actin perturbing drug. *Plant J* 17: 141–154
- Nishimura T, Yokota E, Wada T, Shimmen T, Okada K (2003) An *Arabidopsis* ACT2 dominant-negative mutation, which disturbs F-actin polymerization, reveals its distinctive function in root development. *Plant Cell Physiol* 44: 1131–1140
- Ramachandran S, Christensen HE, Ishimaru Y, Dong CH, Chao-Ming W, Cleary AL, Chua NH (2000) Profilin plays a role in cell elongation, cell shape maintenance, and flowering in *Arabidopsis*. *Plant Physiol* 124: 1637–1647
- Reddy AS, Day IS (2001) Analysis of the myosins encoded in the recently completed *Arabidopsis thaliana* genome sequence. *Genome Biol* 2: research0024
- Reichelt S, Kendrick-Jones J (2000) Myosins. In: Staiger CJ, Baluška F, Volkmann D, Barlow PW (eds) *Actin: a dynamic framework for multiple plant cell functions*. Kluwer Academic, Dordrecht, pp 29–44
- Reichelt S, Knight AE, Hodge TP, Baluška F, Šamaj J, Volkmann D, Kendrick-Jones J (1999) Characterization of the unconventional myosin VIII in plant cells and its localization at the post-cytokinetic cell wall. *Plant J* 19: 555–567
- Ringli C, Baumberger N, Diet A, Frey B, Keller B (2002) ACTIN2 is essential for bulge site selection and tip growth during root hair development of *Arabidopsis*. *Plant Physiol* 129: 1464–1472
- Sakamoto T, Wang F, Schmitz S, Xu Y, Xu Q, Molloy JE, Veigel C, Sellers JR (2003) Neck length and processivity of myosin V. *J Biol Chem* 278: 29201–29207
- Sambrook J, Russell DW (2001) *Molecular cloning: a laboratory manual*. Cold Spring Harbor Laboratory Press, New York
- Shimmen T, Yokota E (1994) Physiological and biochemical aspects of cytoplasmic streaming. *Int Rev Cytol* 155: 97–139
- Sirotkin V, Beltzner CC, Marchand JB, Pollard TD (2005) Interactions of WASp, myosin-I, and verprolin with Arp2/3 complex during actin patch assembly in fission yeast. *J Cell Biol* 170: 637–648
- Szymanski D (2000) The role of actin during *Arabidopsis* trichome morphogenesis. In: Staiger CJ, Baluška F, Volkmann D, Barlow PW (eds) *Actin: a dynamic framework for multiple plant cell functions*. Kluwer Academic, Dordrecht, pp 391–410
- Szymanski DB, Marks MD, Wick SM (1999) Organized F-actin is essential for normal trichome morphogenesis in *Arabidopsis*. *Plant Cell* 11: 2331–2348
- Tominaga M, Kojima H, Yokota E, Orii H, Nakamori R, Katayama E, Anson M, Shimmen T, Oiwa K (2003) Higher plant myosin XI moves processively on actin with 35 nm steps at high velocity. *EMBO J* 22: 1263–1272
- Uyeda TQP, Abramson PD, Spudich JA (1996) The neck region of the myosin motor domain acts as a lever arm to generate movement. *Proc Natl Acad Sci USA* 93: 4459–4464
- Van Gestel K, Kohler RH, Verbelen JP (2002) Plant mitochondria move on F-actin, but their positioning in the cortical cytoplasm depends on both F-actin and microtubules. *J Exp Bot* 53: 659–667
- Van Gestel K, Slegers H, Von Witsch M, Šamaj J, Baluška F, Verbelen JP (2003) Immunological evidence for the presence of plant homologues of the actin-related protein Arp3 in tobacco and maize: subcellular localization to actin-enriched pit fields and emerging root hairs. *Protoplasma* 222: 45–52
- Voigt B, Timmers AC, Šamaj J, Hlavačka A, Ueda T, Preuss M, Nielsen E, Mathur J, Emans N, Stenmark H, Nakano A, Baluška F, Menzel D (2005) Actin-based motility of endosomes is linked to the polar tip growth of root hairs. *Eur J Cell Biol* 84: 609–621
- Yamashita RA, Sellers JR, Anderson JB (2000) Identification and analysis of the myosin superfamily in *Drosophila*: a database approach. *J Muscle Res Cell Motil* 21: 491–505
- Zhang X, Dyachok J, Krishnakumar S, Smith LG, Oppenheimer DG (2005) *IRREGULAR TRICHOME BRANCH1* in *Arabidopsis* encodes a plant homolog of the actin-related protein2/3 complex activator Scar/WAVE that regulates actin and microtubule organization. *Plant Cell* 17: 2314–2326

Publication II

Ojangu E.-L., Tanner K., Pata P., Järve K., Holweg CL., Truve E., Paves H. (2012). Myosins XI-K, XI-1, and XI-2 are required for development of pavement cells, trichomes, and stigmatic papillae in *Arabidopsis*. *BMC Plant Biol.* 12:81.

RESEARCH ARTICLE

Open Access

Myosins XI-K, XI-1, and XI-2 are required for development of pavement cells, trichomes, and stigmatic papillae in *Arabidopsis*

Eve-Ly Ojangu^{1*}, Krista Tanner¹, Pille Pata¹, Kristel Järve¹, Carola L Holweg², Erkki Truve¹ and Heiti Paves¹

Abstract

Background: The positioning and dynamics of vesicles and organelles, and thus the growth of plant cells, is mediated by the acto-myosin system. In *Arabidopsis* there are 13 class XI myosins which mediate vesicle and organelle transport in different cell types. So far the involvement of five class XI myosins in cell expansion during the shoot and root development has been shown, three of which, XI-1, XI-2, and XI-K, are essential for organelle transport.

Results: Simultaneous depletion of *Arabidopsis* class XI myosins XI-K, XI-1, and XI-2 in double and triple mutant plants affected the growth of several types of epidermal cells. The size and shape of trichomes, leaf pavement cells and the elongation of the stigmatic papillae of double and triple mutant plants were affected to different extent. Reduced cell size led to significant size reduction of shoot organs in the case of triple mutant, affecting bolt formation, flowering time and fertility. Phenotype analysis revealed that the reduced fertility of triple mutant plants was caused by delayed or insufficient development of pistils.

Conclusions: We conclude that the class XI myosins XI-K, XI-1 and XI-2 have partially redundant roles in the growth of shoot epidermis. Myosin XI-K plays more important role whereas myosins XI-1 and XI-2 have minor roles in the determination of size and shape of epidermal cells, because the absence of these two myosins is compensated by XI-K. Co-operation between myosins XI-K and XI-2 appears to play an important role in these processes.

Background

The size, shape and growth of plant organs are regulated by genetic and environmental factors [1]. There are several excellent systems in *Arabidopsis* to study epidermal cell development, root hairs, pavement cells, and trichomes are well-studied model systems to investigate the mechanisms of cell growth and morphogenesis [2]. Studies have shown that cytoskeletal dynamics, vesicle transport, small GTPase signaling and endoreduplication all play a role in the development of the specialized shapes of different epidermal cell types. Some mechanisms that determine cell shape and polarity are common between these cell types, while some remain specific to each [3].

Myosins are molecular motors that carry cargo along actin filaments. The actomyosin system plays a crucial role in regulating cellular structures and dynamics [4]. Phylogenetic analysis has revealed that the 17 myosin genes present in the *Arabidopsis* genome fall into two classes: class VIII containing 4 genes and class XI containing 13 genes [5-8]. Class VIII myosins are implicated in new cell wall formation, intercellular transport through plasmodesmata and endocytosis [9-13]. Immunolocalization and co-localization experiments have indicated that class XI myosins are involved in the movement of vesicles and organelles [14-17]. Studies using T-DNA mutant lines, RNA interference or overexpression of dominant-negative myosin forms have confirmed that particular class XI myosins are required for movement of Golgi stacks, mitochondria and peroxisomes [7,18-22]. A novel role in regulation of the actin cytoskeleton and ER dynamics has been shown for class XI myosins [22,23]. In addition, phenotype analysis of T-

* Correspondence: eve-ly.ojangu@ttu.ee

¹Department of Gene Technology, Tallinn University of Technology, Akadeemia tee 15, 12618 Tallinn, Estonia
Full list of author information is available at the end of the article

DNA insertional mutants in each of the 13 class XI myosins has shown that only two class XI myosins are important for normal development of specific epidermal cells: XI-K and XI-2 are required for the tip growth of root hairs and XI-K also plays a role in diffuse growth of trichomes [19,24]. Since mutants in only two of the 13 class XI myosin genes have a distinct phenotype, it has been proposed that the functions of class XI myosins are partially overlapping [19,20]. This hypothesis has been largely proven by phenotype analysis of double, triple and quadruple mutants, which showed that five class XI myosins (XI-1, XI-2, XI-K, XI-B and XI-I) exhibit varying degrees of functional redundancy in *Arabidopsis* [20,22]. Simultaneous inactivation of these myosins in triple and quadruple mutants influenced overall plant growth and fertility, affecting shoot development even more than root development. Triple and quadruple mutant lines exhibited dwarf rosette growth, reduced plant height, late flowering phenotype, reduced fertility and also reduced growth of roots and root hairs. It is now thought that vegetative development of *Arabidopsis* relies on the four myosins (XI-K, XI-2, XI-1, XI-I) and that organelle transport driven by these myosin motors is required both for polarized growth as well as for diffuse growth of plant cells [22].

Myosins represent only one of many different types of actin binding proteins. Actin binding proteins are specialized to regulate dynamics and organization of the actin cytoskeleton. Mutants of these proteins have a wide range of phenotypes. A common characteristic of these mutants is irregular expansion and shape of trichomes, leaf pavement cells, and epidermal cells of the hypocotyl and root [25-28]. A group of mutants, named *distorted*, were initially identified based on a distorted or irregular trichome phenotype. These plants carry mutations in genes coding actin polymerization regulating proteins, like components of ARP2/3 [29,30] and SCAR/WAVE complexes [31-34]. Trichomes of these mutants are smaller, bloated and misshapen due to aberrant

expansion of the stalk and branches [29,30,33,35-38]. Two other phenotypically similar mutants, identified as weak *distorted* mutants are myosin mutant *xi-k* and the WD40/BEACH domain protein mutant *spirrig*. The trichome phenotype of *spirrig* mutants is weaker compared to other *distorted* mutants and the phenotype of *xi-k* in turn is weaker than that of *spirrig* mutants. Partial phenotypic overlap with *distorted* mutants indicated that XI-K and SPIRRIG could be involved in similar growth processes of certain epidermal cells as are ARP2/3 and/or SCAR/WAVE complex proteins [24,39].

To reveal the detailed functions of myosins XI-K, XI-1 and XI-2 in growth and development of epidermal cells we analyzed double and triple T-DNA insertional mutants of these myosins. The results of this current work show that these three myosins contribute to the development of different epidermal cells - not only to the growth of root hairs and leaf pavement cells, but also to the coordinated expansion of trichomes and elongation of the stigmatic papillae. Simultaneous depletion of all three myosins resulted in dwarf growth, delay in bolting and flower development and reduced fertility. Our results indicated that the reduced fertility of triple mutant plants was caused by delayed or insufficient development of floral organs. This manifested in insufficiently developed pistils that were not fully receptive for pollination. Our results also indicate that myosin XI-K plays a more important role in the determination of epidermal cell size and shape than the other two myosins examined.

Results

Myosins XI-1, XI-2 and XI-K have overlapping roles in regulating shoot size

Double mutant lines *xi-1/xi-2*, *xi-1/xi-k*, *xi-2/xi-k* and triple mutant line *xi-1/xi-2/xi-k* were generated, and the genotype combinations were identified by PCR. Single mutant lines used for crossings were analyzed by RT-PCR to confirm the presence or lack of myosin mRNAs

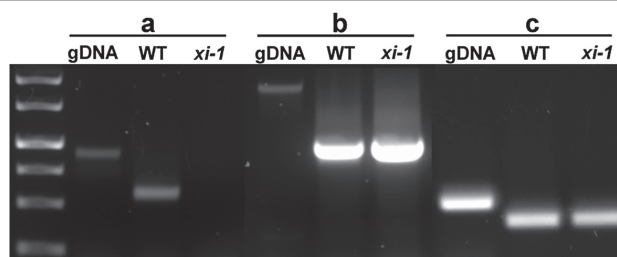


Figure 1 RT-PCR analysis of the *XI-1* T-DNA insertional line Salk_022140. Two different primer pairs were used to amplify two regions within the *XI-1* mRNA: **a** - primers spanning the T-DNA insertion site; **b** - primers for downstream region of the T-DNA insertion site; **c** - control amplified with *GAPB* primers. gDNA - genomic DNA; WT - wild type.

in each mutant. When primers downstream of the T-DNA insertion site were used for RT-PCR, the respective myosin transcript was absent in *xi-2* (data not shown; see [19]), present in *xi-1* (Figure 1) and present in *xi-k* (data not shown; see [19,24]) mutants. When primers spanning the T-DNA insertion site were used, none of the mutant lines produced any transcript (see Figure 1 for *xi-1*). It has been shown previously that no XI-K protein is produced in the *xi-k* mutant, although the corresponding mRNA was present [19]. In *xi-1* mutant, the T-DNA is inserted into the coding region; thus, we assumed that no functional XI-1 protein can be produced in this single mutant as well as in respective double and triple mutant plants. A schematic diagram shows T-DNA insertion sites for mutant lines *xi-1*, *xi-2* and *xi-k* (see Additional file 1).

To uncover the possible functions of myosins XI-1, XI-2 and XI-K in development of various epidermal cell types, we analyzed the overall phenotype of respective double and triple mutant plants. *xi-2/xi-k* double mutants had a slightly decreased rosette size while *xi-1/xi-2/xi-k* triple mutants showed more reduced rosette size (Figure 2A). Rosette size of all single mutants and the double mutants *xi-1/xi-2* and *xi-1/xi-k* was similar to that of wild type and was not investigated further. Rosettes of *xi-2/xi-k* and *xi-1/xi-2/xi-k* were investigated in more detail and both the leaf size as well as the cell area of rosette leaves was measured. Leaf size measurements showed that average length of *xi-2/xi-k* leaf blade was similar to wild type and for *xi-1/xi-2/xi-k* it was 21% ($p < 0.01$) smaller (Figure 2B; Additional file 2). The average width of the leaf blade of *xi-2/xi-k* and *xi-1/xi-2/xi-k* was comparable with wild type. The average length of *xi-2/xi-k* and *xi-1/xi-2/xi-k* petioles was 24% ($p < 0.01$) and 40% ($p < 0.01$) shorter than in wild type, respectively (Figure 2B; Additional file 2). Cell size measurements revealed that pavement cell area of *xi-2/xi-k* and *xi-1/xi-2/xi-k* plants was reduced by 17% ($p < 0.05$) and 35% ($p < 0.01$) and mesophyll cell area by 9% and 20%, respectively (Figure 2C, Additional file 3). In addition, we found that pavement cells of *xi-1/xi-2/xi-k* leaves had slightly less expanded lobes than those of wild type (Figure 2D). Circularity as a quantitative descriptor of cell shape complexity has been used for characterization of several cell types in plants. A perfect circle has the circularity equal to 1.0 and a cell with many deep lobes would have the circularity closer to 0 [40-42]. To characterize the shape of pavement cells, Image-J based circularity value of wild type and *xi-1/xi-2/xi-k* cells of the 5th and 6th rosette leaf was calculated. The average circularity of wild type and *xi-1/xi-2/xi-k* pavement cells was 0.041 and 0.139 ($p < 0.0001$), respectively (Figure 2E, Additional file 4), meaning that the pavement cells of the triple mutant are more round.

The results confirmed that myosins XI-1, XI-2 and XI-K have overlapping roles in shoot development, and that myosins XI-K and XI-2 are more important in this process than the XI-1.

We also noted that both bolt formation and onset of flowering of *xi-1/xi-2/xi-k* plants was delayed for two weeks on average (Additional file 5). In addition, the flowering time of *xi-2/xi-k* plants was occasionally delayed for about a week (data not shown). The average height of the inflorescence shoots of *xi-2/xi-k* and *xi-1/xi-2/xi-k* plants was reduced 9% and 17% ($p < 0.001$), respectively, when compared to wild type (Additional file 6). In addition, the growth of root hairs of double and triple mutant plants was decreased in a similar manner as described previously [20,22] (data not shown).

Distorted trichome phenotype of *xi-k* is amplified in double and triple mutant plants

We have previously shown that myosin mutant *xi-k* partially phenocopies the mild trichome phenotype of *distorted* mutants [24]. Therefore leaf trichomes of myosin double and triple mutant plants were examined. Two parameters were followed to characterize trichomes - cell size and shape. For the size analysis, the length of trichome branches and the height of stalk was measured. The branch length and stalk height in *xi-1* and *xi-2* was similar to wild type (Figure 3A, Additional file 7). The average length of *xi-k* trichome branches was 83% of wild type but the height of the stalk was similar to wild type (Figure 3A, Additional file 7). Size measurements showed that trichomes of *xi-1/xi-2* were comparable with wild type. Trichome branch length of *xi-1/xi-k* was 79% of wild type and comparable with *xi-k*. The length of trichome branches of *xi-2/xi-k* and *xi-1/xi-2/xi-k* plants was 70% ($p < 0.001$) and 40% ($p < 0.001$) of wild type, respectively (Figure 3A, Additional file 7). In contrast, trichome stalks of *xi-1/xi-k* and *xi-2/xi-k* were abnormally elongated compared to wild type. The average height of trichome stalks in *xi-1/xi-k*, and *xi-2/xi-k* were 126% ($p < 0.001$) and 143% ($p < 0.001$) of wild type, respectively (Figure 3A, Additional file 7). The stalk height of *xi-1/xi-2/xi-k* trichomes was similar to wild type. The calculation of the branch and stalk length ratios revealed that in wild type, *xi-1*, *xi-2*, *xi-k* and *xi-1/xi-2* the stalk height constituted approximately half of the branch length (ratio values from 2.1 to 2.8; Figure 3B; Additional file 8). In *xi-1/xi-k* and *xi-2/xi-k*, the trichome stalks were abnormally elongated, and the height of trichome stalk constituted 70% ($p < 0.001$) and 90% ($p < 0.001$) of branch length, respectively (length ratios between 1.3 and 1.5; Figure 3B; Additional file 8). In the case of triple mutant, the length of trichome branches was decreased dramatically and the average height of trichome stalk was equal or slightly longer than the

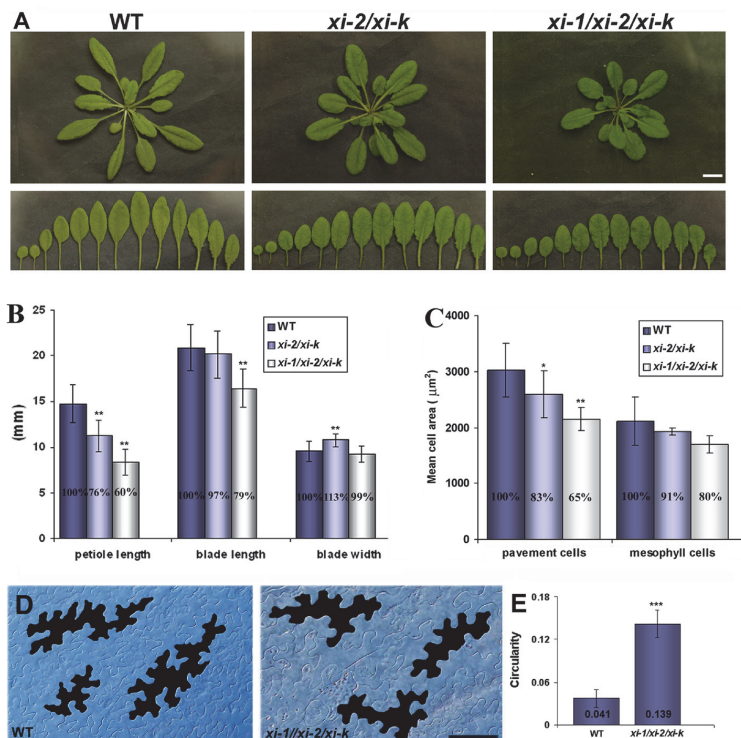
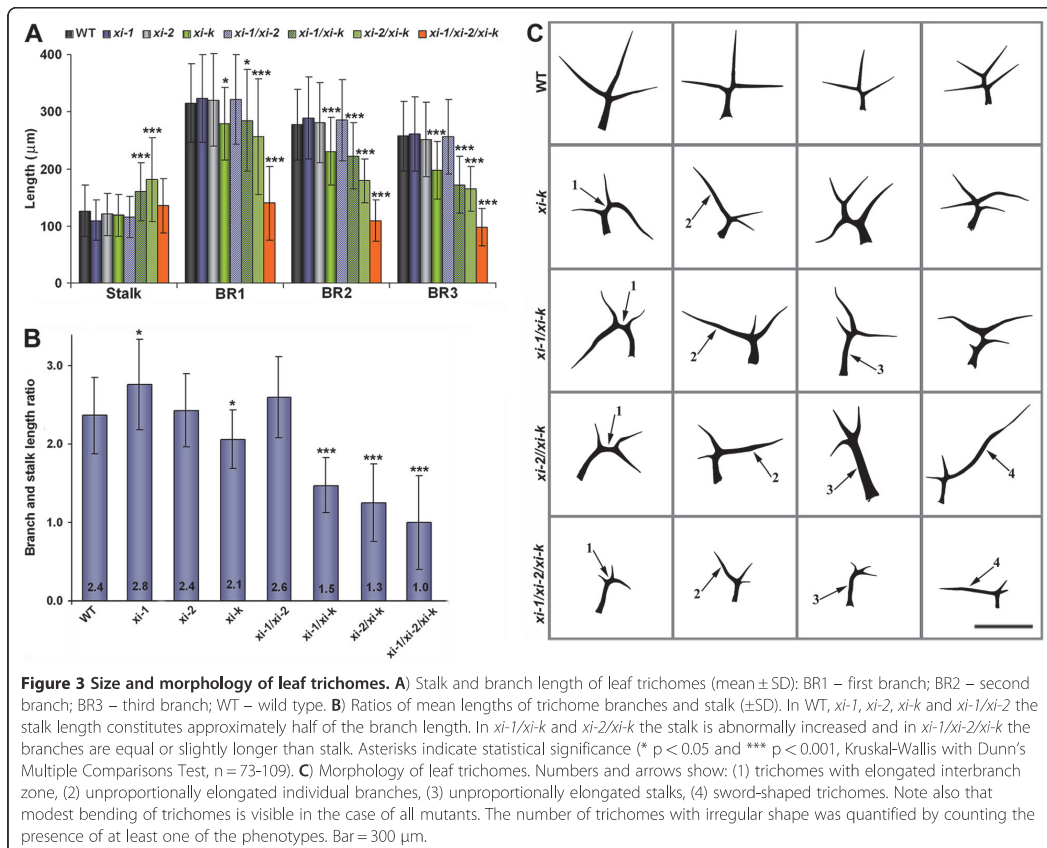


Figure 2 Leaf and cell size. **A)** Size of the rosette leaves of five-week-old plants. Rosette leaves of *xi-2/xi-k* and *xi-1/xi-2/xi-k* in comparison with wild type (WT). Leaves on the lower panel originate from the rosettes on upper panel. Bar = 10 mm. **B)** Mean size of leaf blades and petioles (\pm SD). The 5th to 10th rosette leaves were used for the size measurements. Note shorter petioles and smaller leaf blades of the *xi-2/xi-k* and *xi-1/xi-2/xi-k* plants in comparison with WT. Asterisks indicate statistical significance (** $p < 0.01$, Repeated Measures ANOVA with Dunn's Multiple Comparisons Test, $n = 18$). **C)** Mean cell areas of pavement and mesophyll cells of five-week-old rosette leaves (\pm SD). In the case of *xi-2/xi-k* and *xi-1/xi-2/xi-k* the cell area is smaller compared to WT (* $p < 0.05$ and ** $p < 0.01$, One-Way ANOVA with Dunnett's Multiple Comparisons Test). **D)** Shape of pavement cells of leaf abaxial epidermis. Note less extended lobes of the *xi-1/xi-2/xi-k* pavement cells in comparison with WT (black cells on the image). Bar = 50 μ m. **E)** Circularity values of pavement cells on leaf abaxial epidermis (mean \pm SD). Circularity reflects the ratio of pavement cell area to the perimeter. Cells with values near one are more circular, meaning that *xi-1/xi-2/xi-k* cells have more round morphology than WT cells (***) $p < 0.001$, unpaired t-test with Welch correction, $n = 13-16$).

branch length (ratio value below 1, $p < 0.001$; Figure 3B; Additional file 8).

The number of trichomes with irregular shape was quantified by measuring the frequency at which several types of differences from wild type trichome shape occurred. The differences we measured were: differences in branch positioning (elongated interbranch zone), individual branch length, stalk height or bended shape of the trichome (Figure 3C). The number of irregular trichomes on leaves of *xi-1*, *xi-2* and *xi-1/xi-2* plants was similar to wild type (values from 5% to 8%). In *xi-k* plants, 22% of leaf trichomes exhibited an irregular phenotype. Trichomes on the leaves of the double mutants *xi-1/xi-k*, *xi-2/xi-k* and the triple mutant *xi-1/*

xi-2/xi-k were more irregular than those on the single mutant *xi-k*. Specifically, in the double mutant *xi-1/xi-k*; approximately 38% of leaf trichomes showed irregular phenotype compared to *xi-k*. Very characteristic for *xi-1/xi-k* was the appearance of trichomes with abnormally elongated stalks, a phenotype not found in the single *xi-k* mutant (Figure 3C). Trichome phenotype of *xi-k* was more severe in *xi-2/xi-k* and *xi-1/xi-2/xi-k* plants, where 56% and 90% of trichomes were irregular and frequently exhibited both abnormally elongated stalks as well as abnormally elongated single branches (sword-shaped trichomes) (Figure 3C, Additional files 7 and 8). In the case of *xi-1/xi-k*, *xi-2/xi-k* and *xi-1/xi-2/xi-k* plants, the bent shape of trichomes was more frequent than in *xi-k*.



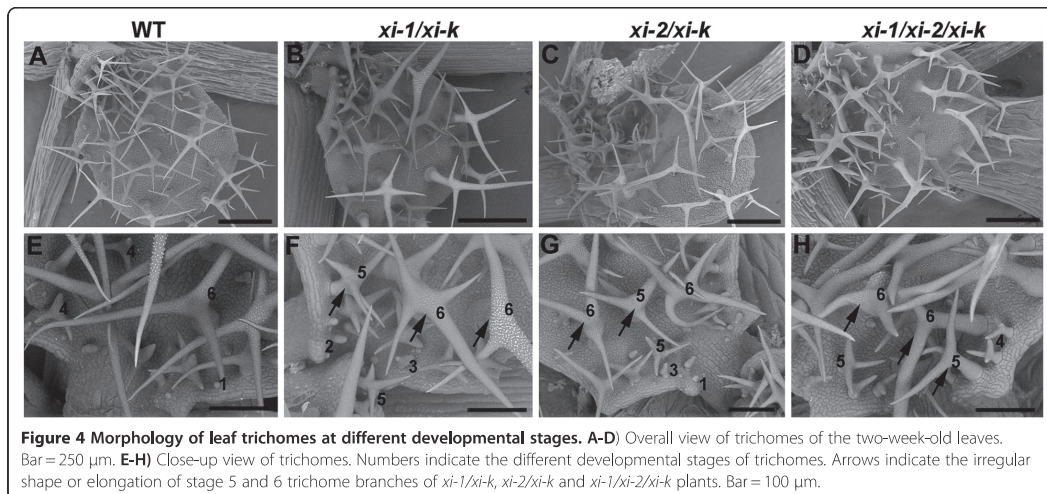
We used scanning electron microscopy to monitor stalk and branch expansion defects during trichome development. Trichome development is divided into six stages based on morphological features. Stage 4 and 5 trichomes were investigated because branches are formed in stage 4 and rapid branch elongation begins in stage 5 [35,43]. We did not detect significant differences between stage 4 trichomes of double mutant, triple mutant and wild type plants. Differences between wild type and mutant trichomes, irregular elongation and modest bending of stalk and branches, were clear in late stage 5 or stage 6 trichomes of *xi-1/xi-k*, *xi-2/xi-k*, and *xi-1/xi-2/xi-k* plants (Figure 4A-H).

The phenotype of double mutants *xi-1/xi-k*, *xi-2/xi-k* and triple mutant *xi-1/xi-2/xi-k* all show more severe mutant phenotypes than any single mutant, suggesting that all three myosins participate in elongation of trichome stalks and branches. Among these mutants *xi-1/xi-k* had the weakest and *xi-1/xi-2/xi-k* had the strongest phenotype. These results indicate that myosin XI-K contributes more

significantly than XI-1 and XI-2 to the trichome development because the absence of both myosins can be compensated by XI-K. Myosin XI-2 in turn plays a more important role in the trichome expansion than XI-1, as the phenotype of *xi-2/xi-k* was stronger than that of *xi-1/xi-k*.

Simultaneous depletion of myosins XI-1, XI-2 and XI-K influences the shape of trichome nuclei

Wild type trichomes undergo approximately four rounds of endoreduplication during maturation leading to a three to four branched cell with an average DNA content of 32 C (32 times the DNA content of the haploid genome) [44-47]. It has been found that mutants with smaller trichomes contain less DNA, whereas mutants with increased cell size were found to have additional endoreduplication rounds [46]. To test whether the smaller size of myosin mutant trichomes could be related to the ploidy level, we quantified the nuclear DNA of fully mature trichomes on 14 days old plants using Hoechst staining. Confocal scanning fluorescence



microscopy measurements showed that the ploidy level of the single, double and triple mutant trichomes was similar to wild type, average DNA content being 32 C (data not shown), suggesting that trichomes of these mutants undergo four successive endoreplication cycles during maturation, as in wild type.

Although we did not detect differences in ploidy level, we found that the nuclei of mutant trichomes exhibited a different shape compared to wild type. Trichomes of all single mutants and double mutants *xi-1/xi-2* and *xi-1/xi-k* had spherically shaped nuclei, similar to wild type. Trichomes of *xi-2/xi-k* and *xi-1/xi-2/xi-k* frequently had abnormally elongated nuclei (Figure 5A). Quantification analysis revealed that the average sphericity of wild type trichome nuclei was 0.65 and that of *xi-1*, *xi-2*, *xi-k*, *xi-1/xi-2* and *xi-1/xi-k* nuclei was between 0.58 and 0.62 (Figure Inter/InternalRef, Additional file 9). The average sphericity of *xi-2/xi-k* and *xi-1/xi-2/xi-k* trichomes was 0.52 ($p < 0.001$) and 0.60 ($p < 0.001$), respectively (Figure 5B, Additional file 9). Taken together, nuclei of wild type trichomes had the most circular shape and nuclei of double mutant *xi-2/xi-k* had the most elongated shape, indicating that co-operation between myosin XI-K and XI-2 is necessary for normal nuclear morphology in trichomes. Since both the irregular trichome shape and the sphericity of nucleus were most dramatically expressed in *xi-2/xi-k* background, a correlation analysis between these phenotypic features in *xi-2/xi-k* was performed. The calculated Pearson's correlation coefficient $r = -0.7120$ ($p < 0.0001$; $n = 32$) shows that smaller nuclear sphericity values (i.e. nucleus is elongated) are correlated with mutant trichome phenotype (Additional file 10).

Simultaneous depletion of myosins XI-1, XI-2 and XI-K influences the growth of floral organs and fertility

To assess the fertility of the analyzed double and triple mutant lines, the number and length of the siliques per plant was measured and the number of seeds per silique was counted. Fertility of single and double mutant lines was comparable to wild type and was therefore not investigated further. For *xi-1/xi-2/xi-k*, variations in the number of normally and abnormally developed siliques were significant (siliques with length from 4 to 10 mm were assessed as abnormal). As an average, *xi-1/xi-2/xi-k* plants had up to 60% ($p < 0.001$) of abnormally developed siliques on main stem, when compared to wild type (Figure 6, Additional file 11).

Moreover, after onset of flowering, up to 60% ($p < 0.001$) of flowers emerged on the primary shoot of *xi-1/xi-2/xi-k* plants remained mostly seedless because the pistils remained unpollinated or were poorly pollinated (Figure 7A-B, Additional file 11). The average length of these siliques was 6.5 mm ($p < 0.001$) containing an average of only two ($p < 0.001$) fertilized ovules (Figure 7A-B; Additional file 12). This process continued approximately two to three weeks after bolting. About three weeks after bolting, there was a "switch" and plants started to produce siliques only slightly underdeveloped or normal in size with average length 12.9 mm (Figure 7A-B, Additional file 12). These siliques contained up to 28% ($p < 0.0001$) of unfertilized ovules (Figure 7C, Additional file 12). The number of unpollinated pistils, underdeveloped and normal siliques varied to a great extent between the *xi-1/xi-2/xi-k* plants. These variations in silique size were prevalent on primary shoots and less on axillary shoots of *xi-1/xi-2/xi-k*

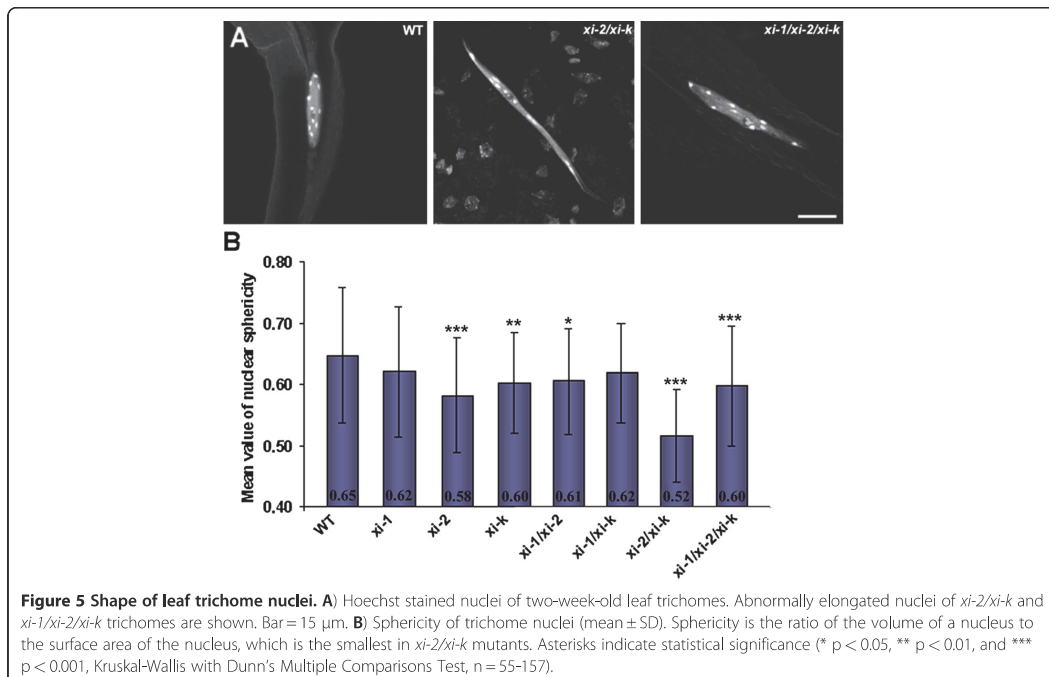


Figure 5 Shape of leaf trichome nuclei. **A**) Hoechst stained nuclei of two-week-old leaf trichomes. Abnormally elongated nuclei of *xi-2/xi-k* and *xi-1/xi-2/xi-k* trichomes are shown. Bar = 15 μ m. **B**) Sphericity of trichome nuclei (mean \pm SD). Sphericity is the ratio of the volume of a nucleus to the surface area of the nucleus, which is the smallest in *xi-2/xi-k* mutants. Asterisks indicate statistical significance (* $p < 0.05$, ** $p < 0.01$, and *** $p < 0.001$, Kruskal-Wallis with Dunn's Multiple Comparisons Test, $n = 55-157$).

plants. In wild type, occasionally the first two flowers on the inflorescence remained seedless and the number of underdeveloped siliques was up to 5% (Additional file 12).

Next, anthers and pistils were examined to identify whether the decreased fertility of triple mutant was caused by defects in male or female reproductive organs. For this, Alexander's staining of pollen, in vitro growth

assays and aniline blue staining of pollen tubes was performed. Alexander's staining showed that the viability of *xi-1/xi-2/xi-k* pollen grains was similar to wild type (Additional file 13). Using in vitro pollen tube growth assay we could not detect differences between triple mutant and wild type pollen tube growth (data not shown). These results indicated that the decreased fertility of *xi-1/xi-2/xi-k* triple mutant plants was not dependent on pollen viability or on the ability of the pollen to form a pollen tube.

Cross-pollination of wild type and *xi-1/xi-2/xi-k* pistils was performed. Aniline blue staining of pollinated pistils demonstrated that when wild type pistils were pollinated with *xi-1/xi-2/xi-k* pollens (WT/*triple*), the growth of pollen tubes in pistils was similar as in self-pollinated wild type (Figure 8). WT/*triple* siliques contained only 2-5% unfertilized ovules counted 9 days after pollination. Inversely, when *xi-1/xi-2/xi-k* pistils were pollinated with wild type pollen (*triple*/WT), pistils developed very heterogeneously. In some cases, the fertilization was normal, but often wild type pollen grains could not attach effectively to the surfaces of *xi-1/xi-2/xi-k* stigmas and form pollen tubes (Figure 8). As a result, *triple*/WT pistils often remained poorly pollinated, no siliques or shorter siliques were formed and a variable amount of ovules (12-53%) in shorter siliques remained unfertilized. We observed a similar phenotype both in cross-

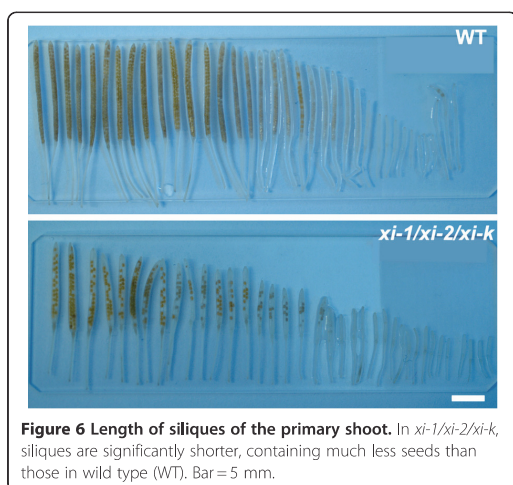


Figure 6 Length of siliques of the primary shoot. In *xi-1/xi-2/xi-k*, siliques are significantly shorter, containing much less seeds than those in wild type (WT). Bar = 5 mm.

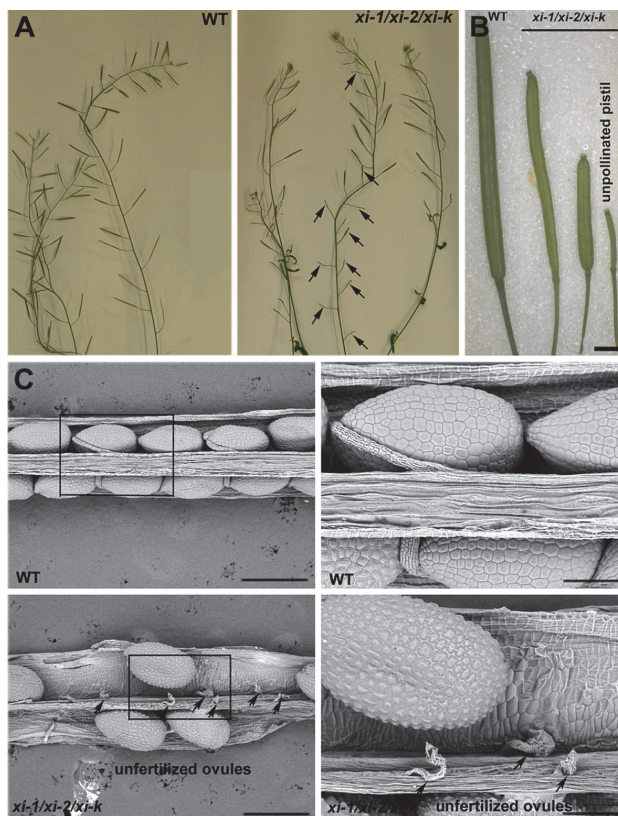


Figure 7 Silique size and seed development. **A**) Shoots of the eight-week-old plants. Arrows indicate the unpollinated pistils on the primary stem of *xi-1/xi-2/xi-k*. **B**) Representative wild type (WT) and *xi-1/xi-2/xi-k* siliques are shown. Note the heterogeneous development of triple mutant siliques on the main stem. Bar = 2 mm. **C**) Scanning electron micrographs of developing seeds in manually opened siliques. Arrows point to the unfertilized ovules in *xi-1/xi-2/xi-k* siliques. Left panel, bar = 500 μ m; right panel, bar = 150 μ m.

pollinated *triple*/WT as well as in self-pollinated *xi-1/xi-2/xi-k* pistils (Additional file 14). Reciprocal crosses between the wild type and triple mutant *xi-1/xi-2/xi-k* revealed that the reduced fertility of triple mutant is female reproductive tract specific.

Making reciprocal crosses it seemed that floral organs of *xi-1/xi-2/xi-k* are significantly smaller than those of wild type and the size and architecture of flowers was therefore examined in more detail (Figure 9A). Indeed, measurements of floral organs showed that *xi-1/xi-2/xi-k* flowers were smaller compared to the wild type (Figure 9B, Additional file 15). The length of peduncles, sepals and petals of *xi-1/xi-2/xi-k* flowers was 88%, 88% ($p < 0.01$) and 83% ($p < 0.001$) of wild type, respectively. The length of *xi-1/xi-2/xi-k* flower buds was only 66% ($p < 0.001$) of wild type (Figure 9B, Additional file 15).

Next, the architecture of the triple mutant and wild type pistils was studied using scanning electron microscopy. Twenty stages of *Arabidopsis* flower development have been distinguished [41]. Floral buds just before pollination (stage 12) and opened flowers (stage 13 or 14) were examined because wild type pistils of these developmental stages are mature and receptive to pollination. We observed that the elongation of stigmatic papillae of stage 12 *xi-1/xi-2/xi-k* buds was delayed, remaining on the level of stage 10 or 11 stigmas (Figure 10A). In stage 13 and 14 flowers the development of *xi-1/xi-2/xi-k* stigmatic papillae varied from normal to stunted. We noticed that in some cases also *xi-1/xi-2/xi-k* pistil itself did not develop to the wild type level even during later stages of development (Figure 10B).

We suggest that the insufficient development of stigmatic papillae, which renders the stigma not fully

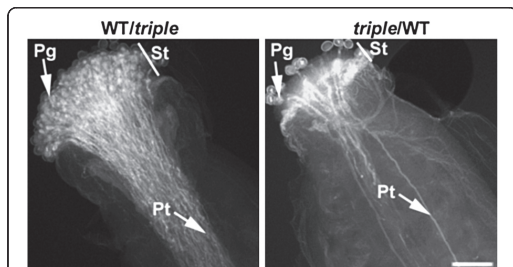


Figure 8 Development of pollen tubes. Pollen tube growth was followed in cross-pollinated pistils: WT/triple – wild type (WT) pistil was pollinated with *xi-1/xi-2/xi-k*; triple/WT – *xi-1/xi-2/xi-k* pistil was pollinated with WT. Note the number of pollen grains attached to the stigmas and the number of pollen tubes formed. In the case of triple/WT, WT pollen grains were not able to attach effectively on the surface of *xi-1/xi-2/xi-k* stigma and only few pollen tubes were formed. Aniline blue staining of pollen tubes was performed 12 hours after hand-pollination. Pg – pollen grains, St – stigma, Pt – pollen tubes. Bar = 50 μ m.

receptive (mature) for pollination, is the main reason for the reduced fertility of *xi-1/xi-2/xi-k* triple mutant plants. These results indicate that myosins XI-1, XI-2 and XI-K together are needed for normal development of floral organs.

Discussion

Characterization of double and triple mutant plants revealed that myosins XI-K, XI-1, and XI-2 have redundant functions not only in development of root hairs and shoots [19,20,22] but also in expansion of trichomes, lobe extension of pavement cells, and in elongation of stigmatic papillae. Our results showed that simultaneous depletion of these three myosins affects several types of epidermal cells thereby influencing the growth and size of leaves, inflorescences, floral organs and the fertility of the plant. Differences between most phenotypic features (dwarf growth, decreased cell size, delayed flowering time and reduced fertility) between triple mutant *xi-1/xi-2/xi-k* and wild type, described in this work are similar and comparable with results published by Peremyslov and coworkers [22], and here we add several new characteristics (disorders in the development of pavement cell lobes, trichome stalk and branches and stigmatic papillae). Results concerning rosette size, plant height and fertility of the double mutants *xi-1/xi-k* and *xi-2/xi-k* are inconsistent with previously published data [20]: we show here that the rosette size and shoot height of the *xi-1/xi-k* plants are similar to the wild type, and on the contrary, the rosette size and shoot height of *xi-2/xi-k* plants are decreased compared to the wild type. Thus, the mutant phenotype (rosette size, shoot height, onset of flowering, and size and shape of trichomes) of *xi-2/*

xi-k plants is always stronger than that of *xi-1/xi-k* plants and the phenotype of *xi-1/xi-2/xi-k* triple mutant plants is always stronger than that of *xi-2/xi-k*. Double and triple mutant lines used in this work were different than those described previously [20,22]: different T-DNA insertional lines of the *xi-1* (Salk_022140) and *xi-2* (Sail_632_D12) but the same for *xi-k* (Salk_067972) were used by us to generate double and triple mutant lines. It is possible that the inconsistency of the shoot phenotype of double mutants can be explained by use of different T-DNA insertional lines for generating double and triple mutant lines. Other aspects like differences in laboratory conditions can cause these differences as well.

The size of plant leaves is determined by a combination of cell number, cell size and intercellular space (reviewed in [48]). Experiments with mericlinal *Nicotiana* chimeras and *Arabidopsis* brassinosteroid receptor mutants have shown that the leaf epidermis has a crucial role in regulating leaf size through influencing mesophyll cell number and cell size [48-50]. We show that double mutant *xi-2/xi-k* and triple mutant *xi-1/xi-2/xi-k* have smaller and less lobed epidermal cells than wild type, and in addition, these leaves are smaller than wild type. Thus, although the primary effect of the depletion of myosins XI-K, XI-1, and XI-2 in the leaf blade may be on epidermal cell size and shape, this ultimately causes smaller leaves, especially in the triple mutant.

Proper organisation of the actin cytoskeleton is important in coordinating directed expansion of trichome branches and, as has been shown for several *distorted* group mutants [26,27,35,51]. The myosin XI-K mutant phenocopies mild trichome phenotype similar to the *distorted* group mutants [24]. However, the irregular trichome phenotype has not been found in the rest of the single mutants of class XI myosin genes. Our characterization of the double and triple mutant plants revealed, however, that myosins XI-1, XI-2 and XI-K have redundant functions in the elongation of trichome stalks and branches. Our results indicated that myosin XI-K has a leading role and XI-1 and XI-2 have minor roles in trichome development, whereas myosin XI-2 contributes to the trichome expansion more than XI-1.

We found also that the irregular size of myosin double and triple mutant trichomes was independent of endoreduplication events. This is also the case in *distorted* mutants [52], which define genes coding actin polymerization regulating proteins, like components of ARP2/3 [29,30] and SCAR/WAVE complexes [31-34]. Although the ploidy level of mutant trichomes did not change, we found that nuclear morphology was markedly affected in double mutant *xi-2/xi-k* trichomes. The abnormally elongated shape of *xi-2/xi-k* nuclei correlated with the mutant trichome phenotype. It is known that

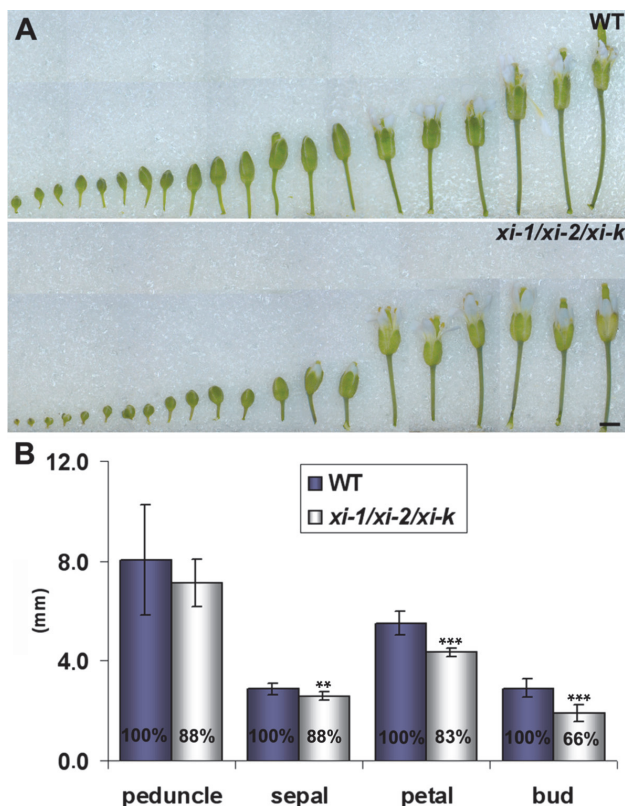


Figure 9 Size of floral organs. **A**) Developmental stages of flowers from inflorescence of the primary shoot are shown. Note the smaller size of *xi-1/xi-2/xi-k* flowers and flower buds. Bar = 1 mm. **B**) Mean length of peduncles, sepals, petals and flower buds (\pm SD). Opened flowers and flower buds of the inflorescences (from main stems) were selected for measurements. The average size of floral organs of *xi-1/xi-2/xi-k* is smaller than in wild type (WT). Asterisks indicate statistical significance (* $p < 0.05$, ** $p < 0.01$, and *** $p < 0.001$, unpaired *t*-test with Welch correction, $n = 6-12$).

nuclear dynamics and morphology occurs in a cell specific manner and is influenced by cell shape and nuclear DNA content [53]. In plant cells the nucleus is positioned within a basket of dense actin filaments connected to the transvacuolar strands and cortical cytoskeleton [54-56]. Recently it has been shown that simultaneous depletion of myosins XI-1, XI-2 and XI-K caused defects in organization of actin filaments in root hairs and in the cells of leaf midvein epidermis [22]. Moreover, Ueda et al. [23] demonstrated that myosin XI-K in co-operation with myosin XI-2 is involved in organizing actin bundles and ER network in epidermal cells of cotyledonary petioles. In addition, transient expression in onion cells showed that GFP-fused head-neck domain of XI-2 had an increased fluorescence signal specifically near the nucleus [57]. Taking this into consideration, it is very likely that the organization of

actin filaments is affected in the trichomes of *xi-1/xi-k*, *xi-2/xi-k* and *xi-1/xi-2/xi-k* plants. It remains to be resolved how myosins XI-K and XI-2 regulate the organization of the nucleus-associated actin bundles, and thus nuclear shape, during trichome development.

Mutations in genes coding various actin related proteins in plants lead to defects in actin filament organization. For example, the organization of cortical actin filaments in the majority of *distorted* mutants is affected [32-34,52,58]. Comparing the phenotypes of myosin double and triple mutant plants and those of group *distorted* mutants revealed apparent similarity in the trichome phenotype of the *xi-1/xi-2/xi-k* with *pirogi* and *xi-2/xi-k* with *spirrig* plants [31,39]. It should be noted that the overall phenotype severity of *xi-2/xi-k* and *xi-1/xi-2/xi-k* plants was weaker than those of *pirogi* and *spirrig* mutants. For example, gaps between adjacent cells in

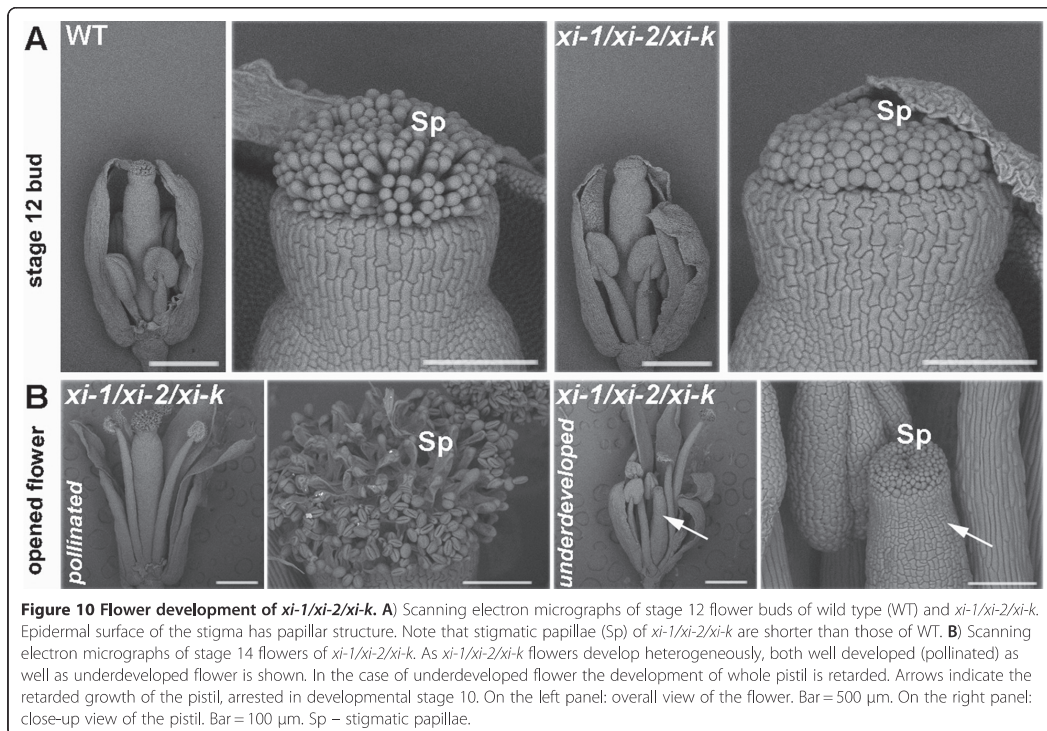


Figure 10 Flower development of *xi-1/xi-2/xi-k*. **A**) Scanning electron micrographs of stage 12 flower buds of wild type (WT) and *xi-1/xi-2/xi-k*. Epidermal surface of the stigma has papillar structure. Note that stigmatic papillae (Sp) of *xi-1/xi-2/xi-k* are shorter than those of WT. **B**) Scanning electron micrographs of stage 14 flowers of *xi-1/xi-2/xi-k*. As *xi-1/xi-2/xi-k* flowers develop heterogeneously, both well developed (pollinated) as well as underdeveloped flower is shown. In the case of underdeveloped flower the development of whole pistil is retarded. Arrows indicate the retarded growth of the pistil, arrested in developmental stage 10. On the left panel: overall view of the flower. Bar = 500 μ m. On the right panel: close-up view of the pistil. Bar = 100 μ m. Sp – stigmatic papillae.

cotyledons and hypocotyls, typical for *distorted* mutants, were not apparent in the analysed myosin mutants. On the other hand, typical characteristics for *xi-1/xi-k*, *xi-2/xi-k* and *xi-1/xi-2/xi-k* trichomes like abnormally elongated trichome stalks have not been reported in *distorted* mutants. The phenotypic similarity between myosin mutants and *distorted* mutants also suggests, that the organization of actin filaments could be affected in trichomes of *xi-1/xi-k*, *xi-2/xi-k* and *xi-1/xi-2/xi-k*.

Changes in branch morphology during stage 4 of trichome development are obvious indicators of aberrant actin function in *distorted* mutants [32-34]. In myosin double and triple mutant plants the irregular trichome phenotype became apparent in late stage 5 or stage 6 trichomes. This reveals that class XI myosins are required for the trichome development during later stages of morphogenesis: during rapid growth of trichome branches or during trichome maturation, when the cell wall thickens and becomes covered with papillae.

Pavement cells of the triple mutant *xi-1/xi-2/xi-k* had less extended lobes. It is known, that the shape of pavement cells and the extension of lobes, depends also on the microfilament dynamics and that most of the *distorted* mutants display less lobed morphology of pavement cells [3,34,59]. Relying on the phenotypic overlap

it is tempting to speculate that the functions of myosins XI-K, XI-2 and perhaps of XI-1 may be related to the mechanisms controlled by ARP2/3 or SCAR/WAVE proteins/complexes.

Reproduction in *Arabidopsis* is dependent on interactions between pollen grains and papillar cells on the surface of the stigma [60]. The stigma is an epidermal structure composed of papillae, i.e. bulbous elongated cells. In the mature pistil the papillae are properly extended and form elongated cells receptive to the recognition, attachment and germination of pollen grains [61,62]. It has been shown that fewer pollen grains can adhere to immature stigmas and germinate. Immature stigmas are able to promote pollen tube growth to some extent, but the immature pistils are often unable to guide pollen tubes to the ovules [60,62,63]. Our current results indicated that the triple mutant *xi-1/xi-2/xi-k* has major deviations in the effectiveness of fertilization. We showed that the reduced fertility of *xi-1/xi-2/xi-k* was caused by delayed or insufficient development of the stigmatic papillae, making pistils less receptive for pollination. This indicates that class XI myosins are required for proper development of *Arabidopsis* pistils and therefore for fertilization.

Apical-basal patterning of *Arabidopsis* gynoecium is auxin dependent, and crosstalk between the actin

cytoskeleton and auxin signaling is well known [64-66]. There are little data available concerning the actin cytoskeleton during pistil development. It has been shown that actin filaments of stigmatic papillae of self-incompatible *Brassica rapa* are differentially organized before and after pollination and that these changes in actin dynamics are associated with pollen hydration and germination [67]. We suggest, that the class XI myosins in the stigmatic papillae may fulfill a similar role as in other tip growing cell types [19,20,24].

In *Arabidopsis* not only stigmatic papillae, but also other epidermal cell types like part of the transmitting tract and the integument of the ovules have the same developmental origin, the meristematic epidermal L1 layer [61]. We do not exclude that defects in these cells may also influence the fertility of the *xi-1/xi-2/xi-k*, as the flowers of triple mutant were smaller than those of wild type and occasionally exhibited retarded growth with completely underdeveloped pistils. Our results indicate that all three myosins (XI-K, XI-2, XI-1) together are required for normal development of *Arabidopsis* shoots and floral organs.

Conclusion

We conclude that (1) myosins XI-1, XI-2 and XI-K have partially redundant roles in the growth of different epidermal cells (pavement cells, trichomes, stigmatic papillae), (2) myosin XI-K has more important role and myosins XI-1 and XI-2 have minor roles in these growth processes, (3) cooperation between myosins XI-K and XI-2 appears to be important for maintaining normal growth of epidermal cells and thus the size of plant organs. We conclude that the decreased size and delayed or insufficient development of floral organs affects the fertility of myosin mutants.

Methods

Plant material and growth conditions

Arabidopsis thaliana (ecotype Columbia-0) seeds of *xi-1* (Salk_022140; At1g17580), *xi-2* (Sail_632_D12; At5g43900) and *xi-k* (Salk_067972; At5g20490) T-DNA mutant lines were obtained from the Nottingham Arabidopsis Stock Centre [68]. Homozygous single mutant lines of *xi-k* (Salk_067972; previously known by allele name *Xlk-2*) and *xi-2* (Sail_632_D12) have been described earlier [19,24]. Homozygous single mutant lines were used to generate the double mutant lines *xi-1/xi-2*, *xi-1/xi-k*, *xi-2/xi-k* and triple mutant line *xi-1/xi-2/xi-k*. Homozygous plants of the double and triple mutant were identified by two PCRs. In the first PCR, a pair of gene-specific primers designed to anneal on either side of the T-DNA insertion were used, which in case of homozygosity does not produce a band of the predicted size. In the subsequent PCR, the T-DNA border specific primer and primers of the first PCR were used. To confirm

the location of the T-DNA insertion in the respective myosin gene, the PCR products were sequenced. Double and triple mutant lines used in this work were partially different than those described previously [20,22]: different T-DNA insertional lines of the *xi-1* and *xi-2* were used to generate double and triple mutant plants.

Seeds from single, double and triple mutant lines were harvested from plants of the same age and stored at least three weeks in the dark at 4°C. Cold stratified seeds were soaked in water at 4°C for 1–4 days and sowed directly in soil (Biolan OY) containing 50% (w/v) of vermiculite. Plants were grown in Sanyo growth chambers at 22 ± 2°C and 60% of relative humidity under long day (16-h light) photoperiod.

RNA isolation and RT-PCR

RNA was extracted from two-week-old seedlings and DNase I (Ambion) treated as described by Oñate-Sánchez and Vicente-Carbajosa [69]. For first-strand synthesis, RevertAid Premium Reverse Transcriptase (Fermentas) and Random Hexamer Primer mixture (Fermentas) were used according to manufacturer's instructions. Equivalent amounts of cDNA template were used for amplification of fragments of *XI-1*, *XI-2* and *XI-K* mRNAs. Two pairs of gene specific primers were used for each single mutant: one pair spanning the T-DNA insertion site and the other pair downstream of the insertion site. In all cases constitutively expressed B subunit of chloroplast glyceraldehydes-3-phosphate dehydrogenase (*GAPB*, At1g42970) specific primers were used to quantify mRNA levels. Primers used for RT-PCR of the *XI-1* and *GAPB* are listed here:

XI-1_022140_LP (5'-AGTCCAGAAGAATTTCCGC CG-3'),

XI-1_022140_RP (5'-GCCTGTCAATTTTCGTTGCT CA-3'),

XI-1_3000_Fw (5'-GCAATTGAAGAAGCAAGTT CAGTTAAT-3'),

XI-1_3900_Rev (5'-CAGAGGGGAAATCTCTTTCT TCATCTT-3'),

GAPB_Fw (5'-CTTAACATATAGTTGTTTCATCAG AC-3'),

GAPB_Rev (5'-GCGCCTCTGTCTCTGTTGAC-3').

Sequencing reactions were performed with BigDye Terminator Cycle Sequencing Kit (Applied Biosystems) according to the protocol provided by the manufacturer and analyzed with DNA analyzer ABIPRISMTM 3130 (Applied Biosystems).

Cell area and circularity measurements

Five-week-old rosette leaves (5th and 6th leaf) were fixed in Carnoy's fixative (ethanol:acetic acid, 3:1), washed with 70% ethanol and mounted in Hoyer's

mounting medium (30 g gum arabic, 50 ml distilled water, 200 g chloral hydrate, 16. ml glycerol).

Images of pavement and mesophyll cells were captured using differential interference contrast (DIC) microscopy by Olympus BX61 microscope with a 20x or 40x objective. For calculating cell areas the total image area was divided with total cell number per image using Adobe Photoshop 7.0.

To quantify the differences in cell shape, circularity of pavement cells (from abaxial side) was measured using ImageJ software (<http://rsb.info.nih.gov/ij/>). Cell circularity was calculated according to the formula $4\pi \cdot \text{area} / \text{perimeter}^2$ [41]. For measuring circularity, black and white binary images of single pavement cells were used. Binary images were generated using Adobe Photoshop 7.0.

Trichome isolation and analysis

Intact trichomes from mature leaves were isolated as described by Zhang and Oppenheimer [70]. Toluidine blue stained trichomes were mounted in Mowiol medium (6 g glycerol; 2.4 g Mowiol 4–88; 6 ml distilled water; 12 ml 0.2 M Tris buffer pH 8.5). Images taken with a 4x or 10x objective of the Olympus BX61 were processed with Adobe Photoshop 7.0. For trichome size analysis, the height of stalks and branches was measured using Image Tool 3.0 (<http://ddsdx.uthscsa.edu/dig/itdesc.html>). The number of trichomes with irregular shape was quantified by counting the presence of at least one of the following phenotypes: elongated interbranch zone, unproportionally elongated individual branches, abnormally elongated stalks, sword-shaped trichomes or slightly twisted shape of trichomes.

For the ploidy and sphericity analysis of trichome nuclei, two-week-old soil grown seedlings were fixed in Carnoy's fixative, washed three times with distilled water (3x15 minutes) and stained overnight with 1 µg/ml of Hoechst 33342 (Molecular Probes). Samples were washed three times with water (3x15 minutes) and mounted in Mowiol medium. Hoechst fluorescence was visualized with 100x objective and 405 nm excitation of laser scanning microscope (Carl Zeiss LSM 510 DUO). Images were quantified using Imaris (Bitplane Scientific Software). Sum of the fluorescence isosurfaces of Hoechst stained nuclei was used for calculation of ploidy levels of wild type and mutant trichomes; at least 50 trichome nuclei per experiment were measured. To calculate total DNA content the fluorescence of trichome nuclei was calibrated using guard cell nuclei, which are considered to be strictly diploid. In mature wild type trichome the total DNA content is 32 C, equal with the four rounds of endoreduplication.

Sphericity of trichome nuclei was calculated using fluorescence isosurfaces of Hoechst stained trichome nuclei. Sphericity (Ψ) of a nucleus is the ratio of the surface

area of a sphere (with the same volume as the given nucleus) to the surface area of the nucleus [71].

To perform correlation analysis, sphericity of trichome nuclei was measured and the overall trichome phenotype was evaluated. Trichomes with normal phenotype (equal to wild type) and mutant phenotype were arbitrarily assigned values of 0 and 1, respectively. The phenotype was considered mutant if the trichome exhibited any of the following features: elongated interbranch zone, irregular branch length, abnormally elongated stalk and sword-shaped trichome.

Analysis of fertility

For floral organ measurements inflorescences of mutant and wild type plants were dissected using double-sided tape, fine needle (G27) and tweezers. Images were captured using stereomicroscope (Zeiss SteREO Discovery V8) and measurements were done using ImageJ software. Fertility was evaluated measuring the length of siliques, counting the number of siliques and the number of developing seeds in siliques.

Alexander's staining of pollens

To stain mature pollen grains, flowers were collected from adult plants and stored in 10% ethanol for at least 2 hours at room temperature. Dehiscent anthers were mounted into a drop of Alexander's stain (10 ml of 95% ethanol, 10 mg Malachite green (1 ml of 1% solution in 95% alcohol), 50 ml of distilled water, 25 ml of glycerol, 5 g of phenol, 5 g of chloral hydrate 50 mg of acid fuchsin (5 ml of 1% solution in water), 5 mg of Orange G (0.5 ml of 1% solution in water) and 2 ml of acetic acid) [72]. A coverslip was placed on the anthers and the slides were incubated overnight at room temperature. Images were taken with a digital camera (Olympus DP70) installed on Olympus BX61 microscope with a 20x objective.

Aniline blue staining of pollen tubes

For pollen tube staining, pistils were opened longitudinally 12 h after pollination and staining was performed as described by Pagnussat et al. [73]. The pistils were fixed overnight in Carnoy's fixative, cleared in 10% chloral hydrate at 65 °C for 5 minutes, washed with water, and softened with 1 M NaOH at room temperature, washed with 0.1 M K_2HPO_4 buffer (pH 10) and stained with 0.1% decolorized aniline blue (in 0.1 M K_2HPO_4 buffer) for 3 hours. Finally pistils were washed briefly with 0.1 M K_2HPO_4 buffer, mounted on a microscope slide using a drop of 80% glycerol. Aniline blue fluorescence was visualized with 10x or 20x objective of laser scanning microscope (Carl Zeiss LSM 510 DUO).

SEM analysis of siliques and pistils

Siliques, flowers and flower buds were dissected on double-sided tape using fine needle (27 G) and tweezers. Images were captured with Hitachi TM-1000 tabletop scanning electron microscope.

Statistical analysis

Statistical analysis was performed with Microsoft Excel and GraphPad InStat software (GraphPad Software Inc., La Jolla, CA). All data are expressed as mean \pm standard deviation (SD). Datasets were first tested for normality using the Kolmogorov-Smirnov test, and an appropriate statistical test was chosen (indicated in Figure legends and Additional files). For all tests, two-sided p-values were calculated. Pearson's correlation coefficient was calculated to determine relationship between the shape of trichomes and sphericity of their nuclei (Additional file 10).

Additional files

Additional file 1: A schematic diagram of *XI-1*, *XI-2*, and *XI-K* genes with the positions of the T-DNA insertions. Black boxes represent exons, black lines introns, and gray boxes represent 5' and 3' untranslated regions. Above the corresponding T-DNA insertion sites are shown.

Additional file 2: Data for Figure 2B: size of the five-week-old rosette leaves (from 5th to 10th, mm).

Additional file 3: Data for Figure 2C: cell areas (μm^2) of pavement and mesophyll cells of five-week-old rosette leaves.

Additional file 4: Data for Figure 2E: circularity of pavement cells on the leaf abaxial epidermis.

Additional file 5: Shoot size of six-week-old plants. Wild type plants are on the left and *xi-1/xi-2/xi-k* plants are on the right. Both bolt formation as well as onset of flowering of *xi-1/xi-2/xi-k* plants delays significantly (two weeks).

Additional file 6: Data for supplementing Additional file 5: inflorescence shoot height (cm).

Additional file 7: Data for Figure 3A: length of trichome stalk and branches (μm).

Additional file 8: Data for Figure 3B: length ratios of the trichome stalk and branches.

Additional file 9: Data for Figure 5B: sphericity of trichome nuclei.

Additional file 10: Data for figure 5B: sphericity data and correlation between the sphericity of the trichome nucleus and the trichome shape.

Additional file 11: Data for Figure 7: number of siliques per main stem.

Additional file 12: Data for Figures 6 and 7: length of the siliques (mm) and number of seeds per silique.

Additional file 13: Pollen viability assessed by Alexander's staining method. Pollen viability (purple-colored cytoplasm of pollen grains) is similar both in wild type (WT) as well as in all double and triple mutant plants. Bar = 100 μm .

Additional file 14: Development of pollen tubes in self-pollinated pistils. Shortly after the onset of flowering first three flowers on the primary shoot were analyzed. A-C) Aniline blue staining of wild type (WT) pistils. D-F) Aniline blue staining of *xi-1/xi-2/xi-k* pistils. In *xi-1/xi-2/xi-k*, pollen grains were not attached to the stigmas and pollen tubes were not formed. Pg – pollen grains; Pt – pollen tubes. Bar = 100 μm .

Additional file 15: Data for Figure 9: size of floral organs (mm), length of the peduncles, sepals, petals and buds.

Acknowledgements

We thank the Arabidopsis Biological Resource Center and the Salk Institute Genomic Analysis Laboratory for providing T-DNA insertion mutants. We thank Birger Illau, Kristina Talts and Illar Pata for carefully reading the manuscript, Signe Nõu for taking care of plants, Olga Volobujeva and Enn Mellikov for providing tabletop SEM for trichome and flower analysis, and Luis Vidali (Worcester Polytechnic Institute) for the assistance with circularity analysis, and Lisa Harper (University of California, Berkeley) for correcting the language of the manuscript. This research was supported by grant number 8604 from the Estonian Science Foundation and by the EU through the European Regional Development Fund (Center of Excellence ENVIRO).

Author details

¹Department of Gene Technology, Tallinn University of Technology, Akadeemia tee 15, 12618 Tallinn, Estonia. ²Nachhaltigkeits-Projekte, Alte Str. 13, 79249 Merzhausen, Germany.

Authors' contributions

EO participated in most of the experimental analyses and wrote the draft of the manuscript. KT did part of the sequencing, RT-PCR, helped with SEM and DIC images and made cell area measurements. PP made statistical analysis of the data. KJ made *xi-1/xi-k* double mutant line and participated in root hair measurements. CH shared T-DNA line of *xi-2* and participated in creating double mutant *xi-2/xi-k* line. ET participated in design of the study and in analysis of the data and helped to draft the manuscript. HP made images and analysis of trichome nuclei; made images of root hairs; participated in design of the study and in analysis of the data and helped to draft the manuscript. All authors read and approved the final manuscript.

Received: 22 August 2011 Accepted: 28 May 2012

Published: 6 June 2012

References

- Bögre L, Magyar Z, López-Juez E: New clues to organ size control in plants. *Genome Biol* 2008, **9**:226.
- Mathur J, Hülkamp M: Microtubules and microfilaments in cell morphogenesis in higher plants. *Curr Biol* 2002, **12**:R669–R676.
- Guimil S, Dunand C: Cell growth and differentiation in Arabidopsis epidermal cells. *J Exp Bot* 2007, **58**:3829–3840.
- Pollard TD, Cooper JA: Actin, a central player in cell shape and movement. *Science* 2009, **326**:1208–1212.
- Reddy AS, Day IS: Analysis of the myosins encoded in the recently completed Arabidopsis thaliana genome sequence. *Genome Biol* 2001, **2**:RESEARCH0024.1-RESEARCH0024.17.
- Foth BJ, Goedecke MC, Soldati D: New insights into myosin evolution and classification. *Proc Natl Acad Sci U S A* 2006, **103**:3681–3686.
- Avisar D, Prokhnevsky AI, Makarova KS, Koonin EV, Dolja VV: Myosin XHK Is Required for Rapid Trafficking of Golgi Stacks, Peroxisomes, and Mitochondria in Leaf Cells of *Nicotiana benthamiana*. *Plant Physiol* 2008, **146**:1098–1108.
- Peremyshlov VV, Mockler TC, Filichkin SA, Fox SE, Jaiswal P, Makarova KS, Koonin EV, Dolja VV: Expression, splicing, and evolution of the myosin gene family in plants. *Plant Physiol* 2011, **155**:1191–1204.
- Reichelt S, Knight AE, Hodge TP, Baluska F, Samaj J, Volkmann D, Kendrick-Jones J: Characterization of the unconventional myosin VIII in plant cells and its localization at the post-cytokinetic cell wall. *Plant J* 1999, **19**:555–567.
- Baluska F, Cvrckova F, Kendrick-Jones J, Volkmann D: Sink Plasmodesmata as Gateways for Phloem Unloading. Myosin VIII and Calreticulin as Molecular Determinants of Sink Strength? *Plant Physiol* 2001, **126**:39–46.
- Avisar D, Prokhnevsky AI, Dolja VV: Class VIII myosins are required for plasmodesmal localization of a closterovirus Hsp70 homolog. *J Virol* 2008, **82**:2836–2843.
- Golomb L, Abu-Abied M, Belausov E, Sadot E: Different subcellular localizations and functions of Arabidopsis myosin VIII. *BMC Plant Biol* 2008, **8**:3.
- Sattarzadeh A, Franzen R, Schmelzer E: The Arabidopsis class VIII myosin ATM2 is involved in endocytosis. *Cell Motil Cytoskeleton* 2008, **65**:457–468.
- Lee Y-RJ, Liu B: Cytoskeletal Motors in Arabidopsis. Sixty-One Kinesins and Seventeen Myosins. *Plant Physiol* 2004, **136**:3877–3883.

15. Hashimoto K, Igarashi H, Mano S, Nishimura M, Shimmen T, Yokota E: Peroxisomal localization of a myosin XI isoform in *Arabidopsis thaliana*. *Plant Cell Physiol* 2005, **46**:782–789.
16. Li J-F, Nebenführ A: Organelle Targeting of Myosin XI Is Mediated by Two Globular Tail Subdomains with Separate Cargo Binding Sites. *J Biol Chem* 2007, **282**:20593–20602.
17. Reisen D, Hanson MR: Association of six YFP-myosin XI-tail fusions with mobile plant cell organelles. *BMC Plant Biol* 2007, **7**:6.
18. Avisar D, Abu-Abied M, Belausov E, Sadot E, Hawes C, Sparkes IA: A Comparative Study of the Involvement of 17 Arabidopsis Myosin Family Members on the Motility of Golgi and Other Organelles. *Plant Physiol* 2009, **150**:700–709.
19. Peremysov VV, Prokhnevsky AI, Avisar D, Dolja VV: Two Class XI Myosins Function in Organelle Trafficking and Root Hair Development in *Arabidopsis*. *Plant Physiol* 2008, **146**:1109–1116.
20. Prokhnevsky AI, Peremysov VV, Dolja VV: Overlapping functions of the four class XI myosins in *Arabidopsis* growth, root hair elongation, and organelle motility. *Proc Natl Acad Sci U S A* 2008, **105**:19744–19749.
21. Sparkes IA, Teany NA, Hawes C: Truncated myosin XI tail fusions inhibit peroxisome, Golgi, and mitochondrial movement in tobacco leaf epidermal cells: a genetic tool for the next generation. *J Exp Bot* 2008, **59**:2499–2512.
22. Peremysov VV, Prokhnevsky AI, Dolja VV: Class XI myosins are required for development, cell expansion, and F-Actin organization in *Arabidopsis*. *Plant Cell* 2010, **22**:1883–1897.
23. Ueda H, Yokota E, Kutsuna N, Shimada T, Tamura K, Shimmen T, Hasezawa S, Dolja VV, Hara-Nishimura I: Myosin-dependent endoplasmic reticulum motility and F-actin organization in plant cells. *Proc Natl Acad Sci U S A* 2010, **107**:6894–6899.
24. Ojangu E-L, Järve K, Paves H, Truve E: *Arabidopsis thaliana* myosin XIX is involved in root hair as well as trichome morphogenesis on stems and leaves. *Protoplasma* 2007, **230**:193–202.
25. Mathur J: The ARP2/3 complex: giving plant cells a leading edge. *Bioessays* 2005, **27**:377–387.
26. Smith LG, Oppenheimer DG: Spatial control of cell expansion by the plant cytoskeleton. *Annu Rev Cell Dev Biol* 2005, **21**:271–295.
27. Szymanski DB: Breaking the WAVE complex: the point of Arabidopsis trichomes. *Curr Opin Plant Biol* 2005, **8**:103–112.
28. Mathur J: Local interactions shape plant cells. *Curr Opin Cell Biol* 2006, **18**:40–46.
29. Li S, Blanchoin L, Yang Z, Lord EM: The putative Arabidopsis arp2/3 complex controls leaf cell morphogenesis. *Plant Physiol* 2003, **132**:2034–2044.
30. Mathur J, Mathur N, Kernebeck B, Hülkamp M: Mutations in actin-related proteins 2 and 3 affect cell shape development in *Arabidopsis*. *Plant Cell* 2003, **15**:1632–1645.
31. Basu D, El-Assal SE-D, Le J, Mallery EL, Szymanski DB: Interchangeable functions of Arabidopsis PIROGI and the human WAVE complex subunit SRA1 during leaf epidermal development. *Development* 2004, **131**:4345–4355.
32. Basu D, Le J, El-Assal SE-D, Huang S, Zhang C, Mallery EL, Koliantz G, Staiger CJ, Szymanski DB: DISTORTED3/SCAR2 is a putative arabidopsis WAVE complex subunit that activates the Arp2/3 complex and is required for epidermal morphogenesis. *Plant Cell* 2005, **17**:502–524.
33. Zhang X, Dyachok J, Krishnakumar S, Smith LG, Oppenheimer DG: IRREGULAR TRICHOME BRANCH1 in *Arabidopsis* encodes a plant homolog of the actin-related protein2/3 complex activator Scar/WAVE that regulates actin and microtubule organization. *Plant Cell* 2005, **17**:2314–2326.
34. Zhang C, Mallery EL, Schlueter J, Huang S, Fan Y, Brankle S, Staiger CJ, Szymanski DB: Arabidopsis SCARs function interchangeably to meet actin-related protein 2/3 activation thresholds during morphogenesis. *Plant Cell* 2008, **20**:995–1011.
35. Szymanski DB, Marks MD, Wick SM: Organized F-actin is essential for normal trichome morphogenesis in *Arabidopsis*. *Plant Cell* 1999, **11**:2331–2347.
36. Le J, El-Assal SE-D, Basu D, Saad ME, Szymanski DB: Requirements for Arabidopsis ATARP2 and ATARP3 during epidermal development. *Curr Biol* 2003, **13**:1341–1347.
37. El-Assal SE-D, Le J, Basu D, Mallery EL, Szymanski DB: Arabidopsis GNARLED encodes a NAP125 homolog that positively regulates ARP2/3. *Curr Biol* 2004, **14**:1405–1409.
38. Zimmermann I, Saedler R, Mutondo M, Hülkamp M: The Arabidopsis GNARLED gene encodes the NAP125 homolog and controls several actin-based cell shape changes. *Mol Genet Genomics* 2004, **272**:290–296.
39. Saedler R, Jakoby M, Marin B, Galiana-Jaime E, Hülkamp M: The cell morphogenesis gene SPIRRI in *Arabidopsis* encodes a WD/BEACH domain protein. *Plant J* 2009, **59**:612–621.
40. Le J, Mallery EL, Zhang C, Brankle S, Szymanski DB: Arabidopsis BRICK1/HSPC300 Is an Essential WAVE-Complex Subunit that Selectively Stabilizes the Arp2/3 Activator SCAR2. *Curr Biol* 2006, **16**:895–901.
41. Vidali L, Augustine RC, Kleinman KP, Bezanilla M: Profilin is essential for tip growth in the moss *Physcomitrella patens*. *Plant Cell* 2007, **19**:3705–3722.
42. Sorek N, Gutman O, Bar E, Abu-Abied M, Feng X, Running MP, Lewinsohn E, Ori N, Sadot E, Henis YI, Yalovsky S: Differential Effects of Prenylation and S-Acylation on Type I and II ROPS Membrane Interaction and Function. *Plant Physiol* 2011, **155**:706–720.
43. Szymanski DB, Jik RA, Pollock SM, Marks MD: Control of GL2 expression in *Arabidopsis* leaves and trichomes. *Development* 1998, **125**:1161–1171.
44. Hülkamp M, Misfa S, Jürgens G: Genetic dissection of trichome cell development in *Arabidopsis*. *Cell* 1994, **76**:555–566.
45. Szymanski DB, Marks MD: GLABROUS1 overexpression and TRIPTYCHON alter the cell cycle and trichome cell fate in *Arabidopsis*. *Plant Cell* 1998, **10**:2047–2062.
46. Hülkamp M, Schnittger A, Folkers U: Pattern formation and cell differentiation: trichomes in *Arabidopsis* as a genetic model system. *Int Rev Cytol* 1999, **186**:147–178.
47. Schnittger A, Hülkamp M: Trichome morphogenesis: a cell-cycle perspective. *Philos Trans R Soc Lond B Biol Sci* 2002, **357**:823–826.
48. Marcotrigiano M: A role for leaf epidermis in the control of leaf size and the rate and extent of mesophyll cell division. *Am J Bot* 2010, **97**:224–233.
49. Savaldi-Goldstein S, Peto C, Chory J: The epidermis both drives and restricts plant shoot growth. *Nature* 2007, **446**:199–202.
50. Savaldi-Goldstein S, Chory J: Growth coordination and the shoot epidermis. *Curr Opin Plant Biol* 2008, **11**:42–48.
51. Mathur J, Spielhofer P, Kost B, Chua N: The actin cytoskeleton is required to elaborate and maintain spatial patterning during trichome cell morphogenesis in *Arabidopsis thaliana*. *Development* 1999, **126**:5559–5568.
52. Schwab B, Mathur J, Saedler R, Schwarz H, Frey B, Scheidegger C, Hülkamp M: Regulation of cell expansion by the DISTORTED genes in *Arabidopsis thaliana*: actin controls the spatial organization of microtubules. *Mol Genet Genomics* 2003, **269**:350–360.
53. Dittmer TA, Richards EJ: Role of LINC proteins in plant nuclear morphology. *Plant Signal Behav* 2008, **3**:485–487.
54. Seagull RW, Falconer MM, Weerdenburg CA: Microfilaments: dynamic arrays in higher plant cells. *J Cell Biol* 1987, **104**:995–1004.
55. Meagher RB, McKinney EC, Kandasamy MK: Isovariant Dynamics Expand and Buffer the Responses of Complex Systems: The Diverse Plant Actin Gene Family. *Plant Cell* 1999, **11**:995–1006.
56. Yu M, Yuan M, Ren H: Visualization of actin cytoskeletal dynamics during the cell cycle in tobacco (*Nicotiana tabacum* L. cv Bright Yellow) cells. *Biol Cell* 2006, **98**:295–306.
57. Walter N, Holweg CL: Head-neck domain of Arabidopsis myosin XI, MYA2, fused with GFP produces F-actin patterns that coincide with fast organelle streaming in different plant cells. *BMC Plant Biol* 2008, **8**:74.
58. Harries PA, Pan A, Quatrano RS: Actin-related protein2/3 complex component ARPC1 is required for proper cell morphogenesis and polarized cell growth in *Physcomitrella patens*. *Plant Cell* 2005, **17**:2327–2339.
59. Qian P, Hou S, Guo G: Molecular mechanisms controlling pavement cell shape in *Arabidopsis* leaves. *Plant Cell Rep* 2009, **28**:1147–1157.
60. Kandasamy MK, Thorsness MK, Rundle SJ, Goldberg ML, Nasrallah JB, Nasrallah ME: Ablation of Papillar Cell Function in Brassica Flowers Results in the Loss of Stigma Receptivity to Pollination. *Plant Cell* 1993, **5**:263–275.
61. Alvarez-Buylla ER, Benitez M, Convera-Poiré A, Cadore AC, de Folter S, de Buen AG, Garay-Arroyo A, García-Ponce B, Jaimes-Miranda F, Pérez-Ruiz RV, Piñeyro-Nelson A, Sánchez-Corrales YE: Flower Development. *The Arabidopsis Book* 2010, **8**:e0127. doi:10.1199/tab.0127.
62. Edlund AF, Swanson R, Preuss D: Pollen and stigma structure and function: the role of diversity in pollination. *Plant Cell* 2004, **16**(Suppl): S84–S97.

63. Nasrallah JB, Stein JC, Kandasamy MK, Nasrallah ME: **Signaling the arrest of pollen tube development in self-incompatible plants.** *Science* 1994, **266**:1505–1508.
64. Nemhauser JL, Feldman LJ, Zambryski PC: **Auxin and ETIN in Arabidopsis gynoecium morphogenesis.** *Development* 2000, **127**:3877–3888.
65. Maisch J, Nick P: **Actin Is Involved in Auxin-Dependent Patterning.** *Plant Physiol* 2007, **143**:1695–1704.
66. Perrot-Rechenmann C: **Cellular responses to auxin: division versus expansion.** *Cold Spring Harb Perspect Biol* 2010, **2**:a001446.
67. Iwano M, Shiba H, Matoba K, Miwa T, Funato M, Entani T, Nakayama P, Shimosato H, Takaoka A, Isogai A, Takayama S: **Actin Dynamics in Papilla Cells of Brassica rapa during Self- and Cross-Pollination.** *Plant Physiol* 2007, **144**:72–81.
68. Alonso JM, Stepanova AN, Leisse TJ, Kim CJ, Chen H, Shinn P, Stevenson DK, Zimmerman J, Barajas P, Cheuk R, Gadrinab C, Heller C, Jeske A, Koesema E, Meyers CC, Parker H, Prednis L, Ansari Y, Choy N, Deen H, Geralt M, Hazari N, Hom E, Karnes M, Mulholland C, Ndubaku R, Schmidt I, Guzman P, Aguilar-Henonin L, Schmid M, Weigel D, Carter DE, Marchand T, Risseeuw E, Brogden D, Zeko A, Crosby WL, Berry CC, Ecker JR: **Genome-wide insertional mutagenesis of Arabidopsis thaliana.** *Science* 2003, **301**:653–657.
69. Oñate-Sánchez L, Vicente-Carbajosa J: **DNA-free RNA isolation protocols for Arabidopsis thaliana, including seeds and siliques.** *BMC Res Notes* 2008, **1**:93.
70. Zhang X, Oppenheimer DG: **A simple and efficient method for isolating trichomes for downstream analyses.** *Plant Cell Physiol* 2004, **45**:221–224.
71. Wadell H: **Volume, Shape, and Roundness of Quartz Particles.** *J Geol* 1935, **43**:250–280.
72. Alexander MP: **Differential staining of aborted and nonaborted pollen.** *Stain Technol* 1969, **44**:117–122.
73. Pagnussat GC, Yu H-J, Sundaresan V: **Cell-Fate Switch of Synergid to Egg Cell in Arabidopsis eostre Mutant Embryo Sacs Arises from Misexpression of the BEL1-Like Homeodomain Gene BLH1.** *Plant Cell* 2007, **19**:3578–3592.

doi:10.1186/1471-2229-12-81

Cite this article as: Ojangu et al.: Myosins XI-K, XI-1, and XI-2 are required for development of pavement cells, trichomes, and stigmatic papillae in *Arabidopsis*. *BMC Plant Biology* 2012 **12**:81.

**Submit your next manuscript to BioMed Central
and take full advantage of:**

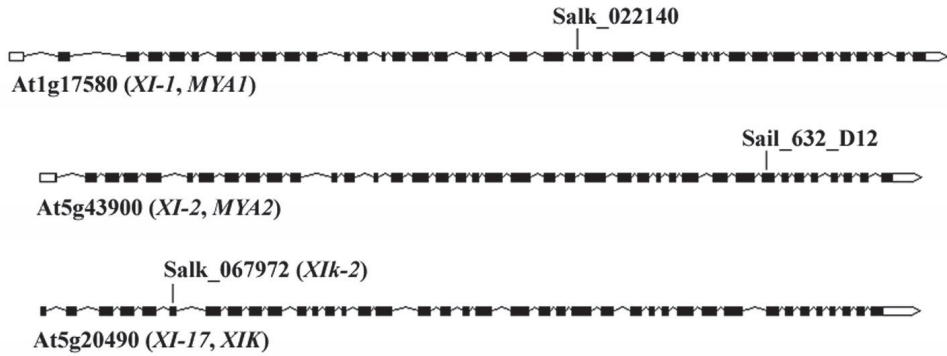
- Convenient online submission
- Thorough peer review
- No space constraints or color figure charges
- Immediate publication on acceptance
- Inclusion in PubMed, CAS, Scopus and Google Scholar
- Research which is freely available for redistribution

Submit your manuscript at
www.biomedcentral.com/submit



Additional file 1

A schematic diagram of XI-1, XI-2, and XI-K genes with the positions of the T-DNA insertions. Black boxes represent exons, black lines introns, and gray boxes represent 5' and 3' untranslated regions. Above the corresponding T-DNA insertion sites are shown.



Additional file 2

Data for Figure 2B: size of the five-week-old rosette leaves (from 5th to 10th; mm).

	MEAN	MEDIAN	STDEV	SEM	n	Repeated Measures ANOVA	Dunn's test WT versus:	%
petiole length								
WT	14.78	15.07	2.07	0.49	18	P<0.0001		100
<i>xi-2/xi-k</i>	11.26	10.75	1.75	0.41	18		P<0.01	76
<i>xi-1/xi-2/xi-k</i>	8.84	9.10	1.26	0.30	18		P<0.01	60
blade length								
WT	20.87	21.17	2.51	0.59	18	P<0.0001		100
<i>xi-2/xi-k</i>	20.17	20.73	2.56	0.60	18		P>0.05	97
<i>xi-1/xi-2/xi-k</i>	16.58	17.30	2.16	0.51	18		P<0.01	79
blade width								
WT	9.55	9.27	1.07	0.25	18	P<0.0001		100
<i>xi-2/xi-k</i>	10.80	10.87	0.71	0.17	18		P<0.01	113
<i>xi-1/xi-2/xi-k</i>	9.48	9.57	0.82	0.19	18		P>0.05	99

Abbreviations: STDEV, standard deviation; SEM, standard error of the mean; n, number of data points.

Statistical analysis: Repeated Measures ANOVA and Dunn's Multiple Comparisons Test.

%. mean values of the wild type (WT) were arbitrarily set at 100% and compared to the mean values of the mutants.

Additional file 3

Data for Figure 2C: cell areas (μm^2) of pavement and mesophyll cells of five-week-old rosette leaves.

*area	MEAN	MEDIAN	STDEV	SEM	**n	One-Way Analysis ANOVA	Dunnett's test WT versus:	%
pavement cells								
WT	3382.7	3450.6	543.4	192.1	8	P<0.0001		100
<i>xi-2/xi-k</i>	2820.4	2794.7	421.1	148.9	8		P<0.05	83
<i>xi-1/xi-2/xi-k</i>	2206.8	2214.6	204.8	72.4	8		P<0.01	65
mesophyll cells								
WT	2113.3	1954.9	434.9	217.5	4	P>0.05		100
<i>xi-2/xi-k</i>	1932.8	1931.2	63.2	31.6	4		P>0.05	91
<i>xi-1/xi-2/xi-k</i>	1699.8	1692.5	155.9	78.0	4		P>0.05	80

Abbreviations: STDEV, standard deviation; SEM, standard error of the mean; n, number of data points.

*Area measurement: the number of cells on the image divided by the image's area, whereas cells on the image over or touching the lines on top and on the left were counted, but cells over or touching the right or bottom lines were ignored.

**n indicates the number of images (each containing 50-80 cells) used for counting cells.

Statistical analysis: One-Way Analysis of Variance ANOVA and Dunnett's Multiple Comparisons Test.

%: mean values of the wild type (WT) were arbitrarily set at 100% and compared to the mean values of the mutants.

Additional file 4

Data for Figure 2E: circularity of pavement cells on the leaf abaxial epidermis.

	MEAN	MEDIAN	STDEV	SEM	n	unpaired <i>t</i> -test with Welch correction
*circularity						P<0.0001
WT	0.041	0.037	0.013	0.003	16	
$\chi^2-1/\chi^2-2/\chi^2-k$	0.139	0.142	0.019	0.005	13	

Abbreviations: STDEV, standard deviation; SEM, standard error of the mean; n, number of data points.

*Cell circularity was calculated according to the following formula $4\pi \cdot \text{area}/\text{perimeter}^2$ using ImageJ software.

Statistical analysis: unpaired *t*-test with Welch correction.

Additional file 5

Shoot size of six-week-old plants. Wild type plants are on the left and *xi-1/xi-2/xi-k* plants are on the right. Both bolt formation as well as onset of flowering of *xi-1/xi-2/xi-k* plants delays significantly (two weeks).



Additional file 6

Data for supplementing Additional file 5: inflorescence shoot height (cm).

	MEAN	MEDIAN	STDEV	SEM	n	Kruskal-Wallis test	Dunn's test WT versus:	%
*shoot height								
WT	31.00	32.00	5.05	1.03	24	P<0.01		100
<i>xt-1/xt-k</i>	29.35	28.00	4.28	0.84	26		P>0.05	95
<i>xt-2/xt-k</i>	28.21	27.50	4.36	0.82	28		P>0.05	91
<i>xt-1/xt-2/xt-k</i>	25.75	26.00	4.61	0.87	28		P<0.01	83

Abbreviations: STDEV, standard deviation; SEM, standard error of the mean; n, number of data points.

* Shoot height of eight week-old plants was measured (after flowering was complete for wild type).

Statistical analysis:Kruskal-Wallis Test and Dunn's Multiple Comparisons test.

%; mean values of the wild type (WT) were arbitrarily set at 100% and compared to the mean values of the mutants.

Additional file 7

Data for Figure 3A: lengths of trichome stalk and branches (μm).

	MEAN	MEDIAN	STDEV	SEM	n	Kruskal Wallis test	Dunn's test WT versus:	%
Stalk						P<0.0001		
WT	126.5	117.9	44.1	4.5	97			100
<i>xi-1</i>	110.2	108.1	34.9	3.6	94		P>0.05	87
<i>xi-2</i>	120.6	114.5	36.9	3.5	109		P>0.05	95
<i>xi-k</i>	118.5	117.5	36.8	3.8	96		P>0.05	94
<i>xi-1/xi-2</i>	115.4	115.4	35.9	3.6	80		P>0.05	91
<i>xi-1/xi-k</i>	159.7	154.3	50.2	4.8	108		P<0.001	126
<i>xi-2/xi-k</i>	181.1	166.9	74.1	7.1	108		P<0.001	143
<i>xi-1/xi-2/xi-k</i>	136.0	132.4	47.7	5.5	73		P>0.05	107
BR1						P<0.0001		
WT	315.2	311.8	68.7	7.0	97			100
<i>xi-1</i>	323.7	324.7	76.7	7.9	94		P>0.05	103
<i>xi-2</i>	320.8	312.4	80.3	7.7	109		P>0.05	102
<i>xi-k</i>	279.7	274.2	63.8	6.5	96		P<0.05	89
<i>xi-1/xi-2</i>	322.2	322.2	78.5	7.8	80		P>0.05	102
<i>xi-1/xi-k</i>	284.7	272.8	88.5	8.5	108		P<0.05	90
<i>xi-2/xi-k</i>	256.7	232.9	101.1	9.7	108		P<0.001	81
<i>xi-1/xi-2/xi-k</i>	139.8	121.3	63.9	7.4	73		P<0.001	44
BR2						P<0.0001		
WT	278.0	268.9	61.9	6.3	97			100
<i>xi-1</i>	289.5	283.5	71.8	7.4	94		P>0.05	104
<i>xi-2</i>	280.9	277.4	70.6	6.8	109		P>0.05	101
<i>xi-k</i>	230.8	221.2	59.3	6.0	96		P<0.001	83
<i>xi-1/xi-2</i>	285.2	285.2	71.2	7.1	80		P>0.05	103
<i>xi-1/xi-k</i>	222.7	213.9	57.8	5.6	108		P<0.001	80
<i>xi-2/xi-k</i>	179.3	173.6	38.2	3.7	108		P<0.001	64
<i>xi-1/xi-2/xi-k</i>	108.9	104.8	35.7	4.1	73		P<0.001	39
BR3						P<0.0001		
WT	257.5	240.8	61.6	6.3	97			100
<i>xi-1</i>	261.0	260.2	65.2	6.7	94		P>0.05	101
<i>xi-2</i>	251.4	239.7	65.6	6.3	109		P>0.05	98
<i>xi-k</i>	197.3	191.4	50.1	5.1	96		P<0.001	77
<i>xi-1/xi-2</i>	256.2	256.2	65.4	6.5	80		P>0.05	99
<i>xi-1/xi-k</i>	171.9	162.5	50.2	4.8	108		P<0.001	67
<i>xi-2/xi-k</i>	165.2	159.5	39.4	3.8	108		P<0.001	64
<i>xi-1/xi-2/xi-k</i>	98.4	93.6	32.7	3.8	73		P<0.001	38

Abbreviations: BR1, branch 1; BR2, branch 2; BR3, branch 3; STDEV, standard deviation;

SEM, standard error of the mean; n, number of data points.

Statistical analysis: Kruskal-Wallis Test and Dunn's Multiple Comparisons Test.

‰: mean values of the wild type (WT) were arbitrarily set at 100% and compared to the mean values of the mutants.

Additional file 8

Data for Figure 3B: length ratios of the trichome stalk and branches.

	MEAN	MEDIAN	STDEV	SEM	n	Kruskal Wallis test	Dunn's test WT versus:
*BR/stalk						P<0.0001	
WT	2.37	2.29	0.49	0.05	97		
<i>xi-1</i>	2.76	2.71	0.57	0.06	94		P<0.05
<i>xi-2</i>	2.43	2.39	0.47	0.04	109		P>0.05
<i>xi-k</i>	2.06	2.06	0.37	0.04	96		P<0.05
<i>xi-1/xi-2</i>	2.60	2.55	0.52	0.05	80		P>0.05
<i>xi-1/xi-k</i>	1.48	1.43	0.35	0.03	108		P<0.001
<i>xi-2/xi-k</i>	1.25	1.18	0.50	0.05	108		P<0.001
<i>xi-1/xi-2/xi-k</i>	1.00	0.86	0.60	0.07	73		P<0.001

Abbreviations: BR, trichome branch; STDEV, standard deviation; SEM, standard error of the mean; n, number of data points.

* BR/stalk ratio: average length of trichome branches (BR1, BR2, BR3) divided with the length of the stalk.

Statistical analysis: Kruskal-Wallis Test and Dunn's Multiple Comparisons Test.

Additional file 9

Data for Figure 5B: sphericity of trichome nuclei.

	MEAN	MEDIAN	STDEV	SEM	n	Kruskal-Wallis test	Dunn's test WT versus:
*Sphericity						0.0001	
WT	0.65	0.67	0.11	0.009	157		
<i>xi-1</i>	0.62	0.64	0.11	0.013	69		P>0.05
<i>xi-2</i>	0.58	0.59	0.09	0.008	151		P<0.001
<i>xi-k</i>	0.60	0.60	0.08	0.010	75		P<0.01
<i>xi-1/xi-2</i>	0.61	0.61	0.09	0.012	55		P<0.05
<i>xi-1/xi-k</i>	0.62	0.62	0.08	0.009	81		P>0.05
<i>xi-2/xi-k</i>	0.52	0.51	0.08	0.008	88		P<0.001
<i>xi-1/xi-2/xi-k</i>	0.60	0.57	0.10	0.010	89		P<0.001

Abbreviations: BR, branch; STDEV, standard deviation; SEM, standard error of the mean; n, number of data points.

*Sphericity is a measure of how spherical (round) an object is, whereas values equal to 1.00 represent a perfect sphere.

Statistical analysis: Kruskal-Wallis Test and Dunn's Multiple Comparisons Test.

Additional file 10

Data for figure 5B: sphericity data and correlation between the sphericity of the trichome nucleus and the trichome shape.

Sphericity	MEAN	MEDIAN	STDEV	SEM	n	Mann-Whitney test (sphericity):	p-value (correlation):
WT	0.83	0.84	0.07	0.01	56	N.A.*	
<i>xi-2/xi-k</i>	0.62	0.60	0.13	0.02	32	$P < 0.0001$	-0.7120 $P < 0.0001$

Abbreviations: BR, branch; STDEV, standard deviation; SEM, standard error of the mean; n, number of data points;

r, Pearson's correlation coefficient; N.A., not applicable.

Statistical analysis: Mann-Whitney Test, Pearson's correlation coefficient.

* Can not be calculated as there is no variance in the shape of WT trichomes.

Additional file 11

Data for Figure 7: number of siliques per main stem of eight week-old plants.

	MEAN	MEDIAN	STDEV	SEM	n	Kruskal-Wallis test	Dunn's test WT versus:	%
WT								
total n of siliques	36.71	39.00	9.47	2.53	14	P>0.05		100
*n of abnormal siliques	1.71	0.00	3.00	0.80		P<0.0001		5
<i>xi-1/xi-k</i>								
total n of siliques	32.75	30.50	7.85	1.96	16		P>0.05	100
n of abnormal siliques	0.13	0.00	0.50	0.13			P>0.05	0
<i>xi-2/xi-k</i>								
total n of siliques	33.77	31.00	7.04	1.95	13		P>0.05	100
n of abnormal siliques	0.00	0.00	0.00	0.00			P>0.05	0
<i>xi-1/xi-2/xi-k</i>								
total n of siliques	30.86	29.00	4.81	1.05	21		P>0.05	100
n of abnormal siliques	18.48	18.00	4.20	0.92			P<0.001	60

Abbreviations: STDEV, standard deviation; SEM, standard error of the mean; n, number of data points.

Statistical analysis: Kruskal-Wallis Test and Dunn's Multiple Comparisons Test.

*Siliques with the length from 4 to 10 mm were evaluated as abnormal.

%: mean number of siliques (per main stem) were taken as 100% and compared to the mean number of abnormal siliques.

Additional file 12

Data for Figures 6 and 7: length of the silique (mm) and number of seeds per silique.

	MEAN	MEDIAN	STDEV	SEM	n	Kruskal-Wallis test	Dunn's test	Mann-Whitney test
WT							WT versus:	WT versus:
silique length	14.48	14.50	0.76	0.20	15	P<0.0001		
seeds per silique	57.60	56.00	2.80	0.72		P<0.0001		
unfertilized ovules	0.73	1.00	1.03	0.27		P<0.0001		
<i>xi-1/xi-2/xi-k</i>								
silique length *I	6.54	6.00	2.56	0.71	13		P<0.001	
seeds per silique I	2.15	1.00	2.91	0.81			P<0.001	
<i>xi-1/xi-2/xi-k</i>								
silique length *II	12.87	13.00	1.78	0.46	15		P>0.05	
seeds per silique II	50.93	51.00	4.22	1.09			P<0.05	
unfertilized ovules II	14.40	12.00	11.93	3.08				P<0.0001

Abbreviations: STDEV, standard deviation; SEM, standard error of the mean; n, number of data points.

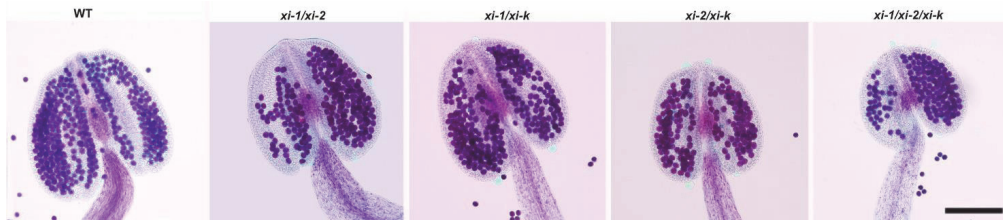
Statistical analysis: Kruskal-Wallis Test, Dunn's Multiple Comparisons Test and Mann-Whitney Test.

*I - siliques developed after onset of flowering (during first two to three weeks) on main stem.

*II - siliques developed "after switch" (starting from three to four weeks after onset of flowering) on main stem.

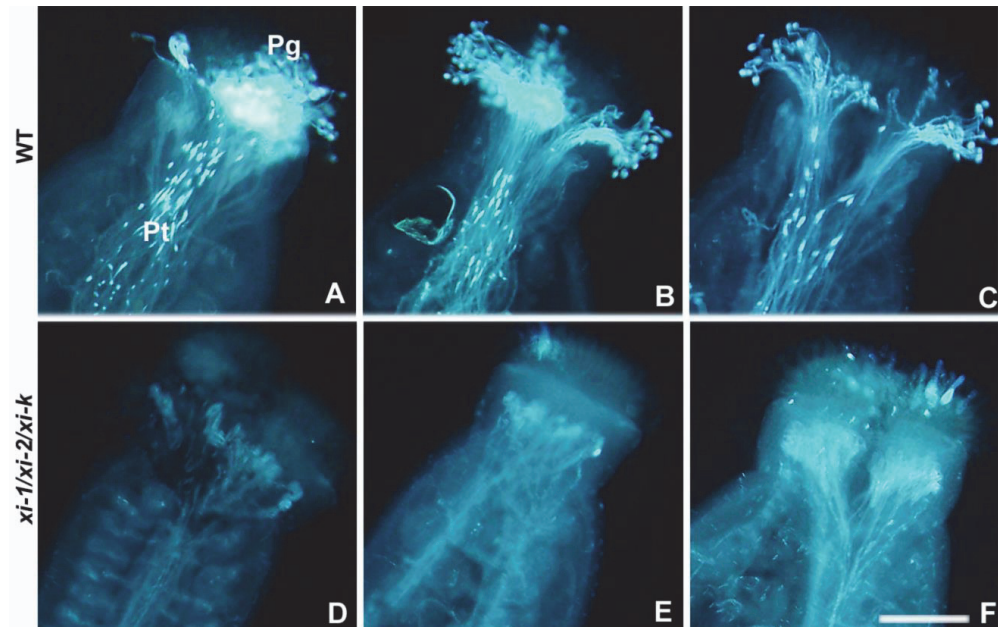
Additional file 13

Pollen viability assessed by Alexander's staining method. Pollen viability (purple-colored cytoplasm of pollen grains) is similar both in wild type (WT) as well as in all double and triple mutant plants.
Bar = 100 μ m.



Additional file 14

Development of pollen tubes in self-pollinated pistils. Shortly after the onset of flowering first three flowers on the primary shoot were analyzed. A-C) Aniline blue staining of wild type (WT) pistils. D-F) Aniline blue staining of *xi-1/xi-2/xi-k* pistils. In *xi-1/xi-2/xi-k*, pollen grains were not attached to the stigmas and pollen tubes were not formed. Pg – pollen grains; Pt – pollen tubes. Bar = 100 μ m.



Additional file 15

Data for Figure 9: size of floral organs (mm), length of the peduncles, sepals, petals and buds.

Floral organs	MEAN	MEDIAN	STDEV	SEM	n	Unpaired <i>t</i> -test with Welch correction	%
WT	Peduncle	8.05	2.21	0.84	7		100
	Sepal	2.94	0.24	0.08	10		100
	Petal	5.31	0.46	0.14	10		100
	Bud	2.91	0.36	0.10	12		100
<i>xi-1/xi-2/xi-k</i>	Peduncle	7.09	0.96	0.39	6	$P > 0.05$	88
	Sepal	2.60	0.17	0.05	12	$P < 0.01$	88
	Petal	4.40	0.44	0.13	12	$P < 0.001$	83
	Bud	1.91	0.33	0.10	12	$P < 0.001$	66

Abbreviations: STDEV, standard deviation; SEM, standard error of the mean; n, number of data points.

Statistical analysis: unpaired *t*-test with Welch correction.

%: mean values of the wild type (WT) were arbitrarily set at 100% and compared to the mean values of the mutants.

Publication III

Ojangu E.-L., Ilau B., Tanner K., Talts K., Ihoma E., Dolja VV., Paves H., Truve E. (2018). Class XI myosins contribute to auxin response and senescence-induced cell death in *Arabidopsis*. *Front. Plant Sci.* 9:1570.



Class XI Myosins Contribute to Auxin Response and Senescence-Induced Cell Death in *Arabidopsis*

Eve-Ly Ojangu^{1*}, Birger Ilau¹, Krista Tanner¹, Kristiina Talts¹, Eliis Ihoma¹, Valerian V. Dolja², Heiti Paves¹ and Erkki Truve¹

¹ Department of Chemistry and Biotechnology, Tallinn University of Technology, Tallinn, Estonia, ² Department of Botany and Plant Pathology, Oregon State University, Corvallis, OR, United States

OPEN ACCESS

Edited by:

Jian Xu,
National University of Singapore,
Singapore

Reviewed by:

Andreas Nebenführ,
The University of Tennessee,
Knoxville, United States
Jie Le,
Institute of Botany (CAS), China

*Correspondence:

Eve-Ly Ojangu
eve-ly.ojangu@ttu.ee

Specialty section:

This article was submitted to
Plant Evolution and Development,
a section of the journal
Frontiers in Plant Science

Received: 29 May 2018

Accepted: 08 October 2018

Published: 27 November 2018

Citation:

Ojangu E-L, Ilau B, Tanner K,
Talts K, Ihoma E, Dolja VV, Paves H
and Truve E (2018) Class XI Myosins
Contribute to Auxin Response
and Senescence-Induced Cell Death
in *Arabidopsis*.
Front. Plant Sci. 9:1570.
doi: 10.3389/fpls.2018.01570

The integrity and dynamics of actin cytoskeleton is necessary not only for plant cell architecture but also for membrane trafficking-mediated processes such as polar auxin transport, senescence, and cell death. In *Arabidopsis*, the inactivation of actin-based molecular motors, class XI myosins, affects the membrane trafficking and integrity of actin cytoskeleton, and thus causes defective plant growth and morphology, altered lifespan and reduced fertility. To evaluate the potential contribution of class XI myosins to the auxin response, senescence and cell death, we followed the flower and leaf development in the triple gene knockout mutant *xi1 xi2 xik* (3KO) and in rescued line stably expressing myosin XI-K:YFP (3KOR). Assessing the development of primary inflorescence shoots we found that the 3KO plants produced more axillary branches. Exploiting the auxin-dependent reporters DR5::GUS and IAA2::GUS, a significant reduction in auxin responsiveness was found throughout the development of the 3KO plants. Examination of the flower development of the plants stably expressing the auxin transporter PIN1::PIN1-GFP revealed partial loss of PIN1 polarization in developing 3KO pistils. Surprisingly, the stable expression of PIN1::PIN1-GFP significantly enhanced the semi-sterile phenotype of the 3KO plants. Further we investigated the localization of myosin XI-K:YFP in the 3KOR floral organs and revealed its expression pattern in floral primordia, developing pistils, and anther filaments. Interestingly, the XI-K:YFP and PIN1::PIN1-GFP shared partially overlapping but distinct expression patterns throughout floral development. Assessing the foliar development of the 3KO plants revealed increased rosette leaf production with signs of premature yellowing. Symptoms of the premature senescence correlated with massive loss of chlorophyll, increased cell death, early plasmolysis of epidermal cells, and strong up-regulation of the stress-inducible senescence-associated gene *SAG13* in 3KO plants. Simultaneously, the reduced auxin responsiveness and premature leaf senescence were accompanied by significant anthocyanin accumulation in 3KO tissues. Collectively, our results provide genetic evidences that *Arabidopsis* class XI myosins arrange the flower morphogenesis and leaf longevity via contributing to auxin responses, leaf senescence, and cell death.

Keywords: *Arabidopsis*, myosin XI, auxin response, PIN1, flower development, senescence, *SAG13*, anthocyanins

INTRODUCTION

The dynamics of actin cytoskeleton, including filament assembly, disassembly and reorganization are regulated by diverse actin binding proteins (ABPs). Various genetic studies have shown that down-regulation of ABPs affects the organization and dynamics of the actin arrays in plant cells (Kandasamy et al., 2005; Henty-Ridilla et al., 2014; Li et al., 2014; Wu et al., 2015; Tang et al., 2017). Actin-dependent molecular motors, myosins, make up a one group of the ABPs that transport endomembranes and other macromolecular cargoes along actin filaments (AFs) in plant cells. In *Arabidopsis*, the cell elongation is affected significantly when multiple class XI myosins are simultaneously eliminated (Prokhnevsky et al., 2008; Peremyslov et al., 2010; Ueda et al., 2010; Ojangu et al., 2012; Cai et al., 2014; Madison et al., 2015; Scheuring et al., 2016; Talts et al., 2016; Abu-Abied et al., 2018). In particular, the stature of myosin XI single, double, triple, quadruple and quintuple knockout plants is decreased progressively along with the reduction in cell size (Ojangu et al., 2007, 2012; Peremyslov et al., 2008, 2010; Prokhnevsky et al., 2008; Ueda et al., 2010; Park and Nebenführ, 2013; Cai et al., 2014; Madison et al., 2015; Abu-Abied et al., 2018). At a subcellular level, myosin XI inactivation in triple knockout mutant *xil xil2 xil3* (3KO) results in reorientation of prominent actin bundles, reduced dynamic behavior of actin arrays, changes in membrane trafficking and deceleration of cytoplasmic streaming (Peremyslov et al., 2010; Ueda et al., 2010; Park and Nebenführ, 2013; Cai et al., 2014; Scheuring et al., 2016). Thus, in the 3KO, cytoplasmic streaming is virtually arrested, the elongation of epidermal and other cell types is decreased and therefore plant size and fertility is affected (Peremyslov et al., 2010; Ueda et al., 2010; Ojangu et al., 2012; Cai et al., 2014; Scheuring et al., 2016).

In addition to being essential for cell integrity, actin cytoskeleton contributes to processes such as polar auxin transport (PAT) (Nick et al., 2009; Zhu and Geisler, 2015; Wu et al., 2015; Zhu et al., 2016; Eggenberger et al., 2017; Huang et al., 2017) and regulation of programmed cell death (PCD) (Kandasamy et al., 2005; Thomas et al., 2006; Breeze et al., 2011; Keech, 2011; Smertenko and Franklin-Tong, 2011).

Various genetic and pharmacological studies have revealed tight interplay between auxin signaling and actin cytoskeleton. On the one hand, the patterning of actin arrays is modulated by auxin; on the other hand, auxin transport depends on the organization and dynamics of microfilaments (Zhu and Geisler, 2015). Auxin regulates both expansion and polarity of individual cells, as well as initiation and patterning of organs. Transient auxin concentration gradients underlie developmental processes such as meristem initiation, organ primordia formation, embryo morphogenesis, lateral root formation, as well as regulation of phyllotaxy and vascular tissue differentiation, photo- and gravitropic responses (Berleth and Sachs, 2001; Vanneste and Friml, 2009; Cardarelli and Cecchetti, 2014; Adamowski and Friml, 2015). Transient auxin concentration gradients result from local biosynthesis and polar cell-to-cell transport of the hormone. PAT is mediated by specific auxin uptake permeases and efflux carrier proteins that localize to plasma membrane in an asymmetric manner. PIN-FORMED (PIN) and ATP-binding

cassette transporters/*P*-glycoprotein (ABCB/PGP) families are principal auxin efflux carriers whereas members of Auxin-Resistant 1/LIKE-AUX1 (AUX1/LAX) family are major auxin uptake carriers (Okada et al., 1991; Bennett et al., 1996; Gälweiler et al., 1998; Luschnig et al., 1998; Marchant et al., 1999; Swarup et al., 2001; Geisler and Murphy, 2006; Kreczek et al., 2009; Zážimalová et al., 2010; Swarup and Péret, 2012; Adamowski and Friml, 2015). The regulation of PAT depends mainly on the action of auxin efflux carriers of the PIN and ABCB/PGP families (Geisler and Murphy, 2006; Vanneste and Friml, 2009; Adamowski and Friml, 2015). Both auxin influx permease AUX1, as well as efflux carriers (PINs and ABCBs) cycle between the plasma membrane and endosomal compartments (Geldner et al., 2001; Kleine-Vehn et al., 2006, 2011; Cho et al., 2007; Kleine-Vehn and Friml, 2008; Titapiwatanakun et al., 2009; Swarup and Péret, 2012; Cho and Cho, 2013; Wang et al., 2013). The crosstalk between auxin and actin is confirmed by findings showing that both localization and recycling of auxin importers and exporters depends partially on AFs (Geldner et al., 2001; Kleine-Vehn et al., 2006; Dhonukshe et al., 2008; Wu et al., 2015; Zhu and Geisler, 2015). However, the exact role of the actin cytoskeleton in PAT is still unresolved. It has been suggested that interactions between auxin and actin are not only dose- and time-dependent, but also species- and organ-dependent (Zhu and Geisler, 2015).

Several recent findings have shown that alterations in the cytoskeleton polymerization status are also critical for triggering PCD in plants (Smertenko et al., 2003; Thomas et al., 2006; Keech et al., 2010; Breeze et al., 2011; Keech, 2011; Smertenko and Franklin-Tong, 2011; Chang et al., 2015). Senescence is the terminal phase in organ development that involves a programmed degradation of cellular components. The resulting degradation products of senescing tissues are reused to support the growth of newly forming organs like leaves, roots, tubers, shoots, flowers, fruits, and seeds (Himmelblau and Amasino, 2001; Maillard et al., 2015). Leaf senescence, the most well studied type of organ senescence in *Arabidopsis*, is characterized by the elevated expression of the senescence-associated genes (SAGs), early auxin-responsive small auxin-up RNA genes (SAURs), loss of chlorophyll, degradation of organelles, autolysis distinguished by fragmentation of the tonoplast and subsequent removal of the cytoplasm (Lohman et al., 1994; Weaver et al., 1998; Lin and Wu, 2004; Zentgraf et al., 2004; Balazadeh et al., 2008; Hou et al., 2013; Watanabe et al., 2013; Woo et al., 2013; Ren and Gray, 2015; Kim et al., 2016). Many SAGs encode proteins that drive breakdown of cellular components, such as short-chain alcohol dehydrogenase SAG13, and cysteine protease SAG12 (Weaver et al., 1997; Buchanan-Wollaston et al., 2003; Lin and Wu, 2004; Zentgraf et al., 2004; Watanabe et al., 2013; Woo et al., 2013; Kim et al., 2016). It has been demonstrated that the *SAG12* is specifically induced by developmental senescence, and *SAG13* by a range of senescence-inducing stress-treatments such as detachment, hormonal treatment, darkness, drought, wounding and pathogen attack. Therefore, it is proposed that *SAG12* could be the marker for age-related developmental senescence, and *SAG13* for stress-induced senescence or general cell-death (Schipper et al., 2007).

Auxin involvement in senescence has been observed to a much longer than the role of cytoskeleton (Hodge and Sacher, 1975;

Noodén and Noodén, 1985; Lim et al., 2010; Kim et al., 2011; Ren and Gray, 2015; Cha et al., 2016). Nevertheless, the precise functions of auxin in leaf senescence remain unclear due to controversial results reporting either negative or positive role of auxin in leaf senescence regulation (Lim et al., 2010; Kim et al., 2011; Hou et al., 2013; Jibrán et al., 2013; Woo et al., 2013; Khan et al., 2014; Ren and Gray, 2015; Cha et al., 2016). However, it has been suggested that auxin may promote leaf senescence through the expression of *SAUR36* gene in *Arabidopsis* (Hou et al., 2013).

Although the auxin impact on secondary metabolism in plants is not well understood, numerous investigations point to the auxin's role in modulating flavonoid biosynthesis (Buer and Muday, 2004; Besseau et al., 2007; Lewis et al., 2011; Kuhn et al., 2016). Flavonoids, in turn, are considered to be endogenous regulators of auxin efflux carriers, suggesting a crosstalk between auxin- and flavonoid-dependent processes (Murphy et al., 2000; Brown et al., 2001; Buer and Muday, 2004; Peer et al., 2004; Besseau et al., 2007; Peer and Murphy, 2007; Santelia et al., 2008; Zažímalová et al., 2010). Flavonoid biosynthesis produces a variety of distinct flavonoid subclasses, including anthocyanins, a group of pink, red, purple or blue pigments widely produced in plants (Harborne and Baxter, 1999). In *Arabidopsis*, anthocyanins accumulate in variable amounts in leaves and stems, depending on light intensity and nutrition (Holton and Cornish, 1995; Gou et al., 2011). Accumulation of anthocyanins and acceleration of senescence are also well documented under certain stress conditions including reduced nitrogen levels and high light intensity (Feild et al., 2001; Peng et al., 2008; Sekhon et al., 2012; Misyura et al., 2013).

Even though myosin and AFs act in concert, the potential role of myosins in auxin responses is starting to be revealed, but the one in senescence and cell death largely remains addressed. It has been reported previously that myosin 3KO roots show moderate unresponsiveness to exogenous auxin treatment, exhibiting partially insensitive vacuoles (Scheuring et al., 2016). Because both the AF architecture and overall actin dynamics are altered in myosin 3KO cells (Peremylov et al., 2010; Ueda et al., 2010; Cai et al., 2014; Scheuring et al., 2016), it is likely that the mutant cells are less responsive to physiological and developmental stimuli such as auxin signaling. Very recent findings of Abu-Abied et al. (2018) showed that the altered root architecture of the 3KO plants was in correlation with the reduced auxin gradient, and partial loss of PIN1 polarization in the stele cells. These results provide first evidence that PAT, at least partially, could be myosin-mediated process in *Arabidopsis*.

In this study, we assessed the potential roles of class XI myosins in mediating auxin response and cell death during floral development and leaf senescence, respectively. We used well-characterized class XI myosin triple gene knockout mutant 3KO (Ojangu et al., 2012) as it has exhibited a prominent phenotype including stunted growth, partially impaired shoot development, and premature leaf yellowing, suggesting a possible connection between myosin function, auxin distribution and senescence signaling. Investigation of the genetically rescued 3KOR (Peremylov et al., 2012) line confirmed that the observed defects have a myosin-dependent nature. Auxin-related processes in 3KO background were monitored through evaluating the

activity of the auxin-responsive reporters DR5::GUS and IAA2::GUS, and comparing the expression patterns of the auxin efflux carrier PIN1::PIN1-GFP and of myosin XI-K::YFP in floral development. Senescence-related processes were analyzed by measuring the contents of chlorophylls and anthocyanins, and following the cell integrity, and patterning of AFs in senescent leaf cells. In addition, relative expression levels of auxin-responsive and senescence-related genes were evaluated. Collectively, our data imply that class XI myosins contribute significantly to auxin responses, stress-induced senescence, and cell death in *Arabidopsis*. At that, we provide first genetic evidences that actomyosin cytoskeleton mediates senescence-processes in *Arabidopsis*. Moreover, our results indicate that there is a mutual crosstalk between actomyosin cytoskeleton, auxin-regulated and senescence-dependent processes, and secondary metabolism.

MATERIALS AND METHODS

Plant Material and Growth Conditions

Arabidopsis thaliana (ecotype Columbia-0) seeds of *xi1* (Salk_022140; At1g17580), *xi2* (Sail_632_D12; At5g43900), *xik* (Salk_067972; At5g20490) T-DNA mutant lines and PIN1::PIN1-GFP (ecotype Landsberg erecta, Ler) line (N23889) were obtained from the Nottingham *Arabidopsis* Stock Centre. Myosin mRNA levels of single mutant T-DNA lines were determined earlier by RT-qPCR (Talts et al., 2016). The myosin triple mutant line *xi1 xi2 xik* (3KO in this work) was published previously (Ojangu et al., 2012). PIN1::PIN1-GFP (Ler) and IAA2::GUS (Ler) lines were backcrossed four times to Columbia-0 (Columbia or Col in this work) prior to phenotypic analyses. The genetic background of the 3KO line transformed with the gene encoding YFP-tagged myosin XI-K, *xi1 xi2 xik XI-K::YFP* (3KOR in this work), was described earlier (Peremylov et al., 2012). Reporter lines DR5::GUS (Col-0) and IAA2::GUS (Ler) were obtained from Malcolm Bennett's lab, and seeds of the 35S::GFP-fABD2-GFP (Wang et al., 2008) line from Alison B. Blancaflor's lab. The genes of DR5::GUS and IAA2::GUS auxin reporters, and the 35S::GFP-fABD2-GFP actin marker were introduced into the 3KO line by crossing the plant lines.

Vernalized seeds were held in water at 4°C for 1 day before sowing in the soil containing 50% (v/v) vermiculite. Plants were grown in growth chambers under 16 h light/8 h dark period at 22 ± 2°C and 60% of relative humidity. For the seedling analysis seeds were surface sterilized and grown on 0.5 × MS medium (Murashige and Skoog, 1962) supplemented with 1% sucrose in climate chambers as described above.

For 1-*N*-naphthylphthalamic acid (NPA) treatments, primary inflorescences were dipped twice (with 3-days interval) with 100 μM NPA (Sigma-Aldrich) and 0.01% (v/v) Silwet L-77 as adapted from Nemhauser et al. (2000). NPA was dissolved in dimethyl sulfoxide (DMSO), and mock treatments were performed with Milli-Q water containing 0.1% (v/v) DMSO and 0.01% Silwet L-77. For latrunculin B (LatB) (Abcam) treatments, 50 mg of 7-day-old seedlings grown on agar plates were incubated for 6 h in 5 ml of liquid MS medium supplemented with 0.5 μM

LatB (dissolved in DMSO), and mock treatments were performed with liquid MS medium containing 0.025% (v/v) DMSO.

Quantitative Analysis of β -Glucuronidase (GUS) Activity in Plant Extracts

The activity of β -glucuronidase (GUS) can be determined in extracts of plant tissue using 4-methylumbelliferyl β -D-glucuronide (4-MUG) as a substrate. The 4-MUG fluorometric assay of plant extracts was performed to measure the GUS activity under the control of the DR5 promoter. For vegetative growth phase analysis 100 mg of 12-day-old seedlings and 23-day-old rosettes were collected and frozen. For generative growth phase analysis, 100 mg of primary inflorescence stems were collected when in height of 10–14 cm (floral transition stage) and 20–25 cm (silique formation stage). Protocol for quantitative GUS activity assay was adapted from Lewis and Muday (2009). Plant extract preparation was as follows: 150 μ l GUS extraction buffer (50 mM sodium phosphate buffer pH 7.0; 10 mM EDTA pH 8.0; 0.1% SDS; 0.1% Triton X-100; 10 mM β -mercaptoethanol; 25 μ g/ μ l PMSF) was added to the 100 mg of frozen tissues, homogenized at 28 Hz/min for 2 min (Qiagen TissueLyser), cell debris was removed by centrifugation (15 min 13,200 rpm at 4°C). The reaction was carried out by adding 50 μ l of plant extract to the 450 μ l pre-warmed reaction mixture (GUS extraction buffer supplemented with 2 mM 4-MUG), incubated 20 h at 37°C in darkness. The reaction was stopped by adding 100 μ l of reaction mixture to 900 μ l of ice-cold 0.2 M Na₂CO₃. 255 μ l of the stopped reaction was loaded to the black 90-well microassay plates (Greiner) and protected from light. Released 4-methylumbelliferone (4-MU) (AppliChem) was excited at 340 nm and emission was measured at 492 nm using Tecan GENios Pro. Total protein content of extracts was measured following BioRad QuickStart 1 \times Bradford protocol. Two to three experiments were performed with each tissue type, including 6–12 biological and two technical replicates per experiment. The GUS activity was expressed as picomoles of 4-MU produced per minute per milligram protein (pmol/min/mg).

Microscopy

The expression pattern analysis of Columbia and 3KO plants stably expressing PIN1::PIN1-GFP, XI-K::YFP or 35S::GFP-ABD2-GFP was performed with Carl Zeiss LSM 510 META confocal laser scanning microscope. GFP or YFP was excited at 488 nm with argon laser and fluorescence was detected with 505–550 nm band-pass filter; band-pass filter 575–615 IR was used for chlorophyll autofluorescence detection. Dissected flower parts, buds, and floral primordia were immersed in 50% glycerol or 95% perfluorodecalin (Sigma-Aldrich). Silicon spacer was applied in between glass slide and cover slip to prevent crushing tissues. Presented images show Z-stacks of confocal images combined into single image by maximal intensity projections using Zeiss LSM Image Browser software.

For histochemical analysis, DR5::GUS and IAA2::GUS plants were treated according to a standard protocol (Weigel and Glazebrook, 2002), immersed in Mowiol mounting medium, and

analyzed under a light microscope. Images of DR5::GUS plants and trypan blue stained leaves were captured with digital camera Nikon D800E using a slide copying adapter ES-1. Images of IAA2::GUS inflorescences and flowers were captured with Zeiss SteREO Discovery.V8.

Scanning electron microscope (SEM) analysis was performed with Carl Zeiss EVO LS15. For flower architecture analysis in *Arabidopsis*, flower parts were dissected on double-sided tape using fine needle (27G) and SEM images of unfixed and uncoated flower tissues were captured using a reduced vacuum mode (100–200 Pa).

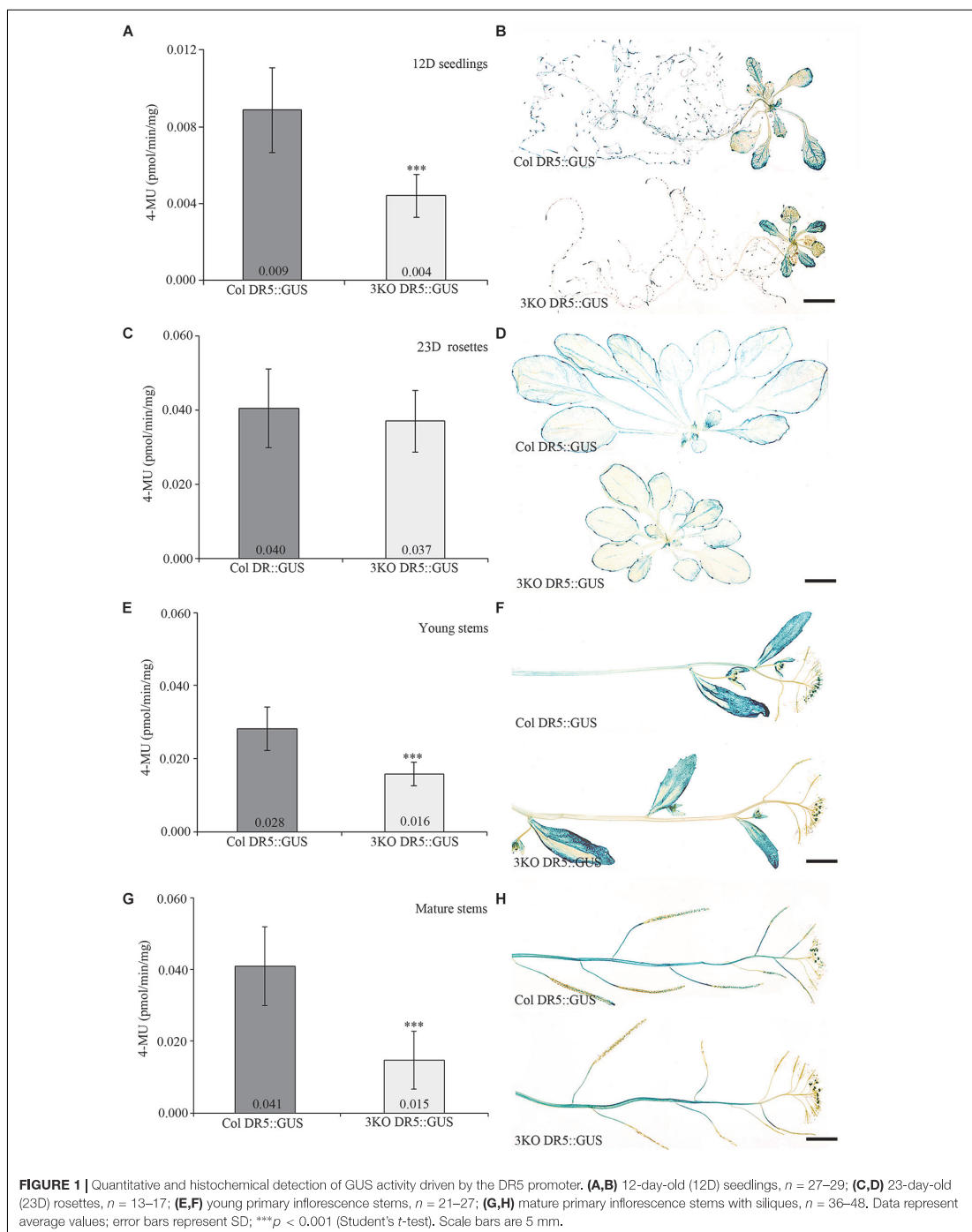
Adobe Photoshop CS6 was used to assemble photographs, indicate details, and measure the intensity of trypan blue staining on leaf photographs (as mean value of the blue channel). ImageJ2 software was used to analyze the PIN1-GFP fluorescence in single optical longitudinal sections (0.71 μ m thick) of outer epidermal cells of stage 8 gynoecia. GFP fluorescence intensities of apical and lateral membranes of each cell was measured as quotients: mean gray values divided by values of selected areas. The ratios of the GFP fluorescence of apical membranes versus lateral membranes of each cell were used to evaluate the distribution of PIN1-GFP: the average ratio value of Columbia cells (3.3) was set as threshold to discriminate the cells with less polarized (<3.3) and more polarized (>3.3) PIN1-GFP distribution. The lower the ratio number was the less the fluorescence between apical and lateral membranes differentiated.

Quantification of Total Chlorophyll Content

For chlorophyll extraction, the fifth and sixth leaves from 23-day-old rosettes (before bolt formation) were dissected and frozen immediately. For dark-induced senescence, dissected leaves were placed in 30 ml of Milli-Q water and incubated for 3 days in growth chamber at darkness. One biological replicate contained six leaves – the fifth and sixth leaves from three different 23-day-old rosettes. Three independent experiments with six biological replicates in each were performed. Chlorophyll was extracted from the rosette leaves before and after dark-treatment as described previously (Hu et al., 2013; Misyura et al., 2013). Briefly, 1 ml of ice cold 80% acetone in 0.2 M Tris-buffer (pH 8.0) was added to frozen samples, homogenized with chrome-steal beads in TissueLyser 20 Hz/min for 1 min, and incubated 12 h in the dark at 4°C. Next day, samples were centrifuged 15 min 3000 rpm at 4°C. The extraction with 80% acetone solution was repeated three times, supernatants of every extraction were collected. 1 ml of extract was transferred to a disposable polymethyl methacrylate (PMMA) cuvette, and absorbance at 645 and 663 nm were measured. The total chlorophyll concentration in fresh weight (mg/g) were calculated using the equation:

$$\text{Chlorophyll } a + b =$$

$$\frac{[(8.05 \times OD_{663}) + (20.29 \times OD_{645})] \times V [\text{extract volume (ml)}]}{1000 \times W [\text{fresh weight (g)}]}$$



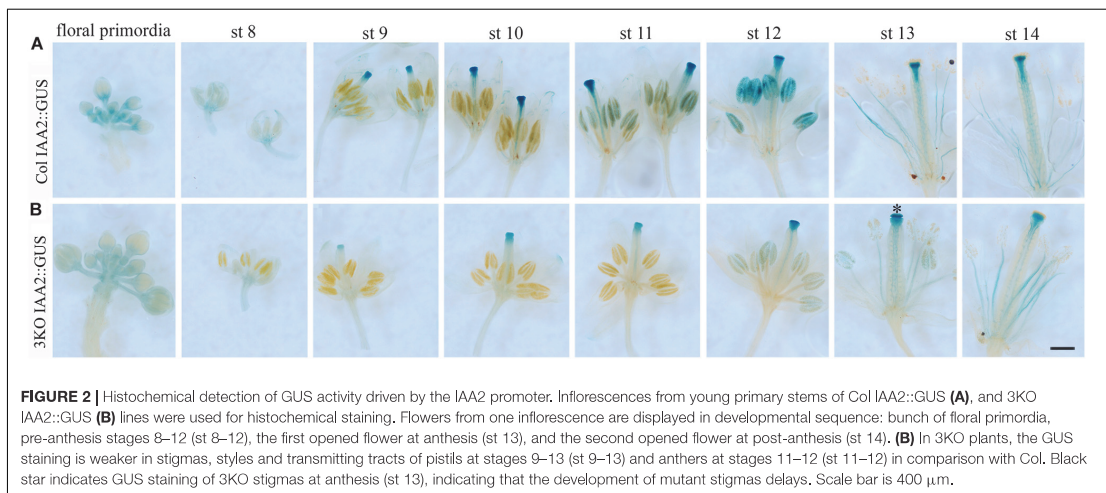


FIGURE 2 | Histochemical detection of GUS activity driven by the IAA2 promoter. Inflorescences from young primary stems of Col IAA2::GUS (**A**), and 3KO IAA2::GUS (**B**) lines were used for histochemical staining. Flowers from one inflorescence are displayed in developmental sequence: bunch of floral primordia, pre-anthesis stages 8–12 (st 8–12), the first opened flower at anthesis (st 13), and the second opened flower at post-anthesis (st 14). (**B**) In 3KO plants, the GUS staining is weaker in stigmas, styles and transmitting tracts of pistils at stages 9–13 (st 9–13) and anthers at stages 11–12 (st 11–12) in comparison with Col. Black star indicates GUS staining of 3KO stigmas at anthesis (st 13), indicating that the development of mutant stigmas delays. Scale bar is 400 μm .

Trypan Blue Staining

For trypan blue staining the fifth leaves from 21-day-old rosettes were selected. Fresh or dark treated leaves were boiled in lactophenol (10 ml of lactic acid, 10 ml of glycerol, 10 ml of liquid phenol, and 10 ml of distilled H_2O) containing 10 mg of trypan blue for 1 min. Tissues were cleared in alcoholic lactophenol (2:1 95% ethanol:lactophenol) for 2 min, washed in 50% ethanol at room temperature, and stored in Milli-Q water. For the analysis, leaves were immersed in Mowiol mounting medium.

Quantification of Anthocyanin Content

Anthocyanin extraction from *Arabidopsis* seedlings was performed as described previously (Nakata and Ohme-Takagi, 2014). In brief, 100 mg of 7-day-old seedlings were frozen in liquid nitrogen, homogenized at 28 Hz/min for 2 min (TissueLyser), and suspended into five volumes of extraction buffer (45% methanol and 5% acetic acid). Cell debris was removed by centrifugation (20 min 13,200 rpm at room temperature). The relative anthocyanin content was calculated from the absorbance at 530 and 657 nm (Shimadzu Biospec Mini) using the equation:

$$\text{Relative anthocyanin content} = \frac{[OD_{530} - (0.25 \times OD_{657})] \times V [\text{extract volume (ml)}]}{1000 \times W [\text{fresh weight (g)}]}$$

RNA Extraction and Reverse Transcription – Quantitative Real-Time PCR (RT-qPCR)

Total RNA was extracted from 50 mg of plant material according to the method described by Oñate-Sánchez and Vicente-Carbajosa (2008). Buffer volumes were scaled up three times. Expression levels of *AUX1*, *IAA2*, *PIN1*, *PIN3*, *PIN4*, *PIN7*, *SAUR36*, *SAG12*, and *SAG13* genes were analyzed. RNA was

extracted from 7-day-old seedlings, 21-day-old leaves before and after dark-induced senescence, and mature inflorescences. cDNA was synthesized from 5 μg of DNase-treated RNA using Maxima Reverse Transcriptase (Thermo Scientific) and random hexamer primer. cDNAs were diluted twofold for qPCR. All RT-qPCR reactions were performed in 384-well plates on the LightCycler 480 instrument (Roche Applied Science). qPCR reactions were performed in duplicate and Cq values were averaged. Each 7 μl reaction contained 1.4 μl 5x HOT FIREPol® EvaGreen® qPCR Mix Plus (no ROX) (Solis Biotec), 0.7 μl diluted cDNA and 3.5 pmol of each primer. qPCR conditions were as follows: initial denaturation at 95°C for 12 min, followed by 45 cycles of 95°C for 15 s, 59°C for 30 s and 72°C for 30 s. All primers used for qPCR experiments were designed for an annealing temperature of 60–62°C. Primers used for qPCR experiments are listed in **Supplementary Table S1**. Primers for reference genes were chosen as described previously (Czechowski et al., 2005; **Supplementary Table S1**). In all experiments, three reference genes were used for normalization: SAND, UBC, and expressed sequence EX70. Five to six biological replicates were analyzed in each experiment. Reference gene stability was analyzed using GeNorm M and coefficient of variation (CV) in qbase^{PLUS} software (Hellemans et al., 2007). Statistical analysis (One-Way ANOVA) was performed with qbase^{PLUS} software.

RESULTS

The Activity of the Auxin-Responsive Reporters Is Reduced in 3KO Plants

Auxin signaling regulates all aspects of plant development, including determination of apical dominance during shoot growth, through finely tuned concentration gradients

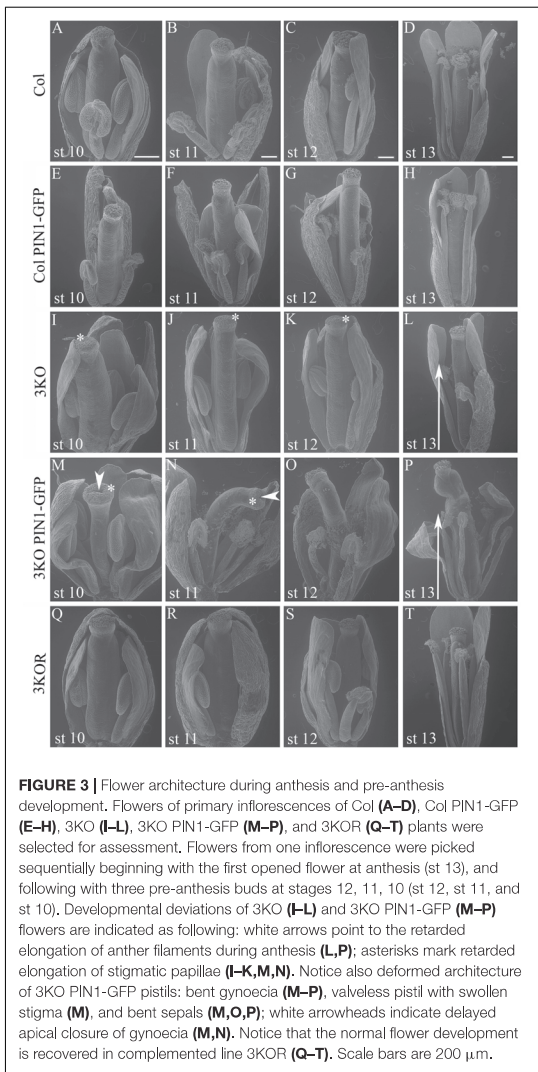


FIGURE 3 | Flower architecture during anthesis and pre-anthesis development. Flowers of primary inflorescences of Col (A–D), Col PIN1-GFP (E–H), 3KO (I–L), 3KO PIN1-GFP (M–P), and 3KOR (Q–T) plants were selected for assessment. Flowers from one inflorescence were picked sequentially beginning with the first opened flower at anthesis (st 13), and following with three pre-anthesis buds at stages 12, 11, 10 (st 12, st 11, and st 10). Developmental deviations of 3KO (I–L) and 3KO PIN1-GFP (M–P) flowers are indicated as following: white arrows point to the retarded elongation of anther filaments during anthesis (L,P); asterisks mark retarded elongation of stigmatic papillae (I–K,M,N). Notice also deformed architecture of 3KO PIN1-GFP pistils: bent gynoceia (M–P), valveless pistil with swollen stigma (M), and bent sepals (M,O,P); white arrowheads indicate delayed apical closure of gynoceia (M,N). Notice that the normal flower development is recovered in complemented line 3KOR (Q–T). Scale bars are 200 μm .

(Berleth and Sachs, 2001; Vernoux et al., 2010). Investigating the overall plant morphology, we noticed that the shoot development of 3KO plants varied significantly as mutant plants frequently displayed partially reduced apical dominance, and increased formation of axillary branches (Supplementary Figure S1). The average number of secondary inflorescences per cm of primary stems in 3KO plants was 1.8-fold, and the one of tertiary inflorescences 2.4-fold higher in comparison with Columbia control (Supplementary Figure S1). To assess if the developmental defects of 3KO plants have auxin-dependent nature, we used the auxin-responsive promoter-reporters DR5::GUS (β -glucuronidase), and

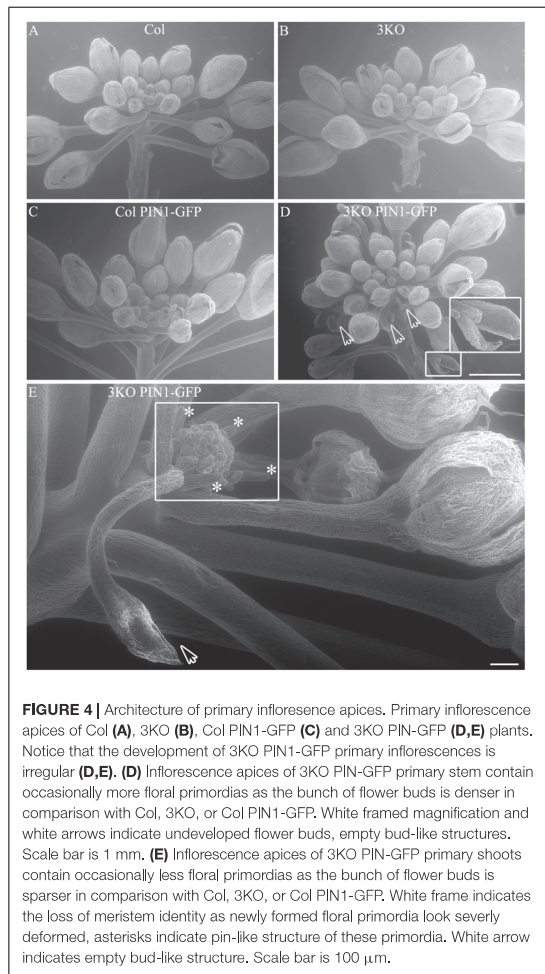


FIGURE 4 | Architecture of primary inflorescence apices. Primary inflorescence apices of Col (A), 3KO (B), Col PIN1-GFP (C) and 3KO PIN1-GFP (D,E) plants. Notice that the development of 3KO PIN1-GFP primary inflorescences is irregular (D,E). (D) Inflorescence apices of 3KO PIN1-GFP primary stem contain occasionally more floral primordias as the bunch of flower buds is denser in comparison with Col, 3KO, or Col PIN1-GFP. White framed magnification and white arrows indicate undeveloped flower buds, empty bud-like structures. Scale bar is 1 mm. (E) Inflorescence apices of 3KO PIN1-GFP primary shoots contain occasionally less floral primordias as the bunch of flower buds is sparser in comparison with Col, 3KO, or Col PIN1-GFP. White frame indicates the loss of meristem identity as newly formed floral primordia look severely deformed, asterisks indicate pin-like structure of these primordia. White arrow indicates empty bud-like structure. Scale bar is 100 μm .

IAA2::GUS which have been widely used as relevant markers to study endogenous auxin responses (Ulmasov et al., 1997; Shibasaki et al., 2009).

Fluorescent GUS assay using 4-methylumbelliferyl- β -D-galactopyranoside (4-MUG) fluorophore was used to measure DR5 promoter activity in plant extracts. Extracts prepared from 3KO seedlings stably expressing DR5::GUS (3KO DR5::GUS) showed 2.3-fold lower DR5 promoter activity when compared to the Columbia wild type control (Col DR5::GUS; Figure 1A). More specifically, histochemical GUS staining revealed reduced coloration in the roots of 3KO DR5::GUS plants (Figure 1B). GUS activity in rosette leaves of 3KO DR5::GUS plants was comparable with Columbia control (Figures 1C,D). Young 10–14 cm inflorescence stems and mature 20–25 cm inflorescence stems of the 3KO DR5::GUS plants showed 1.8-fold (Figure 1E) and 2.7-fold decrease (Figure 1G) in GUS activity, respectively, in

comparison with Columbia control. Histochemical GUS assays revealed reduced GUS activity in the stems (Figure 1F) and siliques (Figure 1H) of 3KO DR5::GUS plants.

The IAA2::GUS reporter was used both for quantitative and histochemical analysis. Quantitative analysis of the IAA2::GUS activity in Columbia and 3KO extracts showed the similar reduction as the DR5::GUS reporter (data not shown). Histochemical staining of young inflorescences of Columbia and 3KO plants stably expressing IAA2::GUS showed similar staining patterns but different staining intensities (Figure 2). Throughout the flower development, the GUS staining in 3KO IAA2::GUS pistils (stigma, style and transmitting tract) (Figure 2B; st 9–13) and anthers (Figure 2B; st 10–11) was weaker than that in Columbia IAA2::GUS line. In addition, the GUS staining of 3KO stigmas at anthesis (Figure 2B; st 13) highlighted the retarded development of 3KO stigmas which was demonstrated previously (Ojangu et al., 2012).

We also analyzed the effect of NPA, the polar auxin transport inhibitor, on the IAA2::GUS expression. For this, inflorescences of Columbia IAA2::GUS and 3KO IAA2::GUS plants were dipped twice with 100 μ M NPA. The histochemical examination of primary inflorescences revealed that NPA-treatment led to increased IAA2::GUS activity both in Columbia and 3KO inflorescences, when compared to DMSO-treated controls (Supplementary Figure S2). However, the responses to NPA were somewhat different in Columbia and 3KO. In NPA-treated Columbia, the strong GUS staining was spread all over the gynoecia, but it did not accumulate in valves of 3KO IAA2::GUS gynoecia (Supplementary Figure S2). Slightly weaker staining of pedicels, petals and sepals was noticeable in 3KO IAA2::GUS also (Supplementary Figure S2).

These results show that the simultaneous inactivation of three class XI myosins reduces the auxin responses of different *Arabidopsis* tissues.

Stable Expression of PIN1-GFP in 3KO Enhances Abnormalities in Flower Formation and Growth

In *Arabidopsis*, developmentally important auxin gradients are generated during PAT by modulating the organization and dynamics of actin cytoskeleton (Geldner et al., 2001; Ivakov and Persson, 2013; Zhu and Geisler, 2015). As the aberrant shoot development in 3KO plants correlated with the reduced auxin response, we further investigated if this was due to possible deviations in the distribution of auxin efflux carrier PIN1, since it plays an essential role in flower and inflorescence formation (Okada et al., 1991). For this, we examined the effect of stable expression of PIN1::PIN1-GFP in 3KO (3KO PIN1-GFP) and Columbia control plants (Col PIN1-GFP).

It is previously described that in 3KO plants, the fertility is slightly decreased as the pistil maturation (elongation of stigmas) partially delays (Ojangu et al., 2012). Interestingly, when examining the flowers at anthesis (stage 13/14) by using SEM, we found that the elongation of stamen filaments in parental 3KO line frequently delayed also (Figure 3L; white arrow). This

indicated that during flower anthesis of the 3KO plants the rapid growth spurt of stamen filaments is partially retarded, and thus stamens often do not reach stigmas in time for proper pollination.

Even more surprising was the finding that previously described semi-sterile phenotype of 3KO plants was exacerbated in the 3KO PIN1-GFP line. SEM imaging revealed that the architecture of inflorescences, formation of floral primordia (Figure 4), and development of floral organs (Figure 3) were significantly affected in 3KO PIN1-GFP plants. The 3KO PIN1-GFP inflorescences displayed very irregular architecture being occasionally denser (Figure 4D and Supplementary Figure S3) or sparser (Figure 4E) in comparison with Columbia, 3KO or Col PIN1-GFP plants, indicating that the inflorescence meristem was partially disturbed. No matter if meristem produced more or less floral primordia (Figures 4D,E) their capability to develop into normal flowers was partially impaired. Some flowers showed completely arrested development (Figures 4D,E) and others exhibited a range of morphologies, from near-normal to severely deformed (Figure 3 and Supplementary Figure S3). Undeveloped flowers did not contain pistils, petals or anthers, and consisted only of one to three sepal-like structures (Figures 4D,E; white arrows). In extreme cases, the inflorescence meristem of the 3KO PIN1-GFP line produced only ~20 near-normal flowers or floral buds. Thereafter, the emergence of new flowers stopped, since only needle-like floral primordia were formed (Figure 4E; asterisks). However, the most prevalent flower deformation was a significantly bent shape of pistils (Figures 3N–P). Delayed apical closure of gynoecia (Figures 3M,N; white arrowheads) and pistils with decreased valves, and swollen style and stigma region (Figure 3M) were frequently observable during late stages of 3KO PIN1-GFP flower development. Besides serious aberrations, the flowers of 3KO PIN1-GFP plants exhibited also same deviations as parental 3KO line: retarded elongation of stamen filaments (anthesis stage 13/14) (Figure 3P; white arrow) and stigmatic papillae (pre-anthesis stage 11) (Figure 3N; asterisk). Modified architecture of 3KO PIN1-GFP inflorescences and flowers indicated that even the modest overexpression of PIN1 under native promoter may disturb auxin responses, and thus affect developmental decisions, when the actomyosin cytoskeleton is simultaneously affected.

Partial Loss of PIN1-GFP Polarization During 3KO Flower Development

Next, the distribution of auxin efflux carrier PIN1 in flower tissues of 3KO and Columbia plants was visualized with expression of the PIN1::PIN1-GFP. Examination of the PIN1-GFP distribution in flower tissues of Columbia plants revealed its presence in septum or valve margins of pistils, as well as in floral primordia (Figure 5A). The PIN1 patterning in the Columbia gynoecia was consistent with previously published data (Zúñiga-Mayo et al., 2014). The overall patterning of the PIN1-GFP in 3KO floral tissues was broadly the same with some exceptions. For instance, in heavily deformed 3KO pistils, such as valveless gynoecia, the PIN1-GFP signal was spread all over the gynoecium (Figure 5B; St 10; white bold arrow). Similarly, PIN-GFP pattern

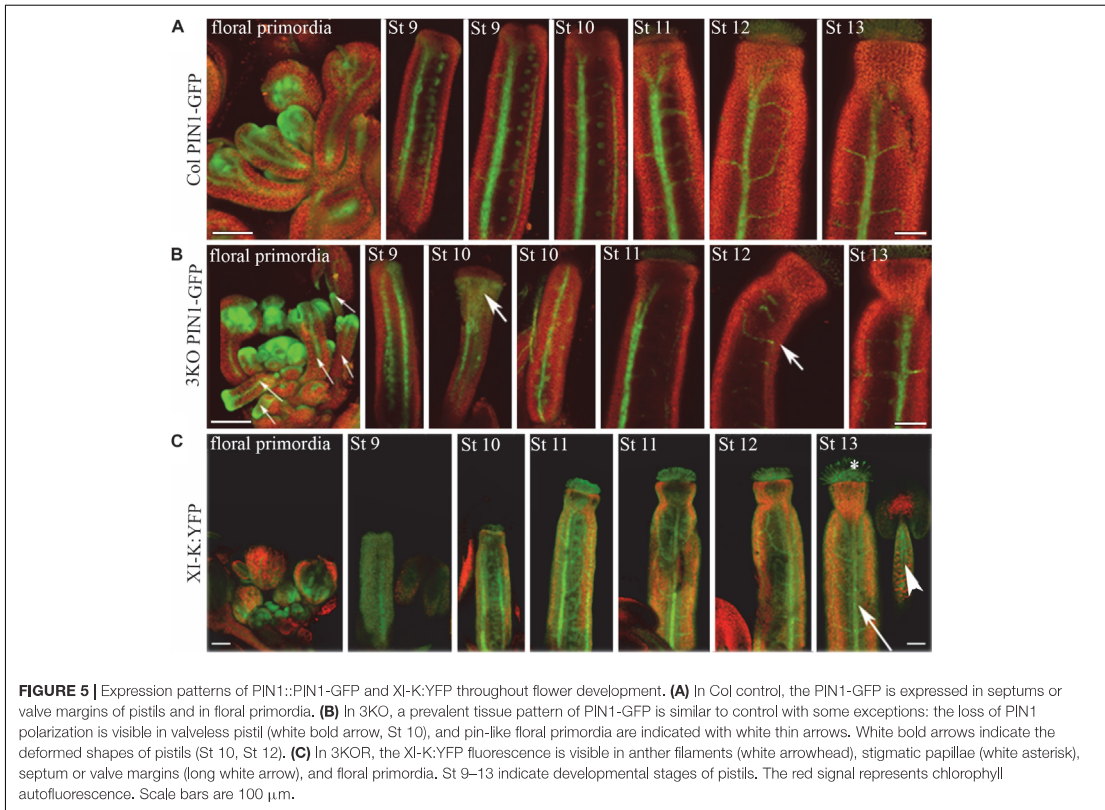


FIGURE 5 | Expression patterns of PIN1::PIN1-GFP and XI-K::YFP throughout flower development. **(A)** In Col control, the PIN1-GFP is expressed in septums or valve margins of pistils and in floral primordia. **(B)** In 3KO, a prevalent tissue pattern of PIN1-GFP is similar to control with some exceptions: the loss of PIN1 polarization is visible in valveless pistil (white bold arrow, St 10), and pin-like floral primordia are indicated with white thin arrows. White bold arrows indicate the deformed shapes of pistils (St 10, St 12). **(C)** In 3KOR, the XI-K::YFP fluorescence is visible in anther filaments (white arrowhead), stigmatic papillae (white asterisk), septum or valve margins (long white arrow), and floral primordia. St 9–13 indicate developmental stages of pistils. The red signal represents chlorophyll autofluorescence. Scale bars are 100 μm .

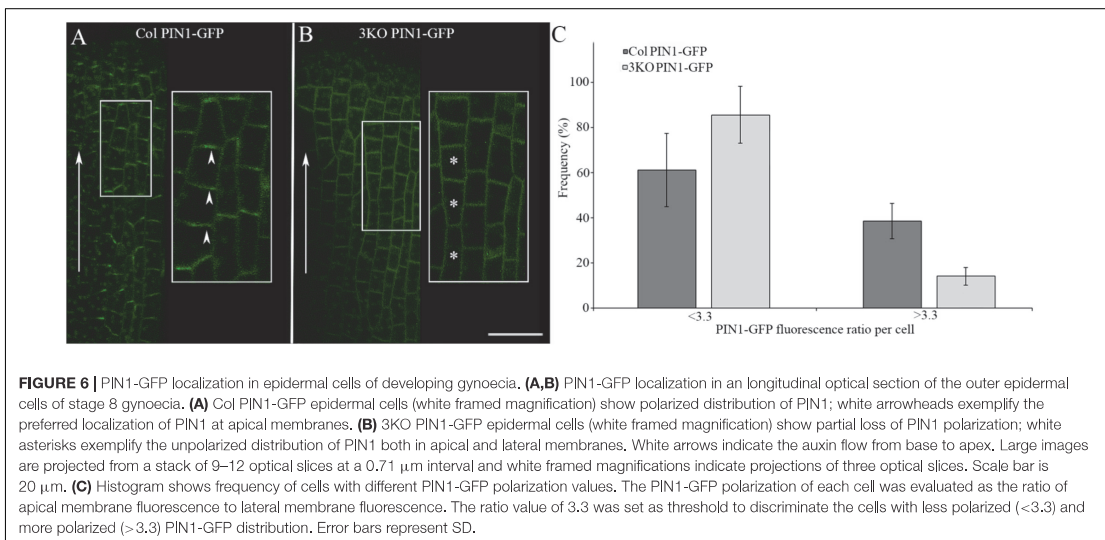


FIGURE 6 | PIN1-GFP localization in epidermal cells of developing gynoecia. **(A,B)** PIN1-GFP localization in a longitudinal optical section of the outer epidermal cells of stage 8 gynoecia. **(A)** Col PIN1-GFP epidermal cells (white framed magnification) show polarized distribution of PIN1; white arrowheads exemplify the preferred localization of PIN1 at apical membranes. **(B)** 3KO PIN1-GFP epidermal cells (white framed magnification) show partial loss of PIN1 polarization; white asterisks exemplify the unpolarized distribution of PIN1 both in apical and lateral membranes. White arrows indicate the auxin flow from base to apex. Large images are projected from a stack of 9–12 optical slices at a 0.71 μm interval and white framed magnifications indicate projections of three optical slices. Scale bar is 20 μm . **(C)** Histogram shows frequency of cells with different PIN1-GFP polarization values. The PIN1-GFP polarization of each cell was evaluated as the ratio of apical membrane fluorescence to lateral membrane fluorescence. The ratio value of 3.3 was set as threshold to discriminate the cells with less polarized (<3.3) and more polarized (>3.3) PIN1-GFP distribution. Error bars represent SD.

in developing 3KO floral primordia was occasionally aberrant (**Supplementary Figure S4**).

We examined the PIN1-GFP polarization in developing gynoecia at the cellular level because the significant pistil deformation was the most prominent phenotype of the 3KO PIN1::PIN1-GFP line. PIN1-GFP localization in longitudinal optical sections of the outer epidermal cell layer of stage 8 gynoecia was evaluated as ratio of apical membrane fluorescence to lateral membrane fluorescence of each cell. In outer epidermal cell layer of Columbia gynoecia, the PIN1-GFP was prominently apically localized (**Figure 6A**; arrowheads), the average ratio of GFP fluorescence of apical membranes versus lateral membranes was 3.3 ± 1.75 ($n = 31$). Epidermal cells of 3KO gynoecia displayed comparable PIN1-GFP fluorescence on both apical and lateral membranes (**Figure 6B**; asterisks), the average ratio of GFP fluorescence of apical membranes versus lateral membranes was 2.3 ± 1.33 [$n = 42$; $p < 0.05$ (Student's *t*-test)]. To further validate the frequency of less and more polarized PIN1-GFP distribution of epidermal cells in Columbia and 3KO gynoecia, the ratio value of 3.3 of the GFP fluorescence was set as threshold (**Figure 6C**). The quantification showed that the ratio values less than 3.3 were observed in 86% of epidermal cells of developing 3KO PIN1-GFP gynoecia (**Figure 6C**) while in Col PIN1-GFP gynoecia, the frequency was 61% (**Figure 6C**). The ratio values higher than 3.3 were observed only in 14% of 3KO PIN1-GFP cells but in 39% of Col PIN1-GFP cells (**Figure 6C**). The gynoecium is the last organ to initiate from the floral meristem (Larsson et al., 2014), and apical domains such as the style and stigma are last structures which emerge during gynoecium development. The partial loss of PIN1 polarization in 3KO PIN1-GFP line is in accordance with severe pistil defects and indicated that the apical domains (style and stigma) of the developing gynoecium may not be sufficiently supplied with auxin in 3KO PIN1-GFP background. These results imply that class XI myosins, at least partially, contribute to the localization of PIN1 during floral development.

Myosin XI-K Is Expressed Throughout Floral Development

Despite the fact that class XI myosins share functional redundancy, it is known that the myosin XI-K plays important roles in such processes as membrane trafficking, cell expansion and division, plant growth, and fertility (Ojangu et al., 2007, 2012; Peremylov et al., 2008, 2010, 2012; Avisar et al., 2012; Park and Nebenführ, 2013; Abu-Abied et al., 2018). Accordingly, to validate the XI-K role in flower development, we performed SEM analysis of the genetically rescued 3KOR line (Peremylov et al., 2012), and found that the normal inflorescence development, including the elongation of stigmas and anther filaments, was restored in this plant line (**Figures 3Q–T**). Further, XI-K:YFP fluorescent signal in floral primordia, pistils and stamen filaments was examined (**Figure 5C**). The expression patterns of XI-K:YFP and PIN1::PIN1-GFP partially overlapped in the floral primordia, as well as in septum and valve margins of developing pistils (**Figure 5C**). At the same time, the XI-K:YFP showed distinct expression patterns in stigmas and anther filaments (**Figure 5C**), in comparison with PIN-GFP

(**Figures 5A,B**). Both the expression pattern analysis, and flower architecture evaluation of the 3KOR line indicate that myosin XI-K contributes to the growth of floral organs, and thus to fertility.

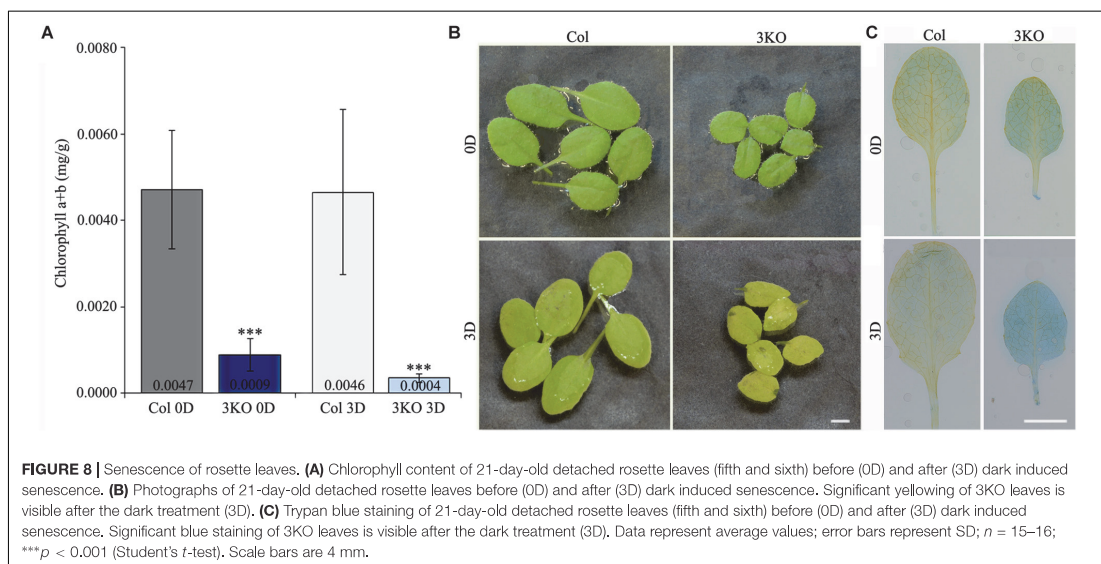
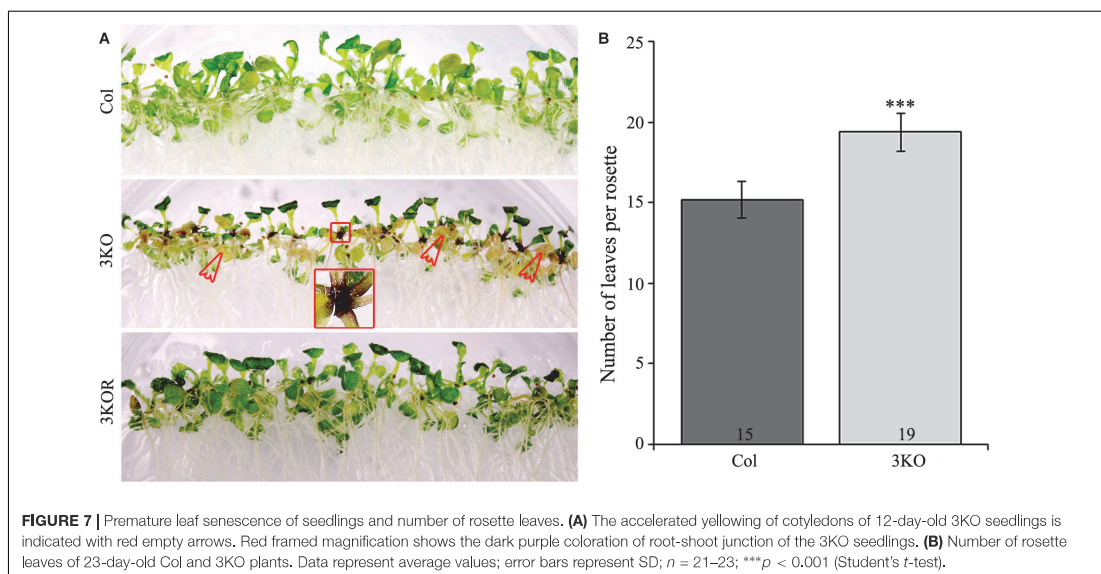
The Senescence and Cell Death of 3KO Leaves Is Accelerated

Despite the delayed bolt formation and extended lifespan, described earlier (Peremylov et al., 2010; Ojangu et al., 2012), we found that the 3KO plants displayed premature senescence of rosette leaves. Physical signs of early aging were particularly striking in the 12-day-old 3KO seedlings, which showed significant yellowing of cotyledons in comparison with Columbia or 3KOR line (**Figure 7A**). At the same time, 23-day-old mature rosettes (at bolt formation) of the 3KO plants produced 27% more leaves than those of Columbia control (**Figure 7B**). Given the very limited data on contributions of cytoskeleton to senescence and cell death in plant cells (Smertenko et al., 2003; Keech et al., 2010; Keech, 2011; Smertenko and Franklin-Tong, 2011), these observations prompted us to further explore myosin's role in these processes.

First, to assess the senescence of 3KO plants, we measured chlorophyll content of detached rosette leaves before and after dark-induced senescence. Chlorophyll was extracted from the fifth and sixth leaves of 21-day-old rosettes. Quantification showed that the chlorophyll content in 3KO leaves before dark-treatment (**Figure 8A**; 3KO 0D) was only 19% of that in Columbia. After 3 days in darkness, the chlorophyll content of 3KO leaves was 9% of that of Columbia (**Figure 8A**; 3KO 3D). Photographs of detached leaves also show significant yellowing of the 3KO leaves after dark-treatment (**Figure 8B**; 3KO 3D).

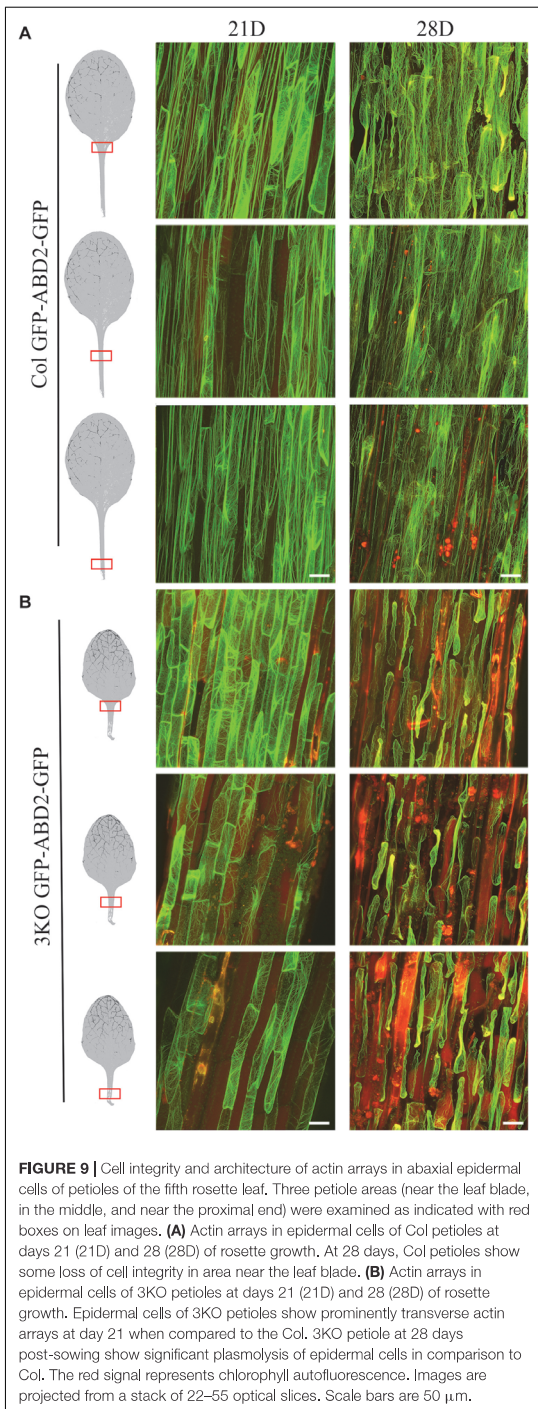
Second, we employed trypan blue staining to distinguish the extent of cell death in rosette leaves before and after dark incubation (**Figure 8C**). Before dark incubation, at day 21 of rosette growth, the fifth leaves of both WT and 3KO plants were weakly stained with trypan blue (**Figure 8C**; Col 0D, 3KO 0D). Measurement of blue channel intensity of leaf pictures showed that after dark incubation, the trypan blue staining of Columbia leaves was 1.6 times, and the one of 3KO leaves 2.1 times more intense in comparison with untreated Columbia (**Figure 8C**; Col 3D, 3KO 3D), indicating the prevalence of dying cells in mutant leaves. In addition, the measurement of total protein content revealed that after dark-treatment, the total protein concentration of 3KO leaves was 2.8-fold lower, and the one of Columbia was 1.6-fold lower in comparison with untreated controls (3KO 0D, Col 0D), respectively (**Supplementary Figure S5**).

Third, to monitor the cell integrity and architecture of actin arrays in abaxial epidermal cells of the fifth rosette leaf's petiole, we used stable expression of an AF tracer GFP-ABD2-GFP under control of the 35S promoter (**Figure 9**). Epidermal cells of leaf petioles were selected for examination as the cell growth, and AF organization defects of 3KO plants are most pronounced in longest cells, such as root hairs and petiole cells, as demonstrated by Peremylov et al. (2010). Since 3KO leaf petioles are 50% shorter than those of Columbia we selected three areas of leaf



petioles for examination: near the leaf blade, in the middle, and near the proximal end (**Figure 9**). The cell integrity and the organization of the AFs was compared between leaves of 21- and 28-day-old rosettes of 3KO and Columbia plants. At day 21 of rosette growth, the petiole cells were intact, and the GFP-ABD2-GFP decorated thick longitudinal cables in epidermal cells of Columbia leaf petioles (**Figure 9A**; Col 21D), and remarkably thin and prominently transverse filaments in 3KO cells (**Figure 9B**; 3KO 21D). At 28 days, GFP-ABD2-GFP labeled

prominently longitudinal cables in Columbia cells (**Figure 9A**; Col 28D) and only traces of AFs in the 3KO petiole cells (**Figure 9B**; 3KO 28D). This was due to massive plasmolysis and cell shape deformation of 3KO petioles. In Columbia, less pronounced changes in AF organization and cell shape were found: 66% of petioles ($n = 12$) showed some plasmolysis at the area near the leaf blade, and only 25% of petioles showed massive plasmolysis (**Figure 9A**; 28D). This indicated that in 3KO plants, at day 28 of rosette growth, the cell death of older rosette



leaves was significantly progressed in comparison with Columbia. Taken together, the results of decreased chlorophyll content, increased trypan blue staining, and premature plasmolysis in 3KO mutant show that the loss of integrity of actomyosin cytoskeleton induces premature senescence and thus cell death in *Arabidopsis* leaves.

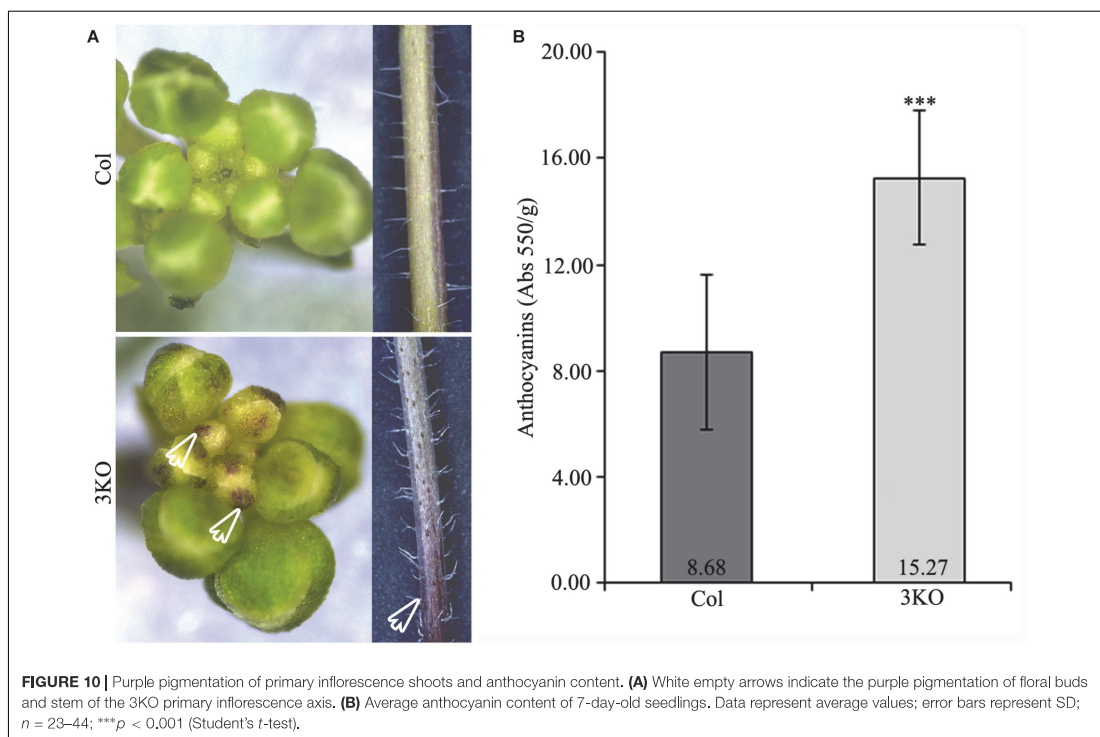
The Anthocyanin Pigments Accumulate in 3KO Tissues

Eventually, when investigating the overall 3KO phenotype, we often observed an accumulation of purple pigments in various tissues including root-shoot junctions of seedlings (Figure 7A; red framed magnification), floral buds and basal parts of inflorescence stems (Figure 10A; white empty arrows). Such increased purple pigmentation of plant tissues is associated primarily with anthocyanin accumulation (Gou et al., 2011; Misyura et al., 2013; Mushtaq et al., 2016). To validate this assumption, the anthocyanin content of 7-day-old seedlings was determined spectrophotometrically (Figure 10B). It was found that anthocyanin content in the 3KO seedlings was 1.9-fold higher than that in Columbia control (Figure 10B). The anthocyanin accumulation rate in the 3KO rosettes and inflorescence stems was similar to that in seedlings (data not shown). This excessive anthocyanin accumulation is likely an accompanying effect related to reduced auxin response and accelerated senescence in the 3KO plants.

Expression of the Auxin-Responsive and Senescence-Associated Genes Is Altered in 3KO

The main mechanism by which auxin- and senescence-responses are converted into cellular responses is via changes in transcription (Zentgraf et al., 2004; Paponov et al., 2008; Kim et al., 2016). To examine, if the elimination of multiple class XI myosins or the stable expression of *PIN1::PIN1-GFP* affect the regulation of the auxin-responsive and senescence-associated genes, we measured the relative expression levels of the selected mRNAs in seedlings, inflorescences, and rosette leaves of the Columbia, 3KO, 3KO *PIN1-GFP*, and Col *PIN1-GFP* plants using RT-qPCR. To assess auxin-related processes, we followed the expressions of auxin importer (*AUX1*) and exporter (*PIN1*, *PIN3*, *PIN4*, *PIN7*) genes whose expressions are related to flower development (Krecek et al., 2009; Lampugnani et al., 2013). We also measured the level of *IAA2* as its expression is closely related to endogenous auxin (Shibasaki et al., 2009). To distinguish stress- and age-induced senescence-related processes, we followed the relative expressions of *SAG13* and *SAG12* genes, respectively (Swartzberg et al., 2006; Schippers et al., 2007; Hou et al., 2013). To assess mutual influences between auxin- and senescence-related processes the level of auxin-responsive *SAUR36* was measured.

First, the expression levels of selected auxin- and senescence-associated genes in the 3KO seedlings, leaves and inflorescences were compared with Columbia control. In the 7-day-old



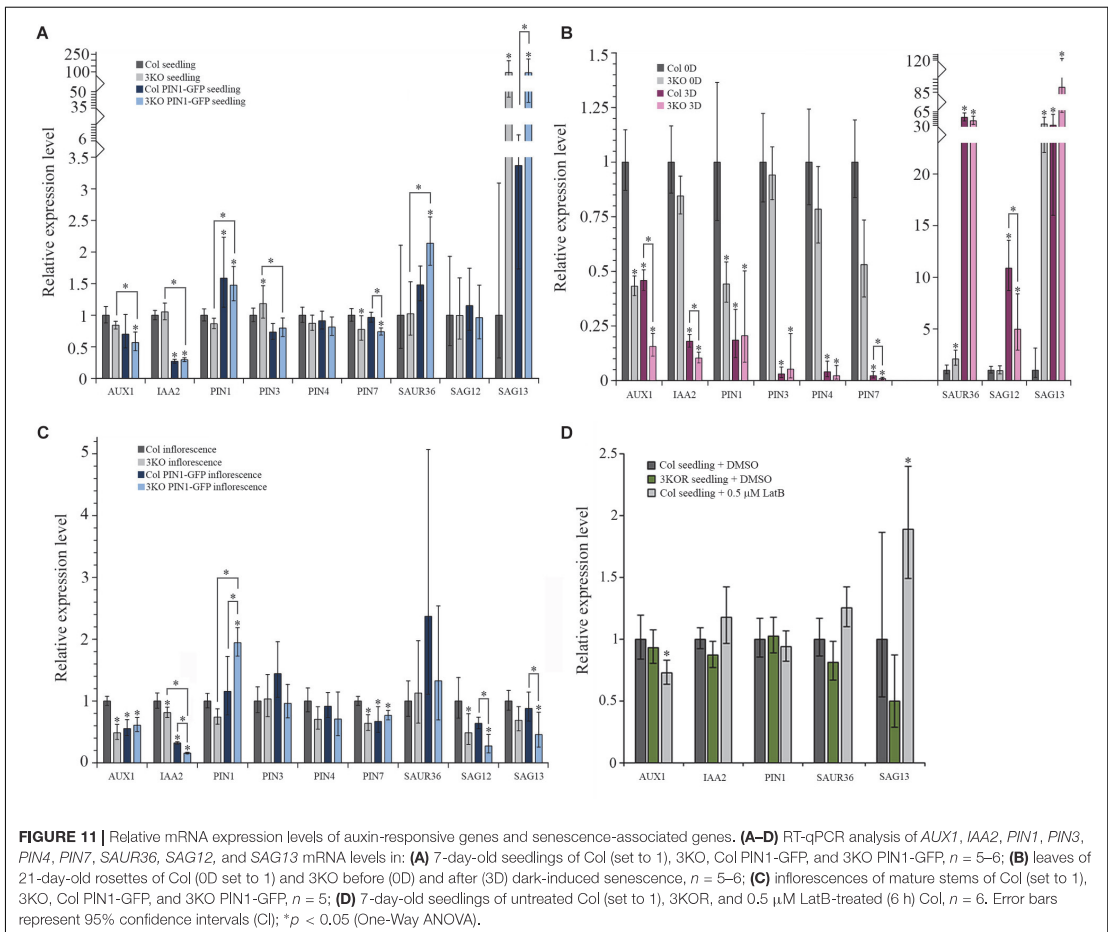
3KO seedlings, early senescence-associated gene *SAG13* was 94-fold up-regulated when compared to the Columbia control (Figure 11A). The down-regulation of *PIN7* in mutant seedlings was moderate, although statistically significant (Figure 11A).

The relative levels of selected genes expressed in rosette leaves of 3KO and Columbia plants were compared before and after dark treatment. Before dark-treatment, at 21 days of growth, 3KO rosette leaves (3KO 0D) showed a 34-fold up-regulation of *SAG13* expression, when compared to untreated Columbia control (Col 0D) (Figure 11B). The expression of *SAUR36* in untreated 3KO (3KO 0D) leaves was twofold increased and those of *AUX1* and *PIN1* were twofold decreased, in comparison with untreated control leaves (Col 0D) (Figure 11B). The dark-treatment of detached leaves significantly affected the expression levels of all selected auxin-responsive and senescence-associated genes both in 3KO (3KO 3D) and Columbia (Col 3D) plants when compared to untreated control (Col 0D) (Figure 11B). However, the changes in 3KO background were more pronounced than those in Columbia. Down-regulation of *AUX1* (7-fold), *IAA2* (10-fold), and *PIN7* (110-fold) in dark-treated 3KO leaves was twice as high as in Columbia (Col 3D) (Figure 11B). It is noteworthy that the up-regulation of *SAG13* in dark-treated Columbia (Col 3D) was comparable with untreated 3KO leaves (3KO 0D), whereas in dark-treated mutant

(3KO 3D), the *SAG13* was already 89-fold up-regulated (Figure 11B).

In 3KO inflorescences, levels of *AUX1* and *SAG12* were down-regulated twofold and those of *IAA2* and *PIN7* moderately, in comparison with Columbia control (Figure 11C). These results show that the onset of leaf senescence of 3KO plants is initiated at transcript level already in the 7-day-old seedlings, as demonstrated by the conspicuously high expression level of the *SAG13* gene. The unchanged levels of *SAG12* mRNA in seedlings and leaves indicates that the premature senescence of 3KO leaves most probably does not result from the activation of a developmental senescence program since the strong expression of *SAG13* suggests the stress-induced senescence and cell death. The relative expression levels of auxin-responsive *AUX1* and *PIN1* in 3KO were affected the most in leaves and inflorescences, implying that defective development of 3KO shoots could be influenced by reduced auxin responses.

The *PIN1* is the principal member of the PIN family involved in development of aerial organs and the lead player in floral development (Gälweiler et al., 1998; Benková et al., 2003; Scarpella et al., 2006; Adamowski and Friml, 2015). Therefore, even the modest overexpression of *PIN1* under native promoter is thought to affect plant phenotype. Therefore, the levels of auxin- and senescence-responsive genes in *PIN1::PIN1*-GFP expressing lines were compared with untransformed

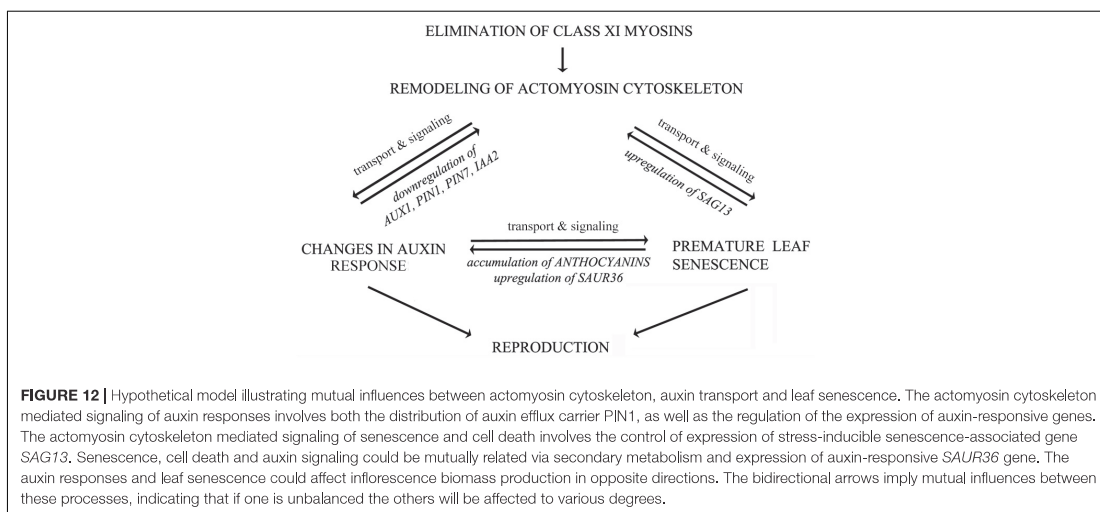


Columbia control. As we expected, both in 3KO PIN1-GFP, as well as in Col PIN1-GFP seedlings the expression of *PIN1* was about 1.5-fold up-regulated in comparison with Columbia control (Figure 11A). The level of *IAA2* was three–fourfold down-regulated in seedlings of PIN1::PIN1-GFP expressing Columbia and 3KO (Figure 11A). In 3KO PIN1-GFP seedlings, the level of *SAG13* was 92-fold up-regulated, similarly like in parental 3KO line (Figure 11A). Likewise, the level of *SAUR36* was also twofold up-regulated in 3KO PIN1-GFP seedlings compared to untransformed Columbia and 3KO (Figure 11A). A moderate down-regulation in levels of *AUX1*, *PIN3*, and *PIN7* in 3KO PIN1-GFP, and *PIN3* in Col PIN1-GFP seedlings was also detectable (Figure 11A).

In 3KO PIN1-GFP inflorescences, the expression of *PIN1* was up-regulated twofold, whereas in Col PIN1-GFP it was comparable with Columbia control (Figure 11C). The level of *IAA2* both in 3KO PIN1-GFP and Col PIN1-GFP inflorescences

was down-regulated six and threefold, respectively (Figure 11C). Relative expression levels of *AUX1* and *PIN7* were down-regulated moderately in both PIN1-GFP expressing lines (Figure 11C). Senescence-associated genes, *SAG12* and *SAG13*, were four and twofold down-regulated in 3KO PIN1-GFP inflorescences, whereas down-regulation of *SAG12* in Col PIN1-GFP shoots was marginal (Figure 11C). These data show that even the mild overexpression of the major non-redundant member of the auxin efflux carrier family, *PIN1*, inevitably affects the expression of auxin-responsive and senescence-associated genes not only in 3KO, but in Columbia background too. These results indicate also that there is a mutual crosstalk between myosin-mediated transport, auxin-signaling and senescence-related processes.

Third, we investigated how the treatment with AF destabilizing drug latrunculin B (LatB) affects the expression levels of *AUX1*, *IAA2*, *PIN1*, *SAUR36*, and *SAG13* in 7-day-old Columbia seedlings in comparison with untreated Columbia and



3KOR seedlings (Figure 11D). Six hours after the application of 0.5 μM LatB the 1.9-fold up-regulation of *SAG13*, and moderate down-regulation of *AUX1* in Columbia seedlings was detectable (Figure 11D). In 3KOR seedlings, the levels of *AUX1*, *IAA2*, *PIN1*, *SAUR36*, and *SAG13* were comparable with untreated Columbia control (Figure 11D). These data show that the latrunculin B-mediated disruption of AFs activates the expression of stress-inducible *SAG13* gene, indicating that the actin cytoskeleton may be necessary for delivering stress-responses in plant cells.

DISCUSSION

Our results show that the three *Arabidopsis* class XI myosins, XI-1, XI-2, and XI-K, contribute to the auxin responses and cell death, and thereby affect developmental decisions during flower growth and leaf senescence. Using triple mutant line 3KO (Ojangu et al., 2012) and complemented line 3KOR (Peremyslov et al., 2012), we demonstrate that simultaneous depletion of these three myosins affects responsiveness of the auxin-dependent promoters and polarization of the PIN1 auxin efflux carrier, causes premature onset of senescence and cell death in leaves, elevates accumulation of anthocyanins, and changes the expression levels of genes related to these processes. We also show that the stable expression of myosin XI-K rescues the decreased fertility and prematurely senescent phenotype in 3KO background. This result implements that myosin XI-K plays important role not only in driving vegetative plant growth (Ojangu et al., 2007, 2012; Peremyslov et al., 2012) and gravitropic response (Talts et al., 2016), but contributes also to floral development and cell death.

Previous works on multiple gene knockout mutants have identified several myosin XI functions in plant development.

In particular, the best studied phenotypes of 3KO plants included stunted growth, delayed bolting, incomplete development of stigmas and reduced fertility (Peremyslov et al., 2010; Ojangu et al., 2012). These phenotypic defects are explained with severe changes at the cellular level: disorganized and more static actin cytoskeleton, reduced membrane trafficking, nearly arrested cytoplasmic streaming (Peremyslov et al., 2010; Ueda et al., 2010; Cai et al., 2014), reduced sensitivity of vacuoles to exogenous auxin, and partial loss of PIN1 polarization in root cells (Scheuring et al., 2016; Abu-Abied et al., 2018).

First, we used flower development of 3KO plants as a model for examining myosin-dependent auxin-responsive processes in *Arabidopsis*. We show that the apical dominance and branching architecture of 3KO shoots is partially affected as the mutant plants produce more axillary branches on primary inflorescence stem. Investigating inflorescence development, four traits are usually evaluated: bolting time, length of the reproductive phase, number of rosette leaves at bolting, number of axillary branches and fruits (Ungerer et al., 2002; Pouteau and Albertini, 2009). In myosin 3KO mutant, all these developmental aspects are partly affected: bolting time delays, reproductive phase is expanded, more rosette leaves are formed, branching architecture is affected, and silique size is decreased. The branching architecture of inflorescence shoots is mainly regulated by auxin, cytokinin, and strigolactone, which control initiation and outgrowth of axillary meristem (Domagalska and Leyser, 2011). Basipetal auxin transport from shoot apex toward the base suppresses axillary meristem outgrowth, and leads to apical dominance (Davies et al., 1966). In *Arabidopsis* and tomato, the axillary meristem initiation is characterized by preparative auxin depletion and the subsequent meristem emergence by a local auxin accumulation (Wang et al., 2014). It has been showed that local auxin gradients necessary during phyllotactic patterning in leaf and inflorescence meristems are regulated by

auxin importers together with PIN1 exporter (Bainbridge et al., 2008). Consistent with this, our results show that the auxin responsiveness is reduced throughout the development of the 3KO plants, with the most pronounced effects in seedlings and inflorescence stems. In addition, as the PIN1 polarization in epidermal cells of developing 3KO gynoecia is partially disturbed, and two major auxin transporter genes, *AUX1* and *PIN1*, are down-regulated in 3KO leaves and inflorescences, a correlation between these processes can be found, indicating that PAT-related processes are disturbed in 3KO background. Interestingly, our results complement recently published data which demonstrated that the production of lateral and adventitious roots in 3KO plants was increased (Abu-Abied et al., 2018). The abnormal formation of the lateral roots was related to changed auxin gradient, which was in correlation with partial loss of PIN1 polarization in stele cells of 3KO plants. Moreover, authors revealed the myosin XI-K role in cell division in both the root and shoot meristem (Abu-Abied et al., 2018). The reduced auxin responsiveness and loss of myosin XI-K function in 3KO meristem was used to explain the altered branching architecture of mutant roots (Abu-Abied et al., 2018). Although these two studies (current work; Abu-Abied et al., 2018) used different models (flowers and leaves versus roots) and different experimental approaches, both highlight myosin-auxin connections.

In this work, we demonstrate for the first time that the myosin XI-K:YFP is expressed in floral primordia and in developing flowers, indicating its role in floral development. Moreover, correlation between the expression pattern of XI-K:YFP and the delayed elongation of stigmas and anther filaments in 3KO can be found, though we do not exclude the roles of myosin XI-1 and XI-2 in these processes.

It is broadly assumed that development of the stamens and gynoecia, the most modified floral organs, require enhanced production of hormones, including auxin (Okada et al., 1991; Sessions et al., 1997; Nemhauser et al., 2000; Aloni et al., 2006; Cheng et al., 2006; Cecchetti et al., 2008; Sundberg and Østergaard, 2009; Hawkins and Liu, 2014). It is proposed that the finely tuned auxin gradient is necessary for gynoecium patterning in general and style and stigma development in particular (Nemhauser et al., 2000). To complete the development of valves, style and stigma, the medial, lateral and apical domains of the growing gynoecium are provided with auxin from the base. This has been demonstrated by Larsson et al. (2014), who showed that the PIN1-GFP localization in outer epidermal cells of stage 7 gynoecia was prominently apical. Interestingly, we found that stable expression of the PIN1::PIN1-GFP augmented a semi-sterile phenotype of the 3KO plants (Peremyslov et al., 2010; Ojangu et al., 2012). Our results indicate that the ability of 3KO PIN1-GFP inflorescence meristem to produce flowers with determined number and shape of inner whorl organs is affected to a variable degree, whereas the gynoecium development is affected the most. Similar gynoecium phenotypes have been described upon direct genetic or pharmacological disruption of auxin signaling (Sessions et al., 1997; Nemhauser et al., 2000; Cheng et al., 2006; Zúñiga-Mayo et al., 2014). The gynoecium is the last organ which emerges from the floral meristem

(Larsson et al., 2014), and the style and stigma are last structures which emerge from the growing gynoecium. The partial loss of PIN1 polarization in developing 3KO PIN1-GFP gynoecia may indicate that the auxin transport from the base may not be sufficient to complete the growth of style, stigma or valves of 3KO PIN1-GFP pistils correctly. Here we demonstrate also that the late phase of stamen development, pre-anthesis filament elongation, often delays both in the parental line as well as in 3KO PIN1-GFP line. Our results indicate that the defective floral development of the 3KO PIN1-GFP line could be due to inability of the disrupted actomyosin cytoskeleton to properly allocate an excess of PIN1 which in turn, via feedback signaling pathway, may affect the expression of auxin-responsive genes. All these results together indicate the possible cooperation between myosin-mediated trafficking and auxin responses in floral development.

Second, we used leaf development of 3KO plants as a model for examining myosin-dependent senescence-associated processes in *Arabidopsis*. It is well documented that late flowering plants have more rosette leaves, and that there is a strong correlation between leaf number and bolting time (Pouteau and Albertini, 2009; Schmalenbach et al., 2014). In accordance with this, rosettes of 3KO plants create more leaves, but at the same time show premature signs of leaf senescence. Premature senescence in 3KO leaves is confirmed by massive loss of chlorophyll, enhanced cell death, premature rupture of petiole epidermal cells, and abnormal accumulation of anthocyanins. Our finding that the *SAG13* is significantly up-regulated prior to observable signs of leaf yellowing both in young 3KO seedlings as well as in rosette leaves, indicates that the premature senescence in this mutant line is highly accelerated at transcript level. In addition, the expression of late senescence-associated gene *SAG12* is not different in the 3KO seedlings and leaves relative to the Columbia. Moreover, the accumulation of anthocyanins in 3KO plants is in accordance with the fact that increased flavonoid production (e.g., anthocyanins) has been also associated with stress responses (Solfanelli et al., 2006). As we detect the anthocyanin accumulation, and *SAG13* up-regulation already in young 3KO seedlings, this supports our assumption that the early leaf senescence of 3KO mutants is not typical developmental senescence but could be caused by cellular stresses such as changes in membrane trafficking, AF rearrangement, and auxin responses. For example, when wild type *Arabidopsis* seedlings are suffering from salt and methyl jasmonate co-stress, the leaf senescence is prematurely initiated as the *SAG13* of transcript level is significantly up-regulated (Chen et al., 2017). In *Arabidopsis accelerated-cell-death11* (*acd11*) mutant, the *SAG13* mRNA is strongly expressed, whereas *SAG12* mRNA does not accumulate. The authors concluded that the cell death in *acd11* does not result from activation of a senescence program, but from PCD as suggested by conspicuously strong *SAG13* expression (Brodersen et al., 2002). It is tempting to speculate that in 3KO cells, the loss of integrity of actomyosin cytoskeleton activates the stress-signaling pathway, and as a consequence of this the senescence and cell death are prematurely initiated.

It has been shown that the integrity of actin cytoskeleton contributes to senescence and cell death through reorganization

of the endoplasmic reticulum (ER) network (Boevink et al., 1998; Kasaras et al., 2012; Xu et al., 2012; Carvalho et al., 2014; Chang et al., 2015) and transcription factor activation (Hao and August, 2005; Breeze et al., 2011; Smertenko and Franklin-Tong, 2011). Smertenko et al. (2003) suggested that the filamentous actin is crucial for the developmentally programmed cell death in the Norway spruce embryos as AFs disappeared significantly later than the microtubules. It has been proposed also that during leaf senescence, a functional actin cytoskeleton could be essential for maintaining the primary metabolism until the cell death (Keech, 2011). Because the integrity of actin arrays, and thus membrane trafficking is affected in 3KO epidermal cells (Peremyslov et al., 2010; Cai et al., 2014), a causal connection between these processes can be suggested. Myosin's potential role in senescence is supported by the facts that ER-streaming is dramatically suppressed in 3KO plants (Ueda et al., 2010), and a portion of the XI-K:YFP is aligned and co-fractionated with a motile ER subdomain (Peremyslov et al., 2012). Intriguingly, myosins XI-K and XI-2 that are inactivated in 3KO are not only broadly expressed throughout plant tissues, but show particularly high expression level in the senescent leaves too (Peremyslov et al., 2011).

In general, the role of auxin in regulating leaf senescence still remains elusive. It has been implied that auxin may promote leaf senescence via *SAUR36* gene since the auxin-inducible transcript accumulation promotes premature senescence of young leaves, whereas in *saur36* null mutant plants senescence delays substantially (Hou et al., 2013). Our findings show that the premature leaf senescence of 3KO leaves is indeed accompanied by up-regulation of *SAUR36*, although it is not clear how the early aging is influenced by reduced auxin responses in this mutant. Up-regulation of *SAG13* and *SAUR36* during leaf senescence, regardless of whether it is induced naturally or by darkness suggests that the senescence mechanism under these two different conditions share common features. It is well known that the dark-induced senescence of detached leaves is radical intervention as major changes in leaf physiology inevitably affect the gene expression. Although, the dark-treatment of detached 3KO leaves does not reflect the situation of natural senescence, the results obtained from these experiments, provide additional clues that myosins contribute to the auxin- and senescence-responsive processes, and indicate that these processes are mutually interconnected.

Accumulation of anthocyanins in plant tissues is related both with auxin signaling and senescence (Brown et al., 2001; Feild et al., 2001; Buer and Munday, 2004; Besseau et al., 2007; Schippers et al., 2007; Falcone Ferreyra et al., 2012). In particular, auxin transport is elevated in inflorescences, hypocotyls, and roots of plants of the flavonoids-deficient mutants (Murphy et al., 2000; Brown et al., 2001; Lewis et al., 2011). During senescence, anthocyanins reduce the risk of photo-oxidative damage in leaf cells and thereby help retrieve nutrients from senescing tissues (Feild et al., 2001; Falcone Ferreyra et al., 2012). We propose that the accumulation of anthocyanins in 3KO tissues is an accompanying effect influenced both by reduced

auxin responses as well as by premature onset of senescence. Collectively, this work highlights the importance of actomyosin cytoskeleton in auxin responsiveness and senescence, and leads to further questions as to how reorganization of metabolism is achieved in cells having a drastically affected actomyosin cytoskeleton. The next critical step in understanding these networks is investigation of the mechanistic contributions of myosins to the function of these networks. It is anticipated that such contributions could involve specific role of myosin-dependent transport in PIN and AUX targeting, overall reduction in cytoplasmic streaming that could affect auxin transport or auxin diffusion, as well as myosin-dependent changes in AF organization. Whether these myosins contribute to auxin responses through shaping actin cytoskeleton or via reorganization of the ER remains to be elucidated. Important aspect of the future studies will be identifying the myosin cargoes that affect auxin signaling and senescence. These cargoes could include MyoB myosin receptors that appear to drive cytoplasmic streaming (Peremyslov et al., 2013, 2015) or newly identified myosin adaptors of MadA and MadB families that presumably mediate more specialized myosin-dependent processes (Kurth et al., 2017).

Taken together, our results provide the genetic evidence that the integrity of actomyosin cytoskeleton, signaling of auxin and senescence, as well as secondary metabolism are functionally intertwined in a finely tuned network as illustrated in a tentative model (Figure 12). According to this, remodeling of actomyosin cytoskeleton affects not only distribution of auxin exporter PIN1, but also the expression of auxin-responsive and senescence-associated genes. Most likely, the levels of auxin-responsive genes are influenced indirectly, through feedback signaling mechanism, mediated by changes in auxin responses. The actomyosin cytoskeleton-mediated signaling of premature leaf senescence involves the control of expression of stress-inducible gene *SAG13*. Senescence and auxin signaling could be mutually regulated by secondary metabolism (e.g., anthocyanin accumulation) and by expression of auxin-responsive *SAUR* genes (e.g., *SAUR36*). All these processes are mutually interconnected, and if one process is unbalanced the others are affected too. It is tempting to speculate that changes in auxin and senescence responses influence reproduction of 3KO plants in opposite directions (Figure 12). From the one hand, the reduced auxin response could disturb flower development; on the other hand, it seems that the premature leaf senescence could constitute a rescue mechanism for supporting the production of inflorescence biomass in conditions where flower development has been compromised.

AUTHOR CONTRIBUTIONS

E-LO, BI, KTaI, HP, ET, and VD contributed to design of the study and interpretation of data. E-LO, BI, KTaI, KTaI, and EI conducted experiments and analyzed data. KTaI performed anthocyanin and chlorophyll measurements, and trypan blue stainings. BI performed RT-qPCR. EI performed

histochemical GUS stainings. K_{Tal} helped with protocol optimization for quantitative MUG assay. HP helped with SEM and confocal imaging, image processing, and data analysis. VD generated 3KOR line. E-LO, BI, K_{Tal}, HP, VD, and ET drafted the manuscript and revised it critically. All authors read and approved the final manuscript, and they agreed to be accountable for all aspects of the work.

FUNDING

This research was supported by institutional research grant IUT 193 from the Estonian Ministry of Education and Research, and Estonian Research Council grant ETF8604. Each of the funding bodies granted the funds based on a research proposal. They had no influence over the experimental design, data analysis, interpretation, or writing the manuscript.

REFERENCES

- Abu-Abied, M., Belausov, E., Hagay, S., Peremyslov, V., Dolja, V., and Sadot, E. (2018). Myosin XI-K is involved in root organogenesis, polar auxin transport and cell division. *J. Exp. Bot.* 69, 2869–2881. doi: 10.1093/jxb/ery112
- Adamowski, M., and Friml, J. (2015). PIN-dependent auxin transport: action, regulation, and evolution. *Plant Cell* 27, 20–32. doi: 10.1105/tpc.114.134874
- Aloni, R., Aloni, E., Langhans, M., and Ullrich, C. I. (2006). Role of auxin in regulating *Arabidopsis* flower development. *Planta* 223, 315–328. doi: 10.1007/s00425-005-0088-9
- Avisar, D., Abu-Abied, M., Belausov, E., and Sadot, E. (2012). Myosin XI-K is a major player in cytoplasm dynamics and is regulated by two amino acids in its tail. *J. Exp. Bot.* 63, 241–249. doi: 10.1093/jxb/err265
- Bainbridge, K., Guyomarc'h, S., Bayer, E., Swarup, R., Bennett, M., Mandel, T., et al. (2008). Auxin influx carriers stabilize phyllotactic patterning. *Genes Dev.* 22, 810–823. doi: 10.1101/gad.462608
- Balazadeh, S., Parlitz, S., Mueller-Roeber, B., and Meyer, R. C. (2008). Natural developmental variations in leaf and plant senescence in *Arabidopsis thaliana*. *Plant Biol.* 10(Suppl. 1), 136–147. doi: 10.1111/j.1438-8677.2008.00108.x
- Benková, E., Michniewicz, M., Sauer, M., Teichmann, T., Seifertová, D., Jürgens, G., et al. (2003). Local, efflux-dependent auxin gradients as a common module for plant organ formation. *Cell* 115, 591–602. doi: 10.1016/S0092-8674(03)00924-3
- Bennett, M. J., Marchant, A., Green, H. G., May, S. T., Ward, S. P., Millner, P. A., et al. (1996). *Arabidopsis* AUX1 gene: a permease-like regulator of root gravitropism. *Science* 273, 948–950. doi: 10.1126/science.273.5277.948
- Berleth, T., and Sachs, T. (2001). Plant morphogenesis: long-distance coordination and local patterning. *Curr. Opin. Plant Biol.* 4, 57–62. doi: 10.1016/S1369-5266(00)00136-9
- Besseau, S., Hoffmann, L., Geoffroy, P., Lapierre, C., Pollet, B., and Legrand, M. (2007). Flavonoid accumulation in *Arabidopsis* repressed in lignin synthesis affects auxin transport and plant growth. *Plant Cell* 19, 148–162. doi: 10.1105/tpc.106.044495
- Boevink, P., Oparka, K., Cruz, S. S., Martin, B., Betteridge, A., and Hawes, C. (1998). Stacks on tracks: the plant Golgi apparatus traffics on an actin/ER network. *Plant J.* 15, 441–447. doi: 10.1046/j.1365-3113X.1998.00208.x
- Breeze, E., Harrison, E., McHattie, S., Hughes, L., Hickman, R., Hill, C., et al. (2011). High-resolution temporal profiling of transcripts during *Arabidopsis* leaf senescence reveals a distinct chronology of processes and regulation. *Plant Cell* 23, 873–894. doi: 10.1105/tpc.111.083345
- Brodersen, P., Petersen, M., Pike, H. M., Olszak, B., Skov, S., Odum, N., et al. (2002). Knockout of *Arabidopsis* accelerated-cell-death11 encoding a sphingosine transfer protein causes activation of programmed cell death and defense. *Genes Dev.* 16, 490–502. doi: 10.1101/gad.218202

ACKNOWLEDGMENTS

We thank prof. Malcolm Bennett from the University of Nottingham for providing DR5::GUS line and prof. Elison B. Blancaflor from The Samuel Roberts Noble Foundation for providing 35S::GFP-ABD2-GFP seeds. We thank Cecilia Sarmiento for thoroughly editing manuscript; Kairi Kärblane for helping with Adobe Photoshop CS6; Signe Nõu for taking care of plants. We sincerely thank the reviewers for their detailed comments, suggestions and constructive criticism for the manuscript.

SUPPLEMENTARY MATERIAL

The Supplementary Material for this article can be found online at: <https://www.frontiersin.org/articles/10.3389/fpls.2018.01570/full#supplementary-material>

- Brown, D. E., Rashotte, A. M., Murphy, A. S., Normanly, J., Tague, B. W., Peer, W. A., et al. (2001). Flavonoids act as negative regulators of auxin transport in vivo in *Arabidopsis*. *Plant Physiol.* 126, 524–535. doi: 10.1104/pp.126.2.524
- Buchanan-Wollaston, V., Earl, S., Harrison, E., Mathas, E., Navabpour, S., Page, T., et al. (2003). The molecular analysis of leaf senescence – A genomics approach. *Plant Biotechnol. J.* 1, 3–22. doi: 10.1046/j.1467-7652.2003.00004.x
- Buer, C. S., and Muday, G. K. (2004). The transparent testa4 mutation prevents flavonoid synthesis and alters auxin transport and the response of *Arabidopsis* roots to gravity and light. *Plant Cell* 16, 1191–1205. doi: 10.1105/tpc.020313
- Cai, C., Henty-Ridilla, J. L., Szymanski, D. B., and Staiger, C. J. (2014). *Arabidopsis* myosin XI: a motor rules the tracks. *Plant Physiol.* 166, 1359–1370. doi: 10.1104/pp.114.244335
- Cardarelli, M., and Cecchetti, V. (2014). Auxin polar transport in stamen formation and development: how many actors? *Front. Plant Sci.* 5:333. doi: 10.3389/fpls.2014.00333
- Carvalho, H. H., Silva, P. A., Mendes, G. C., Brustolini, O. J. B., Pimenta, M. R., Gouveia, B. C., et al. (2014). The endoplasmic reticulum binding protein BiP displays dual function in modulating cell death events. *Plant Physiol.* 164, 654–670. doi: 10.1104/pp.113.231928
- Cecchetti, V., Altamura, M. M., Falasca, G., Costantino, P., and Cardarelli, M. (2008). Auxin regulates *Arabidopsis* anther dehiscence, pollen maturation, and filament elongation. *Plant Cell* 20, 1760–1774. doi: 10.1105/tpc.107.057570
- Cha, J.-Y., Kim, M. R., Jung, I. J., Kang, S. B., Park, H. J., Kim, M. G., et al. (2016). The thiol reductase activity of YUCCA6 mediates delayed leaf senescence by regulating genes involved in auxin redistribution. *Front. Plant Sci.* 7:626. doi: 10.3389/fpls.2016.00626
- Chang, X., Riemann, M., Liu, Q., and Nick, P. (2015). Actin as deathly switch? How auxin can suppress cell-death related defence. *PLoS One* 10:e0125498. doi: 10.1371/journal.pone.0125498
- Chen, Y., Wang, Y., Huang, J., Zheng, C., Cai, C., Wang, Q., et al. (2017). Salt and methyl jasmonate aggravate growth inhibition and senescence in *Arabidopsis* seedlings via the JA signaling pathway. *Plant Sci.* 261, 1–9. doi: 10.1016/j.plantsci.2017.05.005
- Cheng, Y., Dai, X., and Zhao, Y. (2006). Auxin biosynthesis by the YUCCA flavin monooxygenases controls the formation of floral organs and vascular tissues in *Arabidopsis*. *Genes Dev.* 20, 1790–1799. doi: 10.1101/gad.1415106
- Cho, M., and Cho, H.-T. (2013). The function of ABCB transporters in auxin transport. *Plant Signal. Behav.* 8:e22990. doi: 10.4161/psb.22990
- Cho, M., Lee, S. H., and Cho, H.-T. (2007). P-glycoprotein4 displays auxin efflux transporter-like action in *Arabidopsis* root hair cells and tobacco cells. *Plant Cell* 19, 3930–3943. doi: 10.1105/tpc.107.054288
- Czechowski, T., Stitt, M., Altmann, T., Udvardi, M. K., and Scheible, W.-R. (2005). Genome-wide identification and testing of superior reference genes for

- transcript normalization in *Arabidopsis*. *Plant Physiol.* 139, 5–17. doi: 10.1104/pp.105.063743
- Davies, C. R., Seth, A. K., and Wareing, P. F. (1966). Auxin and kinetin interaction in apical dominance. *Science* 151, 468–469. doi: 10.1126/science.151.3709.468
- Dhonukshe, P., Grigoriev, I., Fischer, R., Tominaga, M., Robinson, D. G., Hasek, J., et al. (2008). Auxin transport inhibitors impair vesicle motility and actin cytoskeleton dynamics in diverse eukaryotes. *Proc. Natl. Acad. Sci. U.S.A.* 105, 4489–4494. doi: 10.1073/pnas.0711414105
- Domagalska, M. A., and Leyser, O. (2011). Signal integration in the control of shoot branching. *Nat. Rev. Mol. Cell Biol.* 12, 211–221. doi: 10.1038/nrm3088
- Eggenberger, K., Sanyal, P., Hundt, S., Wadhvani, P., Ulrich, A. S., and Nick, P. (2017). Challenge integrity: the cell-penetrating peptide BP100 interferes with the auxin-actin oscillator. *Plant Cell Physiol.* 58, 71–85. doi: 10.1093/pcp/pcw161
- Falcone Ferreyra, M. L., Rius, S. P., and Casati, P. (2012). Flavonoids: biosynthesis, biological functions, and biotechnological applications. *Front. Plant Sci.* 3:222. doi: 10.3389/fpls.2012.00222
- Feild, T. S., Lee, D. W., and Holbrook, N. M. (2001). Why leaves turn red in autumn. The role of anthocyanins in senescing leaves of red-osier dogwood. *Plant Physiol.* 127, 566–574. doi: 10.1104/pp.010063
- Gälweiler, L., Guan, C., Müller, A., Wisman, E., Mendgen, K., Yephremov, A., et al. (1998). Regulation of polar auxin transport by AtPIN1 in *Arabidopsis* vascular tissue. *Science* 282, 2226–2230. doi: 10.1126/science.282.5397.2226
- Geisler, M., and Murphy, A. S. (2006). The ABC of auxin transport: the role of p-glycoproteins in plant development. *FEBS Lett.* 580, 1094–1102. doi: 10.1016/j.febslet.2005.11.054
- Geldner, N., Friml, J., Stierhof, Y.-D., Jürgens, G., and Palme, K. (2001). Auxin transport inhibitors block PIN1 cycling and vesicle trafficking. *Nature* 413, 425–428. doi: 10.1038/35096571
- Gou, J.-Y., Felippes, F. F., Liu, C.-J., Weigel, D., and Wang, J.-W. (2011). Negative regulation of anthocyanin biosynthesis in *Arabidopsis* by a miR156-targeted SPL transcription factor. *Plant Cell* 23, 1512–1522. doi: 10.1105/tpc.111.084525
- Hao, S., and August, A. (2005). Actin depolymerization transduces the strength of B-cell receptor stimulation. *Mol. Biol. Cell* 16, 2275–2284. doi: 10.1091/mbc.e04-10-0881
- Harborne, J. B., and Baxter, H. (eds.) (1999). *The Handbook of Natural Flavonoids*, Vol. 1 and 2. Chichester: John Wiley and Sons, 889.
- Hawkins, C., and Liu, Z. (2014). A model for an early role of auxin in *Arabidopsis* gynoecium morphogenesis. *Front. Plant Sci.* 5:327. doi: 10.3389/fpls.2014.00327
- Hellema, J., Mortier, G., De Paep, A., Speleman, F., and Vandesompele, J. (2007). qBase relative quantification framework and software for management and automated analysis of real-time quantitative PCR data. *Genome Biol.* 8:R19. doi: 10.1186/gb-2007-8-2-r19
- Henty-Ridilla, J. L., Li, J., Day, B., and Staiger, C. J. (2014). ACTIN DEPOLYMERIZING FACTOR4 regulates actin dynamics during innate immune signaling in *Arabidopsis*. *Plant Cell* 26, 340–352. doi: 10.1105/tpc.113.122499
- Himelblau, E., and Amasino, R. M. (2001). Nutrients mobilized from leaves of *Arabidopsis thaliana* during leaf senescence. *J. Plant Physiol.* 158, 1317–1323. doi: 10.1078/0176-1617-00608
- Hodge, E. T., and Sacher, J. A. (1975). Effects of kinetin, auxin and abscisic acid on ribonuclease and acid phosphatase during senescence of leaf tissue. *Biochem. Physiol. Pflanz.* 168, 433–441. doi: 10.1016/S0015-3796(17)30148-8
- Holton, T., and Cornish, E. (1995). Genetics and biochemistry of anthocyanin biosynthesis. *Plant Cell* 7, 1071–1083. doi: 10.1105/tpc.7.7.1071
- Hou, K., Wu, W., and Gan, S.-S. (2013). SAUR36, a small auxin up RNA gene, is involved in the promotion of leaf senescence in *Arabidopsis*. *Plant Physiol.* 161, 1002–1009. doi: 10.1104/pp.112.212787
- Hu, X., Tanaka, A., and Tanaka, R. (2013). Simple extraction methods that prevent the artifactual conversion of chlorophyll to chlorophyllide during pigment isolation from leaf samples. *Plant Methods* 9:19. doi: 10.1186/1746-4811-9-19
- Huang, X., Maisch, J., and Nick, P. (2017). Sensory role of actin in auxin-dependent responses of tobacco BY-2. *J. Plant Physiol.* 218, 6–15. doi: 10.1016/j.jplph.2017.07.011
- Ivakov, A., and Persson, S. (2013). Plant cell shape: modulators and measurements. *Front. Plant Sci.* 4:439. doi: 10.3389/fpls.2013.00439
- Jibrán, R., A Hunter, D., and P Dijkwel, P. (2013). Hormonal regulation of leaf senescence through integration of developmental and stress signals. *Plant Mol. Biol.* 82, 547–561. doi: 10.1007/s11103-013-0043-2
- Kandasamy, M. K., McKinney, E. C., Deal, R. B., and Meagher, R. B. (2005). *Arabidopsis* ARP7 is an essential actin-related protein required for normal embryogenesis, plant architecture, and floral organ abscission. *Plant Physiol.* 138, 2019–2032. doi: 10.1104/pp.105.065326
- Kasaras, A., Melzer, M., and Kunze, R. (2012). *Arabidopsis* senescence-associated protein DMP1 is involved in membrane remodeling of the ER and tonoplast. *BMC Plant Biol.* 12:54. doi: 10.1186/1471-2229-12-54
- Keech, O. (2011). The conserved mobility of mitochondria during leaf senescence reflects differential regulation of the cytoskeletal components in *Arabidopsis thaliana*. *Plant Signal. Behav.* 6, 147–150. doi: 10.4161/psb.6.1.14307
- Keech, O., Pesquet, E., Gutierrez, L., Ahad, A., Bellini, C., Smith, S. M., et al. (2010). Leaf senescence is accompanied by an early disruption of the microtubule network in *Arabidopsis*. *Plant Physiol.* 154, 1710–1720. doi: 10.1104/pp.110.163402
- Khan, M., Rozhon, W., and Poppenberger, B. (2014). The role of hormones in the aging of plants – A mini-review. *Gerontology* 60, 49–55. doi: 10.1159/000354334
- Kim, J., Woo, H. R., and Nam, H. G. (2016). Toward systems understanding of leaf senescence: an integrated multi-omics perspective on leaf senescence research. *Mol. Plant* 9, 813–825. doi: 10.1016/j.molp.2016.04.017
- Kim, J. I., Murphy, A. S., Baek, D., Lee, S.-W., Yun, D.-J., Bressan, R. A., et al. (2011). YUCCA6 over-expression demonstrates auxin function in delaying leaf senescence in *Arabidopsis thaliana*. *J. Exp. Bot.* 62, 3981–3992. doi: 10.1093/jxb/err094
- Kleine-Vehn, J., Dhonukshe, P., Swarup, R., Bennett, M., and Friml, J. (2006). Subcellular trafficking of the *Arabidopsis* auxin influx carrier AUX1 uses a novel pathway distinct from PIN1. *Plant Cell* 18, 3171–3181. doi: 10.1105/tpc.106.042770
- Kleine-Vehn, J., and Friml, J. (2008). Polar targeting and endocytic recycling in auxin-dependent plant development. *Annu. Rev. Cell Dev. Biol.* 24, 447–473. doi: 10.1146/annurev.cellbio.24.110707.175254
- Kleine-Vehn, J., Wabnik, K., Martinière, A., Langowski, Ł., Willig, K., Naramoto, S., et al. (2011). Recycling, clustering, and endocytosis jointly maintain PIN auxin carrier polarity at the plasma membrane. *Mol. Syst. Biol.* 7:540. doi: 10.1038/msb.2011.72
- Krecek, P., Skupa, P., Libus, J., Naramoto, S., Tejos, R., Friml, J., et al. (2009). The PIN-FORMED (PIN) protein family of auxin transporters. *Genome Biol.* 10:249. doi: 10.1186/gb-2009-10-12-249
- Kuhn, B. M., Errafi, S., Bucher, R., Dobrev, P., Geisler, M., Bigler, L., et al. (2016). 7-Rhamnosylated flavonols modulate homeostasis of the plant hormone auxin and affect plant development. *J. Biol. Chem.* 291, 5385–5395. doi: 10.1074/jbc.M115.701565
- Kurth, E. G., Peremyshov, V. V., Turner, H. L., Makarova, K. S., Iranzo, J., Mekhedov, S. L., et al. (2017). Myosin-driven transport network in plants. *Proc. Natl. Acad. Sci. U.S.A.* 114, E1385–E1394. doi: 10.1073/pnas.1620577114
- Lampugnani, E. R., Kilinc, A., and Smyth, D. R. (2013). Auxin controls petal initiation in *Arabidopsis*. *Development* 140, 185–194. doi: 10.1242/dev.084582
- Larsson, E., Roberts, C. J., Claes, A. R., Franks, R. G., and Sundberg, E. (2014). Polar auxin transport is essential for medial versus lateral tissue specification and vascular-deiated valve outgrowth in *Arabidopsis* gynoecia. *Plant Physiol.* 166, 1998–2012. doi: 10.1104/pp.114.245951
- Lewis, D. R., and Muday, G. K. (2009). Measurement of auxin transport in *Arabidopsis thaliana*. *Nat. Protoc.* 4, 437–451. doi: 10.1038/nprot.2009.1
- Lewis, D. R., Ramirez, M. V., Miller, N. D., Vallabhaneni, P., Ray, W. K., Helm, R. F., et al. (2011). Auxin and ethylene induce flavonol accumulation through distinct transcriptional networks. *Plant Physiol.* 156, 144–164. doi: 10.1104/pp.111.172502
- Li, G., Liang, W., Zhang, X., Ren, H., Hu, J., Bennett, M. J., et al. (2014). Rice actin-binding protein RMD is a key link in the auxin-actin regulatory loop that controls cell growth. *Proc. Natl. Acad. Sci. U.S.A.* 111, 10377–10382. doi: 10.1073/pnas.1401680111
- Lim, P. O., Lee, I. C., Kim, J., Kim, H. J., Ryu, J. S., Woo, H. R., et al. (2010). Auxin response factor 2 (ARF2) plays a major role in regulating auxin-mediated leaf longevity. *J. Exp. Bot.* 61, 1419–1430. doi: 10.1093/jxb/erq100

- Lin, J.-F., and Wu, S.-H. (2004). Molecular events in senescing *Arabidopsis* leaves. *Plant J.* 39, 612–628. doi: 10.1111/j.1365-3113.2004.02160.x
- Lohman, K. N., Gan, S., John, M. C., and Amasino, R. M. (1994). Molecular analysis of natural leaf senescence in *Arabidopsis thaliana*. *Physiol. Plant.* 92, 322–328. doi: 10.1111/j.1399-3054.1994.tb05343.x
- Luschnig, C., Gaxiola, R. A., Grisafi, P., and Fink, G. R. (1998). EIR1, a root-specific protein involved in auxin transport, is required for gravitropism in *Arabidopsis thaliana*. *Genes Dev.* 12, 2175–2187. doi: 10.1101/gad.12.14.2175
- Madison, S. L., Buchanan, M. L., Glass, J. D., McClain, T. F., Park, E., and Nebenführ, A. (2015). Class XI myosins move specific organelles in pollen tubes and are required for normal fertility and pollen tube growth in *Arabidopsis*. *Plant Physiol.* 169, 1946–1960. doi: 10.1104/pp.15.01161
- Maillard, A., Diquélou, S., Billard, V., Lainé, P., Garnica, M., Prudent, M., et al. (2015). Leaf mineral nutrient remobilization during leaf senescence and modulation by nutrient deficiency. *Front. Plant Sci.* 6:317. doi: 10.3389/fpls.2015.00317
- Marchant, A., Kargul, J., May, S. T., Muller, P., Delbarre, A., Perrot-Rechenmann, C., et al. (1999). AUX1 regulates root gravitropism in *Arabidopsis* by facilitating auxin uptake within root apical tissues. *EMBO J.* 18, 2066–2073. doi: 10.1093/emboj/18.8.2066
- Misyura, M., Colasanti, J., and Rothstein, S. J. (2013). Physiological and genetic analysis of *Arabidopsis thaliana* anthocyanin biosynthesis mutants under chronic adverse environmental conditions. *J. Exp. Bot.* 64, 229–240. doi: 10.1093/jxb/ers328
- Murashige, T., and Skoog, F. (1962). A revised medium for rapid growth and bio assays with tobacco tissue cultures. *Physiol. Plant.* 15, 473–497. doi: 10.1111/j.1399-3054.1962.tb08052.x
- Murphy, A., Peer, W. A., and Taiz, L. (2000). Regulation of auxin transport by aminopeptidases and endogenous flavonoids. *Planta* 211, 315–324. doi: 10.1007/s004250000300
- Mushtaq, M. A., Pan, Q., Chen, D., Zhang, Q., Ge, X., and Li, Z. (2016). Comparative leaves transcriptome analysis emphasizing on accumulation of anthocyanins in *Brassica*: molecular regulation and potential interaction with photosynthesis. *Front. Plant Sci.* 7:311. doi: 10.3389/fpls.2016.00311
- Nakata, M., and Ohme-Takagi, M. (2014). Quantification of anthocyanin content. *BIO-Protoc.* 4:e1098. doi: 10.21769/BioProtoc.1098
- Nemhauser, J. L., Feldman, L. J., and Zambryski, P. C. (2000). Auxin and ETTIN in *Arabidopsis* gynoecium morphogenesis. *Development* 127, 3877–3888.
- Nick, P., Han, M.-J., and An, G. (2009). Auxin stimulates its own transport by shaping actin filaments. *Plant Physiol.* 151, 155–167. doi: 10.1104/pp.109.140111
- Noodén, L. D., and Noodén, S. M. (1985). Effects of morphactin and other auxin transport inhibitors on soybean senescence and pod development. *Plant Physiol.* 78, 263–266. doi: 10.1104/pp.78.2.263
- Ojangu, E.-L., Järve, K., Paves, H., and Truve, E. (2007). *Arabidopsis thaliana* myosin XI-K is involved in root hair as well as trichome morphogenesis on stems and leaves. *Protoplasma* 230, 193–202. doi: 10.1007/s00709-006-0233-8
- Ojangu, E.-L., Tanner, K., Pata, P., Järve, K., Holweg, C. L., Truve, E., et al. (2012). Myosins XI-K, XI-1, and XI-2 are required for development of pavement cells, trichomes, and stigmatic papillae in *Arabidopsis*. *BMC Plant Biol.* 12:81. doi: 10.1186/1471-2229-12-81
- Okada, K., Ueda, J., Komaki, M., Bell, C., and Shimura, Y. (1991). Requirement of the auxin polar transport system in early stages of *Arabidopsis* floral bud formation. *Plant Cell* 3, 677–684. doi: 10.1105/tpc.3.7.677
- Oñate-Sánchez, L., and Vicente-Carbajosa, J. (2008). DNA-free RNA isolation protocols for *Arabidopsis thaliana*, including seeds and siliques. *BMC Res. Notes* 1:93. doi: 10.1186/1756-0500-1-93
- Papouov, I. A., Papouov, M., Teale, W., Menges, M., Chakrabortee, S., Murray, J. A. H., et al. (2008). Comprehensive transcriptome analysis of auxin responses in *Arabidopsis*. *Mol. Plant* 1, 321–337. doi: 10.1093/mp/ssp021
- Park, E., and Nebenführ, A. (2013). Myosin XI-K of *Arabidopsis thaliana* accumulates at the root hair tip and is required for fast root hair growth. *PLoS One* 8:e76745. doi: 10.1371/journal.pone.0076745
- Peer, W. A., Bandyopadhyay, A., Blakeslee, J. J., Makam, S. N., Chen, R. J., Masson, P. H., et al. (2004). Variation in expression and protein localization of the PIN family of auxin efflux facilitator proteins in flavonoid mutants with altered auxin transport in *Arabidopsis thaliana*. *Plant Cell* 16, 1898–1911. doi: 10.1105/tpc.021501
- Peer, W. A., and Murphy, A. S. (2007). Flavonoids and auxin transport: modulators or regulators? *Trends Plant Sci.* 12, 556–563. doi: 10.1016/j.tplants.2007.10.003
- Peng, M., Hudson, D., Schofield, A., Tsao, R., Yang, R., Gu, H., et al. (2008). Adaptation of *Arabidopsis* to nitrogen limitation involves induction of anthocyanin synthesis which is controlled by the NLA gene. *J. Exp. Bot.* 59, 2933–2944. doi: 10.1093/jxb/ern148
- Peremylov, V. V., Cole, R. A., Fowler, J. E., and Dolja, V. V. (2015). Myosin-powered membrane compartment drives cytoplasmic streaming, cell expansion and plant development. *PLoS One* 10:e0139331. doi: 10.1371/journal.pone.0139331
- Peremylov, V. V., Klocko, A. L., Fowler, J. E., and Dolja, V. V. (2012). *Arabidopsis* myosin XI-K localizes to the motile endomembrane vesicles associated with F-actin. *Front. Plant Sci.* 3:184. doi: 10.3389/fpls.2012.00184
- Peremylov, V. V., Mockler, T. C., Filichkin, S. A., Fox, S. E., Jaiswal, P., Makarova, K. S., et al. (2011). Expression, splicing, and evolution of the myosin gene family in plants. *Plant Physiol.* 155, 1191–1204. doi: 10.1104/pp.110.170720
- Peremylov, V. V., Morgun, E. A., Kurth, E. G., Makarova, K. S., Koonin, E. V., and Dolja, V. V. (2013). Identification of myosin XI receptors in *Arabidopsis* defines a distinct class of transport vesicles. *Plant Cell* 25, 3022–3038. doi: 10.1105/tpc.113.113704
- Peremylov, V. V., Prokhnovsky, A. I., Avisar, D., and Dolja, V. V. (2008). Two class XI myosins function in organelle trafficking and root hair development in *Arabidopsis*. *Plant Physiol.* 146, 1109–1116. doi: 10.1104/pp.107.11.13654
- Peremylov, V. V., Prokhnovsky, A. I., and Dolja, V. V. (2010). Class XI myosins are required for development, cell expansion, and F-actin organization in *Arabidopsis*. *Plant Cell* 22, 1883–1897. doi: 10.1105/tpc.110.076315
- Pouteau, S., and Albertini, C. (2009). The significance of bolting and floral transitions as indicators of reproductive phase change in *Arabidopsis*. *J. Exp. Bot.* 60, 3367–3377. doi: 10.1093/jxb/erp173
- Prokhnovsky, A. I., Peremylov, V. V., and Dolja, V. V. (2008). Overlapping functions of the four class XI myosins in *Arabidopsis* growth, root hair elongation, and organelle motility. *Proc. Natl. Acad. Sci. U.S.A.* 105, 19744–19749. doi: 10.1073/pnas.0810730105
- Ren, H., and Gray, W. M. (2015). SAUR proteins as effectors of hormonal and environmental signals in plant growth. *Mol. Plant* 8, 1153–1164. doi: 10.1016/j.molp.2015.05.003
- Santelia, D., Henrichs, S., Vincenzetti, V., Sauer, M., Bigler, L., Klein, M., et al. (2008). Flavonoids redirect PIN-mediated polar auxin fluxes during root gravitropic responses. *J. Biol. Chem.* 283, 31218–31226. doi: 10.1074/jbc.M710122200
- Scarpella, E., Marcos, D., Friml, J., and Berleth, T. (2006). Control of leaf vascular patterning by polar auxin transport. *Genes Dev.* 20, 1015–1027. doi: 10.1101/gad.1402406
- Scheuring, D., Löffke, C., Krüger, F., Kittelman, M., Eisa, A., Hughes, L., et al. (2016). Actin-dependent vacuolar occupancy of the cell determines auxin-induced growth repression. *Proc. Natl. Acad. Sci. U.S.A.* 113, 452–457. doi: 10.1073/pnas.1517445113
- Schippers, J., Jing, H.-C., Hille, J., and Dijkwel, P. (2007). Developmental and hormonal control of leaf senescence. *Annu. Plant Rev.* 26, 145–170. doi: 10.1002/978047098855.ch7
- Schmalenbach, I., Zhang, L., Reymond, M., and Jiménez-Gómez, J. M. (2014). The relationship between flowering time and growth responses to drought in the *Arabidopsis* Landsberg erecta x Antwerp-1 population. *Front. Plant Sci.* 5:609. doi: 10.3389/fpls.2014.00609
- Sekhon, R. S., Childs, K. L., Santoro, N., Foster, C. E., Buell, C. R., de Leon, N., et al. (2012). Transcriptional and metabolic analysis of senescence induced by preventing pollination in maize. *Plant Physiol.* 159, 1730–1744. doi: 10.1104/pp.112.199224
- Sessions, A., Nemhauser, J. L., McColl, A., Roe, J. L., Feldmann, K. A., and Zambryski, P. C. (1997). ETTIN patterns the *Arabidopsis* floral meristem and reproductive organs. *Development* 124, 4481–4491.
- Shibasaki, K., Uemura, M., Tsurumi, S., and Rahman, A. (2009). Auxin response in *Arabidopsis* under cold stress: underlying molecular mechanisms. *Plant Cell* 21, 3823–3838. doi: 10.1105/tpc.109.069906
- Smertenko, A., and Franklin-Tong, V. E. (2011). Organisation and regulation of the cytoskeleton in plant programmed cell death. *Cell Death Differ.* 18, 1263–1270. doi: 10.1038/cdd.2011.39

- Smertenko, A. P., Bozhkov, P. V., Filonova, L. H., von Arnold, S., and Hussey, P. J. (2003). Re-organisation of the cytoskeleton during developmental programmed cell death in *Picea abies* embryos. *Plant J.* 33, 813–824. doi: 10.1046/j.1365-313X.2003.01670.x
- Solfanelli, C., Poggi, A., Loreti, E., Alpi, A., and Perata, P. (2006). Sucrose-specific induction of the theanthocyanin biosynthetic pathway in *Arabidopsis*. *Plant Physiol.* 140, 637–646. doi: 10.1104/pp.105.072579
- Sundberg, E., and Østergaard, L. (2009). Distinct and dynamic auxin activities during reproductive development. *Cold Spring Harb. Perspect. Biol.* 1:a001628. doi: 10.1101/cshperspect.a001628
- Swartzberg, D., Dai, N., Gan, S., Amasino, R., and Granot, D. (2006). Effects of cytokinin production under two SAG promoters on senescence and development of tomato plants. *Plant Biol.* 8, 579–586. doi: 10.1055/s-2006-924240
- Swarup, R., Friml, J., Marchant, A., Ljung, K., Sandberg, G., Palme, K., et al. (2001). Localization of the auxin permease AUX1 suggests two functionally distinct hormone transport pathways operate in the *Arabidopsis* root apex. *Genes Dev.* 15, 2648–2653. doi: 10.1101/gad.210501
- Swarup, R., and Péret, B. (2012). AUX/LAX family of auxin influx carriers — An overview. *Front. Plant Sci.* 3:225. doi: 10.3389/fpls.2012.00225
- Talts, K., Ilau, B., Ojangu, E.-L., Tanner, K., Peremylov, V. V., Dolja, V. V., et al. (2016). *Arabidopsis* myosins XI1, XI2, and XIK are crucial for gravity-induced bending of inflorescence stems. *Front. Plant Sci.* 7:1932. doi: 10.3389/fpls.2016.01932
- Tang, L. P., Li, X. M., Dong, Y. X., Zhang, X. S., and Su, Y. H. (2017). Microfilament depolymerization is a pre-requisite for stem cell formation during in vitro shoot regeneration in *Arabidopsis*. *Front. Plant Sci.* 8:158. doi: 10.3389/fpls.2017.00158
- Thomas, S. G., Huang, S., Li, S., Staiger, C. J., and Franklin-Tong, V. E. (2006). Actin depolymerization is sufficient to induce programmed cell death in self-incompatible pollen. *J. Cell Biol.* 174, 221–229. doi: 10.1083/jcb.200604011
- Titapiwatanakun, B., Blakeslee, J. J., Bandyopadhyay, A., Yang, H., Mravec, J., Sauer, M., et al. (2009). ABCB19/PGP19 stabilises PIN1 in membrane microdomains in *Arabidopsis*. *Plant J.* 57, 27–44. doi: 10.1111/j.1365-313X.2008.03668.x
- Ueda, H., Yokota, E., Kutsuna, N., Shimada, T., Tamura, K., Shimmen, T., et al. (2010). Myosin-dependent endoplasmic reticulum motility and F-actin organization in plant cells. *Proc. Natl. Acad. Sci. U.S.A.* 107, 6894–6899. doi: 10.1073/pnas.0911482107
- Ulmasov, T., Murrlett, J., Hagen, G., and Guilfoyle, T. J. (1997). Aux/IAA proteins repress expression of reporter genes containing natural and highly active synthetic auxin response elements. *Plant Cell* 9, 1963–1971. doi: 10.1105/tpc.9.11.1963
- Ungerer, M. C., Halldorsdottir, S. S., Modliszewski, J. L., Mackay, T. F. C., and Purugganan, M. D. (2002). Quantitative trait loci for inflorescence development in *Arabidopsis thaliana*. *Genetics* 160, 1133–1151.
- Vanneste, S., and Friml, J. (2009). Auxin: a trigger for change in plant development. *Cell* 136, 1005–1016. doi: 10.1016/j.cell.2009.03.001
- Vernoux, T., Besnard, F., and Traas, J. (2010). Auxin at the shoot apical meristem. *Cold Spring Harb. Perspect. Biol.* 2:a001487. doi: 10.1101/cshperspect.a001487
- Wang, C., Yan, X., Chen, Q., Jiang, N., Fu, W., Ma, B., et al. (2013). Clathrin light chains regulate clathrin-mediated trafficking, auxin signaling, and development in *Arabidopsis*. *Plant Cell* 25, 499–516. doi: 10.1105/tpc.112.108373
- Wang, Q., Kohlen, W., Rossmann, S., Vernoux, T., and Theres, K. (2014). Auxin depletion from the leaf axil conditions competence for axillary meristem formation in *Arabidopsis* and tomato. *Plant Cell* 26, 2068–2079. doi: 10.1105/tpc.114.123059
- Wang, Y.-S., Yoo, C.-M., and Blancaflor, E. B. (2008). Improved imaging of actin filaments in transgenic *Arabidopsis* plants expressing a green fluorescent protein fusion to the C- and N-termini of the fimbrin actin-binding domain 2. *New Phytol.* 177, 525–536. doi: 10.1111/j.1469-8137.2007.02261.x
- Watanabe, M., Balazadeh, S., Tohge, T., Erban, A., Giavalisco, P., Kopka, J., et al. (2013). Comprehensive dissection of spatiotemporal metabolic shifts in primary, secondary, and lipid metabolism during developmental senescence in *Arabidopsis*. *Plant Physiol.* 162, 1290–1310. doi: 10.1104/pp.113.217380
- Weaver, L. M., Gan, S. S., Quirino, B., and Amasino, R. M. (1998). A comparison of the expression patterns of several senescence-associated genes in response to stress and hormone treatment. *Plant Mol. Biol.* 37, 455–469. doi: 10.1023/A:1005934428906
- Weaver, L. M., Himelblau, E., and Amasino, R. M. (1997). Leaf senescence: gene expression and regulation. *Genetic Eng.* 19, 215–234. doi: 10.1007/978-1-4615-5925-2_12
- Weigel, D., and Glazebrook, J. (2002). *Arabidopsis: A Laboratory Manual*. New York, NY: CSHL Press, 355.
- Woo, H. R., Kim, H. J., Nam, H. G., and Lim, P. O. (2013). Plant leaf senescence and death — Regulation by multiple layers of control and implications for aging in general. *J. Cell Sci.* 126, 4823–4833. doi: 10.1242/jcs.109116
- Wu, S., Xie, Y., Zhang, J., Ren, Y., Zhang, X., Wang, J., et al. (2015). VLN2 regulates plant architecture by affecting microfilament dynamics and polar auxin transport in rice. *Plant Cell* 27, 2829–2845. doi: 10.1105/tpc.15.00581
- Xu, G., Li, S., Xie, K., Zhang, Q., Wang, Y., Tang, Y., et al. (2012). Plant ERD2-like proteins function as endoplasmic reticulum luminal protein receptors and participate in programmed cell death during innate immunity. *Plant J.* 72, 57–69. doi: 10.1111/j.1365-313X.2012.05053.x
- Zažimalová, E., Murphy, A. S., Yang, H., Hoyerová, K., and Hošek, P. (2010). Auxin transporters — Why so many? *Cold Spring Harb. Perspect. Biol.* 2:a001552. doi: 10.1101/cshperspect.a001552
- Zentgraf, U., Jobst, J., Kolb, D., and Rentsch, D. (2004). Senescence-related gene expression profiles of rosette leaves of *Arabidopsis thaliana*: leaf age versus plant age. *Plant Biol.* 6, 178–183. doi: 10.1055/s-2004-815735
- Zhu, J., Bailly, A., Zwiewka, M., Sovero, V., Di Donato, M., Ge, P., et al. (2016). TWISTED DWARF1 mediates the action of auxin transport inhibitors on actin cytoskeleton dynamics. *Plant Cell* 28, 930–948. doi: 10.1105/tpc.15.00726
- Zhu, J., and Geisler, M. (2015). Keeping it all together: auxin-actin crosstalk in plant development. *J. Exp. Bot.* 66, 4983–4998. doi: 10.1093/jxb/erv308
- Zúñiga-Mayo, V. M., Reyes-Olalde, J. I., Marsch-Martinez, N., and de Folter, S. (2014). Cytokinin treatments affect the apical-basal patterning of the *Arabidopsis gynoecium* and resemble the effects of polar auxin transport inhibition. *Front. Plant Sci.* 5:191. doi: 10.3389/fpls.2014.00191

Conflict of Interest Statement: The authors declare that the research was conducted in the absence of any commercial or financial relationships that could be construed as a potential conflict of interest.

Copyright © 2018 Ojangu, Ilau, Tanner, Talts, Ihoma, Dolja, Paves and Truve. This is an open-access article distributed under the terms of the Creative Commons Attribution License (CC BY). The use, distribution or reproduction in other forums is permitted, provided the original author(s) and the copyright owner(s) are credited and that the original publication in this journal is cited, in accordance with accepted academic practice. No use, distribution or reproduction is permitted which does not comply with these terms.

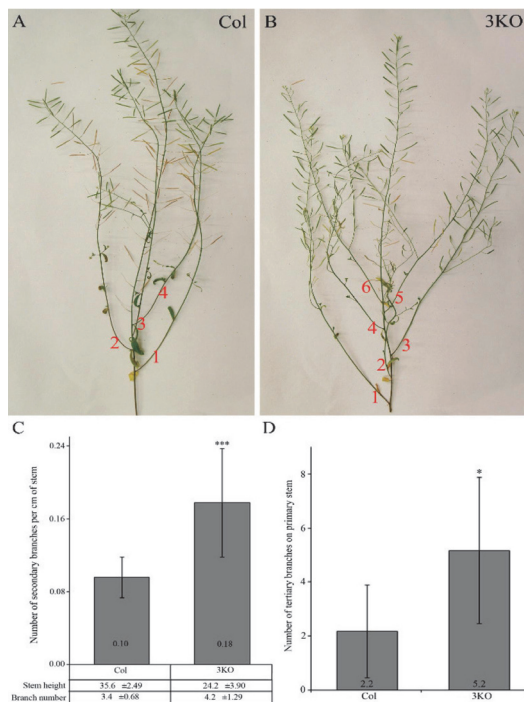
Supplementary Material

Class XI myosins contribute to polar auxin transport and senescence-induced programmed cell death in Arabidopsis

Eve-Ly Ojangu*, Birger Ilau, Krista Tanner, Kristiina Talts, Eliis Ihoma, Valerian V. Dolja, Heiti Paves, Erkki Truve

* Correspondence: Eve-Ly Ojangu: eve-ly.ojangu@ttu.ee

1 Supplementary figure 1



Supplementary Figure 1. Branching architecture of primary inflorescence shoots. (A) Primary inflorescence shoot of Columbia plant formed four axillary branches, and 3KO plant (B) six axillary branches. Red numbers illustrate the number of axillary branches. (C) Number of secondary branches per cm of primary inflorescence stem. Stem height and branch number was measured after flower formation was ended. Data represent average values; error bars represent SD; $n = 17-19$; *** $p < 0.001$ (Student's t-test). (D) Number of tertiary branches on primary inflorescence stem. Data represent average values; error bars represent SD; $n = 6$; * $p < 0.001$ (Student's t-test).

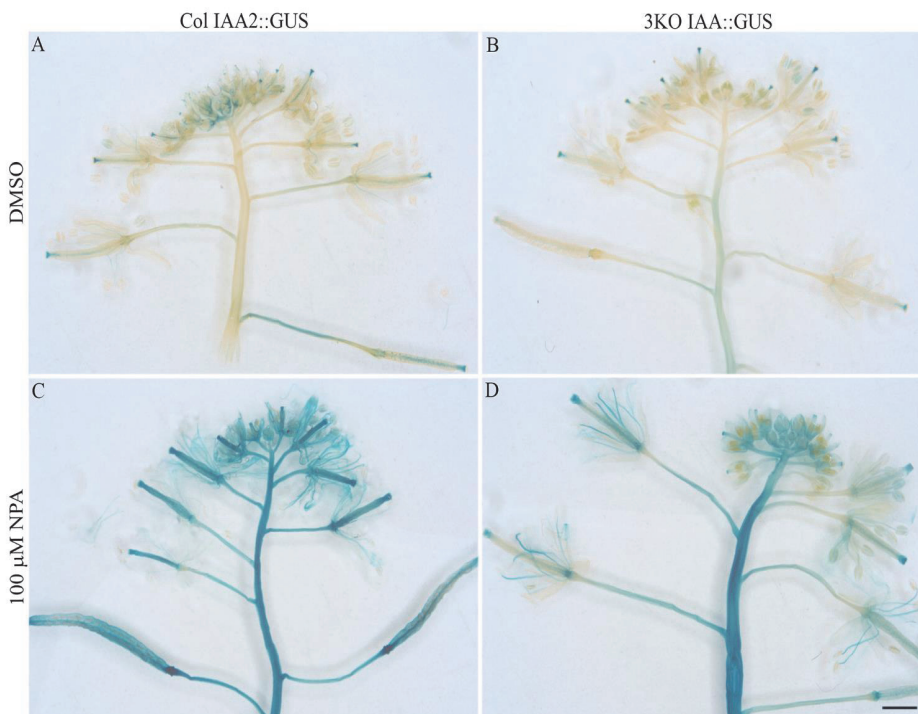
Supplementary Material

Class XI myosins contribute to auxin response and senescence-induced cell death in Arabidopsis

Eve-Ly Ojangu*, Birger Ilau, Krista Tanner, Kristiina Talts, Eliis Ihoma, Valerian V. Dolja, Heiti Paves, Erkki Truve

* Correspondence: Eve-Ly Ojangu: eve-ly.ojangu@ttu.ee

1 Supplementary figure 2



Supplementary Figure 2. Effect of NPA-treatment on IAA2::GUS expression. Primary inflorescences of Col IAA2::GUS (A) and 3KO IAA2::GUS (B) were dipped twice with 100 μ M NPA (C-D). Histochemical staining was performed one week after NPA-treatment. NPA-treatment led to increased IAA2::GUS activity both in Col (C) and 3KO (D) inflorescences. In NPA-treated 3KO IAA2::GUS flowers, the GUS staining does not accumulate in valves of gynoecia. Somewhat weaker staining of pedicles, petals and sepals is noticeable in 3KO IAA2::GUS also. Scale bar is 1 mm.

Supplementary Material

Class XI myosins contribute to auxin response and senescence-induced cell death in Arabidopsis

Eve-Ly Ojangu*, Birger Ilau, Krista Tanner, Kristiina Talts, Eliis Ihoma, Valerian V. Dolja, Heiti Paves, Erkki Truve

* Correspondence: Eve-Ly Ojangu: eve-ly.ojangu@ttu.ee

1 Supplementary figure 3



Supplementary Figure 3. Variety of inflorescence and flower development in 3KO PIN1::PIN1-GFP plants. The irregular architecture of (A) primary inflorescence and (B) axillary (secondary) inflorescence of 3KO PIN1::PIN1-GFP plants. (C) Post-anthesis flowers were dissected from primary inflorescence (A) according to developmental sequence. Notice the variability of under- and undeveloped flowers. Scale bar is 1mm.

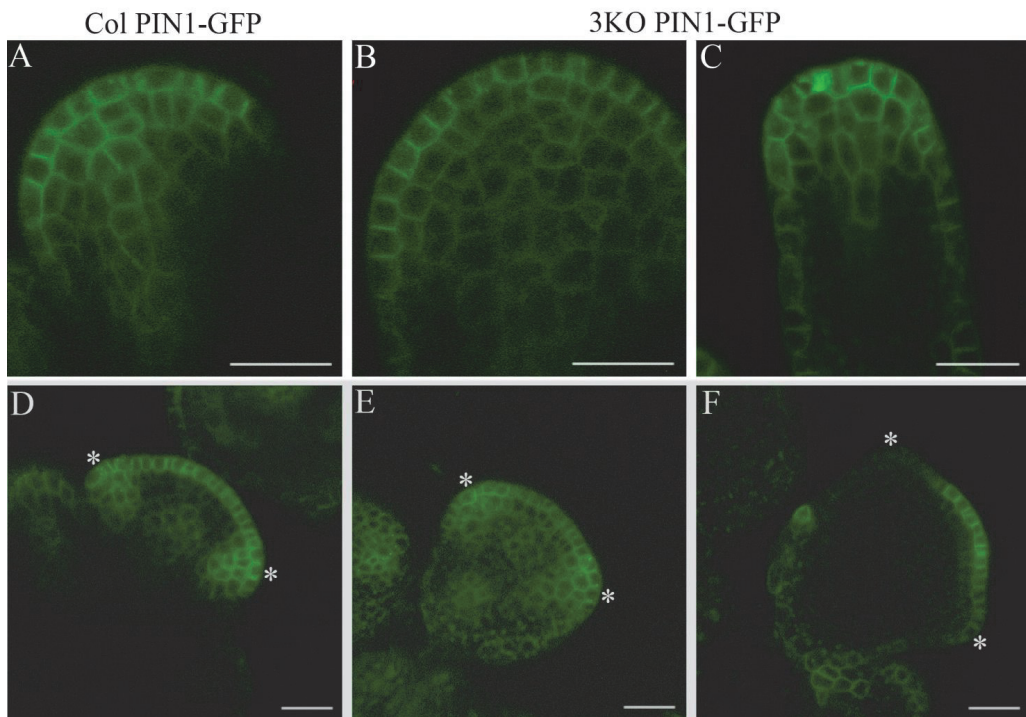
Supplementary Material

Class XI myosins contribute to auxin response and senescence-induced cell death in Arabidopsis

Eve-Ly Ojangu*, Birger Ilau, Krista Tanner, Kristiina Talts, Eliis Ihoma, Valerian V. Dolja, Heiti Paves, Erkki Truve

* Correspondence: Eve-Ly Ojangu: eve-ly.ojangu@ttu.ee

1 Supplementary figure 4



Supplementary Figure 4. The PIN1-GFP expression in early stages of floral primordia development. (A-C) Upper panel represents very early stage of primordium development. In 3KO PIN1-GFP plants, the shapes of primordia vary occasionally, notice the pin-like shape of 3KO PIN1-GFP primordium (C). (D-F) Lower panel represents later stage of primordium development where PIN1-GFP accumulation defines the sites of petal initiation (white asterisks). The PIN1-GFP patterning in developing 3KO floral primordia is partially aberrant since the PIN1 accumulation is occasionally absent at the sites of petal emergence (F). Images represent single optical slices. Scale bars are 20 μm .

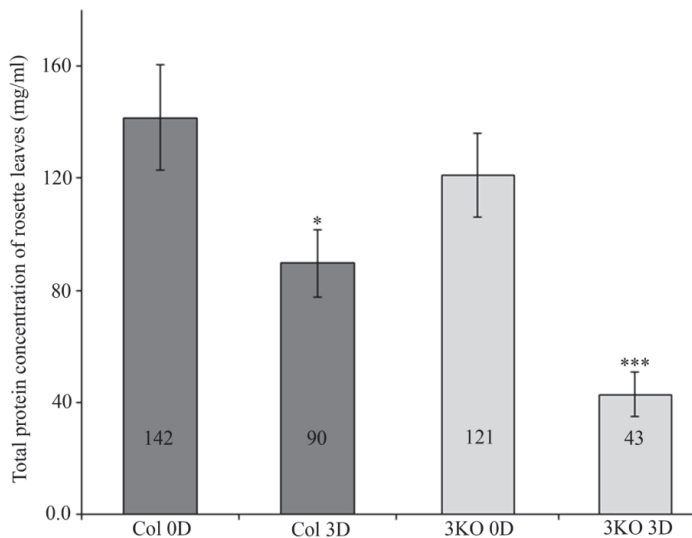
Supplementary Material

Class XI myosins contribute to auxin response and senescence-induced cell death in Arabidopsis

Eve-Ly Ojangu*, Birger Ilau, Krista Tanner, Kristiina Talts, Eliis Ihoma, Valerian V. Dolja, Heiti Paves, Erkki Truve

* **Correspondence:** Eve-Ly Ojangu: eve-ly.ojangu@ttu.ee

1 Supplementary figure 5



Supplementary Figure 5. The total protein content of leaf extracts before and after dark treatment. After dark-treatment, the total protein concentration of Col leaves was 1.6-fold lower (Col 3D) and the one of 3KO leaves was 2.8-fold lower (3KO 3D), in comparison with untreated controls (Col 0D, 3KO 0D), respectively. Data represent average values; error bars represent SD; n = 4; * $p < 0.05$, *** $p < 0.001$ (Student's *t*-test).

Supplementary Material

Class XI myosins contribute to auxin response and senescence-induced cell death in Arabidopsis

Eve-Ly Ojangu*, Birger Ilau, Krista Tanner, Kristiina Talts, Eliis Ihoma, Valerian V. Dolja, Heiti Paves, Erkki Truve

* **Correspondence:** Eve-Ly Ojangu: eve-ly.ojangu@ttu.ee

1 Supplementary Table

Supplementary Table S1. RT-qPCR primers.

Gene name	AGI code	Primer sequence
<i>SAND</i>	AT2G28390	5' - AACTCTATGCAGCATTGATCCACT - 3'
		5' - TGATTGCATATCTTTATCGCCATC - 3'
<i>UBC</i>	AT5G25760	5' - CTGCGACTCAGGGAATCTTCTAA - 3'
		5' - TTGTGCCATTGAATTGAACCC - 3'
expressed sequence (EX70)	AT2G32170	5' - ATCGAGCTAAGTTTGGAGGATGTAA - 3'
		5' - TCTCGATCACAAACCCAAAATG - 3'
<i>AUX1</i>	AT2G38120	5' - TGTTATCAGGAATAGTACTTCAGATC - 3'
		5' - AGTATGAACCAAGTAATCCATCAAG - 3'
<i>IAA2</i>	AT3G23030	5' - AGAACAACAACAGTGTGAGCTAC - 3'
		5' - CTCTCACAATATTCACCAATCATGA - 3'
<i>PIN1</i>	AT1G73590	5' - CGACACTCCCCAACACTCTAG - 3'
		5' - AGCTTAGCTCCACGGTACTC - 3'
<i>PIN3</i>	AT1G70940	5' - AAAGATTGGAAGATGAAGACAACCTTA - 3'
		5' - CTGGAACAAGGGAATATTCAAATC - 3'

<i>PIN4</i>	AT2G01420	5'- GGATCTTGTCTTCATTAGACGC - 3'
		5'- GTATAAACCACTTAACTAGAACTTCA - 3'
<i>PIN7</i>	AT1G23080	5'- TCGCACTACCGATTACACTTGTT - 3'
		5'- CATTTCGTGTTACATTACATTTTCTAG - 3'
<i>SAUR36</i>	AT2G45210	5'- GTGATTAGCATGGGGACACTTA - 3'
		5'- ATCTTGAGTAGACCCATATAGAGAA - 3'
<i>SAG12</i>	AT5G45890	5'- TGATGAGCAAGCACTGATGAAG - 3'
		5'- TTCGCCGTATCCAATCGCAG - 3'
<i>SAG13</i>	AT2G29350	5'- AGCTTGCCCACCCATTGTTAAA - 3'
		5'- CCAGCTGATTCATGGCTCCT - 3'



CURRICULUM VITAE

Personal data

Name: Eve-Ly Ojangu
Date of birth: 29.01.1974
Place of birth: Tallinn
Citizenship: Estonian

Contact information

Address: Department of Chemistry and Biotechnology, Tallinn University of Technology, Akadeemia tee 15, 12618, Tallinn
Tel.: +372-56562291
E-mail: eve-ly.ojangu@ttu.ee

Education

2001–2007 Tallinn University of Technology, Faculty of Science, Department of Gene Technology, doctoral studies
1997–1999 University of Tartu, Faculty of Biology and Geography, Institute of Molecular and Cell Biology, Master of Science (MSc)
1992–1997 University of Tartu, Faculty of Biology and Geography, Institute of Molecular and Cell Biology, Bachelor's degree (BSc)
1981–1992 Tallinn 43. High School (Tallinn High School of Technology)

Professional employment

2017– ... Tallinn University of Technology, School of Science, Department of Chemistry and Biotechnology, engineer
2016–2017 Tallinn University of Technology, Faculty of Science, Department of Gene Technology, Chair of Gene Technology, engineer
2004–2016 Tallinn University of Technology, Faculty of Science, Department of Gene Technology, Chair of Gene Technology, researcher
2000–2004 National Institute of Chemical Physics and Biophysics, engineer
1999–2000 University of Tartu, Faculty of Science and Technology, Institute of Molecular and Cell Biology, University of Tartu, Chair of Genetics, engineer

Courses and conferences

November 2017 Plant Phenotyping Forum, poster presentation. Tartu, Estonia.
August 2017 27th Congress of the Scandinavian Plant Physiology Society, poster presentation. Naantali, Finland.
September 2015 VI Congress of Baltic Genetic Research, oral presentation. Tartu, Estonia.
April 2015 Botanical Microscopy Meeting, poster presentation. Exeter, UK.
April 2011 Botanical Microscopy Meeting, poster presentation. Wageningen, Netherlands.
August 2010 Gordon Conference on "Plant and fungal cytoskeleton", poster presentation. Andover, New Hampshire, USA.

- April 2008 Theoretical course “The usage of GMOs in laboratory: licence and quality”. Tallinn, Estonia.
- March 2008 Theoretical course “Environmental risk assessment in GMO analysis”. Tallinn, Estonia.
- August 2008 Gordon Conference on “Plant and fungal cytoskeleton”, poster presentation. Italy.

Supervised dissertations

Krista Tanner, MSc, 2016:

Supervised by Eve-Ly Ojangu, Heiti Paves and Erkki Truve
Activity of auxin promoters and senescence of rosette leaves in *Arabidopsis thaliana* class XI myosin triple mutant *xi-2/xi-k/xi-h*.

Eliis Ihoma, MSc, 2016:

Activity of auxin promoters and polar auxin transport in *Arabidopsis thaliana* class XI myosin triple mutant. Supervised by Eve-Ly Ojangu, Heiti Paves and Erkki Truve.

Eliis Ihoma, BSc, 2013:

Activity of auxin promoters in *Arabidopsis thaliana* class XI myosin triple mutant. Supervised by Eve-Ly Ojangu and Kristiina Talts.

Krista Tanner, BSc, 2010:

Overlapping role of class XI myosins in epidermis development of *Arabidopsis thaliana*. Supervised by Eve-Ly Ojangu and Erkki Truve.

Birger Ilau, MSc, 2005:

Expression of *GUS* reporter gene in transgenic plants under the control of the promoters of *Arabidopsis thaliana* myosins *ATM1* and *MYA1*. Supervised by Eve-Ly Ojangu, Erkki Truve and Heiti Paves.

Kristel Järve, MSc, 2005:

Arabidopsis thaliana myosin XIX is essential for normal development of root hairs. Supervised by Erkki Truve, Heiti Paves and Eve-Ly Ojangu.

Birger Ilau, BSc, 2003:

Characterization of MPB2C, the tobacco mosaic virus movement protein interacting protein in *Nicotiana benthamiana*. Supervised by Eve-Ly Ojangu and Erkki Truve.

Kristel Järve, BSc, 2003:

The analysis of T-DNA insertional mutants of *Arabidopsis thaliana* myosins. Supervised by Erkki Truve and Eve-Ly Ojangu.

Publications

Ojangu E.-L., Ilau B., Tanner K., Talts K., Ihoma E., Dolja VV., Paves H., Truve E. (2018). Class XI myosins contribute to auxin response and senescence-induced cell death in *Arabidopsis*. *Front. Plant Sci.* 9:1570.

Talts K., Ilau B., **Ojangu E.-L.**, Tanner K., Peremyslov VV., Dolja VV., Truve E., Paves H. (2016). *Arabidopsis* myosins XI1, XI2, and XIK are crucial for gravity-induced bending of inflorescence stems. *Front. Plant Sci.* 7:1932.

Ojangu E.-L., Tanner K., Pata P., Järve K., Holweg CL., Truve E., Paves H. (2012). Myosins XI-K, XI-1, and XI-2 are required for development of pavement cells, trichomes, and stigmatic papillae in *Arabidopsis*. *BMC Plant Biol.* 12:81.

Ojangu E.-L., Järve K., Paves H., Truve E. (2007). *Arabidopsis thaliana* myosin XIK is involved in root hair as well as trichome morphogenesis on stems and leaves. *Protoplasma* 230:193–202.

Curin M., **Ojangu E.-L.**, Trutnyeva K., Ilau B., Truve E., Waigmann E. (2007). MPB2C, a microtubule-associated plant factor, is required for microtubular accumulation of tobacco mosaic virus movement protein in plants. *Plant Physiol.* 143:801–811.

Tover A., **Ojangu E.-L.**, Kivisaar M. (2001). Growth medium composition-determined regulatory mechanisms are superimposed on CatR-mediated transcription from the pheBA and catBCA promoters in *Pseudomonas putida*. *Microbiology* 147:2149–2156.

Ojangu E.-L., Tover A., Teras R., Kivisaar M. (2000). Effects of combination of different -10 hexamers and downstream sequences on stationary-phase-specific sigma factor sigma(S)-dependent transcription in *Pseudomonas putida*. *J. Bacteriol.* 182:6707–6713.

ELULOOKIRJELDUS

Isikuandmed

Nimi: Eve-Ly Ojangu
Sünniaeg: 29.01.1974
Sünnikoht: Tallinn
Kodakondsus: Eesti

Kontaktandmed

Address: Keemia ja biotehnoloogia instituut, Tallinna Tehnikaülikool, Akadeemia tee 15, 12618 Tallinn
Tel.: +372-56562291
E-post: eve-ly.ojangu@ttu.ee

Hariduskäik

2001–2007 Tallinna Tehnikaülikool, doktoriõpe
1997–1999 Tartu Ülikool, magistrikraad (MSc)
1992–1997 Tartu Ülikool, bakalauresusekraad (BSc)
1981–1992 Tallinna 43. Keskkool (Tallinna Tehnikagümnaasium)

Teenistuskäik

2017– ... Tallinna Tehnikaülikool, Loodusteaduskond, Keemia ja biotehnoloogia instituut, insener
2016–2017 Tallinna Tehnikaülikool, Matemaatika-loodusteaduskond, Geenitehnoloogia instituut, Geenitehnoloogia õppetool, insener
2004–2016 Tallinna Tehnikaülikool, Matemaatika-loodusteaduskond, Geenitehnoloogia instituut, Geenitehnoloogia õppetool, teadur
2000–2004 Keemilise ja Bioloogilise Füüsika Instituut, insener
1999–2000 Tartu Ülikool, Loodus- ja tehnoloogiateaduskond, Tartu Ülikooli Molekulaar- ja Rakubioloogia Instituut, Geneetika õppetool, insener

Kursused ja konverentsid

November 2017 “Plant Phenotyping Forum”, posterettekanne. Tartu, Eesti.
August 2017 “Nordic plant biology days: 27th SPPS congress”, posterettekanne. Naantali, Soome.
September 2015 VI Balti geneetika kongress, suuline ettekanne. Tartu, Estonia.
Aprill 2015 Botaanilise mikroskoopia konverents, posterettekanne. Exeter, Ühendkuningriigid.
Aprill 2011 Botaanilise mikroskoopia konverents, posterettekanne. Wageningen, Holland.
August 2010 Taimede ja seente rakuskeleti konverents (Gordon Conferences), posterettekanne. Andover, New Hampshire, Ameerika Ühendriigid.

Aprill 2008	Koolitus "GMO-de kasutamine laboris: luba ja kvaliteet". Tallinn, Eesti.
Märts 2008	GMOde riskianalüüsi koolitus. Tallinn, Eesti.
August 2008	Taimede ja seente rakuskeleti konverents (Gordon conferences), posterettekanne. Itaalia.

Juhendatud diplomitööd

Krista Tanner, MSc, 2016:

Auksiini promootorite aktiivsus ning rosetilehtede vananemine müürlooga klass XI müosiinide kolmikmutandis *xi-2/xi-k/xi-h*. Juhendajad Eve-Ly Ojangu, Heiti Paves ja Erkki Truve

Eliis Ihoma, MSc, 2016:

Auksiini promootorite aktiivsus ning auksiini polaarne transport müürlooga klass XI müosiinide kolmikmutandis. Juhendajad Eve-Ly Ojangu, Heiti Paves ja Erkki Truve

Eliis Ihoma, BSc, 2013:

Auksiini promootorite aktiivsus müürlooga klass XI müosiinide kolmikmutandis. Juhendajad Eve-Ly Ojangu ja Kristiina Talts

Krista Tanner, BSc, 2010:

Klass XI müosiinide kattuv roll müürlooga epidermise arengus. Juhendajad Eve-Ly Ojangu ja Erkki Truve

Birger Ilau, MSc, 2005:

Arabidopsis thaliana müosiinide *ATM1* ja *MYA1* promootorite poolt suunatud *GUS* reportergeeni ekspressioon transgeensetes taimedes. Juhendajad Eve-Ly Ojangu, Erkki Truve ja Heiti Paves

Kristel Järve, MSc, 2005:

Arabidopsis thaliana müosiin XI-K on vajalik juurekarvade normaalseks arenguks. Juhendajad Erkki Truve, Heiti Paves ja Eve-Ly Ojangu

Birger Ilau, BSc, 2003:

Tubaka mosaiigiviiruse liikumisvalguga seonduva valgu MPB2C iseloomustamine *Nicotiana benthamiana*'s. Juhendajad Eve-Ly Ojangu ja Erkki Truve

Kristel Järve, BSc, 2003:

Arabidopsis thaliana müosiinide insertiooniliste T-DNA mutantide analüüs. Juhendajad Erkki Truve ja Eve-Ly Ojangu

Publikatsioonid

Ojangu E.-L., Ilau B., Tanner K., Talts K., Ihoma E., Dolja VV., Paves H., Truve E. (2018). Class XI myosins contribute to auxin response and senescence-induced cell death in *Arabidopsis*. *Front. Plant Sci.* 9:1570.

Talts K., Ilau B., **Ojangu E.-L.**, Tanner K., Peremyslov VV., Dolja VV., Truve E., Paves H. (2016). *Arabidopsis* myosins XI1, XI2, and XIK are crucial for gravity-induced bending of inflorescence stems. *Front. Plant Sci.* 7:1932.

Ojangu E.-L., Tanner K., Pata P., Järve K., Holweg CL., Truve E., Paves H. (2012). Myosins XI-K, XI-1, and XI-2 are required for development of pavement cells, trichomes, and stigmatic papillae in *Arabidopsis*. *BMC Plant Biol.* 12:81.

Ojangu E.-L., Järve K., Paves H., Truve E. (2007). *Arabidopsis thaliana* myosin XIK is involved in root hair as well as trichome morphogenesis on stems and leaves. *Protoplasma* 230:193–202.

Curin M., **Ojangu E.-L.**, Trutnyeva K., Ilau B., Truve E., Waigmann E. (2007). MPB2C, a microtubule-associated plant factor, is required for microtubular accumulation of tobacco mosaic virus movement protein in plants. *Plant Physiol.* 143:801–811.

Tover A., **Ojangu E.-L.**, Kivisaar M. (2001). Growth medium composition-determined regulatory mechanisms are superimposed on CatR-mediated transcription from the pheBA and catBCA promoters in *Pseudomonas putida*. *Microbiology* 147:2149–2156.

Ojangu E.-L., Tover A., Teras R., Kivisaar M. (2000). Effects of combination of different -10 hexamers and downstream sequences on stationary-phase-specific sigma factor sigma(S)-dependent transcription in *Pseudomonas putida*. *J. Bacteriol.* 182:6707–6713.